

DESIGN AND CHARACTERISATION OF  
PARALLEL MINIATURE  
BIOREACTORS FOR BIOPROCESS  
OPTIMISATION AND SCALE-UP

Naveraj Kaur Gill

A thesis submitted for the degree of  
Doctor of Philosophy  
to the  
University of London

Department of Biochemical Engineering  
University College London  
Torrington Place  
London  
WC1E 7JE

UMI Number: U593299

All rights reserved

INFORMATION TO ALL USERS

The quality of this reproduction is dependent upon the quality of the copy submitted.

In the unlikely event that the author did not send a complete manuscript and there are missing pages, these will be noted. Also, if material had to be removed, a note will indicate the deletion.



UMI U593299

Published by ProQuest LLC 2013. Copyright in the Dissertation held by the Author.  
Microform Edition © ProQuest LLC.

All rights reserved. This work is protected against  
unauthorized copying under Title 17, United States Code.



ProQuest LLC  
789 East Eisenhower Parkway  
P.O. Box 1346  
Ann Arbor, MI 48106-1346

'I, Naveraj Kaur Gill, confirm that the work presented in this thesis is my own. Where information has been derived from other sources, I confirm that this has been indicated in the thesis.'

# ABSTRACT

---

---

The establishment of a high productivity microbial fermentation process requires the experimental investigation of many interacting variables. In order to speed up this procedure a novel miniature stirred bioreactor system is described which enables parallel operation of 4-16 independently controlled fermentations. Each miniature bioreactor is of standard geometry (100 mL maximum working volume) and is fitted with a magnetically driven six-blade miniature turbine impeller ( $d_i = 20$  mm,  $d_i/d_T = 1/3$ ) operating in the range 100 - 2000 rpm. Aeration is achieved via a sintered sparger at flow rates in the range of 0 - 2 vvm. Continuous on-line monitoring of each bioreactor is possible using miniature pH, dissolved oxygen and temperature probes, while PC-based software enables independent bioreactor control and real-time visualisation of parameters monitored on-line. Initial characterisation of the bioreactor involved quantification of the volumetric oxygen mass transfer coefficient as a function of agitation and aeration rates. The maximum  $k_L a$  value obtained was  $0.11 \text{ s}^{-1}$ . The reproducibility of *E. coli* TOP10 pQR239 and *B. subtilis* ATCC6633 fermentations was shown in four parallel fermentations of each organism. For *E. coli* (1000 rpm, 1 vvm) the maximum specific growth rate,  $\mu_{\max}$ , was  $0.68 \pm 0.01 \text{ h}^{-1}$  and the final biomass concentration obtained,  $X_{\text{final}}$ , was  $3.8 \pm 0.05 \text{ g.L}^{-1}$ . Similarly for *B. subtilis* (1500 rpm, 1 vvm)  $\mu_{\max}$  was  $0.45 \pm 0.01 \text{ h}^{-1}$  and  $X_{\text{final}}$  was  $9.0 \pm 0.06 \text{ g.L}^{-1}$ . Biomass growth kinetics increased with increases in agitation and aeration rates and the implementation of gas blending for control of DOT levels enabled  $\mu_{\max}$  and  $X_{\text{final}}$  values as high as  $0.93 \text{ h}^{-1}$  and  $8.1 \text{ g.L}^{-1}$  respectively to be achieved.

The value of the miniature bioreactor design for high throughput experimentation was further demonstrated when Design of Experiments (DoE) techniques were employed to assess three variables; temperature, pH and inducer concentration, for the optimisation of CHMO expression in *E. coli* TOP10 pQR239. The optimised regression model derived from the results of 20 fermentations concluded that only temperature and inducer concentration had a significant influence, predicting a

maximum specific CHMO activity of 105.9 U.g<sup>-1</sup> at 37.1 °C and 0.11 %w/v. This was in good agreement with the experimentally determined results at these conditions.

In order to enable the predictive scale-up of miniature bioreactor results, the engineering characterisation of the miniature turbine impeller predicted a Power number of 3.5 based on experimental ungasged power consumption measurements. As a result of the numerous literature correlation relating  $k_{La}$ , gassed power per unit volume and superficial gas velocity being designed for much larger scale bioreactors, a similar correlation has been specifically derived for the miniature bioreactor scale. Constant  $k_{La}$  has been shown to be the most reliable basis for predictive scale-up of fermentation results from the miniature bioreactor to conventional laboratory scale. This was confirmed over a range of  $k_{La}$  values (0.04-0.11 s<sup>-1</sup>), with good agreement between final biomass concentrations and maximum specific growth rates. In addition successful scale-up of the DoE results for optimum CHMO expression in *E. coli* at a constant  $k_{La}$  value of 0.04 s<sup>-1</sup> yielded final biomass concentrations of 4.9 g.L<sup>-1</sup> and 5.1 g.L<sup>-1</sup> respectively in the miniature bioreactor and the 2 L vessel, and the CHMO activity obtained was 105.9 U.g<sup>-1</sup> and 105.2 U.g<sup>-1</sup> respectively.

Finally, alternative on-line methods for monitoring cell growth within the miniature bioreactors without the need for repeated sampling have been described. The application of a novel optical density probe for monitoring biomass growth kinetics on-line has shown that comparable results for calculated maximum specific growth rates were obtained from off-line and on-line OD measurements; 0.67 and 0.68 h<sup>-1</sup> respectively. Thermal profiling techniques were also investigated as an alternative means for monitoring cell growth based on the natural heat generated by a microbial culture. Initial results showed that the heat generated during *E. coli* TOP10 pQR239 fermentations followed the same pattern as the off-line growth curve. The maximum specific growth rates calculated from off-line and on-line thermal data were also in good agreement, 0.66 0 ± 0.04 h<sup>-1</sup> and 0.69 0 ± 0.05 h<sup>-1</sup> respectively. In summary the miniature bioreactor system designed and evaluated here provides a useful tool for the rapid optimisation and scale-up of microbial fermentation processes.

# ACKNOWLEDGMENTS

---

---

I would like to thank Professor Gary Lye for his supervision, support and advice during this project. His words of encouragement and praise have allowed me to perform throughout this work with great enthusiasm and content. I wish to express my gratitude to Dr. Mark Appleton for his valuable support and advice throughout this project, and for making my time spent at HEL 'as well as can be expected'!

I would also like to thank all those people within the Department of Biochemical Engineering at UCL (past and present) and HEL who have helped me during my research. In particular I would like to thank Dr. Steve Doig for much practical discussion and advice, Billy Doyle and Ian Buchanan for their invaluable technical support throughout the project. My thanks also go to Keith Habben and Tim Windsor for the mechanical construction of the miniature bioreactor system, Paul Shuttleworth for writing the control and software and Ron Griffiths for all the electronics support.

On a personal level I would like to thank all the members of the Department of Biochemical Engineering with whom I shared the good days and bad days these last four years and who have made my time at UCL most entertaining and enjoyable. In particular I am thankful to Dr. Martina Micheletti, a great friend and mentor, who made time spent in London so memorable. I would also like to express many thanks to all my dear friends Talar, Ida, Priti, Chau, Surj, Priya and Kolya for all the encouragement and priceless memories.

Finally, but most importantly I want to express my deepest gratitude to my parents and brothers, Dilraj and Haran, for all your love and for having faith in me over the years. This would not have been possible without them. I would like to dedicate this thesis to my mum and dad; they have always been my strength and inspiration.

# CONTENTS

---

---

| Section      |   | Page      |
|--------------|---|-----------|
|              | <b>ABSTRACT</b>   | <b>3</b>  |
|              | <b>ACKNOWLEDGEMENTS</b>   | <b>5</b>  |
|              | <b>CONTENTS</b>   | <b>6</b>  |
|              | <b>LIST OF FIGURES</b>  | <b>12</b> |
|              | <b>LIST OF TABLES</b>   | <b>18</b> |
|              | <b>NOMENCLATURE</b>   | <b>21</b> |
|              | <b>ABBREVIATIONS</b>  | <b>24</b> |
| <b>1</b>     | <b>INTRODUCTION</b>   | <b>26</b> |
| <b>1.1</b>   | <b>High Throughput Experimentation (HTE) and Bioprocess Design</b>                                      | <b>26</b> |
| <i>1.1.1</i> | <i>Need for Scale-down Systems</i>  | <i>26</i> |
| <i>1.1.2</i> | <i>Small Scale Bioreactor Systems Available for High Throughput Cell Cultivation</i>                    | <i>29</i> |
| 1.1.2.1      | Shake Flasks  | 29        |
| 1.1.2.2      | Microtitre Plates (MTP's)   | 32        |
| 1.1.2.3      | Miniature Stirred Bioreactors   | 34        |
| <b>1.2</b>   | <b>Scale-up of Microbial Fermentation Processes</b>   | <b>36</b> |
| <i>1.2.1</i> | <i>Predictive Scale-up Techniques</i>   | <i>36</i> |
| <i>1.2.2</i> | <i>Scale-up Concepts</i>  | <i>38</i> |
| <i>1.2.3</i> | <i>Most Commonly Applied Criteria of Scale-up</i>   | <i>41</i> |
| 1.2.3.1      | Constant Volumetric Mass Transfer Coefficient   | 43        |
| 1.2.3.2      | Constant Power per Unit Volume  | 44        |
| 1.2.3.3      | Constant Impeller Tip Speed or Shear Rate   | 45        |
| 1.2.3.4      | Constant Mixing Time  | 45        |
| 1.2.3.5      | Constant Reynolds Number  | 46        |
| 1.2.3.6      | Constant Volumetric Gas Flow Rate per Unit Volume of Liquid (vvm) or Superficial Gas Velocity ( $u_s$ ) | 46        |
| <b>1.3</b>   | <b>On-line Fermentation Monitoring</b>  | <b>47</b> |
| <i>1.3.1</i> | <i>On-line Sensors</i>  | <i>47</i> |
| <i>1.3.2</i> | <i>Calorimetry</i>  | <i>50</i> |
| 1.3.2.1      | Heat as a Quantitative Indicator of Cell Growth and Metabolism  | 50        |
| 1.3.2.2      | Biological Reaction Calorimeters  | 52        |

|            |   |           |
|------------|---|-----------|
| 1.3.2.2.1  | Micro-calorimetry   | 52        |
| 1.3.2.2.2  | Macro-calorimetry   | 54        |
| <b>1.4</b> | <b>Aims of the project</b>  | <b>56</b> |
| <b>2</b>   | <b>MATERIALS AND METHODS</b>  | <b>59</b> |
| <b>2.1</b> | <b>Reagents and Suppliers</b>   | <b>59</b> |
| <b>2.2</b> | <b>Source and Maintenance of Microorganisms</b>                           | <b>59</b> |
| 2.2.1      | <i>Escherichia coli TOP10 pQR239</i>                                      | 59        |
| 2.2.2      | <i>Bacillus subtilis ATCC6633</i>   | 60        |
| <b>2.3</b> | <b>Miniature Bioreactor Design, Instrumentation and Control</b>           | <b>62</b> |
| 2.3.1      | <i>Design of Individual Bioreactors</i>                                   | 62        |
| 2.3.2      | <i>Instrumentation of Individual Bioreactors</i>                          | 64        |
| 2.3.2.1    | Standard On-line Probes   | 64        |
| 2.3.2.2    | Novel Optical Density Probe   | 66        |
| 2.3.2.3    | Thermal Profiling Studies   | 66        |
| 2.3.3      | <i>Design and Control of Parallel Bioreactor Systems</i>                  | 68        |
| <b>2.4</b> | <b>Characterisation of Bioreactor Oxygen Transfer Rates</b>               | <b>71</b> |
| <b>2.5</b> | <b>Characterisation of Bioreactor Power Input</b>                         | <b>71</b> |
| <b>2.6</b> | <b>Demonstration of Parallel Bioreactor Operation and Reproducibility</b> | <b>74</b> |
| 2.6.1      | <i>E.coli TOP10 pQR239 Fermentations</i>                                  | 74        |
| 2.6.1.1    | Inoculum Preparation  | 74        |
| 2.6.1.2    | Miniature Bioreactor Operation  | 74        |
| 2.6.1.3    | Oxygen Enrichment Fermentations   | 75        |
| 2.6.2      | <i>B. subtilis ATCC6633 Fermentation</i>                                  | 75        |
| 2.6.2.1    | Inoculum Preparation  | 75        |
| 2.6.2.2    | Miniature Bioreactor Fermentation Operation                               | 75        |
| <b>2.7</b> | <b>Fermentation Optimisation using Design of Experiments</b>              | <b>76</b> |
| 2.7.1      | <i>Design of Experiments (DOE)</i>  | 76        |
| 2.7.2      | <i>Fermentation Operation and CHMO Induction</i>                          | 77        |
| <b>2.8</b> | <b>Scale-up of Miniature Bioreactor Fermentations</b>                     | <b>78</b> |
| 2.8.1      | <i>Miniature Bioreactor Fermentations</i>                                 | 78        |
| 2.8.2      | <i>2 L Laboratory Scale Bioreactor</i>                                    | 78        |
| 2.8.2.1    | Bioreactor Design and Instrumentation                                     | 78        |



|              |  |            |
|--------------|--|------------|
| 2.8.2.2      | Bioreactor Operation at Matched $P_g/V$ and $k_L a$                                  | 79         |
| 2.8.2.3      | Scale-up of DOE Optimised Fermentation Conditions                                    | 79         |
| <b>2.9</b>   | <b>Analytical Techniques</b>   | <b>80</b>  |
| <b>2.9.1</b> | <b><i>Biomass Quantification</i></b>   | <b>80</b>  |
| 2.9.1.1      | Dry Cell Weight (DCW) Measurement  | 80         |
| 2.9.1.2      | Optical Density (OD) Measurement   | 80         |
| <b>2.9.2</b> | <b><i>Spectrophotometric Measurement of CHMO Activity</i></b>                        | <b>81</b>  |
| 2.9.2.1      | Preparation of Crude Cell Extract  | 81         |
| 2.9.2.2      | NADPH Linked Spectrophotometric Assay  | 81         |
| <b>3</b>     | <b>MINIATURE BIOREACTOR DESIGN AND EVALUATION</b>                                    | <b>83</b>  |
| <b>3.1</b>   | <b>Introduction and Aims</b>   | <b>83</b>  |
| <b>3.2</b>   | <b>Miniature Bioreactor Design, Operation and Control</b>                            | <b>84</b>  |
| <b>3.3</b>   | <b>Characterisation of Bioreactor Oxygen Transfer Capability</b>                     | <b>86</b>  |
| <b>3.4</b>   | <b>Parallel Batch Fermentation Kinetics</b>  | <b>91</b>  |
| 3.4.1        | <i>Reproducibility of Parallel E. coli Fermentations</i>                             | 91         |
| 3.4.2        | <i>Reproducibility of Parallel B. subtilis Fermentations</i>                         | 95         |
| <b>3.5</b>   | <b>Influence of Agitation and Aeration Conditions on <i>E.coli</i> Fermentations</b> | <b>99</b>  |
| <b>3.6</b>   | <b>Comparison with Other Miniature Bioreactors</b>                                   | <b>102</b> |
| <b>3.7</b>   | <b>Discussion</b>  | <b>105</b> |
| <b>4</b>     | <b>APPLICATION TO FERMENTATION PROCESS OPTIMISATION</b>                              | <b>107</b> |
| <b>4.1</b>   | <b>Introduction and Aims</b>   | <b>107</b> |
| 4.1.1        | <i>Statistical Design of Experiments (DoE)</i>                                       | 107        |
| 4.1.2        | <i>Model System and Aims</i>   | 109        |
| <b>4.2</b>   | <b>Initial Evaluation of Cell Growth and Enzyme Expression</b>                       | <b>110</b> |

|          |   |            |
|----------|---|------------|
| 4.3      | <b>Optimisation of Enzyme Expression: Selection of Variables and Ranges</b>                       | 112        |
| 4.4      | <b>DoE Results, Model Formulation and Optimisation</b>  | 116        |
| 4.4.1    | <i>DoE Results and Modelling</i>  | 116        |
| 4.4.2    | <i>Response Variable: Biomass Concentration</i>   | 116        |
| 4.4.3    | <i>Response Variable: CHMO Activity</i>   | 118        |
| 4.4.4    | <i>Analysis and Verification of Optimisation Model</i>  | 122        |
| 4.5      | <b>Response Surface Plot: Optimisation of Enzyme Expression</b>                                   | 125        |
| 4.5.1    | <i>Response Variable: Biomass Concentration</i>   | 125        |
| 4.5.2    | <i>Response Variable: CHMO Activity</i>   | 125        |
| 4.6      | <b>Discussion</b>   | 127        |
| <b>5</b> | <b>SCALE-UP OF MINIATURE BIOREACTOR PERFORMANCE</b>   | <b>130</b> |
| 5.1      | <b>Introduction and Aims</b>  | 130        |
| 5.2      | <b>Power Characteristics of the Miniature Turbine Impeller</b>                                    | 131        |
| 5.2.1    | <i>Variation of <math>P_g/P_{ug}</math> Ratio with Flow Number</i>                                | 135        |
| 5.3      | <b>Correlation of Miniature Bioreactor Energy Dissipation Rates</b>                               | 138        |
| 5.4      | <b>Correlation of Miniature Bioreactor <math>k_L a</math> Values</b>                              | 141        |
| 5.5      | <b>Fermentation Scale Translation at Matched <math>P_g/V</math> and <math>k_L a</math> Values</b> | 145        |
| 5.5.1    | <i>Scale-up Based on Constant <math>P_g/V</math></i>  | 145        |
| 5.5.2    | <i>Scale-up Based on Constant <math>k_L a</math></i>  | 148        |
| 5.6      | <b>Scale-up of Optimised Conditions for Cell Growth and Enzyme Expression</b>                     | 148        |
| 5.7      | <b>Discussion</b>   | 153        |
| <b>6</b> | <b>IN-SITU MONITORING OF CELL GROWTH DURING PARALLEL BIOREACTOR</b>                               | <b>156</b> |

|              |   |            |
|--------------|---|------------|
|              | <b>OPERATION</b>  |            |
| 6.1          | <b>Introduction and Aims</b>  | <b>156</b> |
| 6.2          | <b><i>In-situ</i> Optical Density Measurements</b>  | <b>157</b> |
| 6.3          | <b><i>In-situ</i> Culture Heat Generation Measurements</b>  | <b>161</b> |
| 6.3.1        | <b><i>Thermal Profiling of Cell Growth</i></b>  | <b>161</b> |
| 6.3.2        | <b><i>Analysis of the Thermal Profiling Results during E.coli TOP10 pQR239 Fermentations</i></b>  | <b>162</b> |
| 6.4          | <b>Discussion</b>   | <b>164</b> |
| 7            | <b>CONCLUSIONS AND FUTURE WORK</b>  | <b>168</b> |
| 7.1          | <b>Conclusions</b>  | <b>168</b> |
| 7.2          | <b>Future Work</b>  | <b>170</b> |
| 8            | <b>REFERENCES</b>   | <b>173</b> |
| Appendix I   | <b>COMMERCIAL EVALUATION, DESIGN AND VALIDATION OF A PARALLEL MINIATURE BIOREACTOR SYSTEM FOR USE IN THE BIOTECHNOLOGY-BASED INDUSTRIES</b> | <b>194</b> |
| A.I.1        | <b>Initial Market Survey</b>  | <b>194</b> |
| A.I.2        | <b>Required Features for Bioreactor Design and Operation</b>  | <b>199</b> |
| A.I.3        | <b>Validation of Prototype Bioreactor Design</b>  | <b>200</b> |
| Appendix II  | <b>MECHANICAL DRAWINGS OF THE MINIATURE BIOREACTOR SYSTEM</b>   | <b>203</b> |
| Appendix III | <b>CALIBRATION OF OFF-LINE OD<sub>600</sub> MEASUREMENTS WITH BIOMASS DRY CELL WEIGHT</b>   | <b>211</b> |
| Appendix IV  | <b>QUANTIFICATION OF INTRACELLULAR CHMO ACTIVITY BASED ON THE SPECTROPHOTOMETRIC ASSAY</b>  | <b>212</b> |

|                          |   |            |
|--------------------------|---|------------|
| <b>Appendix<br/>V</b>    | <b>K<sub>L</sub>A DETERMINATION BASED ON THE<br/>FERMENTATION KINETICS OF A TYPICAL <i>B.</i><br/><i>SUBTILIS</i> ATCC6633 FERMENTATION</b> | <b>214</b> |
| <b>Appendix<br/>VI</b>   | <b>DERIVATION OF THE PARAMETERS FOR THE<br/>MINIATURE BIOREACTOR K<sub>L</sub>A CORRELATION</b>   | <b>216</b> |
| <b>Appendix<br/>VII</b>  | <b>QUANTIFICATION OF REQUESTED HEATER POWER<br/>USING A PT100 CALIBRATION HEATER</b>  | <b>219</b> |
| <b>Appendix<br/>VIII</b> | <b>ENGD PROFORMAS</b>   | <b>221</b> |

# LIST OF FIGURES

---

---

- Figure 1.1.** Comparison of the degree of experimental throughput and information available over a range of scales for a variety of cultivation systems. Figure reproduced from Doig *et al.*, (2006).
- Figure 1.2.** Comparison of the time required to prepare four bioreactors in parallel at three different scales.
- Figure 1.3.** The scale-up window defining the operating boundaries for aeration and agitation for the scale-up of fermentation conditions. Figure adapted from Lilly (1983).
- Figure 2.1.** Mechanical drawing showing key design features and dimensions of an individual miniature bioreactor: (A) cross section through bioreactor; (B) plan view of head plate.
- Figure 2.2.** Miniature probes for continuous on-line monitoring of each bioreactor: (A) thermocouple; (B) pH probe; (C) dissolved oxygen probe; (D) optical density probe.
- Figure 2.3.** Schematic diagram of *in-situ* optical density probe: (A) dimensions of probe; (B) arrangement of light source and detectors.
- Figure 2.4.** Photograph of prototype four-pot miniature bioreactor system
- Figure 2.5.** Main features of the WinBio software showing: (A) simultaneous display of all four individual bioreactor supervisory windows; (B) an example of an experimental plan and the various terminating conditions; (C) real time interactive graphs showing culture progress
- Figure 2.6.** Mechanical drawing showing key design features and dimensions of a single miniature bioreactor and the novel magnetically driven turbine impeller design.
- Figure 3.1.** Results from a typical sterile hold test, which involved sterilising a miniature bioreactor containing 100 mL of growth media. The bioreactor was then agitated at 1000 rpm and aerated at 1 vmm for a period of four days with continuous on-line measurement of dissolved oxygen tension, pH, temperature and optical density: (–) DOT; (□) pH; (o) temperature and (- - -) OD.
- Figure 3.2.** Controller response for pH and temperature during a typical *E.coli* TOP10 pQR239 fermentation. (A) pH was controlled at a set point value of  $7 \pm 0.1$  by metered addition of acid and base: measured pH of fermentation broth (----); volume of base added (-); volume of acid added (.....). (B) Temperature was controlled at a set point

value of  $37^{\circ}\text{C} \pm 0.2$  by the automatic adjustment of the electrical heater: measured temperature of fermentation broth (-); requested power of the electrical heater required to maintain set point temperature (---).

**Figure 3.3.** Influence of bioreactor operating conditions on oxygen uptake kinetics during dynamic gassing out experiments. From left to right: (— -- —) 2000 rpm, 2 vvm; (— - —) 2000 rpm, 1vvm; (---) 1500 rpm, 1vvm; (— —) 1000 rpm, 2 vvm; (—) 1000 rpm, 1.5 vvm; (——) 1000 rpm, 1 vvm.

**Figure 3.4.** Bioreactor oxygen mass transfer coefficient ( $k_{La}$ ) as a function of stirrer speed and aeration rate for aeration with atmospheric air: (◆) 1 vvm; (■) 1.5 vvm; (▲) 2 vvm. Values of  $k_{La}$  calculated from the dynamic gassing out data shown in Figure 3.3 using Equation 2.1.

**Figure 3.5.** Parallel batch fermentation kinetics of *E. coli* TOP10 pQR239 grown under identical conditions: (■) biomass concentration; (-) DOT. Experiments performed at 1000 rpm and aerated with 1 vvm atmospheric air. B1 – B4 refer to bioreactors one to four respectively.

**Figure 3.6.** Parallel batch fermentation kinetics of *B. subtilis* ATCC6633 grown under identical conditions: (■) biomass concentration; (-) DOT. Experiments performed at 1500 rpm and aerated with 1 vvm atmospheric air. B1 – B4 refer to bioreactors one to four respectively.

**Figure 3.7.** Influence of agitation and aeration rates on batch fermentation kinetics of *E. coli* TOP10 pQR239: (■) biomass concentration; (-) DOT. Experimental conditions: (A) 2000 rpm, 1 vvm; (B) 1000 rpm, 2 vvm.

**Figure 3.8.** Influence of oxygen enrichment on batch fermentation kinetics of *E. coli* TOP10 pQR239: (■) biomass concentration; (-) DOT. Experimental conditions: (A) 2000 rpm, 1 vvm and DOT controlled at 30%; (B) 2000 rpm, 1 vvm and DOT controlled at 50%.

**Figure 4.1.** The reaction scheme for the CHMO catalysed bioconversion studied in this work.

**Figure 4.2.** Results from a typical 100 mL *E. coli* TOP10 pQR239 fermentation at pH 7,  $37^{\circ}\text{C}$  and induced with 0.1 % w/v L-arabinose. (A) Cell growth and volumetric CHMO activity versus time: (■) biomass concentration; (◆) specific CHMO activity. (B) Online measurement of pH, temperature and DOT: (- -) pH; (-) temperature; (-) DOT.

**Figure 4.3.** CCF design region using three variables can be modelled on a cube to represent the experimental region being explored. Each corner of the cube represents a combination of the factors used in an experiment, with additional points at the centres of the faces to

approximate a sphere. A centre point is included and in this case has been replicated six times to determine reproducibility and detect non-linear responses.

- Figure 4.4.** Coefficient plot with confidence intervals (set at 95%) for biomass concentration. The size of each bar (or coefficient) represents the relative importance upon *E.coli* cell growth.
- Figure 4.5.** Coefficient plot with confidence intervals (set at 95%) for CHMO activity. The size of each bar (or coefficient) represents the relative importance upon *E.coli* cell growth.
- Figure 4.6.** Coefficient plot for final optimisation model for CHMO activity, complete with confidence intervals (set at 95%) for CHMO activity ( $Y$  transformed as  $Y^2$ ). The original model consisted of 9 terms. However terms whose confidence intervals included the value zero were deemed insignificant and so were removed in a hierarchical manner.
- Figure 4.7.** Parity plot of experimental and predicted CHMO activities used to produce the regression model. Experimental values taken from experiments described in Table 4.1. Predicted values calculated from refined regression model, Equation 4.2.
- Figure 4.8.** Response surface plot showing variation of expressed CHMO activity and the strong interaction effects between temperature and L-arabinose concentration. Response surface generated based on the data in Table 4.1 and using Equation 4.2.
- Figure 5.1.** Ungassed and gassed power requirements of the miniature turbine impeller over a range of agitation rates: (♦)ungassed power; gassed power with aerating at (□) 1 vvm, (▲) 1.5 vvm and (○) 2 vvm.
- Figure 5.2.** Variation of the measured Power number with increasing Reynolds number for the miniature turbine impeller: (A) in water; (B) in clarified fermentation broth.
- Figure 5.3.** Comparison of the ratio of gassed/ungassed power,  $P_g/P_{ug}$ , against Flow number for the miniature bioreactor and the results reported by Hall *et al.* (2005) for a miniature reactor with a 0.045m vessel diameter. Miniature bioreactor aeration rates: (■) 1 vvm, (▲) 1.5 vvm and (●) 2 vvm. Hall *et al.* (2005) miniature reactor aeration rate of 0.5 vvm: (×) sparger positioned beneath the impeller axis; (◇) sparger positioned away from the impeller.
- Figure 5.4.** Parity plot comparing the measured  $P_g/V$  at an aeration rate of 1.5 vvm, with those predicted from the most commonly reported literature correlations: (□) Hughmark (1980); (▲) Michel and Miller (1962); (x) Cui et al. (1996); (◇) Luong and Volesky (1979); (●) Mockel et al. (1990). Experimental measurements as shown in Figure 5.1. Correlations as described in Table 5.1.

- Figure 5.5.** Comparison of the experimentally determined  $k_{La}$  values at an aeration rate of 1 vvm, with those predicted from the miniature bioreactor correlation and various literature correlations (Table 5.2): (◆) Measured values; (—) miniature bioreactor correlation; (—) van't Riet (1979); (—) Vilaca *et al.* (2000); (— - - —) Linek *et al.* (2004); (—) Smith *et al.* (1977); (----) Zhu (2001). Experimental  $k_{La}$  values taken from Figure 3.4.
- Figure 5.6.** Comparison of growth and DOT profiles for batch *E. coli* TOP10 pQR239 fermentations carried out at matched  $P_g/V$  at miniature (100 mL) and conventional laboratory bioreactor (1.5 L) scales: (A)  $P_g/V = 657 \text{ W.m}^{-3}$ ; (B)  $P_g/V = 1487 \text{ W.m}^{-3}$ ; (C)  $P_g/V = 2960 \text{ W.m}^{-3}$ . Miniature bioreactor: (■) cell density, (—) DOT; laboratory bioreactor: (○) cell density, (---) DOT. Matched  $P_g/V$  operating conditions as described in Table 5.3.
- Figure 5.7.** Comparison of growth and DOT profiles for batch *E. coli* TOP10 pQR239 fermentations carried out at matched  $k_{La}$  at miniature (100 mL) and conventional laboratory bioreactor (1.5 L) scales: (A)  $k_{La} = 0.06 \text{ s}^{-1}$ ; (B)  $k_{La} = 0.08 \text{ s}^{-1}$ ; (C)  $k_{La} = 0.11 \text{ s}^{-1}$ . Miniature bioreactor: (■) cell density, (—) DOT; laboratory bioreactor: (○) cell density, (---) DOT.
- Figure 5.8.** The optimum fermentation conditions for enzyme expression in *E. coli* TOP10 pQR239 derived from the DOE investigation in Section 4.5.2 were scaled-up to the 2 L bioreactor based on a constant  $k_{La}$  value of  $0.04 \text{ s}^{-1}$ : (■) cell density, (—) DOT, (○) specific CHMO activity. Dashed line represents time point used in original DoE experiments with miniature bioreactor (chapter 4).
- Figure 6.1.** On-line measurement of optical density in *E. coli* TOP10 pQR239 fermentations. (A) Comparison of the off-line OD and uncalibrated voltage output of the OD probe. (B) Comparison of off-line and calibrated on-line biomass growth kinetics from an individual fermentation: (■) off-line optical density; (—) on-line optical density.
- Figure 6.2.** Parity plot of on-line and off-line optical density data from nine identical fermentations. Linear Regression gives an  $R^2$  value of 0.96. Experiments performed at 1000 rpm and 1 vvm.
- Figure 6.3.** On-line heat measurements during a typical *E. coli* TOP10 pQR239 fermentation. (A) On-line dissolved oxygen profile and the power supplied by the heater to maintain the fermentation temperature at  $37 \text{ }^\circ\text{C}$ : (○) DOT; (-) heater power. (B) Comparison of biomass growth kinetics from off-line  $\text{OD}_{600}$  measurements and the heat generation: (■) biomass concentration; (-) heat generation.
- Figure 6.4.** Comparison of biomass growth kinetics from a typical *E. coli* TOP10 pQR239 fermentation, off-line  $\text{OD}_{600}$  measurements and the integrated heat generation curve: (■) biomass concentration; (-) integrated heat curve.



- Figure A.I.1.** Market survey questionnaire distributed to individuals in several pharmaceutical companies involved in fermentation processes. .
- Figure A.I.2.** Temperature mapping and pressure tests for *in-situ* sterilisation of the miniature bioreactor without an external steam supply: (■) pressure, (Δ) temperature of the reactor contents, (x) headspace temperature.
- Figure A.II.1.** Design and dimensions of miniature bioreactor glass vessel.
- Figure A.II.2.** Design and dimensions of the four equally spaced removable baffles.
- Figure A.II.3.** Design and dimensions of the miniature bioreactor headplate, detailing the positions and sizes of the various ports
- Figure A.II.4** Design and dimensions of the multiport fitting that screws into the bioreactor headplate. Up to five additions can be made using sterile hypodermic needles via a self-sealing septum. The centre of the multiport consists of a long hollow tube which functions as a sampling tube.
- Figure A.II.5.** Design and dimensions of the magnetically driven, miniature six-blade turbine impeller. The impeller has been designed to incorporate a flat disk at the end of the impeller drive shaft, this disc housed a total of eight cylindrical magnets
- Figure A.II.6.** Design and dimensions of the hollow stirrer shaft, which also functions as a thermowell to hold the thermocouple. The miniature turbine impeller is mounted on the bottom half of the shaft and held in place with a nut. The top of the stirrer shaft is fitted with an o-ring and screws into the underside of the bioreactor headplate.
- Figure A.II.7.** Design and dimensions of the full length sparger tube. The tube is bent at right angles approximately 22 mm from the end to fit into the miniature bioreactor vessel. It is then fitted with a 15 μm stainless steel sinter. The top of the sparger tube is fitted with an o-ring and screws into the underside of the bioreactor headplate.
- Figure A.II.8.** Design and dimensions of the off-gas condenser fitted onto the gas outlet port of the bioreactor headplate. Cooling was achieved using a chilled water supply.
- Figure A.III.1.** Calibration curve of off-line OD<sub>600</sub> measurements from *E.coli* TOP10 pQR239 fermentation with DCW measurements.
- Figure A.IV.1.** Example of the background absorbance change with time and the absorbance change with time after addition of the cyclohexanone substrate for a typical spectrophotometric assay of CHMO in a clarified *E.coli* TOP10 pQR239 lysate.
- Figure A.V.1.** Determination of  $k_{La}$  value based on fermentation data from a

typical *B.subtilis* fermentation as shown in Figure 3.5 (B2). Linear least square fitting gave an  $R^2$  value of 0.958.

**Figure A.VI.1.** Determination of exponents  $\alpha$  and  $\beta$ : (A) constant aeration rate of 2 vvm, gradient gives  $\alpha$ ; (B) constant agitation rate of 2000 rpm, gradient gives  $\beta$ .

**Figure A.VII.1.** Calibration of the requested power of the electrical heater (-) used for controlling the temperature of the miniature bioreactor. A known quantity of power was introduced to the vessel using a calibration heater (---).

# LIST OF TABLES

---

---

- Table 1.1.** Comparison of miniature bioreactor systems that have recently been reported for parallel operation. The table shows key design features and operating characteristics. Quoted working volumes, number of parallel units and stirrer speeds indicate maximum reported values. Nomenclature: T = temperature, DOT = dissolved oxygen, OD = optical density, N/A = not applicable, N/R = not reported.
- Table 1.2.** Process parameter and coefficients implicated in mixing, aeration and oxygen transfer that are a suitable as scale-up variables to be kept constant alone or in combination with each other or other process relevant variables (Schmidt, 2005).
- Table 1.3.** Most frequently used on-line monitoring techniques currently available for cell cultures.
- Table 1.4.** Comparison of the various published work that used biocalorimetry as a tool for continuous on-line monitoring. Table shows the various types of modified calorimeter devices used, quoted working volumes, microorganisms investigated and heat production. N/R – not reported.
- Table 2.1.** Composition of the growth medium used in all *E.coli* TOP10 pQR239 fermentations.
- Table 2.2.** Composition of the growth medium used in all *B. subtilis* ATCC6633 fermentations.
- Table 3.2.** Reproducibility of batch *B. subtilis* ATCC6633 fermentation kinetics from four parallel fermentations. Kinetic parameters derived from the fermentation profiles shown in Figure 3.6. B1-B4 refer to bioreactors one to four respectively, while  $B_{AV}$  indicates the mean values of the kinetic parameters.
- Table 3.1.** Reproducibility of batch *E. coli* TOP10 pQR239 fermentation kinetics from four parallel fermentations. Kinetic parameters derived from the fermentation profiles shown in Figure 3.5. B1-B4 refer to bioreactors one to four respectively, while  $B_{AV}$  indicates the mean values of the kinetic parameters.
- Table 3.3.** Variation of bioreactor oxygen mass transfer coefficient and *E. coli* TOP10 pQR239 fermentation kinetics as a function of agitation and aeration conditions including the use of oxygen enrichment to control DOT levels. (A1) and (B1) correspond to the fermentation profiles shown in Figure 3.7; (A2) and (B2) correspond to the

fermentation profiles shown in Figure 3.8.

- Table 4.1.** Central Composite Face (CCF) design matrix of uncoded independent variables for the optimisation of CHMO expression in miniature bioreactor experiments. Table also shows the corresponding biomass concentration results and, experimental and predicted CHMO activities. Experiments performed as described in Section 2.7.2. Experimental measurements were 420 minutes after induction. Predicted CHMO activity values based on Equation 4.2.
- Table 4.2.** Estimated regression coefficients of the reduced optimisation model (Equation 4.1) for CHMO expression. The corresponding p-values and confidence intervals are also shown.  $X_1$  = temperature and  $X_2$  = L-arabinose concentration.
- Table 4.3.** ANOVA results for analysis of the reduced optimisation model (Equation 4.2) for CHMO expression. Model terms as described in Table 4.2.
- Table 5.1.** Comparison of the most commonly reported gassed to un-gassed power ( $P_g/P_{ug}$ ) correlations for smaller scale vessels.
- Table 5.2.** Comparison of the most commonly reported correlations relating  $k_{La}$  to gassed power per unit volume and superficial gas velocity. NR: Figures not reported as a variety of previously published data was analysed, vessel volumes ranged from 0.002 -2.6 m<sup>3</sup>.
- Table 5.3.** Summary of batch *E. coli* TOP10 pQR239 fermentations carried out in miniature and conventional laboratory bioreactors using constant  $P_g/V$  as a basis for scale translation. Kinetic parameters derived from data in Figure 5.6.
- Table 5.4.** Summary of batch *E. coli* TOP10 pQR239 fermentations carried out in miniature and conventional laboratory bioreactors using constant  $k_{La}$  as a basis for scale translation. Kinetic parameters derived from data in Figure 5.7.
- Table 5.5.** Comparison of the optimum fermentation conditions for enzyme expression in *E.coli* TOP10 pQR239 derived from the DOE investigation in Section 4.5.2 and corresponding conditions in the 2 L bioreactor for scale-up on the basis of constant  $k_{La}$ .
- Table A.I.1.** Comparison of miniature bioreactor systems that are commercially available for parallel operation. Table shows key design features and operating characteristics. Quoted working volumes, number of parallel units and range of agitation rates reported. Nomenclature: T = temperature, DOT = dissolved oxygen, OD = optical density, Agt = agitation rate, Ant = antifoam, OUR = oxygen uptake rate, CER = carbon dioxide excretion rate, RQ = respiratory quotient. All information last updated 01.08.06.
- Table A.I.2.** Results from the initial market survey questionnaire from Figure

A.I.1. Nomenclature: T = temperature, DOT = dissolved oxygen, OD = optical density, Agt = agitation rate, Ant = antifoam, OUR = oxygen uptake rate, CER = carbon dioxide evolution rate, RQ = respiratory quotient, G = residual glucose, Lp = residual lipid/ phosphates, F = feed, Agt = agitation rate.

# NOMENCLATURE

---

---

|            |  |
|------------|--|
| $A$        | Area ( $\text{m}^2$ )  |
| $A_{340}$  | Absorbance at 340 nm   |
| $b_t$      | Impeller blade thickness (m)   |
| $C$        | Constant   |
| $c$        | NADPH concentration in cuvette ( $\mu\text{molml}^{-1}$ )                        |
| $C_L$      | Actual liquid phase oxygen concentration ( $\text{kgm}^{-3}$ )                   |
| $C_p$      | Normalised oxygen concentration ( $\text{kg.m}^{-3}$ )                           |
| $C^*$      | Saturated dissolved oxygen concentration ( $\text{kg.m}^{-3}$ )                  |
| $d_B$      | Width of baffle (mm)   |
| $d_i$      | Diameter of impeller (mm)  |
| $d_T$      | Diameter of vessel (mm)  |
| $DOT$      | Dissolved oxygen tension (%)   |
| $F$        | Force (N)  |
| $Fl$       | Flow number  |
| $g$        | Acceleration of gravity ( $\text{m.s}^{-2}$ )                                    |
| $g_{DCW}$  | Grams of dry cell weight   |
| $h_i$      | Distance between centre line of impeller and base of vessel (mm)                 |
| $h_T$      | Height of the vessel (mm)  |
| $k_La$     | Volumetric oxygen mass transfer coefficient ( $\text{s}^{-1}$ )                  |
| $l$        | Light path length (cm)   |
| $m_{O_2}$  | Oxygen required for cell maintenance ( $\text{mol.g}_{DCW}^{-1}.\text{h}^{-1}$ ) |
| $N$        | Impeller speed ( $\text{s}^{-1}$ )   |
| $N_P$      | Power number   |
| $N_{CD}$   | Minimum agitation rate for complete dispersion ( $\text{s}^{-1}$ )               |
| $OD_{600}$ | optical density at 600 nm  |
| $OTR$      | oxygen transfer rate ( $\text{mmol.L}^{-1}.\text{h}^{-1}$ )                      |
| $OUR$      | oxygen uptake rate ( $\text{mmol.L}^{-1}.\text{h}^{-1}$ )                        |
| $P$        | Power input (W)  |
| $P_g$      | Gassed power requirement of the STR (W)  |
| $P_{ug}$   | Ungassed power requirement of the STR (W)  |
| $P_{ch}$   | Power of the heater (W)  |
| $Q_g$      | Volumetric gas flow rate aeration rate ( $\text{m}^3\text{s}^{-1}$ )             |

|                                      |   |
|--------------------------------------|---|
| $R$                                  | Length of the arm pressing against the force sensor (m)                             |
| $Re$                                 | Reynolds number   |
| $Re_i$                               | Impeller Reynolds number  |
| $R_{ch}$                             | Resistance of the calibration of heater ( $\Omega$ )                                |
| $SS_{resid}$                         | Residual sum of squares   |
| $SS_{lof}$                           | Lack of fit sum of squares  |
| $SS_{pe}$                            | Pure error sum of squares   |
| $t$                                  | Time (s)  |
| $t_m$                                | Mass transfer time, $1/k_L a$ (s)   |
| $T_m$                                | Mixing time (s)   |
| $t_{DOT}$                            | Time at which the DOT falls to zero (min)   |
| $U$                                  | Units of enzyme activity ( $\mu\text{molmin}^{-1}$ )                                |
| $u_S$                                | Superficial gas velocity ( $\text{m}\cdot\text{s}^{-1}$ )                           |
| $V$                                  | Volume (L)  |
| $V_{ch}$                             | Voltage (V)   |
| $W$                                  | Impeller blade width (m)  |
| $X$                                  | Biomass concentration ( $\text{g}_{\text{DCW}}\cdot\text{L}^{-1}$ )                 |
| $X_{final}$                          | Final biomass concentration ( $\text{g}_{\text{DCW}}\cdot\text{L}^{-1}$ )           |
| $x_i$                                | Dimensionless value of an independent variable (here $i$ is the predicted response) |
| $X_i$                                | Real value of an independent variable   |
| $\bar{X}_i$                          | Real value of an independent variable at the centre point                           |
| $\Delta X_i$                         | Step change value   |
| $Y_i$                                | Dependent variables or response   |
| $Y_{XO_2}$                           | Yield of biomass on oxygen ( $\text{g}\cdot\text{mol}^{-1}$ )                       |
| $Z$                                  | Constant, depends on the number of stirrers for Mockel et al. (1990)                |
| $\alpha, \beta$                      | Exponents   |
| $\beta_0$                            | Offset term   |
| $\beta_1, \beta_2, \beta_3$          | Linear effects  |
| $\beta_{11}, \beta_{22}, \beta_{33}$ | Squared effects   |
| $\beta_{12}, \beta_{13}, \beta_{23}$ | Interaction terms   |
| $\varepsilon$                        | Extinction coefficient ( $\text{ml}\mu\text{mol}^{-1}\text{cm}^{-1}$ )              |
| $\rho$                               | Density ( $\text{kg}\cdot\text{m}^{-3}$ )   |
| $\mu_{\max}$                         | Maximum specific growth rate ( $\text{h}^{-1}$ )                                    |
| $\mu$                                | Specific growth rate ( $\text{h}^{-1}$ )  |
| $\mu_v$                              | Viscosity   |
| $\omega$                             | Angular velocity ( $\text{s}^{-1}$ )  |

|                  |   |
|------------------|---|
| $\sigma$         | Air-liquid surface tension ( $\text{N}\cdot\text{m}^{-1}$ ) |
| $\tau_p$         | Probe response time (s)                                     |
| $u_{\text{tip}}$ | Tip speed ( $\text{m}\cdot\text{s}^{-1}$ )                  |



# ABBREVIATIONS

---

---

|                   |   |
|-------------------|---|
| Agt               | Agitation rate  |
| ANOVA             | Analysis of variance                                  |
| Ant               | Antifoam  |
| Arab              | L-arabinose   |
| Are               | Aeration rate   |
| CCF               | Central composite face design                         |
| CER               | Carbon dioxide evolution rate                         |
| CHMO              | Cyclohexanone monooxygenase                           |
| D1                | Detector 1  |
| D2                | Detector 2  |
| DCW               | Dry cell weight                                       |
| DoE               | Design of experiments                                 |
| DOT               | Dissolved oxygen tension                              |
| F                 | Feed  |
| G                 | Residual glucose                                      |
| HTE               | High throughput experimentation                       |
| LED               | Light emitting diode                                  |
| Lp                | Residual lipid/phosphates                             |
| LS                | Light source  |
| MTP               | Microtitre plates                                     |
| NADPH             | Nicotinamide adenine dinucleotide phosphate (reduced) |
| N/R               | Not reported  |
| OD                | Optical density                                       |
| OD <sub>600</sub> | Optical density at 600 nm                             |
| OFAT              | One factor at a time                                  |
| PEEK              | Poly-ether ether ketone                               |
| PID               | Proportional integral derivative control              |

|                     |   |
|---------------------|---|
| PWM                 | Pulse width modulation                                    |
| $Q^2$               | Fraction of the response variation predicted by the model |
| $R^2$               | Fraction of the response variation explained by the model |
| RO                  | Reverse osmosis   |
| rpm                 | Revolutions per minute                                    |
| RQ                  | Respiratory quotient                                      |
| RSM                 | Response surface methodology                              |
| SIP                 | Sterilisation in place                                    |
| $SS_{\text{lof}}$   | Lack of fit sum of squares                                |
| $SS_{\text{pe}}$    | Pure error sum of squares                                 |
| $SS_{\text{resid}}$ | Residual sum of squares                                   |
| StSt                | Stainless steel   |
| STR                 | Stirred tank reactor                                      |
| T                   | Temperature   |
| Temp                | Temperature   |
| vvm                 | Volumetric air flow per volume of broth per minute        |
| v/v                 | Volume per unit volume                                    |
| w/v                 | Weight per unit volume                                    |

# 1. INTRODUCTION

---

---

## 1.1 High Throughput Experimentation (HTE) and Bioprocess Design

### 1.1.1. *Need for Scale-down Systems*

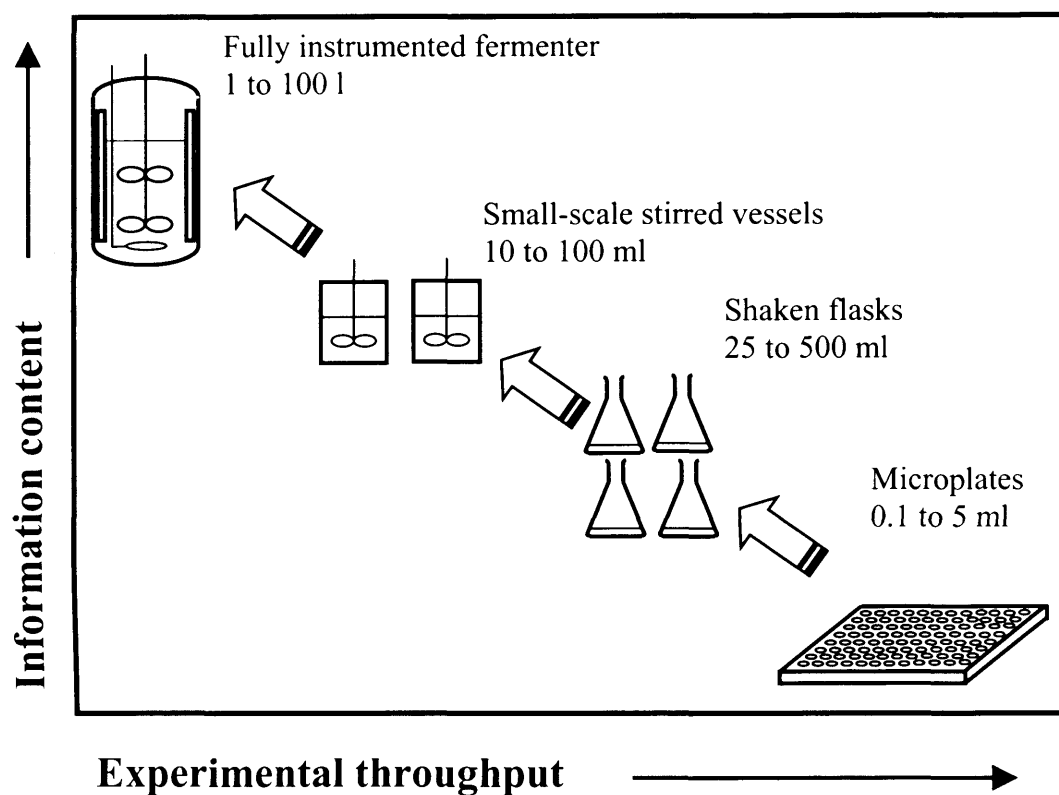
The design and optimisation of industrial fermentation processes generally involves four key stages, including: (i) identification of a strain that produces the product of interest, (ii) strain enhancement, (iii) process optimisation and (iv) scale-up (Doig *et al.*, 2006). Having identified a small number of the most promising strains based on simple screens for product yield or activity, productivity is further enhanced using readily available genetic and metabolic engineering techniques (Puskeiler *et al.*, 2005a). Such advances in metabolic engineering and protein evolution techniques make feasible the rapid creation of large libraries of recombinant microorganisms (Hibbert *et al.*, 2005) that need to be evaluated. The initial design and optimisation of such a process requires the experimental investigation of many interacting biological and physical variables. Optimisation of the chosen strains leads to further investigation of culture medium composition, nutrient feeding regimes and physical variables such as temperature, pH and dissolved oxygen levels. This requires a large number of experiments to be performed because of the number of experimental variables requiring investigation per strain. Even with the aid of statistical process design the total number of experiments required would generally not reduce to less than 100 (Freyer *et al.*, 2004). Finally, once a production strain is identified, further experimental investigation over a range of scales is necessary to establish the operating boundaries and robustness of the process for validation purposes (Doig *et al.*, 2006). At this stage virtually all processes would be performed in stirred bioreactors because of the dominance of this design in the chemical and biopharmaceutical sectors.

The use of traditional laboratory bioreactors for the initial stages of development is not practical or cost effective given the large number of experiments required. However, the use of small scale bioreactor systems and high throughput methodologies is now proving to be an effective tool for bioprocess development. Systems that enable parallel and automated operation of several fermentations simultaneously have the potential to increase the rate at which the necessary experiments are performed allowing reduced development times (Lye *et al.*, 2003; Kumar *et al.*, 2004; Fernandes and Cabral, 2006). This approach also provides significant reduction in labour intensity, cost for media components and has less space requirements as compared to the use of conventional bioreactors (Lye *et al.*, 2003; Kumar *et al.*, 2004; Betts and Baganz, 2006).

In recent years various types of parallel bioreactor systems have been reported e.g. shake flasks, microtitre plates (MTPs), stirred miniature bioreactors. These are discussed in detail in Section 1.1.2. These systems aim to satisfy all the requirements for rapid fermentation process development and have capability of higher throughput operation compared to conventional bioreactors. However, some of these designs are less instrumented and limited in terms of off-line sampling due to the smaller process volumes (0.1 mL to approximately 100 mL). As a result there is normally a trade-off between experimental throughput and the information content of the data obtained from each experiment. This is illustrated in Figure 1.1.

This trade-off is most clear when comparing related developments in microwell fermentations (Dutez *et al.*, 2000; Elmahdi *et al.*, 2003; John *et al.*, 2003) with small scale stirred bioreactor designs. Irrespective of the approach taken for high throughput fermentation process development, it will be important that advances in throughput are matched by the creation of microscale downstream processing operations. In this regard the generation of quantitative process data from a number of microwell-based downstream unit operations has recently been reported (Lye *et al.*, 2003; Rege *et al.*, 2006; Jackson *et al.*, 2006) as has the automated operation of linked process sequences (Ferreira-Torres *et al.*, 2005; Micheletti *et al.*, 2006).

In addition to all the benefits of automated high throughput operation, it is important that miniature bioreactor systems used for assessing potential production strains, are



**Figure 1.1.** Comparison of the degree of experimental throughput and information available over a range of scales for a variety of cultivation systems. Figure reproduced from Doig *et al.*, (2006).

capable of accurately mimicking laboratory and pilot scale bioreactors. By doing this the growth kinetics and product expression optimised at miniature scale can be expected to be scaled up quantitatively (Betts and Baganz, 2006).

### ***1.1.2. Small Scale Bioreactor Systems Available for High Throughput Cell Cultivation***

When designing a system for cell cultivation careful consideration of several factors is necessary regardless of the scale of operation. These include, maintenance of sterility and control of physical and engineering parameters, particularly: temperature, pH and dissolved oxygen (Doran, 2000). These parameters have been included in various designs of small scale systems and a selection those that have been reported over the years are listed in Table 1.1 and those that are commercially available have been detailed in Appendix I. The most commonly used small scale systems are briefly described in the following sections.

#### **1.1.2.1. Shake Flasks**

The most widely and traditionally used cultivation vessel in process development is the shake flask. These are typically operated with working volumes between 25-100 mL (Buchs, 2001; Freyer *et al.*, 2004; Fernandes and Cabral, 2006). Shake flasks are cheap, easy to operate and capable of high throughput operation with up to several hundred vessels being attached to a base tray in dedicated temperature controlled shaking incubators (Weuster-Botz, 2005).

Liquid mixing and oxygen mass transfer is achieved via the rotary action of the incubator tray. The key factors affecting liquid mixing and oxygen mass transfer include: flask shape and size, shaking frequency, shaking diameter, fill volume and surface properties (Maier and Buchs, 2001). The major limitation of these vessels is their reliance on surface aeration, leading to reduced oxygen transfer rates compared to stirred tank bioreactors (Betts and Baganz, 2006). Values for the oxygen mass transfer coefficient ( $k_{La}$ ) in a variety of shake flasks have been reported and range

**Table 1.1.** Comparison of miniature bioreactor systems that have recently been reported for parallel operation. The table shows key design features and operating characteristics. Quoted working volumes, number of parallel units and stirrer speeds indicate maximum reported values. Nomenclature: T = temperature, DOT = dissolved oxygen, OD = optical density, N/A = not applicable, N/R = not reported.

| Bioreactor Design  | Working Volume (mL) | No. of Parallel Units | Agitation  | Aeration             | Mode of Operation                | Sterilisation | On-line Monitoring | Max. $k_L a$ ( $s^{-1}$ ) | Maximum Biomass Concentration ( $g_{DCW} \cdot L^{-1}$ )          | Reference   |
|--|---------------------|-----------------------|--|----------------------|----------------------------------|---------------|--------------------|---------------------------|---|---|
| <b>(a) Stirred Bioreactors</b>   |                     |                       |  |                      |                                  |               |                    |                           |   |   |
| Xplorer<br>Bioxplore, UK<br><a href="http://www.Bioxplore.net">www. Bioxplore. net</a>             | 100                 | 16                    | Miniature turbine<br>Magnetic drive<br>(2000 rpm)        | Sparger              | Batch<br>Fed-batch<br>Continuous | Autoclave     | T, pH,<br>DOT, OD  | 0.11                      | <i>E. coli</i> TOP10<br>8.1<br><i>B. subtilis</i> ATCC6633<br>9.0 | Gill et al., 2007   |
| Bioreactor block   | 10                  | 48                    | Gas inducing<br>impeller<br>Magnetic drive<br>(4000 rpm) | Surface/<br>impeller | Batch<br>Fed-batch               | Disposable    | T, pH,<br>DOT, OD  | 0.40                      | <i>E. coli</i> K12<br>36.9<br><i>B. subtilis</i> RB50<br>45-50    | Puskeiler et al., 2005a;<br>2005b; Knorr <i>et al.</i> , 2006 |
| Miniature bioreactor   | 7                   | N/R                   | Flat blade turbine<br>Mechanical drive<br>(15000 rpm)    | Sparger              | Batch                            | Chemical      | T, pH,<br>DOT, OD  | 0.11                      | <i>E. coli</i> DH5a<br>4  | Lamping et al., 2003;<br>Betts et al., 2006                   |
| Cellstation<br>Fluorometrix, USA<br><a href="http://www.fluorometrix.com">www.fluorometrix.com</a> | 35                  | 12                    | Stirrer bar<br>Magnetic drive<br>(1000 rpm)              | Sparger              | Batch                            | Chemical      | T, pH,<br>DOT, OD  | 0.01                      | <i>E. coli</i> JM105<br>2.3                                       | Kostov et al., 2001   |
| <b>(b) Bubble Columns</b>  |                     |                       |  |                      |                                  |               |                    |                           |   |   |
| Profors,<br>Infors, Switzerland<br><a href="http://www.infors-ht.com">www.infors-ht.com</a>        | 200                 | 16                    | N/A  | Sparged              | Batch                            | Autoclave     | T, pH,<br>DOT      | 0.16                      | <i>S. carnosus</i> TM300<br>12.5                                  | Dilsen et al., 2001;<br>Weuster-Botz et al., 2001a            |

|   |     |    |                |         |                                  |           |               |      |                                     |                            |
|---|-----|----|----------------|---------|----------------------------------|-----------|---------------|------|-------------------------------------|----------------------------|
| Bubble column block                               | 2   | 48 | N/A            | Sparged | Batch                            | N/R       | T, pH,<br>DOT | 0.06 | <i>B. subtilis</i> ATCC6633<br>10.4 | Doig et al., 2004          |
| <b>(c) Shake Flasks</b>                           |     |    |                |         |                                  |           |               |      |                                     |                            |
| Fedbatch-pro,<br>DasGip,Germany<br>www.dasgip.com | 100 | 16 | Orbital shaker | Surface | Batch<br>Fed-batch               | Autoclave | T, pH         | N/R  | <i>E. coli</i> BL21<br>5.1          | Weuster-Botz et al., 2001b |
| Shaken bioreactor                                 | 40  | 4  | Orbital shaker | Sparged | Batch<br>Fed-batch<br>Continuous | Autoclave | N/R           | N/R  | <i>S. cerevisiae</i> H1022<br>2.7   | Akgün et al., 2004         |



from 0.01-0.06 s<sup>-1</sup> (Kato and Tanaka, 1998; Wittmann *et al.*, 2003). In addition the limited mixing action of most shaking incubators only permit the liquid to move in circular motions around the vessel resulting is significantly less efficient liquid mixing compared to stirred bioreactors (Doig *et al.*, 2006). Mixing and oxygen transfer can be enhanced to a certain degree by the use of baffled vessels (Kumar *et al.*, 2004).

Given the geometry of the vessel and mode of operation they have proved difficult to instrument (Doig *et al.*, 2004). These challenges have been overcome to some degree by modified designs integrating pH probes (Weuster-Botz *et al.*, 2001b), as demonstrated by the Shakeflask Pro system (DasGip, Germany). The potential for optical sensing methods has also been reported by Wittmann and co-workers (2003), using optical sensor spots immobilized on the bottom of a shake flask for oxygen sensing. A coaster holding an optical fibre for detection is placed beneath the flask. This technology has been applied for on-line measurements of the respiration activities such as OUR, CTR and RQ for the RAMOS- Respiratory Activity Monitoring System (HiTech Zang, GmbH, Germany).

Despite the recent advancements making shake flasks an attractive screening tool, the level of information provided when compared to laboratory bioreactors is still limited. This limits their application to the initial steps of bioprocess development. In addition the reaction conditions in these systems are often not representative of the conditions experienced at the larger scale (Freyer *et al.*, 2004). Thus results frequently can not be transferred to production scale due to the limited capability for scale-up (Doig *et al.*, 2006) and further validation of the processes at larger scales is necessary.

#### 1.1.2.2. Microtitre Plates (MTP's)

Microtitre plates have been used industrially for many years, initially in medical diagnostic tests and later for pharmaceutical and combinatorial chemistry applications (Kumar *et al.*, 2004). Only in recent years have they been used for small scale fermentation and biocatalysis processes (Betts and Baganz, 2006). MTP's are commercially available in various sizes and geometries ranging from 4-1536 wells per

plate and nominal volumes of each well in the microtitre plate can vary from 0.2  $\mu\text{L}$  to 5 mL (Fernandes and Cabral, 2006). The most attractive feature of MTP's is the potential for carrying out huge numbers of parallel experiments in identically shaped wells. Wells may be of square or circular shape. Experiments with MTP's are almost completely automated using dedicated platforms and robotics for liquid handling. Mixing is most commonly achieved by mounting the plate on a small shaking platform. Other options include, using pipette aspiration or miniature magnetic stirrer bars.

Square MTP geometries have shown approximately 50% higher oxygen transfer rates compared to the corresponding round well of the same size range by mimicking the action of baffles providing better mixing (Kumar *et al.*, 2004). Nevertheless oxygen transfer rates still continue to be significantly lower compared to stirred bioreactors (Doig *et al.*, 2004), with  $k_{\text{L}}a$  values in the same range as shake flasks, reaching between 0.03- 0.05  $\text{s}^{-1}$  (Betts and Baganz, 2006). In most cases this would lead to severe oxygen limitations which can have detrimental affects on growth and product formation. Evaporation can also be a problem with slow growing cultures. However, researchers have attempted to remedy this by using suitable closures/films on top of the plate (Duetz *et al.*, 2000; Zimmerman *et al.*, 2003; Wittmann *et al.*, 2003).


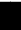











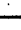
















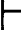










Further limitations result from the risk of cross contamination from aerosol formation at high shaking rates (Dutez and Witholt. 2001). Conventional instrumentation and monitoring becomes difficult with the MTP's operated on shaking platforms. MTP's integrated with sensors- pH measurement are commercially available (Weiss *et al.*, 2002; Harms *et al.*, 2002) and some researchers have also added optical sensors for DOT and OD monitoring (John *et al.*, 2003; Puskeiler *et al.*, 2005b). However, in a majority of cases shaking needs to stop in order to take readings, this further complicates the process automation and can have severe affects on the cultivation. This type of optical sensing technology has been integrated into the Micro-24 device (Applikon, UK) that is based on a 24-well MTP. However, the major drawback of these systems is still the lack of suitable scale-up criteria given that the design and operating conditions do not entirely mimic a standard laboratory bioreactor.

### 1.1.2.3. Miniature Stirred Bioreactors

In recent years miniature stirred bioreactors have successfully bridged the gap between the large scale, fully instrumented and controlled bioreactors and the simple moderately or uncontrolled systems such as shake flasks. These systems are generally miniature versions of a traditional, independently operated bench scale bioreactor (Kumar *et al.*, 2004), providing the additional advantage of parallel operation with up to 48 independent experiments running simultaneously. With working volumes of 7-500 mL the quantity and cost of raw materials is significantly reduced, while the smaller footprint reduce floor space requirements (Doig *et al.*, 2006).


Figure 1.2 shows a simple analysis of the time taken to setup several stirred tank fermentations to the point of inoculation at three different scales; 100 mL, 2 L and 7 L. There is clearly a significant reduction in the preparation time alone of up to approximately five hours when replacing the larger scale systems with miniature bioreactors. Also given the speed of preparation, potentially a larger number of miniature vessels can be handled by a single operator. More importantly in some cases these miniature stirred systems have been designed to be geometrically similar to conventional stirred bioreactors and provide well defined, realistic engineering environments. Therefore it is a huge advantage to be able to replace larger scale vessels with several miniature systems that can also facilitate predictive scale-up of desired bioprocesses.

The monitoring and control capabilities of miniature stirred bioreactors are also comparable to their larger scale counterparts and all key process variables including temperature, stirrer speed, pH, DOT and in some cases OD can be individually monitored and controlled in each parallel unit. These parameters have been reported to be measured either by miniature versions of conventional probes or in most cases optical probes. For the majority of the designs listed in Table 1.1 and Appendix I agitation is achieved via a magnetic drive assembly except for the vessel described by Betts *et al.* (2006) which is directly mechanically driven. The agitation and aeration strategy provides flexibility for achieving various mixing and mass transfer capabilities that are significantly higher than shake flasks and MTP's, with oxygen


| Action                              | Bioreactor Scale  |   |   |
|-------------------------------------|---|---|---|
|                                     | 100 mL  | 2 L   | 7 L   |
| Batch media preparation             |    |    |    |
| Calibration of pH and DOT probes    | <br><br>       | <br><br>       | <br><br>       |
| Acid and base reservoir preparation |    | <br><br>       | <br><br>       |
| Sterilisation                       | <br>Autoclave  | <br>Autoclave   | <br><br>In-situ   |
| Prime pumps and make Additions      | <br><br>  | <br><br>  | <br><br>  |
| Inoculate                           | <br><br> | <br><br> | <br><br> |
| Number of operators                 | 1   | 1-2   | 2   |
| Total Preparation Time (h)          | 3.5   | 6.8   | 8.8   |

**KEY**

 10 minutes

 60 minutes

 All four bioreactors in parallel

 Individual preparation of each bioreactor

**Figure 1.2.** Comparison of the time required to prepare four bioreactors in parallel at three different scales.

mass transfer rates reaching up to  $0.4 \text{ s}^{-1}$  (Pukelier *et al.*, 2005a). These miniature bioreactor systems are discussed in further detail in Section 3.6.

Despite the benefits of miniature stirred bioreactors that have been reported in Table 1.1, both bioreactor block (Pukelier *et al.*, 2005a) and Cellstation<sup>TM</sup> (Kostov *et al.*, 2001) are fitted with non standard impellers and lack geometric similarity compared to conventional scale bioreactors. This could potentially make subsequent predictive scale-up of processes rather difficult. To date only Betts *et al.* (2006) have reported on some scale-up studies based on constant  $P_g/V$ . In terms of flexible operation, the bioreactor block is limited since operation relies completely on an interface with a robotic platform, which significantly increases expenses. Furthermore some of the miniature stirred bioreactors in Table 1.1 handle process volumes less than 50 mL this may be a huge advantage for carrying out large numbers of screening experiments. However such low process volumes are not realistic in cases where repeated sampling is necessary for off-line analysis.

## **1.2 Scale-up of Microbial Fermentation Processes**

### ***1.2.1 Predictive Scale-up Techniques***

Scale-up studies are inevitable for the industrialisation of bioprocesses. Traditionally bioprocesses are developed at at least three scales: 1) laboratory scale, where initial studies are carried out; 2) pilot plant, where the optimal operating conditions are ascertained; and 3) plant scale, where the process is brought to economic fruition (Ju and Chase, 1992). However in recent years given the increasing number of strains requiring evaluation an additional stage precedes the first stage, involving small scale bioreactor systems (shake flasks, miniature bioreactors, etc) for initial design and optimisation of a given process.

The objective of scale-up is to reproduce at a larger scale the behaviour of fermentations performed and optimised at small scale (Diaz and Acevedo, 1999; Oldshue, 1985). In addition it is highly advantageous to assess the performance of the

bioprocess at small scale since evaluation of optimum conditions at production scale is expensive and time consuming. It would also be beneficial to know whether a particular process will work properly before it is constructed in full size (Doran, 2000). The traditional approach to scale-up is based on the theory of similarity. However, despite the extensive literature that is available there seems to be no common, generally applicable strategy established for scale-up. For a given product, process and facility, a suitable scale-up strategy has to be specifically designed (Schmidt, 2005). The problem is complicated by the fact that complete similarity is not possible; therefore different scale-up criteria and strategies have been proposed (Abia *et al.*, 1973; Wang *et al.*, 1979). A viable scale-up strategy consists of comprehensive and detailed process characterisation to identify key stress factors and parameters influencing product yield and quality the most (Schmidt, 2005). Appropriate process control and process design must also be taken into consideration in order to ensure optimum mixing and reaction conditions (Schmidt, 2005).

Fermentations in general can be evaluated based on a combination of physical factors (mass transfer, heat transfer, mixing, shear, and power consumption), chemical factors (medium composition and concentration) and process factors (number of precultures, sterilisation conditions). Many physical and chemical parameters that influence the behaviour and environment of the cultured microorganisms are interrelated and change as the scale of the process becomes larger (Ju and Chase, 1992; Hosobuchi and Yoshikawa, 1999). The most critical environmental parameters prone to be affected by scale include (Stanbury *et al.*, 2003):

- a. Nutrient availability
- b. pH
- c. Temperature
- d. Dissolved oxygen concentration
- e. Hydrodynamic shear
- f. Dissolved carbon dioxide concentration
- g. Foam production

All the above parameters are affected by agitation and aeration, either in terms of bulk mixing (a, b, c and e) or providing oxygen (d, e, f and g). Thus agitation and aeration

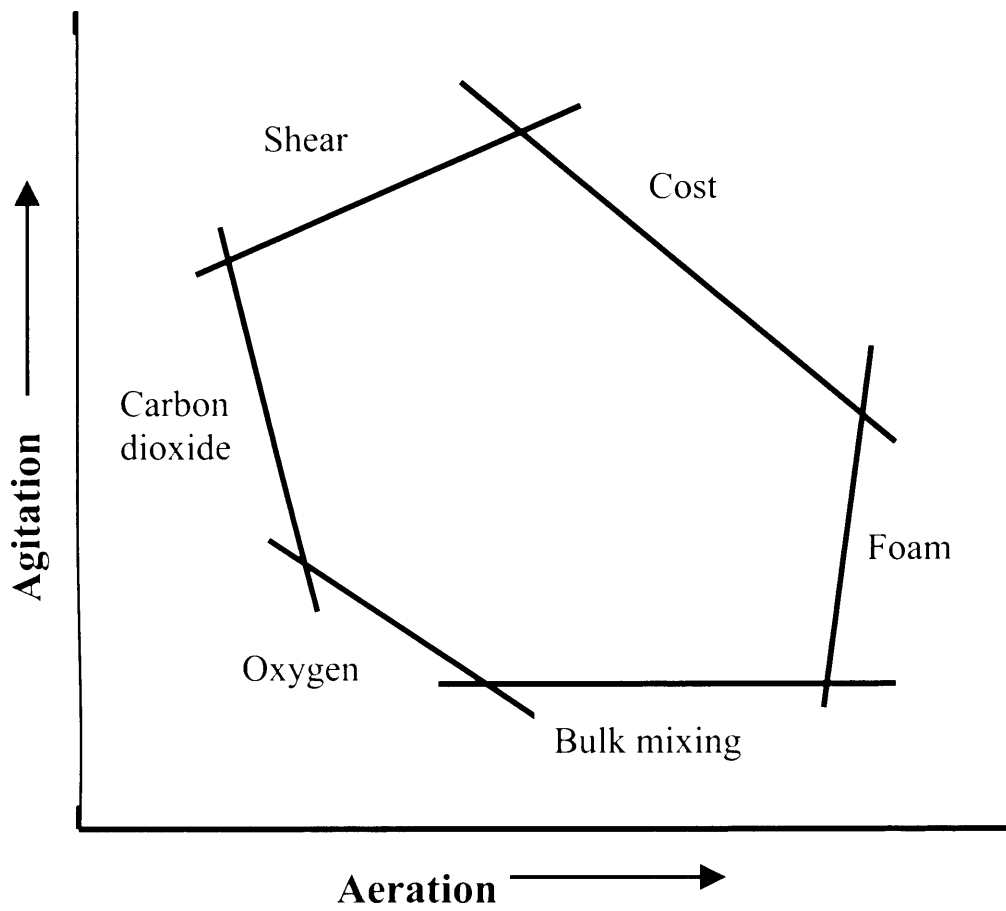
considerations tend to dominate the scale up literature (Stanbury *et al.*, 2003). From the list above it is obviously unlikely that all the conditions of the small-scale fermentations will be successfully replicated at the large scale. The most important criteria for a given fermentation must be established and the scale-up be based on those characteristics.

The issues of aeration and agitation scale-up have been addressed previously based on the 'scale-up window' (Lilly, 1983). This analogy illustrates the boundaries imposed by both the environmental parameters and the cost on the aeration and agitation regime. From Figure 1.3 it can be seen that suitable mixing and oxygen transfer can be achieved over a range of aeration and agitation conditions. These boundaries are defined by the limits of the oxygen supply, carbon dioxide accumulation, shear damage to the microorganism, cost, foam production and bulk mixing. The specific shape of the window depends on individual fermentations and the parameters of major importance.

### 1.2.2 Scale-up Concepts

The initial concept of scale-up stems from the principle of similarity. Uhl and von Essen (1987) have described the applications of the principles of similarity to be conceptually useful, however having little direct application value. The similarity states that are generally applicable for agitation include (Johnston and Thring, 1957):

- **Geometric similarity** – both systems must be the same shape and the ratio of any two linear dimensions between scale equal i.e.  $(d_i/d_T)_1 = (d_i/d_T)_2$ ;  $(h_T/d_T)_1 = (h_T/d_T)_2$ ;  $(h_i/d_T)_1 = (h_i/d_T)_2$ ;  $(d_B/d_T)_1 = (d_B/d_T)_2$
- **Kinematic similarity** – similar flow patterns in both vessels, i.e. velocities at corresponding points must have a constant ratio



**Figure 1.3.** The scale-up window defining the operating boundaries for aeration and agitation for the scale-up of fermentation conditions. Figure adapted from Lilly (1983).



- **Dynamic similarity** – all significant forces (Reynolds number, Power number, Froude number etc) should have a constant ratio in two geometrically similar systems.

The initial approach to scale-up was to apply geometric similarity (Nagata, 1975). This is feasible going from say bench scale to pilot scale, therefore it is important to account for some degree of geometric similarity in smaller scale systems preceding bench scale tests. However it may prove difficult to apply this strategy to commercial vessels as the configurations may change due to process and economic reasons (Uhl and von Essen, 1987). In reality kinematic and dynamic similarity can not be widely applied to a range of different process situations and it is difficult to integrate them for many mixing applications. In the case of kinematic similarity, this can not be readily maintained due to the increase of liquid velocities with scale resulting in a significant increase in power requirement. Also for dynamic similarity, since the surface area of the vessel increases with volume approximately as  $V^{2/3}$ , it is impossible to maintain the balance between circulation rate and intensity of turbulence for a given process fluid.

Oosterhuis and Kossen (1985) have subsequently suggested four different approaches for scale-up:

- **Fundamental methods** – require a lot of information for accuracy and are based on solving micro-balances for momentum, mass and heat transfer. If applied for scale up of stirred vessels, the balances must account for transport in three dimensions and complicated boundary conditions. Typically the momentum balances are usually used for homogenous fluids; however this is not very realistic for an aerated fermentation broth. As a result, the momentum balance can not be readily solved. The use of the fundamental methods is thus applicable to very simple systems with well defined flow conditions.
- **Semi-fundamental methods** – this is a simplified approach based on simple flow models, and so avoids the problems associated with solving the momentum balances. Most of these flow models refer to bulk flow and do not provide any

information about the flow near important regions such as the impeller blades and vessel walls. These models are usually based on small scale observations with limited information available for larger scale vessels, making scale-up based on these flow models unreliable.

- **Dimensional analysis** – this is based on maintaining constant values of dimensionless groups of parameters during scale-up. These include ratios of rates or time constants for the different mechanisms involved. Therefore, in theory, if all the dimensionless groups are kept constant, the relative importance of the mechanisms involved in the process should not change during scale-up. To use this method geometric similarity can be important. However it is impossible to keep all the dimensionless groups constant for scale-up and the most significant groups must be determined for a given process. In some cases this may lead to unrealistic predictions for certain parameters, such as power consumption and stirrer speed.
- **Rules of thumb** – these include the most commonly used basis for scale-up, such as constant power per unit volume, volumetric mass transfer coefficient, impeller tip speed and constant dissolved oxygen concentration. These are discussed further in Section 1.2.3.

It should be noted that the different scale-up criterion can determine very different process conditions at production scale and it is impossible to maintain all the parameters in the same ratio to one another. In practical application these scale up criteria can be used in combination to satisfy the scale-up requirements of a given process and some trial and error studies may also be necessary to determine the optimum scale-up criterion.

### ***1.2.3 Most Commonly Applied Criteria of Scale-up***

Given that there is no standard method for fermentation scale-up and since the methodology of scale-up is very much related to the characteristics of the

microorganism and individual process, the process characteristics which have been most commonly suggested to be maintained constant during scale-up (Stanbury *et al.*, 2002; Ju and Chase, 1992; Oosterhuis and Kossen, 1985; Hosobuchi and Yoshikawa, 1999) are shown in Table 1.2.

As discussed in Section 1.2.2, geometric similarity is almost always a useful starting point when considering scale-up of processes, since all empirical correlations for scale-up that have been developed to date have been experimentally based on geometrically similar vessels at different scales. Nevertheless, for non-geometric scale-up a range of ratios for impeller diameter to reactor diameter ( $d_i/d_T$ ), capable of delivering sufficient gas dispersion are available (Oldshue, 1966).

Table 1.2. Process parameter and coefficients implicated in mixing, aeration and oxygen transfer that are suitable as scale-up variables to be kept constant alone or in combination with each other or other process relevant variables (Schmidt, 2005).

| Parameter/ Coefficient                                     | Mathematical Characterisation           |
|--|---|
| Volumetric mass transfer coefficient ( $s^{-1}$ )          | $k_L a = C(P/V)^{\alpha} (u_s)^{\beta}$ |
| Power per unit volume (W)                                  | $P/V = N_p \rho N^3 d_i^5$              |
| Oxygen transfer rate ( $kgO_2 \cdot m^{-3} \cdot h^{-1}$ ) | $OTR = k_L a (C^* - C_L)$               |
| Impeller tip speed ( $m \cdot s^{-1}$ )                    | $v_{tip} = 2\pi N d_i$                  |
| Mixing time (s)  | $T_m = V/Q$                             |
| Volumetric gas flow rate per unit volume of liquid         | $Q/V$ or vvm                            |
| Superficial gas velocity ( $m \cdot s^{-1}$ )              | $u_s = Q/A$                             |
| Impeller Reynolds number                                   | $Re_i = (\rho N d_i) / \mu_v$           |

### 1.2.3.1 Constant Volumetric Mass Transfer Coefficient

The volumetric oxygen mass transfer coefficient,  $k_{L,a}$ , is currently the most widely applied physical scale-up criterion when dealing with aerobic fermentations (Schmidt, 2005). Approximately 30% of industrial processes opt for this as the basis for scale-up (Mavituna, 1996). This criterion accounts for the relevant parameters influencing gas-liquid mass transport, such as agitation (via power input) and aeration (superficial gas velocity) (Yawalkar, 2002). Oxygen is sparingly soluble in culture broth at the conditions typically used for bioprocess, and as a result the oxygen supply to growing cells is usually a rate-limiting operation as scale increases (Shin *et al.*, 1996). This is especially true when dealing with high cell density cultures of fast growing aerobes such as *Escherichia coli* or when the rheological properties of the fermentation broth offer high resistance to mass transfer (mycelial fermentations and production of extracellular polysaccharides) (Diaz and Acevedo, 1999). Conditions involving even temporary depletion of dissolved oxygen during aerobic fermentations could result in irreversible cell damage (Ju and Chase, 1992) and significant reduction of product yield (Hosobuchi and Yoshikawa, 1999). Therefore, a strong emphasis has been put on maintaining constant  $k_{L,a}$  in process scale-up to ensure the same oxygen supply rate to satisfy the oxygen demand of the desired cultivation.

The same  $k_{L,a}$  values can be achieved in different sized vessels by adjusting the operating conditions i.e. stirrer speed and aeration rates on the larger scale to match the optimum  $k_{L,a}$  conditions determined in the small-scale studies (Stanbury *et al.*, 2003). Several correlations estimating  $k_{L,a}$  have been developed over the years for a range of different vessel sizes (Van't Riet 1979; Vilaca *et al.* 2000; Linek *et al.* 2004; Smith *et al.* 1977; Zhu *et al.* 2001). Selected correlations are listed later in Table 5.2.  $k_{L,a}$  is also readily determined experimentally using methods such as sulfite oxidation and dynamic gassing out techniques (Stanbury *et al.*, 2003).

Several researchers have successfully scaled-up from bench scale to pilot scale based on constant  $k_{L,a}$  or in conjunction with another scale-up parameter. These studies concluded that results produced at smaller scale were maintained on scaling up (Shin *et al.*, 1996; Flores *et al.*, 1997; Wong *et al.* 2002; Pérez *et al.*, 2006). Shukla and co-workers (2006) have also used constant  $k_{L,a}$  to scale-up from a 100 mL shake flask to

5 L bioreactor, demonstrating the wide range over which this criterion can be used. Diaz and Acevedo (1999) have stated that the oxygen transfer capacity, indicated by  $k_L a$  value is not the most important process relevant parameter, but the effective oxygen transfer potential, i.e the difference between the  $pO_2$  values in the gas and the liquid phase, and suggest an OTR based scale up strategy. However these researchers have not experimentally proved this.

#### 1.2.3.2 Constant Power per Unit Volume

Maintaining equal power per unit volume is another popular scale-up method, and has been successfully applied as a primary scale-up parameter for many antibiotic fermentations (Ju and Chase, 1992; Schmidt, 2005). Typically a power per unit volume ratio of 1-2  $kW.m^{-3}$  has been used (Aiba *et al.*, 1973). Since most bioprocesses are aerobic, it is the gassed power that is used at the basis for scale translation. Under gassed conditions the power input required can reduce by 60-65% compared to ungassed conditions (Wang *et al.*, 1979), since the transfer of power from the impeller to the fluid is greatly influenced by aeration. This power reduction is due to the formation of cavities behind the impeller blades and the different density of the fluid under gassed and ungassed conditions (Sensel *et al.*, 1993). As a result, several researchers have suggested correlations for the prediction of gassed power requirement (Cui *et al.* 1996; Mockel *et al.* 1983; Hughmark 1980; Michel and Miller 1962; Luong and Volesky 1979). Selected correlations are listed later in Table 5.1.

If scale-up is conducted using constant power per unit volume with geometric similarity, then circulation time, mixing time and impeller tip speed increase (Brown, 1982), but the size of eddies does not change (Oosterhuis and Kossen, 1985). The power per unit volume required to provide a certain OTR generally decreases with scale (Ju and Chase, 1992). Scale-up based on this criterion can result in larger than necessary motor size, and it becomes more difficult to accommodate higher power per unit volume inputs at larger scale due to practical limitations in motor size (Junker, 2004; Hosobuchi and Yoshikawa, 1999). Pérez *et al.* (2006) have demonstrated scaled-up from a 1.5 L to 50 L bioreactor using constant power per unit of volume as

main scaling criteria, combined with constant oxygen mass transfer coefficient to adjust the optimal aeration conditions.

#### 1.2.3.3 Constant Impeller Tip Speed or Shear Rate

Shear can be of critical importance when dealing with fermentations involving insect and filamentous cultures. These organisms have been found to be affected by shear or the absolute value of the impeller tip speed (Ju and Chase, 1992; Maranga, *et al.*, 2004). High shear conditions can cause cell damage and a significant reduction in productivity (Junker, 2004). Oldshue (1966) showed the relationship between impeller tip speed and the amount of nucleic acid related compounds leaked from the cells. Since shear stress is considered to be proportional to the tip speed of the impeller. As a general rule cell damage can occur at tip speeds above  $3.2 \text{ m}\cdot\text{s}^{-1}$ , although this value can be affected by many factors such as broth rheology (Charles and Wilson, 1999). Although tip speed is a valuable consideration for branched yeast, filamentous bacteria and fungal fermentations for estimation of hyphal breakage and thus changes in broth morphology, it is much less useful for single cell bacterial or yeast fermentations (Junker, 2004). It should be noted that scale-up based on constant tip speed can result in a reduced value of gassed power per unit volume, which in turn will adversely affect the aeration efficiency. This can potentially be remedied by increasing the number of impellers in the larger scale vessel, and maintaining both the tip speed and gassed power per unit volume constant in combination (Brown, 1982).

#### 1.2.3.4 Constant Mixing Time

Mixing time is defined as “the period of time which is needed for a liquid droplet passing into an agitated vessel filled with a fluid with the same physical properties as the droplet to be completely mixed with the bulk of the fluid” (Abia *et al.*, 1973). As scale increases, the contents of bioreactors become less homogenous, and this can lead to localised concentration gradients for nutrients and oxygen (Larsson *et al.*, 1996), and temperature gradients as well as oscillations in pH. These can affect the productivity of the process (Bonvillani *et al.*, 2006). Various correlations have been

developed to accomplish scale-up for geometrically similar vessels based on mixing time (Ju and Chase, 1992; Reisman, 1993, Junker *et al.*, 2004). Mixing time needs to be evaluated relative to nutrient mass transfer rates for fed-batch cultures in the presence of cellular nutrient uptake. For fast growing cultures that reach high cell densities (yeast and *E.coli*) nutrients such as oxygen and glucose can be depleted in a matter of seconds, thus longer mixing times can cause locally high glucose concentrations which in turn cause locally low dissolved oxygen levels owing to higher cell metabolism (Junker *et al.*, 2004). This can result in local areas of mixed acid *E.coli* fermentations, producing overall lower biomass yields upon scale-up. Therefore mixing time can be a significant parameter for the basis of scale-up when dealing with fed-batch yeast and *E.coli* cultures, especially at high densities.

#### 1.2.3.5 Constant Reynolds Number

Scale up can also be achieved based on constant impeller Reynolds number. However, on its own this is not a reliable scale-up criterion given that it does not account for the effect of aeration on the process (Ju and Chase, 1992). Other dimensionless groups have also been assessed for scale-up with limited success, due to technically unrealistic equipment and operating parameters (Junker, 2004). As it is difficult to maintain all dimensional parameters constant upon scale-up, those most important to the process must be accurately defined.

#### 1.2.3.6 Constant Volumetric Gas Flow Rate per Unit Volume of Liquid or Superficial Gas Velocity

Scale-up based on constant volumetric gas flow rate per unit volume of liquid (vvm) can also be considered to check that the resulting values for superficial gas velocity are reasonable. If the vvm remains constant on scale-up, there is a problem with the superficial gas velocity increasing to the point of flooding in production scale vessels (Ju and Chase, 1992). This is usually an unsatisfactory scale-up parameter (Oosterhuis and Kossen, 1985). Conversely, the superficial gas velocity is also an important factor in bioreactor design as it strongly affects the mixing energy required to disperse the

gas stream. However, maintaining this parameter constant for scale-up, results in larger values of vvm to be used at smaller scale. Typical values of vvm range from 1-1.67, with the values generally decreasing at larger scale (Junker, 2004).

## **1.3 On-line Fermentation Monitoring**

### ***1.3.1 On-line Sensors***

In order to achieve optimal exploitation of the particular production organism, the advancement of bioprocesses to improve monitoring and control capabilities is essential to reduce production costs and increase yield while at the same time maintaining the quality of the product. Satisfying economic needs and given the complex nature of microbial growth and product formation in batch and fed-batch cultivations represents an ever-increasing engineering challenge. As a result a great number of the current processes are still far from optimal mainly due to limited process monitoring capabilities (Clementschtch and Bayer, 2006). The current state of bioprocess monitoring has evolved from chemical engineering and as a result sensors useful for *in situ* monitoring of biotechnological processes are comparatively few; they measure physical and chemical variables rather than biological ones (Sonnleitner, 1999). The reasons are generally due to the fact that biologically relevant variables are much more difficult and complex to measure than others. Although there is vigorous research being done on sensor development only a small fraction of new sensors are suitable for use in fermentations (Harms *et al.*, 2002) as a result of the restricting requirements. It is therefore critical that sensors used *in-situ* need to satisfy the following criteria:

- Withstand repeated sterilisation.
- Maintain aseptic conditions and any components, liquids or ions, must not leach out into the culture (biocompatibility).
- Remain stable and reliable over extended periods without recalibration as bioprocesses may potentially run for weeks.



- Robust enough to tolerate the harsh environments of bioprocesses as growing cultures can infiltrate sensors and surface growth can occur.

Table 1.3 shows a list some of the on-line techniques widely used in many academic biochemical engineering laboratories for monitoring key bioprocess parameters..

**Table 1.3.** Most frequently used on-line monitoring techniques currently available for cell cultures.

| Parameter        | Method                                    | Frequency  |
|------------------|---|------------|
| Temperature      | Thermocouple                              | Continuous |
| pH               | pH electrode<br>Optical sensor            | Continuous |
| Dissolved Oxygen | Polarographic electrode<br>Optical sensor | Continuous |
| Optical Density  | OD probe<br>Optical sensor                | Continuous |

As bioprocesses are scaled down, taking large numbers of samples becomes unrealistic and alternative methods for continuous on-line monitoring to obtain the same type of information has become increasingly important. Some researchers have integrated commercially available optical density probes for continuous monitoring of biomass growth to replace repeated offline sampling (Sarrafzadeh *et al.*, 2005; Wu *et al.*, 1995).

More recently, optical sensors have provided alternative, non-invasive methods to obtain the same type of information (Marose *et al.*, 1999). Optical sensors enable continuous and simultaneous monitoring of several parameters at once, without disturbing the observed bioprocess or increasing the risk of contamination. Fiber-optic sensors (known as optodes) are based on a change in the optical properties (such as absorption or luminescence) of a particular indicator. For instance, fiber-optic oxygen sensors are produced by the immobilization of suitable oxygen-sensitive dyes at the

tip of an optical fiber. The principle of these measurements is the decrease in fluorescence intensity of a dye, caused by the interaction with oxygen. The light of a blue light-emitting-diode (LED) is guided through an optical fiber, on the tip of which the dye is immobilized; the fluorescence of this dye offers information about the oxygen concentration (Stärk *et al.*, 2002). If the oxygen-sensitive dye is replaced with a pH sensitive dye, optical pH sensors can be produced (Marose *et al.*, 1999).

A number of commercially available optical sensors allow the on-line determination of microbial growth by measuring light absorption (turbidity) or scattering continuously in the visible and near-infrared (NIR) ranges. These devices allow accurate on-line determination of cell density with no need for intermittent calibration procedures (Konstantinov *et al.*, 1994). Several researchers working with small scale bioreactor systems have integrated such optical sensors for monitoring important parameters including pH, dissolved oxygen and optical density (Lamping *et al.*, 2003; Gupta and Rao, 2003; Doig *et al.*, 2004; Puskeiler *et al.*, 2005a; Betts *et al.*, 2006; Harms *et al.*, 2006). While conventional sensing probes remain a popular and robust choice, they are not practical at very low process volumes. Hence, optical sensors have become increasingly useful for ultra-scale down applications using MTP's as they are more readily miniaturised compared to the electrochemical probes (Scheper *et al.*, 1996; Harms *et al.*, 2002).

Although optical probes offer several advantages over conventional sensors, there are a number of drawbacks. Ambient light can interfere with the measurement of optical signals (Narayanaswamy, 1993). Therefore either the sensors must be used in dark environments or the optical signal must be modulated to resolve it from ambient light. However, more recently some optical sensors utilising modulated light and selective detecting systems that are not sensitive to changes in the ambient light have become available (Dybko, 2001). They have a limited dynamic range in comparison to electronic sensors and their response times may be slow due to the time of mass transfer of analytes to the reagent phase (Mehrvar *et al.*, 2000). Long-term stability could also be a problem with optical sensors as they are dependent on the amount of indicator dye immobilized at the sensor tip and the detector sensitivity. Therefore, intensity-based optical sensors are prone to drift due to aging of the light source and detector, fluorophore leaching, and photodegradation (Orellana, 2004). Frequent

replacement or service of the sensors can also be necessary. This can be time consuming and expensive (Kane, 2006).

### **1.3.2 Calorimetry**

The broad applicability of calorimetry stems primarily from one central theme that virtually every process liberates or consumes some finite amount of energy (Landau, 1996). Perhaps one of the greatest attributes of calorimetry is its relative simplicity. Hence it is not surprising to discover that the non-invasive nature of this technology makes it quite attractive for a very broad range of applications, with examples ranging from drug design in the pharmaceutical industry (Giron, 2002; Barnes *et al.*, 1993; Cooper, 2003), to quality control of processes in the chemical industry (Singh, 1997; Zogg, 2004; de Buruaga 1997), and the study of metabolic rates in biological systems. The history, application and development of bio-calorimetry has been extensively reported in literature (von Stockar and Marison, 1989; Zentgraf, 1991; Kemp 1993; Wadso, 1997; Battley, 1998).

It is clear that quantitative measurements of heat exchange rates might serve as a powerful indicator of the nature of the on-going chemical or biological processes (von Stockar and Briou, 1989). Such an indicator not only constitutes a potentially valuable diagnostic tool for laboratory work, but also holds promising potential for control of such processes on an industrial scale. Despite the obvious potential of on-line calorimetry for bioprocess monitoring and control, it has rarely been exploited. The reason for this is probably the result of difficulties in investigating and developing this concept in laboratory experiments.

#### **1.3.2.1 Heat as a Quantitative Indicator of Cell Growth and Metabolism**

A wealth of information can be inferred from simple measurements of heat production by microbes which can be valuable for assessing the state of the culture and deciding on corrective actions ensuring proper control of the process. This proves to be particularly useful for the study and control of biological processes, where no other

measurements are available. Monitoring abrupt changes in the thermal power release can provide valuable information about all kinds of metabolic events such as shifts from one substrate to another, shifts from one type of catabolism to another, occurrence of limitations, inhibitions and overflow metabolism which will cause characteristics changes in the heat curves (von Stockar *et al.*, 1997). Given some experience with the respective type of culture, these events can be identified and used for control. This has been illustrated using yeast cultures grown on glucose (von Stockar *et al.*, 1992). During aerobic growth, metabolism is completely oxidative. When grown in the absence of oxygen, the metabolism is reductive producing ethanol and both biomass yields and heat evolution are also reduced. Therefore by monitoring the overall heat effect on-line it is possible to determine the oxidative and reductive fractions in the overall metabolism and to detect changes toward one or the other. There are also difficulties with monitoring and controlling glucose feed on-line during fed-batch operations of yeast, since the maximum allowable glucose for completely oxidative metabolism increases exponentially during exponential growth. However simple heat measurements have been shown to perform as an on-line sensor for glucose enabling optimal feed control (Randolph *et al.*, 1990).

Heat measurements are also of interest for the study of dynamic behaviour in microbial cultures. Since microbial heat is directly released into the culture broth, the effect of changes in behaviour can be expected without a significant delay. Heat measurements thus have an advantage over off-gas analysis, which suffers from a delay in response due to tubing and mixing in the bioreactor head space. Duboc *et al.* (1999) have discussed the merits and inconvenience of using heat generation as compared to other on-line measurements as a control variable, when dealing with feed control. They show that calorimetric measurements react faster and therefore show more details than other alternatives, which are delayed by mass transfer effects, accumulation terms, mixing phenomenon and transport through line samples.

Another technique involves using heat measurements as a substitute for the oxygen uptake rate measurement, since heat production during aerobic processes closely follows oxygen uptake. Therefore these measurements can provide independent data to be used as a check on the oxygen uptake measurements (van Kleeff *et al.*, 1993; von Stockar *et al.*, 1997).

### 1.3.2.2 Biological Reaction Calorimeters

Calorimetry has essentially been developed in two main directions micro-calorimetry and macro-calorimetry (bench scale). Table 1.4 lists a selection of work that has been reported using various calorimetric instruments for investigating the heat generation for a range of different microorganisms.

#### 1.3.2.2.1 Micro-calorimetry

In the first approach, microcalorimetric devices with small working volumes (1-100 mL) have been used by many researchers to study the thermodynamics of bioreactions (Turker, 2004). Microcalorimeters were developed first and reached sufficient sensitivity for measuring the relatively weak heat generation rates accompanying biological processes (Hansen and Eatough, 1983). However, this approach suffers from the disadvantage that it is not possible to simulate and maintain realistic process conditions found in technical bioreactors such as pH control and vigorous agitation and aeration conditions, or monitoring the process by either on-line or off-line analysis (Turker, 2004; Voisard *et al.*, 2002).

This problem has only been partially resolved by the development of flow through microcalorimeters (Suurkuusk and Wadso, 1982; Wadso, 1993; Kemp and Guan 1999, Loureiro-Dias and Arrabaca, 1982; Brettel *et al.*, 1980) coupled with a standard lab bioreactor. This strategy has been used by many researchers, particularly for studies involving Baker's yeast, *Saccharomyces cerevisiae*, for investigating heat evolution of aerobic batch cultures (Brettel *et al.*, 1980; Loureiro-Dias and Arrabaca, 1982) and for testing the osmo-tolerance and growth for different physiological states of the culture (Blomberg *et al.*, 1988). In these cases the bioreactor culture may be carefully controlled and new developments in the measuring cell of the flow calorimeter, enable agitation and even sample aeration. Experience has shown, however that the time lag in the sample line between the bioreactor and the calorimeter measuring cell may result in depletion of carbon and energy sources as well as oxygen, which again makes interpretation of data, particularly under aerobic conditions difficult.

**Table 1.4.** Comparison of the various published work that used biocalorimetry as a tool for continuous on-line monitoring. Table shows the various types of modified calorimeter devices used, quoted working volumes, microorganisms investigated and heat production. N/R – not reported.

|                           | Reference                          | Working Volume (L) | Microorganism  | Heat Production (W.L <sup>-1</sup> ) | Biomass (g.L <sup>-1</sup> ) |
|---------------------------|------------------------------------|--------------------|--|--------------------------------------|------------------------------|
| <b>Micro-calorimeters</b> | Higuera-Guisset <i>et al.</i> 2005 | 0.0006             | <i>E.coli</i> K12 CGSC 5073  | 0.069                                | N/R                          |
|                           | Brettel <i>et al.</i> , 1980       | 1                  | <i>Saccharomyces cerevisiae</i>  | 1.8                                  | N/R                          |
|                           | Antoce <i>et al.</i> 2001          | 0.03 – 0.05        | <i>Saccharomyces cerevisiae</i> No. 9302                               | N/R                                  | N/R                          |
|                           | Ishikawa <i>et al.</i> 1981        | 1.2                | <i>E.coli</i> K12  | 0.016                                | N/R                          |
| <b>Macro-calorimeters</b> | <b>RCI Calorimeter</b>             |                    |  |                                      |                              |
|                           | Jassen <i>et al.</i> 2005          | 1.5                | <i>Chorella vulgaris</i> CCAP 211/11B                                  | 1                                    | N/R                          |
|                           | Voisard <i>et al.</i> 2002         | 1.5                | <i>Bacillus sphaericus</i> 1593M                                       | 9.33                                 | 7.5                          |
|                           | Bou-Diab <i>et al.</i> 2001        | 2                  | <i>Saccharomyces cerevisiae</i> GIV 2009                               | 2.55                                 | 21                           |
|                           | Voisard <i>et al.</i> 1998         | 2                  | <i>Bacillus sphaericus</i> 1593M<br><i>Saccharoployspora erythraea</i> | 1.65<br>1.43                         | N/R                          |
|                           | Vellanki 1998                      | 2                  | <i>Bacillus thuringiensis var galleriae</i>                            | 3.15                                 | N/R                          |
|                           | Randolph 1990                      | 2                  | <i>Saccharomyces cerevisiae</i> CBS 426                                | 7.8                                  | N/R                          |
|                           | <b>BSC-81 Calorimeter</b>          |                    |  |                                      |                              |
|                           | von Stockar and Birou 1989         | 1.35               | <i>Kluyveromyces fragilis</i> NRRL 1109                                | 0.7                                  | 1.9                          |
|                           | Birou <i>et al.</i> 1987           | 1.8                | <i>Kluyveromyces fragilis</i> NRRL<br><i>E.coli</i> W                  | 7.9<br>2.2                           | 7<br>2.3                     |
|                           | Marison and von Stockar 1985       | 1.8                | <i>E.coli</i> W  | 2.3                                  | 1.15                         |
|                           | <b>BFK calorimeter</b>             |                    |  |                                      |                              |
|                           | Maskow and Babel 1998              | 2                  | <i>Alcaligenes eutrophus</i> JMP 134                                   | 2                                    | N/R                          |
|                           | <b>Modified Bioreactor</b>         |                    |  |                                      |                              |
|                           | van Kleeff <i>et al.</i> 1992      | 1.5                | <i>Candida utilis</i>  | 4.67                                 | N/R                          |
|                           | This work                          | 0.1                | <i>E.coli</i> TOP10 pQR239   | 0.15                                 | 4.9                          |

This method also suffers from wall growth, particularly on the measuring cell, and blockages of sample lines with cultures of high cell density (Marison and von Stockar 1985; Voisard *et al.*, 2002).

Some workers have attempted to further overcome some of these difficulties by equipping small Calvet-type twin calorimeters with agitation and aeration devices (Ishikawa *et al.*, 1981). A fermenter vessel with similar characteristics to the calorimeter is operated in parallel under identical conditions, from which samples can be removed for analysis. Since this method is not *in-situ* and it is assumed that the growth conditions are identical in each vessel, these factors must be considered in the interpretation of the results (Marison and von Stockar 1985).

In more recent years a multiplex calorimeter that enables the monitoring of 24 microbial cultures simultaneously has been developed (Antoce *et al.*, 2001). This apparatus consists of an aluminium heat sink that holds 24 glass vials (30-50 mL) in individual copper wells. Initial studies with *Saccharomyces cerevisiae* have shown promising results for using calorimetric data to monitor cell growth. Higuera-Guisset and co-workers (2005) have reported on a miniaturised calorimeter (0.6 mL volume), based on silicon integrated thermopile chips for determining growth related heat production of microbial cultures. Studies were carried out using *E.coli* under different conditions, with the thermal profiles matching the typical exponential growth kinetics for the culture. Although these systems can provide valuable information about microbial growth kinetics based on heat measurements alone with potentially high throughput operation, they fail to simulate the conditions that would be experienced in a traditional bioreactor and lack the ability to monitor other critical process parameters such as pH and DOT.

#### 1.3.2.2.2 Macro-calorimetry

The challenging drawbacks of micro-calorimetry have been overcome by the advent of bench-scale calorimeters (macro-calorimeters), which closely resemble standard laboratory bioreactors with working volumes of at least 1 L (Marison *et al.*, 1998). Operation at this scale readily facilitates *in-situ* measuring techniques (Marison and

von Stockar, 1985). Developed first for chemical processes (Landau, 1996; Regenass, 1985), several researchers have adapted this technique to the study of living organisms (Marison and von Stockar, 1985; Birou *et al.*, 1987; von Stockar and Briou 1989; van Kleeff *et al.*, 1993; Marison *et al.*, 1998). As a result they have become very powerful tools for quantitative thermodynamic studies (Duboc and von Stockar, 1995) and for the reliable monitoring and control of many bioprocesses (Marison and von Stockar, 1986; Birou *et al.*, 1987; Randolph *et al.*, 1989; Meier-Schneiders *et al.*, 1995; van Kleeff *et al.*, 1996; von Stockar *et al.*, 1997; Voisard *et al.*, 1998; Duboc *et al.*, 1999).

The most widely reported bench-scale calorimeters that have been used for bioprocess applications include the RC1 (Marison *et al.*, 1998) developed by Mettler-Toledo AG, Switzerland and the BSC-81 (Meier-Schneiders *et al.*, 1995) calorimeter developed by Ciba-Geigy AG, Switzerland. Although these systems were originally associated with chemical reaction systems, they were modified to enable the cultivations of microorganisms under defined and sterile conditions similar to those in operation with a standard laboratory bioreactor.

The BioRC1 has been extensively used for studying a wide range of microbial and animal cell bioprocesses under batch, fed-batch and continuous operation. Voisard *et al.* (2002) successfully adapted the BioRC1 to perform as a conventional bioreactor and provide real-time quantitative and accurate measurements of the heat associated with a process. This work was validated by application to fed-batch cultures of *Bacillus sphaericus* 1593M. In these fed batch cultures, the nutrient feed was controlled using measurement of the metabolic heat release, since the latter is proportional to the substrate uptake rates for a given metabolic state. Earlier this strategy was used for the production of the antibiotic erythromycin by batch culture of *Saccharolopolyspora erythraea* (Voisard *et al.*, 1998). It was shown that calorimetry can indicate the two main phases of the process (growth and sporulation), the exact moment of any substrate depletion and the nature of the depleted substrate.

Consistent results have also been obtained using the BSC-81 biocalorimeter for a whole range of microbial strains and different carbon and energy substrates, showing that heat production correlates linearly with process variables such as biomass growth



and oxygen consumption (Birou *et al.*, 1987). This system has also been applied for investigation of different growth processes, growth by respiration and growth by fermentation for *K. fragilis* under aerobic and anaerobic conditions respectively (von Stockar and Birou, 1988).

Another route for incorporating heat measurements for monitoring and controlling bioprocesses simply involves equipping a standard bioreactor with the controls and measurements needed for a calorimeter (van Kleeff *et al.*, 1992; Meier-Schneiders and Schafer, 1996; Zentgraf 1996). The Berghof fermentation (BFK) calorimeter (Berghof Labor- und Automationstechnik GmbH, Germany) is a dedicated commercially available calorimeter for use in bioprocess applications (Meiers-Schneiders *et al.*, 1995; Maskow and Babel, 1998).

## **1.4 Aims of the project**

The overall aim of this work is to design and construct a novel miniature stirred bioreactor system which enables several experiments to be carried out in parallel and which is predictive of larger scales of operation. The need for such a device stems from the fact that there is not a single system available (Table 1.1) that has been demonstrated to satisfy all the requirements for fermentation process development in both industry and academia. As discussed in Sections 1.1.2.1 and 1.1.2.2 shake flasks and MTPs are popular for discovery research and initial screening studies given their medium to low cost and time constraints. However their application becomes limiting due to lack of instrumentation and the fact that these systems are not able to accurately mimic the conditions experienced in conventional bioreactors. Ideally any high throughput culture device should be able to evaluate as many key development stages as possible under production scale conditions. This enables the operator to potentially identify problems that may arise at larger scale and more importantly facilitate scale-up of desired process using defined scale up criteria. Miniature stirred bioreactors (Section 1.1.2.3) appear to fulfil the three key requirements and so will be the focus of this study: not only does the miniature bioreactor have the capability to mimic the conditions of larger scale vessels, but also provides same quantity of

information for a given process due to the high level of instrumentation available; also the time and cost of running several experiments is significantly reduced.

As already described in Table A.I.1 there are currently various miniature bioreactor system commercially available. A majority of these systems offer parallel operation with some level of instrumentation. However most of these are stirred using magnetic stirring bars or orbital shakers, hence failing to imitate the aeration and agitation conditions typically experienced in conventional bioreactors. Ultimately scale-up of processes is essential and there is limited information to suggest that the currently available systems have successfully demonstrated this. Also all the commercially available systems are instrumented with conventional probes or fluorescence sensors, and while the miniature bioreactor described herein is similarly instrumented, alternative methods of non-invasive on-line monitoring are also possible.

The primary objectives of the investigation are summarised below:

- The initial objective is to establish the design, construction and instrumentation of a novel, parallel miniature bioreactor system. The detailed design and instrumentation is discussed in Section 2.3, while Appendix I describes some of the commercial factors taken into account when first considering the design. Once fabricated, characterisation of the oxygen transfer capabilities as a function of agitation and aeration rates and parallel operation and control of the four pot miniature bioreactor system using *E. coli* TOP10 pQR239 and *B. subtilis* ATCC6633 is demonstrated. This is not only to confirm reproducibility of the results obtained but also to show that the system is sensitive to differences between microorganisms and operating conditions. The results of this work are presented and discussed in Chapter 3.
- Once the system has been characterised and reproducibility confirmed, its applicability as a tool for high throughput fermentation process development will be demonstrated. This will be via the use of Design of Experiments (DoE) and the demonstration of parallel experimentation. This study will also illustrate the operation of the miniature bioreactors over a range of operating conditions and set

points. The model system chosen for this investigation is based on optimising cell growth and cyclohexanone monooxygenase (CHMO) expression in *E.coli* TOP10 pQR239 by evaluating three critical factors: temperature, pH and L-arabinose concentration. These parameters are thought to have a significant effect on cell growth and enzyme production (Doig *et al.*, 2001; Stanbury *et al.*, 2003; Qader *et al.*, 2006). The DoE approach generates a series of experiments that allows the investigation of the key combinations of the critical parameters on the production of CHMO (Montgomery, 2005). Therefore fewer more relevant experiments are required providing more useful and precise information. The results of this work are presented and discussed in Chapter 4.

- The miniature bioreactor system will be further characterised in terms of power input and oxygen transfer. These results will be used to establish a predictive correlation for the miniature bioreactor relating  $P_g/V$  and  $k_{L,a}$  to bioreactor operating conditions. Scale-up based on constant  $P_g/V$  and  $k_{L,a}$  values will be assessed to establish the most suitable basis for scale translation from the miniature bioreactor to a conventional 2 L bioreactor. The most suitable scale-up criterion will be further verified and used for the scale-up of the DoE results from chapter 4, in order to achieve accurate reproduction of the optimum miniature bioreactor results at the laboratory scale. The results of this work are presented and discussed in Chapter 5.
- Given the ability for one operator to run multiple miniature bioreactors in parallel, the final objective of this work is to establish a number of on-line methods to facilitate the on-line estimation of biomass growth. This will enable *in-situ* collection and quantification of biomass growth kinetic data. In particular two approaches will be examined, a novel optical density probe for monitoring changes in culture absorbance and thermal profiling techniques for monitoring changes in culture heat generation. The results of this work are presented and discussed in Chapter 6.

## 2. MATERIALS AND METHODS

---

---

### 2.1 Reagents and Suppliers

All reagents used in this work were of the highest purity available and were obtained from Sigma-Aldrich (Dorest, UK), apart from the following: tryptone, yeast extract, glycerol, polypropylene glycol 2000 and L-arabinose, all of which were obtained from BDH (Dorset, UK). Reverse osmosis (RO) water was used in all experimental work.

### 2.2 Source and Maintenance of Microorganisms

#### 2.2.1. *Escherichia coli* TOP10 pQR239

*E. coli* TOP10 pQR239 was available within the Department of Biochemical Engineering, UCL, having been engineered for previous studies (Doig *et al.*, 2001; Lander 2003). Stock cultures for this project were prepared initially from an individual colony grown overnight at 37 °C on an agar plate containing LB nutrient broth and 50 mg.L<sup>-1</sup> ampicillin. This was inoculated into a sterile 1 L shake flask containing 100 mL of the growth medium described in Table 2.1, to which 50 mg.L<sup>-1</sup> ampicillin had been added via a 0.2 µm syringe filter (Fisher Scientific, UK). When the culture had grown to a biomass concentration of approximately 1 g.L<sup>-1</sup>, 50 % v/v of sterile glycerol was mixed in aseptically and 1 mL aliquots were frozen and stored at -80 °C. These stock cultures were then used throughout the rest of this work.

*E. coli* TOP10 pQR239, expresses the cyclohexanone monooxygenase (CHMO) from *Acinetobacter calcoaceticus* upon induction with L-arabinose. The engineering of this strain involved first cloning the CHMO gene from *A. calcoaceticus* into the *E. coli* expression vector pKK223-3. This was then subcloned into the pBAD vector thus

allowing L-arabinose inducible expression of CHMO. The methods used and detailed cloning procedures have been previously described by Doig and co-workers (2001).

**Table 2.1.** Composition of the growth medium used in all *E.coli* TOP10 pQR239 fermentations.

| Medium Component | Concentration (g.L <sup>-1</sup> ) |
|------------------|------------------------------------|
| Yeast extract    | 10.0                               |
| Tryptone         | 10.0                               |
| Glycerol         | 10.0                               |
| NaCl             | 10.0                               |
| Antifoam         | 0.2                                |

### 2.2.2. *Bacillus subtilis* ATCC6633

*B. subtilis* ATCC6633 was sourced from a stock culture available within the Department of Biochemical Engineering, UCL and fresh stock cultures for use in this project were prepared initially from an individual colony grown overnight at 32 °C on an agar plate containing LB nutrient broth. This was then inoculated into a sterile 1 L shake flask containing 100 mL of the chemically defined growth medium described in Table 2.2. This growth medium was prepared and sterilised in five separate fractions as indicated in Table 2.2. When the culture had grown to a biomass concentration of approximately 2 g.L<sup>-1</sup>, 50 % v/v of sterile glycerol was mixed in aseptically and 1 mL aliquots were frozen and stored at -80 °C. These stock cultures were then used throughout the rest of this investigation.

**Table 2.2.** Composition of the growth medium used in all *B. subtilis* ATCC6633 fermentations. Note that fraction 5, the trace metals were prepared as an acidified solution (pH 1).

| Medium Fraction | Volume (mL) per Litre of Complete Medium | Medium Component                                     | Concentration (g.L <sup>-1</sup> ) |
|-----------------|--|--|------------------------------------|
| 1               | 100                                      | D-glucose  | 200.0                              |
| 2               | 895                                      | (NH <sub>4</sub> ) <sub>2</sub> SO <sub>4</sub>      | 11.2                               |
|                 |  | KH <sub>2</sub> PO <sub>4</sub>                      | 15.2                               |
|                 |  | K <sub>2</sub> HPO <sub>4</sub>                      | 12.1                               |
|                 |  | Na <sub>2</sub> HPO <sub>4</sub>                     | 4.0                                |
|                 |  | Antifoam   | 1.1                                |
| 3               | 2  | MgSO <sub>4</sub> .7H <sub>2</sub> O                 | 246.0                              |
| 4               | 1  | CaCl <sub>2</sub> .2H <sub>2</sub> O                 | 147.0                              |
| 5               | 2  | FeSO <sub>4</sub> .7H <sub>2</sub> O                 | 40.0                               |
|                 |  | MnSO <sub>4</sub> .H <sub>2</sub> O                  | 5.0                                |
|                 |  | CoCl <sub>2</sub> .6H <sub>2</sub> O,                | 2.0                                |
|                 |  | ZnSO <sub>4</sub> .7H <sub>2</sub> O,                | 1.0                                |
|                 |  | MoO <sub>4</sub> Na <sub>2</sub> .2H <sub>2</sub> O, | 1.0                                |
|                 |  | CuCl <sub>2</sub> .2H <sub>2</sub> O                 | 0.5                                |
|                 |  | H <sub>3</sub> BO <sub>3</sub>                       | 2.0                                |

## 2.3 Miniature Bioreactor Design, Instrumentation and Control

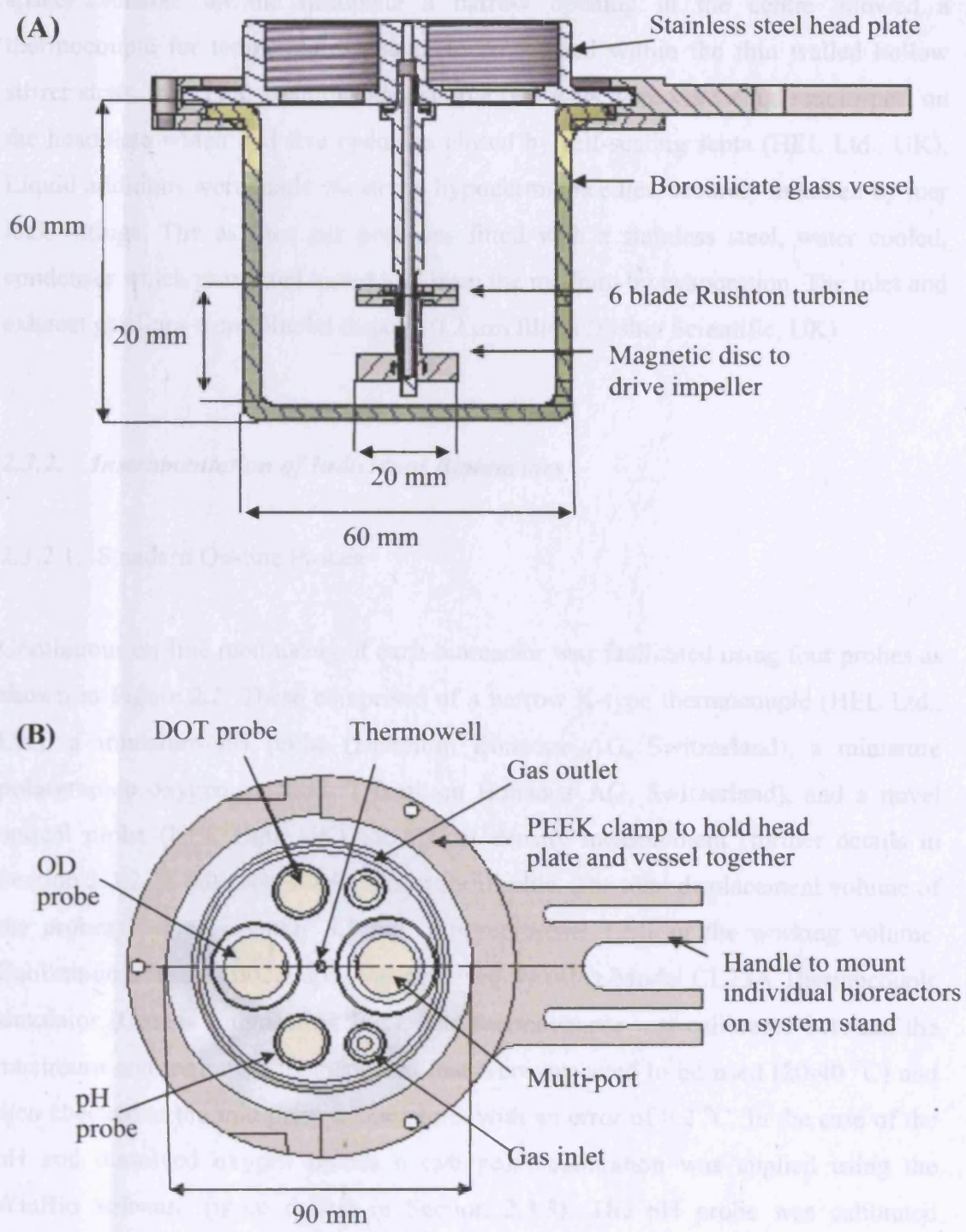
### 2.3.1. Design of Individual Bioreactors

Each miniature bioreactor was designed to be as geometrically similar to conventional laboratory scale stirred fermenters as possible. All bioreactors consisted of a borosilicate glass vessel (100 mL maximum working volume), allowing visual inspection of the contents. This was sealed with a stainless steel head plate, as shown in Figure 2.1 (detailed mechanical drawings can be seen in Appendix A.II).

Mixing of the bioreactor was achieved by a magnetically driven, six-blade Rushton turbine impeller ( $d_i = 20$  mm,  $d_i/d_T = 1/3$ ) fabricated from PEEK (poly-ether ether ketone). There was a distance of 20 mm between the centre line of the Rushton turbine and the base of the vessel ( $d_i/h_i = 1$ ). Eight cylindrical magnets (3 mm in diameter and 2 mm long) were uniformly distributed and embedded into a small PEEK disc 10 mm below the Rushton turbine as shown in Figure 2.1(A). The whole PEEK impeller structure was mounted onto a hollow, non-rotating stainless steel stirrer shaft that screwed into the headplate of the bioreactor. This design eliminated the need for rotating mechanical seals and increased the area available on the headplate for other ports. The PEEK impeller assembly, which was magnetically driven from below, had a stirring range of 100 - 2000 rpm.

Each bioreactor was also equipped with four equally spaced removable baffles of width 6 mm ( $d_B/d_T = 1/10$ ). Aeration of the vessel was via a narrow sparger located directly beneath the Rushton turbine. The sparger was fitted with a 15  $\mu\text{m}$  stainless steel sinter to create finer gas bubbles and promote more efficient oxygen transfer. The air flow rate was manually regulated by a standard laboratory rotameter in the range 0 - 200  $\text{mL}\cdot\text{min}^{-1}$  (Fisher Scientific, UK) and it was possible to use atmospheric air alone or oxygen-enriched air via a gas blending system (HEL Ltd., UK).

As shown in Figure 2.1(B), the headplate accommodated a total of four probes for continuous on-line monitoring of pH, dissolved oxygen tension (DOT), optical density (OD) and temperature as described in Section 2.3.2. As a result of the limited



**Figure 2.1.** Mechanical drawing showing key design features and dimensions of an individual miniature bioreactor: (A) cross section through bioreactor; (B) plan view of head plate. Further details given in Section 2.3.1.



space available on the headplate a narrow opening in the centre allowed a thermocouple for temperature sensing to be located within the thin walled hollow stirrer shaft. All liquid additions and sample removals were via a single multi-port on the headplate which had five openings closed by self-sealing septa (HEL Ltd., UK). Liquid additions were made via sterile hypodermic needles, securely mounted by luer lock fittings. The exhaust gas port was fitted with a stainless steel, water cooled, condenser which prevented liquid loss from the medium by evaporation. The inlet and exhaust gas lines were filtered through 0.2  $\mu\text{m}$  filters (Fisher Scientific, UK).

### **2.3.2. Instrumentation of Individual Bioreactors**

#### **2.3.2.1. Standard On-line Probes**

Continuous on-line monitoring of each bioreactor was facilitated using four probes as shown in Figure 2.2. These comprised of a narrow K-type thermocouple (HEL Ltd., UK), a miniature pH probe (Hamilton Bonaduz AG, Switzerland), a miniature polarographic oxygen electrode (Hamilton Bonaduz AG, Switzerland), and a novel optical probe (HEL Ltd., UK) for optical density measurement (further details in Section 2.3.2.2). All probes were steam sterilisable. The total displacement volume of the probes is approximately 3.5 mL, this represents 3.5% of the working volume. Calibration of the thermocouple was achieved by using Model CL23A Thermocouple simulator (Omega Engineering Inc.). The thermocouple was calibrated between the maximum and minimum temperatures that were expected to be used (20-40 °C) and then checked at the mid point temperature, with an error of 0.2 °C. In the case of the pH and dissolved oxygen probes a two point calibration was applied using the WinBio software (more details in Section 2.3.3). The pH probe was calibrated between pH 4 and 7. The dissolved oxygen probe was calibrated *in-situ* in bio-medium, following sterilisation at the fermentation operating temperature. The probe was calibrated at 100% in media saturated with compressed air, while zero was set by sparging to 0% using nitrogen gas.

### 2.3.2.2 Novel Optical Density Probe

The optical probe was designed for biomass growth. Figure 2.2 (A) shows the thermocouple probe, which had a FLUKA body and was used to measure the temperature of the culture. Figure 2.3 (B) had a white light source and a photodiode detector. The light source and detector were placed directly opposite each other and the probe was inserted into the bioreactor at an angle to the direction of the light beam. The output of the probe was a signal that was proportional to the optical density of the broth. The light source was a white light emitting diode (LED) and the detector was a photodiode. The light source and detector were housed in a stainless steel probe with a diameter of 1.5 mm. The optical density of the broth was measured at a wavelength of 660 nm. The optical density of the broth was measured at a wavelength of 660 nm. The optical density of the broth was measured at a wavelength of 660 nm.



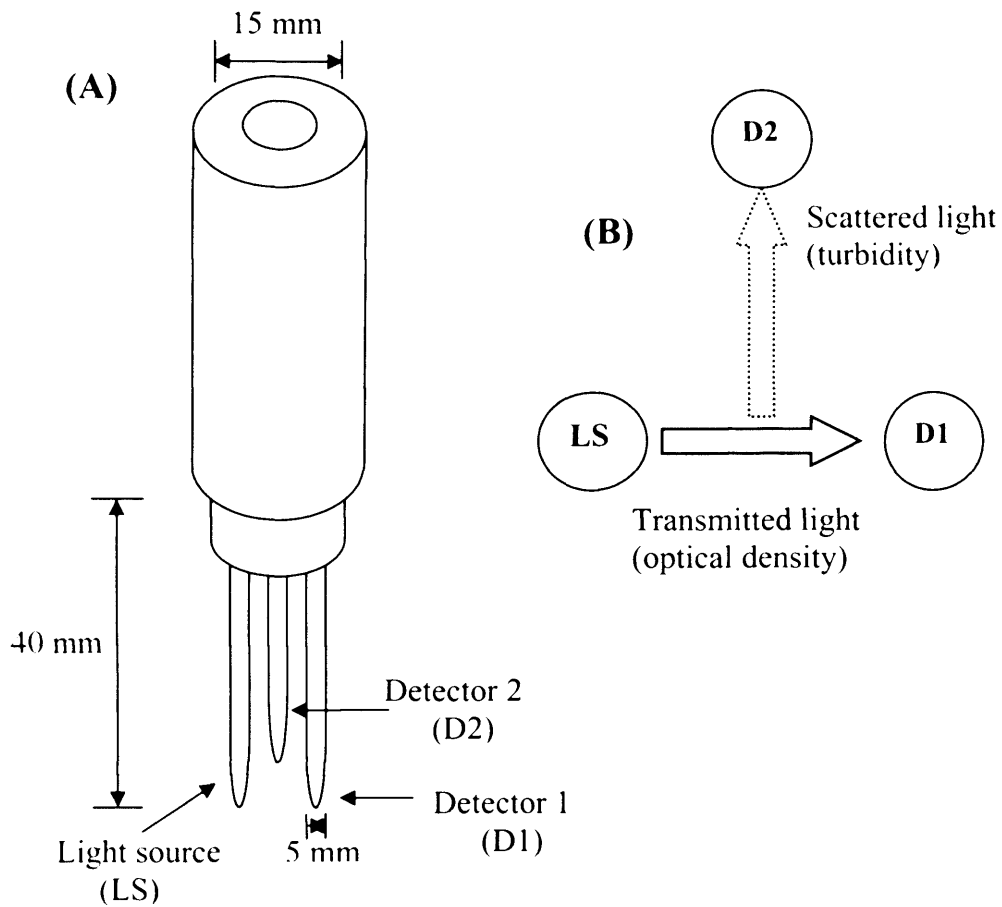
**Figure 2.2.** Miniature probes for continuous on-line monitoring of each bioreactor: (A) thermocouple; (B) pH probe; (C) dissolved oxygen probe; (D) optical density probe.

#### 2.3.2.2. Novel Optical Density Probe

The optical probe provided continuous on-line information for biomass growth. Figure 2.3 (A) shows a schematic diagram of the probe which had a PEEK body and was sized to fit each bioreactor headplate. The end of the probe, Figure 2.3 (B), had a white light source and two detectors that were each located in sealed glass tubes. The light source (LS) and one of the detectors (D1) were positioned directly opposite each other approximately 10 mm apart. D1 thus gave a direct measurement of the optical density of the broth. A second detector (D2) was placed at right angles to the direction of transmitted light approximately 5 mm away from the beam. The output of this second detector measured the amount of light scattered by the broth. The light source had a sufficiently narrow angle of emission such that any light reaching the right-angle detector (D2) by direct transmission was considered negligible. In this work only the data from the optical density signal (D1) is reported. The optical density probe was calibrated using clear sterile biomedium and a solution of known optical density.

#### 2.3.2.3. Thermal Profiling Studies

The miniature bioreactor design also incorporated the possibility to perform thermal profiling studies. Any heat generated within the bioreactor as a result of microbial growth was indirectly measured by monitoring the requested power of the external heater placed beneath the vessel throughout the fermentation. Initially the heater turned on at a given level to achieve the required temperature; it then constantly adjusted its level (increasing or decreasing) according to the surrounding environment to ensure the temperature remained at the set point value throughout the experiment; this is discussed in further detail in Section 6.3. A calibration curve translating the requested power of the heater into a more useful measurement of power generated by the microbial culture was constructed and is shown in more detail in Appendix A.VIII. Subsequent energy calculations were carried out with the aid of IQ software (HEL Ltd., UK).



**Figure 2.3.** Schematic diagram of *in-situ* optical density probe: (A) dimensions of probe; (B) arrangement of light source and detectors. Further details given in Section 2.3.2.2.

All the *E. coli* TOP10 pQR239 fermentations carried out in the miniature bioreactor for the thermal profiling studies were set-up and performed as described in Sections 2.6.1.1 and 2.6.1.2. The agitation and aeration rates for all fermentations were controlled at 1000 rpm and 1 vvm respectively. In addition to this, the miniature bioreactor was heavily lagged with glass fibre insulating wool (HEL Ltd, UK) to ensure heat losses remained constant throughout the experiment.

### **2.3.3. Design and Control of Parallel Bioreactor Systems**

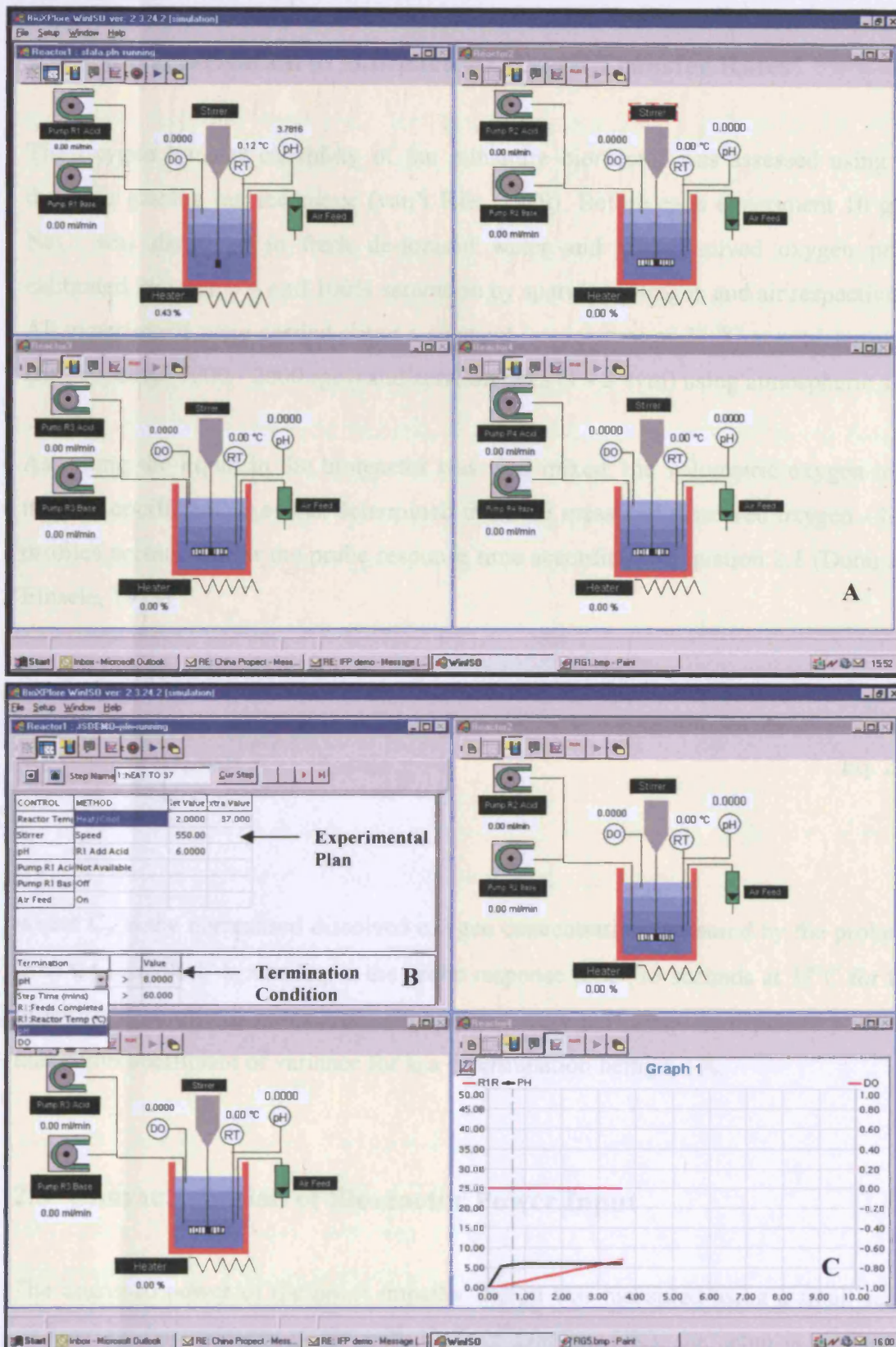
To support the individual bioreactors a prototype modular base unit was designed and built which securely located four miniature bioreactors and their respective peristaltic pumps (RS Components Ltd, UK), rotameters and magnetic drive assemblies. Electrical disc heaters for temperature control were also integrated into the base unit and positioned beneath each miniature bioreactor. Cables from the various probes plugged into the base unit which housed all the associated electronics creating a compact unit with a footprint of 480 by 362 mm, Figure 2.4. Up to four of these modular base units can be used in a single system.

A custom piece of PC-based software (WinBio) was written which allowed independent monitoring and control of up to 16 miniature bioreactors. This was based on an architecture originally used for control of automated chemical reactors that has been reported to be easily programmed and simple to use (Van Loo and Lengowski, 2002). Experiments with multiple operating conditions and set points could be conducted by generating an experimental plan that dictated which piece of equipment should be running and what it was required to do. Each experimental plan can consist of several steps with each step being carried out automatically in sequence. The end to each step is specified by a terminating condition, which is any parameter defined by the user, e.g., time, temperature, pH, OD, DOT etc. The software also enabled key parameters such as pH, DOT, temperature and optical density to be displayed in real time on interactive graphs for each bioreactor. Figure 2.5 further illustrates the main features and screens that can be viewed when operating the WinBio software.



**Figure 2.4.** Photograph of prototype four-pot miniature bioreactor system

Figure 2.4 shows a feature of the WinCC software showing: (A) simultaneous display of all four individual bioreactor supervisory windows; (B) an example of an experimental plan and the various terminating conditions; (C) real time interactive graphs showing culture progress.



**Figure 2.5.** Main features of the WinBio software showing: (A) simultaneous display of all four individual bioreactor supervisory windows; (B) an example of an experimental plan and the various terminating conditions; (C) real time interactive graphs showing culture progress.

## 2.4 Characterisation of Bioreactor Oxygen Transfer Rates

The oxygen transfer capability of the miniature bioreactor was assessed using the dynamic gassing out technique (van't Riet, 1979). Before each experiment 10 g.L<sup>-1</sup> NaCl was dissolved in fresh de-ionised water and the dissolved oxygen probe calibrated between 0% and 100% saturation by sparging nitrogen and air respectively. All experiments were carried out at a constant temperature of 37 °C at predetermined stirrer speeds (1000 - 2000 rpm) and aeration rates (1 - 2 vvm) using atmospheric air.

Assuming the liquid in the bioreactor was well mixed, the volumetric oxygen mass transfer coefficient,  $k_La$ , was determined from the measured dissolved oxygen - time profiles accounting for the probe response time according to Equation 2.1 (Dunn and Einsele, 1975):

$$C_p = \frac{1}{t_m - \tau_p} \left[ t_m \exp\left(\frac{-t}{t_m}\right) - \tau_p \exp\left(\frac{-t}{\tau_p}\right) \right] \quad \text{Eq. 2.1}$$

where  $C_p$  is the normalised dissolved oxygen concentration measured by the probe at time  $t$ ,  $t_m$  equals  $1/k_La$  and  $\tau_p$  is the probe response time (18 seconds at 37°C for the probe used here). All gassing out experiments were performed in triplicate with the maximum coefficient of variance for  $k_La$  determination being 6.1%.

## 2.5 Characterisation of Bioreactor Power Input

The ungasped power of the novel impeller design was measured using a small scale air bearing dynamometer (University College London, UK); the setup is similar to that described by Nienow and Miles (1969). The glass vessel from the miniature bioreactor ( $d_T = 60$  mm) fitted with four equidistant baffles containing 100 mL of RO water, was mounted onto the top plate of the air bearing (96 mm Ø). The miniature



bioreactor impeller ( $d_i = 20$  mm) was then located vertically in the vessel. In order to facilitate power measurements this was driven by an overhead electric motor, and positioned such that there was clearance of 20 mm from the base of the vessel. Further details of the impeller are given in Figure 2.6.

The air bearing consisted of two main elements: one static (lower section) and the other a floating top plate (upper section), air was introduced into the static section, enabling free and essentially frictionless movement of the top plate. The resulting torque generated by the rotating stirrer in the liquid caused the vessel to freely rotate with the top plate in the same direction as the impeller. A rigid arm that was fixed to the top plate of the air bearing enabled the torque to be measured as a force transmitted to a pre-calibrated force sensor (FS Series, Honeywell, USA). From these measurements the power draw can be calculated from:

$$P = FR\omega \quad \text{Eq. 2.2}$$

where  $P$  is the power,  $F$  is the force applied,  $R$  is the length of the arm pressing against the force sensor and  $\omega$  is the angular velocity, given by:

$$\omega = 2\pi N \quad \text{Eq. 2.3}$$

where  $N$  is the stirrer speed. The gassed power input of the impeller was measured in exactly the same way as described above but, with a sintered sparger fitted along side the stirrer in the vessel. Aeration rates were varied between 1-2 vvm. All measurements of power were performed in triplicate with the maximum coefficient of variance of 3.5%.

## 2.6 Description of Parallel Bioreactor Operation and Reproducibility

### 2.6.1. Effect of Parallel Bioreactor Configuration

#### 2.6.1.1.

#### 2.6.1.2.

#### 2.6.1.3.

#### 2.6.1.4.

#### 2.6.1.5.

#### 2.6.1.6.

#### 2.6.1.7.

#### 2.6.1.8.

#### 2.6.1.9.

#### 2.6.1.10.

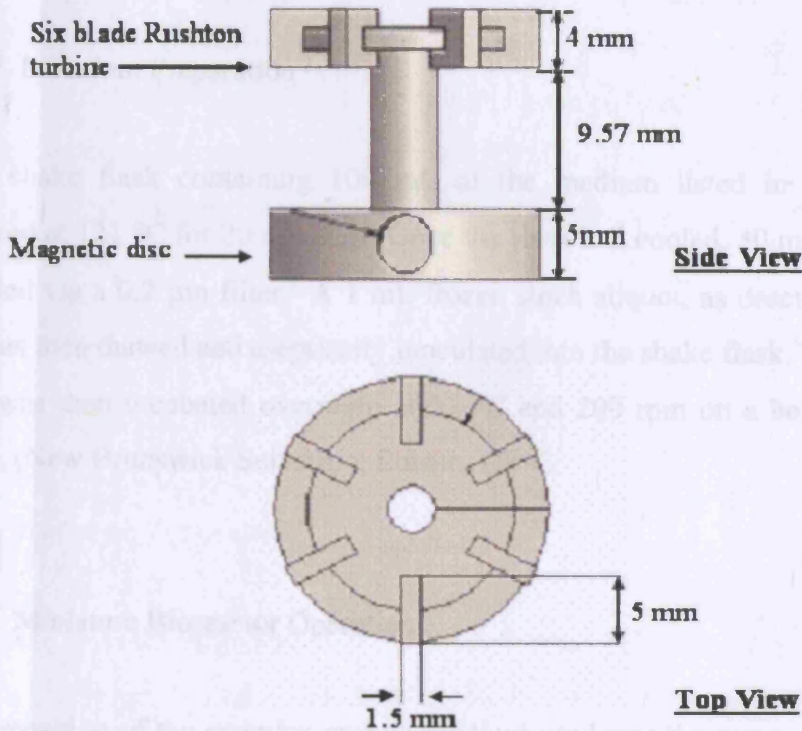
#### 2.6.1.11.

#### 2.6.1.12.

#### 2.6.1.13.

#### 2.6.1.14.

#### 2.6.1.15.



**Figure 2.6.** Mechanical drawing showing key design features and dimensions of a single miniature bioreactor and the novel magnetically driven turbine impeller design. Further details given in Sections 2.3.1 and 2.5.

## 2.6 Demonstration of Parallel Bioreactor Operation and Reproducibility

### 2.6.1. *E.coli TOP10 pQR239 Fermentations*

#### 2.6.1.1. Inoculum Preparation

A 1 L shake flask containing 100 mL of the medium listed in Table 2.1 was autoclaved at 121 °C for 20 minutes. Once the flask had cooled, 50 mg.L<sup>-1</sup> ampicillin was added via a 0.2 µm filter. A 1 mL frozen stock aliquot, as described in Section 2.2.1, was then thawed and aseptically inoculated into the shake flask. The shake flask culture was then incubated overnight at 37 °C and 200 rpm on a horizontal shaken platform (New Brunswick Scientific, Edison, USA).

#### 2.6.1.2. Miniature Bioreactor Operation

The composition of the complex growth medium used was the same as for inoculum preparation and is shown in Table 2.1. Each miniature bioreactor was sterilised as a complete unit (121°C for 20 minutes) containing 100 mL of all media components (apart from ampicillin) and 0.2 mL.L<sup>-1</sup> of added antifoam (polypropylene glycol 2000). After cooling the temperature was maintained at 37 °C, and filter sterilised (0.2 µm) ampicillin was added immediately prior to inoculation. Each bioreactor was inoculated with 2 mL (2% v/v inoculum) of overnight culture, prepared as described in Section 2.6.1.1. The pH was controlled at 7 (± 0.1) by the metered addition of 3M NaOH and 3M H<sub>3</sub>PO<sub>4</sub>. Agitation rates in the miniature bioreactors were varied between 1000 - 2000 rpm and aeration rates varied between 1 - 2 vvm. Fermentations were performed in parallel on a four pot system either under identical agitation and aeration conditions (to show reproducibility) or under different agitation and aeration conditions (to show parallel evaluation of fermentation conditions). All fermentations were performed in batch mode. The progress of the fermentation was monitored by on-line measurements (Section 2.3.2) as well as by taking regular OD<sub>600</sub> measurements, as described in Section 2.9.1.2.

### 2.6.1.3. Oxygen Enriched Fermentations

A gas blending device was integrated into the four pot miniature bioreactor system providing aeration using oxygen enriched air and allowing the DOT to be accurately controlled at specific set point values. A number of experiments were performed with the DOT set point of 30% or 50%. Both air and oxygen were fed into the gas blender and mixed according to the demand of the fermentation. Preparation and operation for all oxygen enriched fermentations were carried out as described in Section 2.6.1.1 and 2.6.1.2. Aeration and agitations rates were maintained at 2000 rpm and 2 vvm respectively.

### 2.6.2. *B. subtilis ATCC6633 Fermentation*

#### 2.6.2.1. Inoculum Preparation

A 1 L shake flask containing medium fraction 2 listed in Table 2.2 was autoclaved at 121 °C for 20 minutes. The remaining 4 medium fractions were autoclaved separately under identical conditions and aseptically added to the shake flask following sterilisation. Following this a 1 mL frozen stock aliquot, as described in Section 2.2.2, was then thawed and aseptically inoculated into the shake flask. The culture was then incubated for 24 h at 32 °C and 300 rpm on a horizontal shaken platform.

#### 2.6.2.2. Miniature Bioreactor Fermentation Operation

The composition of the chemically defined growth medium used was the same as for inoculum preparation and is shown in Table 2.2. The media components were prepared and sterilised (121°C for 20 minutes) in five separate groups. Each miniature bioreactor was sterilised as a complete unit (121°C for 20 minutes) containing only group 2 media components. After cooling the temperature was maintained at 32 °C and the remaining groups of media components were added aseptically immediately prior to inoculation. Each bioreactor was inoculated with 10 mL (10% v/v inoculum)

of broth from a shake flask culture, prepared as described in Section 2.6.2.1. The pH was controlled at 6.8 ( $\pm 0.1$ ) by the metered addition of 3M NaOH and 3M H<sub>3</sub>PO<sub>4</sub>. Agitation and aeration rates for all four miniature bioreactors were controlled at 1500 rpm and 1 vmm respectively. The progress of the fermentation was monitored by on-line measurements (Section 2.3.2) as well as by taking regular OD<sub>600</sub> measurements, as described in Section 2.9.1.2.

## 2.7 Fermentation Optimisation using Design of Experiments

### 2.7.1. Design of Experiments (DOE)

Response surface methodology (RSM) consists of mathematical techniques devoted to the evaluation of the relationship between a group of controlled experimental factors and the measured response, according to one or more selected criteria. Some prior knowledge and understanding of the process and process variables under investigation is necessary to achieve the most realistic model of process performance (Adinarayana and Ellaiah, 2002). The central composite face (CCF) experimental design was used to optimise biomass growth and CHMO expression in *E.coli* TOP10 pQR239. The experiments were designed using MODDE 7 software (Umetrics Ltd, UK).

Temperature, L-arabinose (inducer) concentration and pH were the key independent variables chosen for investigation, and the range specified for each variable was 35-39 °C, 0.05-0.15 % w/w L-arabinose concentration and pH 6-8 respectively. The CCF design determined a total of twenty experiments with six replicates at the centre points needed for the optimisation of these three independent variables. In developing the regression equation the variables were coded according to the equation:

$$x_i = \frac{(X_i - \bar{X}_i)}{\Delta X_i} \quad i = 1, 2, 3, \dots, k, \quad \text{Eq. 2. 4}$$

where  $x_i$  is a dimensionless value of an independent variable,  $X_i$  is the real value of an independent variable,  $\bar{X}_i$  is the real value of an independent variable at the centre point and  $\Delta X_i$  is the step change value.

The biomass concentration and CHMO activity were taken as the dependent variables or response,  $Y_i$ . Regression and graphical analysis was performed on the data obtained from twenty experiments using MODDE 7 software. A second order polynomial, Equation 2.5, which includes all the interacting terms, is used to calculate the predicted response:

$$Y_i = \beta_0 + \beta_1 x_1 + \beta_2 x_2 + \beta_3 x_3 + \beta_{11} x_1^2 + \beta_{22} x_2^2 + \beta_{33} x_3^2 + \beta_{12} x_1 x_2 + \beta_{13} x_1 x_3 + \beta_{23} x_2 x_3$$

Eq. 2.5

where  $Y_i$  is the predicted response,  $x_1$ ,  $x_2$  and  $x_3$  are independent variables,  $\beta_0$  is the constant term,  $\beta_1$ ,  $\beta_2$  and  $\beta_3$  are linear effects,  $\beta_{11}$ ,  $\beta_{22}$  and  $\beta_{33}$  are squared effects, and  $\beta_{12}$ ,  $\beta_{13}$  and  $\beta_{23}$  are interaction terms. Using the software package the second order polynomial coefficients ( $\beta_i$ ) were calculated to estimate the responses of the dependent variables. The optimum combinations of the selected independent variables were determined by optimising the regression equation and also by analysing the response surface plot using MODDE 7.

### **2.7.2. Fermentation Operation and CHMO Induction**

Fermentations carried out as part of the DoE investigation were prepared and operated as described in Section 2.6.1.1 and 2.6.1.2, with agitation and aeration rates maintained to 1000 rpm and 1 vvm throughout all fermentations. Temperature and pH were controlled at 35, 37 or 39 °C and 6, 7, or 8 respectively according to the experimental design matrix (Table 4.1). Induction was performed during the mid log phase at approximately 240 minutes into the fermentation when the DOT was less than 5% (Doig *et al.*, 2001). Concentrated L-arabinose solution was added via a 0.2  $\mu$

m filter to a final concentration of 0.05, 0.1 or 0.15 % w/v as required. This induced the expression of CHMO by the recombinant *E.coli* TOP10 pQR239 cells. Biomass and CHMO activity assays were performed after 420 minutes for each fermentation as described in Section 2.9.1.1 and 2.9.2.

## **2.8 Scale-up of Miniature Bioreactor Fermentations**

### **2.8.1. Miniature Bioreactor Fermentations**

All miniature bioreactor fermentations performed for scale comparison purposes were prepared and operated as described in Sections 2.6.1.1 and 2.6.1.2. Fermentations were performed at three different  $P_g/V$  and  $k_{La}$  values of, 657, 1487 and 2960  $W.m^3$  and 0.06, 0.08 and 0.11  $h^{-1}$  respectively. The corresponding agitation and aeration rates in the miniature bioreactors are given in Table 5.3 and 5.4.

### **2.8.2. 2 L Laboratory Scale Bioreactor**

#### **2.8.2.1. Bioreactor Design and Instrumentation**

The laboratory scale fermentations were carried out in a 2 L (1.5 L working volume) LH 210 series laboratory scale bioreactor (Bioprocess Engineering Services, Kent, UK). The bioreactor itself comprised a glass vessel fitted with four equally spaced baffles and two top driven six blade Rushton turbines. The ratio of the impeller diameter to the vessel diameter ( $d_i/d_T$ ) was 0.33. pH was measured using a steam sterilisable Ingold pH probe (Ingold Messtechnik, Urdorf, Switzerland) and controlled at pH 7 ( $\pm 0.05$ ) by the metered addition of 3M NaOH and 3M  $H_3PO_4$ . Dissolved oxygen was measured using a polarographic oxygen electrode (Ingold Messtechnik, Urdorf, Switzerland) and the temperature was maintained at 37 °C using a temperature probe and heating element. The inlet and exhaust gases were filtered through 0.2  $\mu m$  filters (Fisher Scientific, UK). Data logged from the fermenter itself, e.g. impeller speed, pH, DOT etc. and exhaust gas measurements were recorded with

the RT-DAS program (real-time data acquisition system) (Acquisition Systems, Guildford, Surrey, UK).

#### 2.8.2.2. Bioreactor Operation at Matched $P_g/V$ and $k_{La}$

The composition of the complex growth medium used is shown in Table 2.1 and is identical to that used in miniature bioreactor experiments. In addition antifoam (polypropylene glycol 2000) was added to a final concentration of approximately  $0.2 \text{ mL.L}^{-1}$  in the bioreactor. The bioreactor, containing initially 1.5 L of medium and ancillary equipment was sterilised by autoclaving at  $121 \text{ }^\circ\text{C}$  for 20 minutes. After cooling the fermenter to  $37 \text{ }^\circ\text{C}$ , aqueous ampicillin solution was added via a  $0.2 \text{ }\mu\text{m}$  filter prior to inoculation. The bioreactor was inoculated with 30 mL of overnight culture (2% v/v inocula) prepared as described in Section 2.6.1.1.  $P_g/V$  and  $k_{La}$  values used in the corresponding miniature bioreactor experiments and vessel agitation and aeration rates are summarised in Table 5.3 and 5.4. The progress of the fermentation was followed by taking  $\text{OD}_{600}$  measurements, as described in Section 2.9.1.2.

#### 2.8.2.3. Scale-up of DoE Optimised Fermentation Conditions

In order to further assess the most reliable scale-up criteria established from experiments in Section 2.8.2.2, the optimum combinations of operating parameters (temperature, pH and L-arabinose) predicted by the DoE analysis were scaled up to the 2 L laboratory scale. These experiments were performed at matched  $k_{La}$  of  $0.04 \text{ s}^{-1}$ . The 2 L bioreactor fermentations were carried out as described in Section 2.8.2.1 and 2.8.2.2. In this case CHMO expression was induced with the predicted optimum concentration of L-arabinose solution which was added to the vessel via a  $0.2 \text{ }\mu\text{m}$  syringe filter. This was performed during the late log phase at approximately four hours into the fermentation when the DOT was less than 5%.



## **2.9 Analytical Techniques**

### ***2.9.1. Biomass Quantification***

#### **2.9.1.1. Dry Cell Weight (DCW) Measurement**

To pre-dried and pre-weighed 2.2 mL Eppendorf tubes, 2 mL aliquots of cell culture were added and the tubes centrifuged (Eppendorf AG, Germany) at 13000 rpm for 2 minutes. The supernatant was discarded and the cell pellets were washed once with 10 g.L<sup>-1</sup> NaCl solution and dried at 100°C for 24 hours. The DCW of the culture could then be calculated. All the biomass concentrations subsequently reported in this thesis are on a DCW basis. The coefficient of variance for an individual DCW measurement was determined from triplicate measurements of each of seven cell suspensions (concentration range 2.0-6.3 g.L<sup>-1</sup>) and found to be  $\pm 7.7\%$ .

#### **2.9.1.2. Optical Density (OD) Measurement**

In addition to on-line OD measurements used to quantify biomass concentrations (Section 2.2.2 and 6.2), OD was also measured off-line at 600 nm (OD<sub>600</sub>) using a Ultraspec 4000 variable wavelength spectrophotometer (Pharmacia Biotech, USA). A small quantity of culture medium was withdrawn from the bioreactors and diluted appropriately with RO water so that the optical density measurement was between 0.1-0.8 absorbance units. A calibration curve linking the OD<sub>600</sub> measurement from a serial dilution of broth sample to the corresponding DCW measurement was constructed and is shown in Appendix A.III.

## 2.9.2. Spectrophotometric Measurement of CHMO Activity

### 2.9.2.1. Preparation of Crude Cell Extract

Since CHMO is produced intracellularly by the recombinant *E.coli* TOP10 pQR239, it was first necessary to prepare a crude cell extract for the subsequent assay. 1 mL samples of the fermentation broth were centrifuged for 2 minutes at 13,000 rpm (Biofuge 13, Heraeus Sepatech, Brentwood, Essex, UK) and the resulting cell pellet resuspended in reaction buffer (50 mM Tris-HCl with 7.14 g.L<sup>-1</sup> bovine serum albumin at pH 9). The sample was sonicated (cycling programme of 5 x 10 s on, 10 s off) on ice at an amplitude of 8µm (Soniprep 150 MSE, Sanyo, Crawley, West Sussex, UK) followed by re-centrifugation for 2 minutes at 13,000 rpm to remove any insoluble cell debris. The resulting supernatant was kept on ice and then variously diluted with reaction buffer prior to the enzyme assay.

### 2.9.2.2. NADPH Linked Spectrophotometric Assay

The spectrophotometric assay for measurement of isolated CHMO activity was based on the rate of NADPH utilisation upon the addition of cyclohexanone and NADPH to CHMO containing samples. NADPH absorbs strongly at 340nm ( $\epsilon = 6.22 \text{ mL} \cdot \mu\text{mol}^{-1} \text{ cm}^{-1}$ ) and its consumption is stoichiometrically linked to product formation in reactions catalysed by CHMO. The protocol used for this assay was based on a modified method as first described by Trudgill (1990).

The assay was carried out in an Aquarius variable wavelength spectrophotometer (Cecil Instruments Ltd, Cambridgeshire, UK) fitted with a thermostated cell. The temperature of the cell was controlled at 30°C throughout the whole assay. In a final volume of 1 mL, the following reagents were added to a 1.5 mL quartz cuvette, expressed as final concentrations: 700 µL of 50 mM Tris-HCl, pH 9 containing 7.14 g.L<sup>-1</sup> bovine serum albumin; 100 µL of approximately diluted cell extract; 100 µL of 0.161 mM NADPH.

The background rate of NADPH consumption was measured over 2 minutes prior to the addition of 100  $\mu$ L of 2 mM cyclohexanone to the cuvette. The resulting rate of change was measured for a further two minutes until all the NADPH in the cuvette was consumed. The CHMO activity was measured as the difference between the background rate of NADPH consumption and the rate observed upon the addition of cyclohexanone. The activity of the enzyme extract was expressed in Units (U) with one unit being defined as the amount of CHMO which catalyses the cyclohexanone induced oxidation of 1  $\mu$ mol of NADPH per minute. A sample curve generated by the spectrophotometer and CHMO activity calculation are shown in Appendix A.IV. The coefficient of variance for an individual activity measurements was determined from triplicate measurements of five samples of induced cells and was found to be  $\pm$  12 %.

# 3. MINIATURE BIOREACTOR DESIGN AND EVALUATION<sup>†</sup>

---

---

## 3.1 Introduction and Aims

In recent years various designs of parallel miniature bioreactors have been reported including stirred tanks, bubble columns and shake flasks as described in Section 1.1.2. These all aim to enable parallel and potentially automated operation of several fermentations simultaneously. The key engineering design features of many of these systems have been summarised in Table 1.1. In each case there is the potential to increase the rate at which the necessary experiments are performed thus reducing fermentation development times and costs (Lye *et al.*, 2003). To date, there has been little or no detailed engineering characterisation and scale-up evaluation for any of the systems reported in Table 1.1.

The aim of this chapter is to describe the initial design, construction and operation of a novel, parallel miniature bioreactor system prior to its engineering characterisation and evaluation of scale-up potential. Some of the detailed design and instrumentation features have already been described in Section 2.3. The key objectives of this chapter include:

- Demonstrate maintenance of aseptic and controlled operation over prolonged periods.
- Evaluation of oxygen transfer capabilities over a range of operating conditions.

---

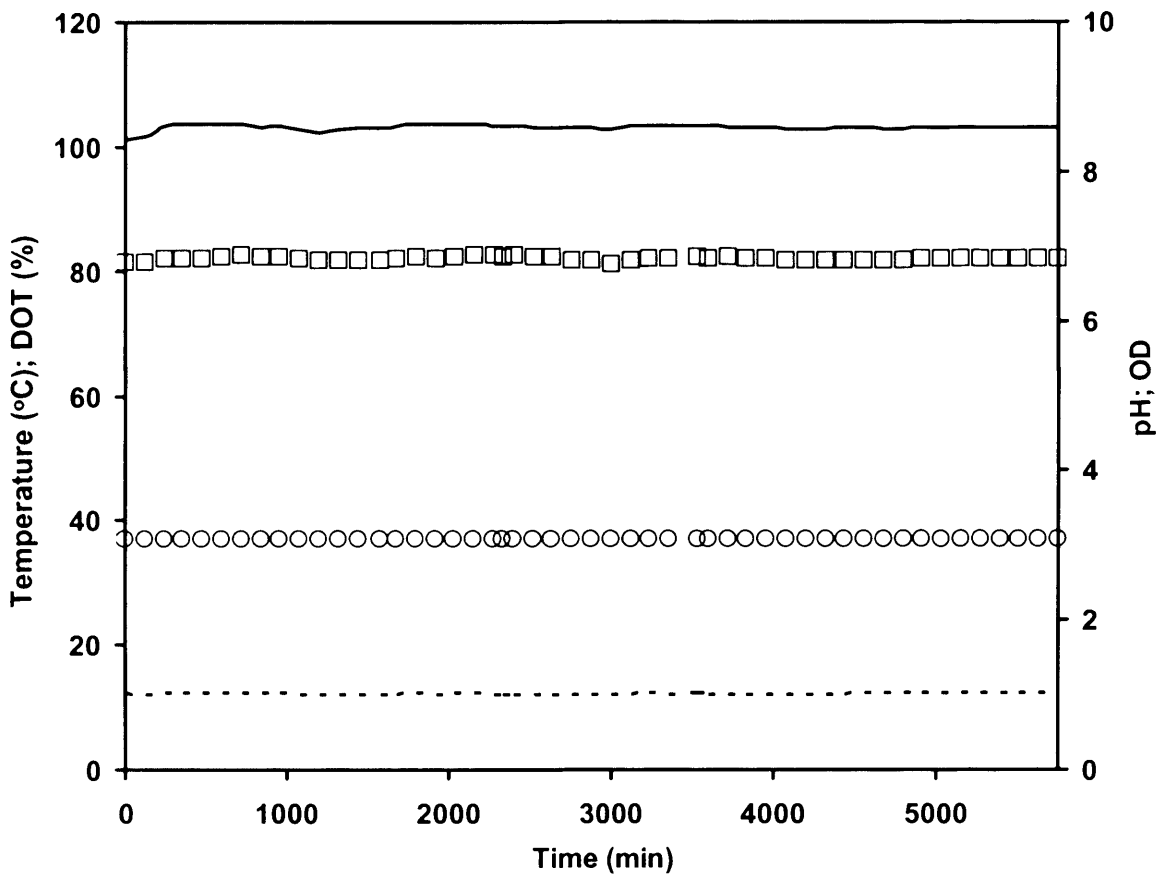
<sup>†</sup> The majority of the results in this chapter have been submitted for publication as: N. K. Gill, M. Appleton, F. Baganz, G. J. Lye, Design and Characterisation of a Miniature Stirred Bioreactor System for Parallel Microbial Fermentations, *Biochem. Eng. J.* (2007) accepted.

- Demonstrate reproducible operation of the parallel, 4-pot system and the accurate quantification of fermentation kinetics parameters with a number of microorganisms, namely *E. coli* TOP10 pQR239 and *B. subtilis* ATCC6633.
- Evaluation of gas blending and DOT set point on cell growth.

### **3.2 Miniature Bioreactor Design, Operation and Control**

The primary basis of the miniature bioreactor design was that it should be as geometrically similar as possible to conventional laboratory scale bioreactors and be agitated by a miniature turbine impeller. This was dictated by the desire to obtain quantitative and scaleable data from each miniature bioreactor and efficient oxygen transfer during microbial fermentations. In practice these constraints limited the volume of each bioreactor to a minimum of 100 mL, based on calculations of average energy consumption rates and mechanical fabrication issues. In order to simplify the assembly of each unit, and to minimise any risk of contamination, the need for a rotating mechanical seal on the impeller drive shaft was overcome by opting for a magnetically driven stirrer. This was only possible by compromising on the design of the impeller by the incorporation of a flat disk at the end of the impeller drive shaft as shown in Figure 2.1(A). This was necessary to ensure coupling of the impeller with the magnetic drive at agitation rates of up to 2000 rpm and with liquids of viscosity up to 100 cp. Given these modifications to the impeller design, visual observation showed uniform distribution of gas bubbles throughout the entire liquid volume of each vessel at agitation rates of 1000 rpm or above.

To facilitate parallel operation, four miniature bioreactors could be assembled and sterilised simultaneously in a typical laboratory autoclave. A hydrostatic pressure test indicated that each vessel could typically withstand an applied pressure of 8 bar before rupturing. An initial medium sterilisation and hold test, in which DOT, pH and OD were monitored over 4 days showed no signs of contamination (Figure 3.1). Aseptic operation was confirmed by the absence of any colonies from medium samples withdrawn periodically and grown on nutrient agar plates at 37°C for 24 hours.



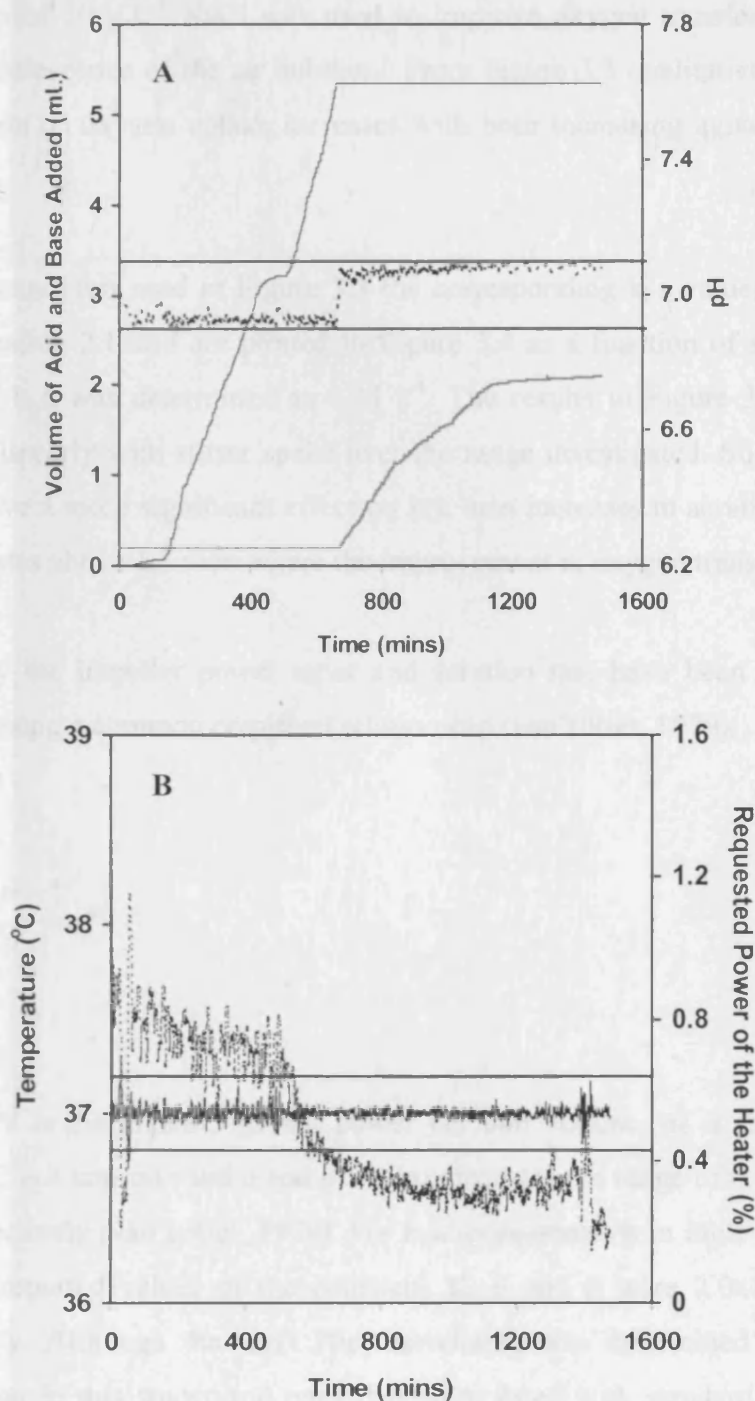
**Figure 3.1.** Results from a typical sterile hold test, which involved sterilising a miniature bioreactor containing 100 mL of growth media. The bioreactor was then agitated at 1000 rpm and aerated at 1 vmm for a period of four days with continuous on-line measurement of dissolved oxygen tension, pH, temperature and optical density: (—) DOT; (□) pH; (o) temperature and (- - -) OD. Sterilisation performed as described in Section 2.6.1.2.

To further facilitate parallel and unattended operation of multiple units each bioreactor was instrumented with pH, temperature and dissolved oxygen probes as well as a novel on-line optical density probe (as described in Section 2.3.2). The small area of each bioreactor head plate meant that it was necessary to source the smallest available probes. In order to then have sufficient ports for liquid additions, sampling and the possibility of continuous bioreactor operation all liquid handling operations took place via a specially designed multi-port. Finally, it was possible to independently monitor and control up to sixteen miniature bioreactors using custom-written, PC-based software. The key features of the software have been specified in Section 2.3.3.

Figure 3.2 shows the good performance of the pH and temperature control systems during a typical *E.coli* fermentation (as described later in Section 3.4.1). Both parameters are controlled by a PID controller. The corrective action of the pH controller is shown by the delivery of acid and base during fermentation (Figure 3.2 (A)), initially only base is added as the fermentation broth became more acidic due to secretion of metabolic by-products. After 540 minutes the cells entered stationary phase, however the fermentation was run for a prolonged period to test the robustness of the pH controller. It can be seen from Figure 3.2 (B) that from 661 minutes base addition stopped and acid addition commenced in order to maintain the pH at the set-point value of  $7 \pm 0.1$ . In the case of the temperature control, the power required from the heater continuously adjusted itself in order to maintain the set-point value of  $37 \text{ }^{\circ}\text{C} \pm 0.2$ .

### 3.3 Characterisation of Bioreactor Oxygen Transfer Capability

Since the majority of industrial fermentations use aerobic microorganisms (Shay *et al.*, 1987) the oxygen transfer capability of the miniature bioreactor is of great interest. Parameters such as  $k_L a$  are also useful for comparing different bioreactor designs and provide a useful criterion for scale-up. A series of dynamic gassing out experiments were thus performed at different stirrer speeds (1000-2000 rpm) and aeration rates (1-2 vvm) for aeration with atmospheric air, as described in Section 2.4.



**Figure 3.2.** Controller response for pH and temperature during a typical *E.coli* TOP10 pQR239 fermentation. (A) pH was controlled at a set point value of  $7 \pm 0.1$  by metered addition of acid and base: measured pH of fermentation broth (---); volume of base added (-); volume of acid added (.....). (B) Temperature was controlled at a set point value of  $37^{\circ}\text{C} \pm 0.2$  by the automatic adjustment of the electrical heater: measured temperature of fermentation broth (-); requested power of the electrical heater required to maintain set point temperature (---). Fermentations performed as described in Section 2.6.1.2.



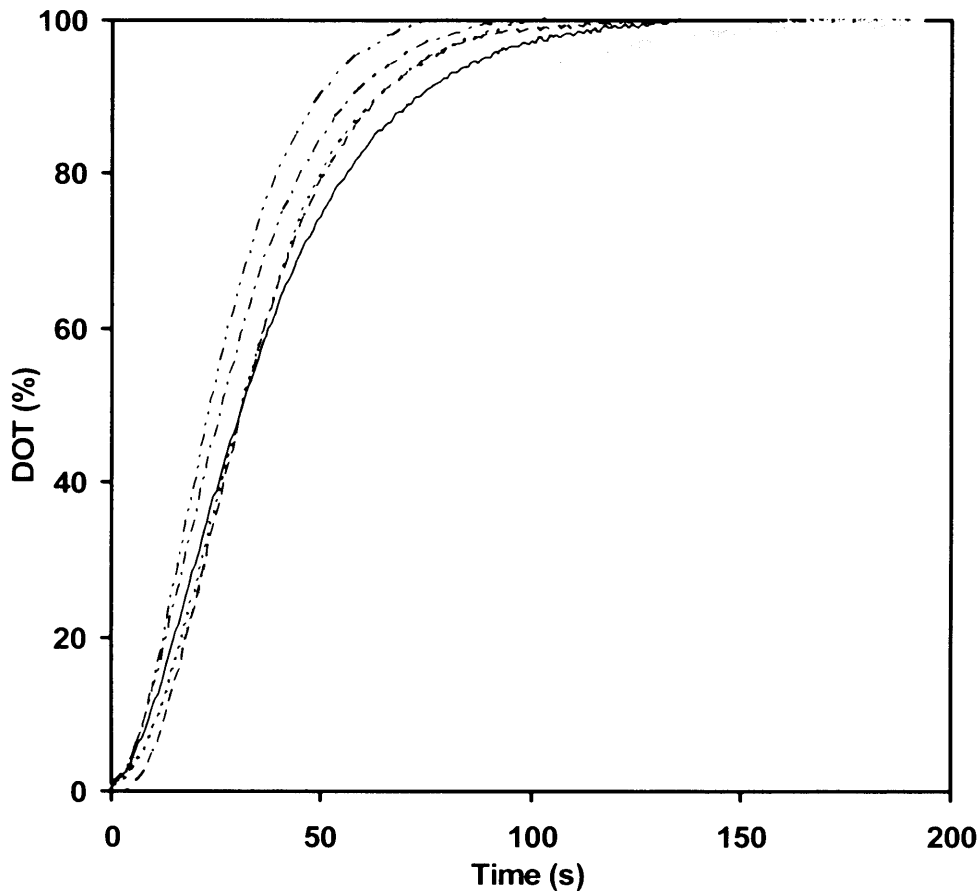
A solution of 10 g.L<sup>-1</sup> NaCl was used to improve oxygen transfer by reducing the level of coalescence of the air bubbles. From Figure 3.3 qualitatively it can be seen that the rate of oxygen uptake increases with both increasing agitation and aeration rates.

For each condition used in Figure 3.3 the corresponding k<sub>L</sub>a values were calculated using Equation 2.1 and are plotted in Figure 3.4 as a function of stirrer speed. The maximum k<sub>L</sub>a was determined as 0.11 s<sup>-1</sup>. The results in Figure 3.4 show that k<sub>L</sub>a increases linearly with stirrer speed over the range investigated. Stirrer speed is also seen to have a more significant effect on k<sub>L</sub>a than increases in aeration particularly at aeration rates above 1.5 vvm where the improvement in oxygen transfer is minimal.

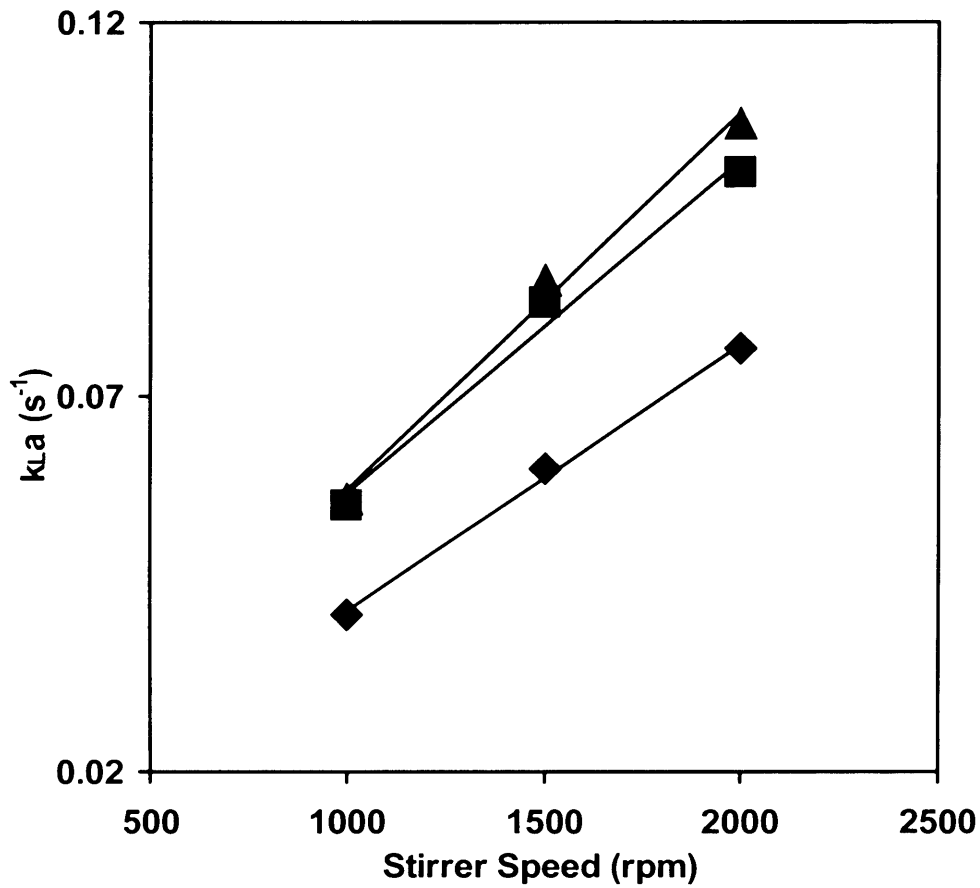
Classically the impeller power input and aeration rate have been correlated in the literature using a common empirical relationship (van't Riet, 1979):

$$k_L a = C \left( \frac{P_g}{V} \right)^\alpha u_s^\beta \quad \text{Eq. 3.1}$$

where P<sub>g</sub>/V is the impeller gassed power per unit volume, u<sub>s</sub> is the superficial gas velocity, C is a constant and α and β are exponents in the range of 0.4 < α < 1 and 0 < β < 0.7 respectively (van't Riet, 1979). For k<sub>L</sub>a measurements in ionic solutions as used here, the reported values of the constants K, α and β were 2.0×10<sup>-3</sup>, 0.7 and 0.2 respectively. Although the van't Riet correlation was determined for much larger vessels than in this study, and ones that were fitted with standard Rushton turbine impellers, the stronger dependency of k<sub>L</sub>a on P<sub>g</sub>/V (and hence stirrer speed) than on u<sub>s</sub> (Figure 3.4) initially suggests that results for the miniature bioreactor are consistent with the established theory. Further discussions and results regarding impeller power measurements will be presented in Chapter 5.



**Figure 3.3.** Influence of bioreactor operating conditions on oxygen uptake kinetics during dynamic gassing out experiments. From left to right: (— -- —) 2000 rpm, 2 vvm; (— - — ) 2000 rpm, 1vvm; (---) 1500 rpm, 1vvm; (— —) 1000 rpm, 2 vvm; (—) 1000 rpm, 1.5 vvm; (—) 1000 rpm, 1 vvm. Experiments performed at 37°C in a 10 g.L<sup>-1</sup> NaCl solution as described in Section 2.4.



**Figure 3.4.** Bioreactor oxygen mass transfer coefficient ( $k_{L,a}$ ) as a function of stirrer speed and aeration rate for aeration with atmospheric air: (◆) 1 vvm; (■) 1.5 vvm; (▲) 2 vvm. Values of  $k_{L,a}$  calculated from the dynamic gassing out data shown in Figure 3.3 using Equation 2.1. Solid lines fitted by linear regression.

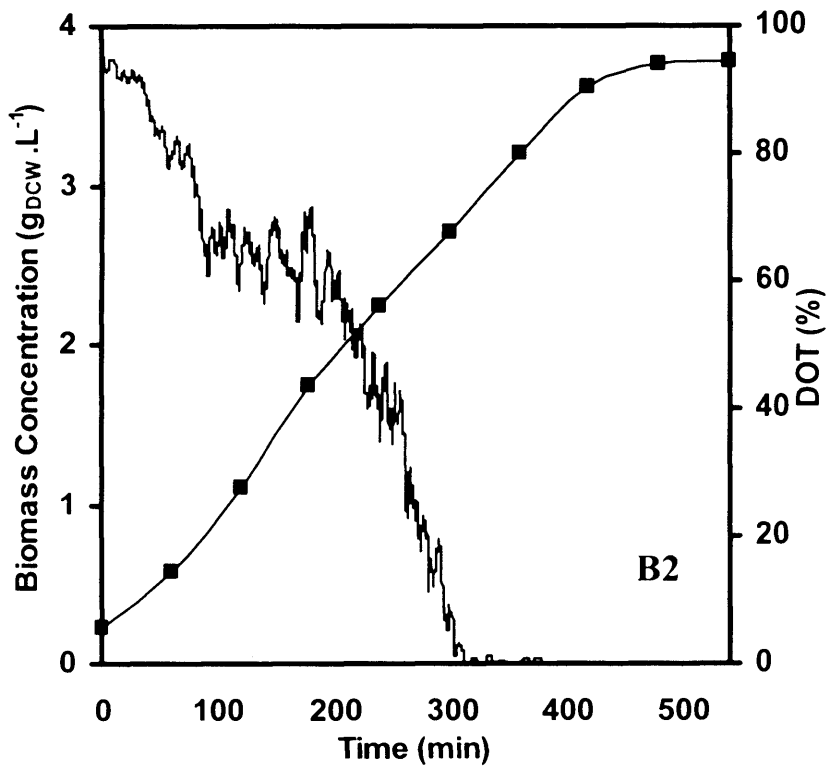
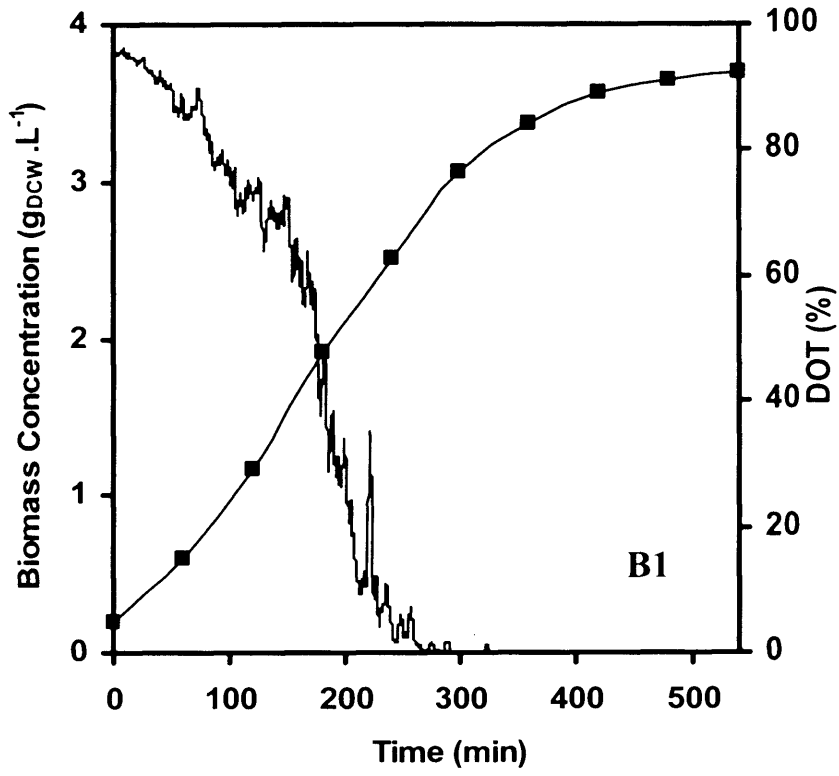
## 3.4 Parallel Batch Fermentation Kinetics

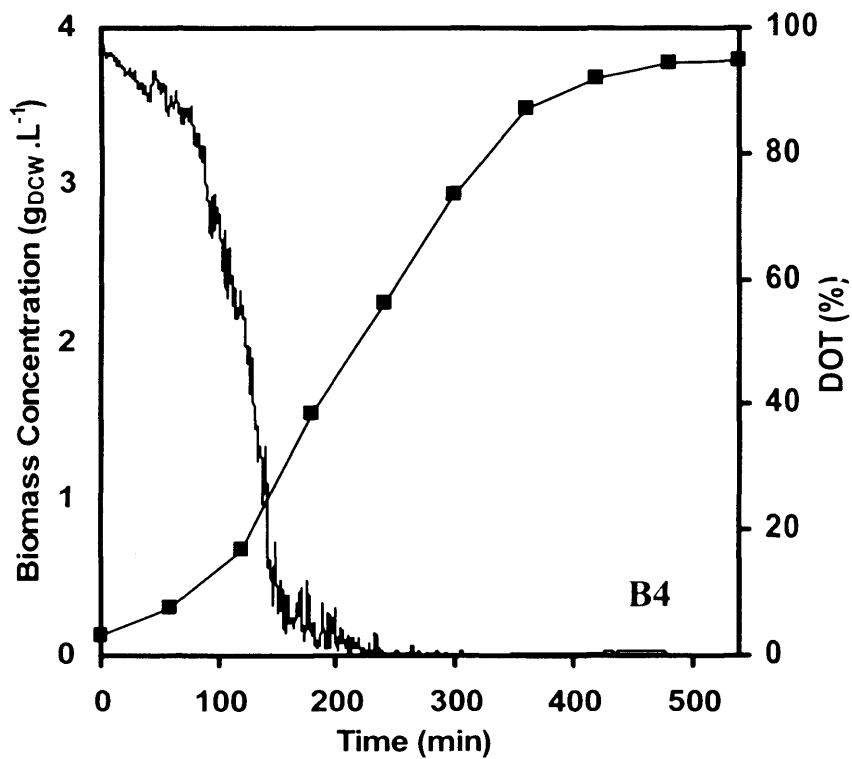
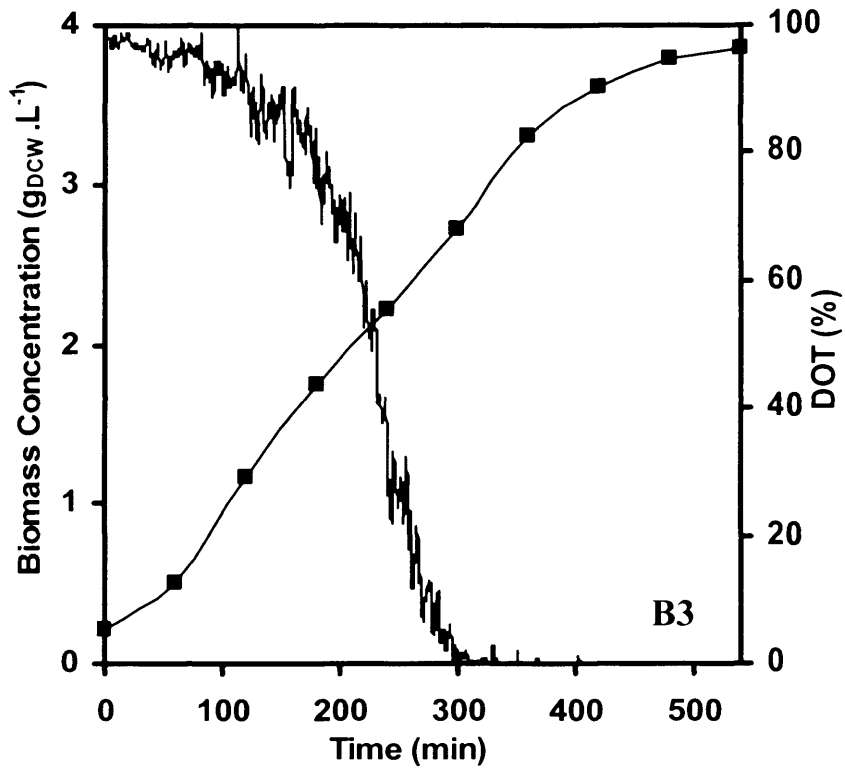
### 3.4.1. Reproducibility of Parallel *E. coli* Fermentations

A key requirement of any parallel bioreactor system is that cultivations in separate bioreactors should be highly reproducible if performed under identical operating conditions. Figure 3.5 shows biomass growth kinetics and dissolved oxygen tension (DOT) profiles for typical parallel *E. coli* (facultative anaerobe) fermentations in the four-pot miniature bioreactor system, with the temperature and pH controlled at  $37\text{ }^{\circ}\text{C} \pm 0.2$  and  $7 \pm 0.1$  respectively. All fermentations were carried out at a fixed impeller speed and aeration rate of 1000 rpm and 1 vvm (atmospheric air) respectively which gave a relatively low  $k_{\text{L}}a$  value of  $0.04\text{ s}^{-1}$ . All biomass concentrations are reported as dry cell weight based on off-line  $\text{OD}_{600}$  measurements as described in Section 2.9.1.

Considering the data from bioreactor B1, (Figure 3.5), the entire fermentation is seen to last a total of 540 minutes with the end of the exponential cell growth phase occurring around 300 minutes (based on plots of  $\ln(X)$  versus  $t$ ). This coincided with the point at which oxygen mass transfer limitation occurred and the measured DOT reached zero. The particular strain of *E. coli* used here is known to have a high specific oxygen demand (Doig *et al.*, 2001) so the fact that the measured DOT reached zero for operation at a relatively low  $k_{\text{L}}a$  value is not surprising. The period of exponential growth was followed by an almost linear increase in biomass concentration for a further 160 minutes at which point the culture entered stationary phase and ceased to grow. The biomass growth kinetics and dissolved oxygen profiles for the other three bioreactors are very similar apart from the DOT profile in bioreactor B4 which reached zero DOT somewhat earlier.

Table 3.1 shows the key kinetic parameters derived from the individual fermentation profiles shown in Figure 3.5. The maximum specific growth rates were very similar, giving an average value of  $0.68 \pm 0.01\text{ h}^{-1}$  as were the final biomass concentrations achieved where the average value was  $3.8 \pm 0.05\text{ g.L}^{-1}$ . The time at which the measured DOT reached zero was also comparable in the majority of cases. Overall





**Figure 3.5.** Parallel batch fermentation kinetics of *E. coli* TOP10 pQR239 grown under identical conditions: (■) biomass concentration; (-) DOT. Experiments performed at 1000 rpm and aerated with 1 vvm atmospheric air as described in Section 2.6.1.2. B1 – B4 refer to bioreactors one to four respectively.

these results indicate excellent reproducibility of the four-pot system as determined by *E.coli* cell growth.

**Table 3.1.** Reproducibility of batch *E. coli* TOP10 pQR239 fermentation kinetics from four parallel fermentations. Kinetic parameters derived from the fermentation profiles shown in Figure 3.5. B1-B4 refer to bioreactors one to four respectively, while B<sub>AV</sub> indicates the mean values of the kinetic parameters (error indicated represents one standard deviation).

| Parameter   | B1   | B2   | B3   | B4   | B <sub>AV</sub> |
|---|------|------|------|------|-----------------|
| $\mu_{\max}$ (h <sup>-1</sup> )                             | 0.68 | 0.66 | 0.68 | 0.69 | 0.68 ± 0.01     |
| X <sub>final</sub> (g.L <sup>-1</sup> )                     | 3.7  | 3.8  | 3.8  | 3.8  | 3.8 ± 0.05      |
| t <sub>DOT=0</sub> (min)                                    | 290  | 300  | 300  | 243  | 283 ± 27.2      |
| OUR <sub>max</sub> (mmol.L <sup>-1</sup> .h <sup>-1</sup> ) | 18.1 | 18.4 | 18.4 | 18.4 | 18.3 ± 0.15     |

At the point where the measured DOT first reaches zero, it can be assumed that the maximum oxygen uptake rate (OUR<sub>max</sub>) and the maximum oxygen transfer rate (OTR<sub>max</sub>) are equal. The OUR<sub>max</sub> can thus be estimated from:

$$OUR_{\max} = \frac{\mu X}{Y_{X,O_2}} + m_{O_2} X \quad \text{Eq.3.2}$$

where  $\mu$  is the specific growth rate at the time point when the DOT first reaches zero, X is the corresponding biomass concentration,  $Y_{X,O_2}$  is the yield of biomass on oxygen, which was taken to be 1.92 g.g<sup>-1</sup> for *E.coli* (Atkinson and Mavituna, 1999) and m is the oxygen required for cell maintenance which was taken to be 0.003 molO<sub>2</sub>.g<sup>-1</sup>.h<sup>-1</sup> (Atkinson and Mavituna, 1999). Similarly, the OTR can be estimated from:

$$OTR = k_L a (C^* - C_L) \quad \text{Eq. 3.3}$$

where  $C^*$  is the saturation dissolved oxygen concentration in the medium, taken to be  $6.9 \text{ mg.L}^{-1}$  (Bailey and Ollis, 1986) and  $C_L$  is the actual concentration of dissolved oxygen. At the point where the measured DOT first reaches zero,  $C_L$  is also zero and so Equation 3.3 reduces to:

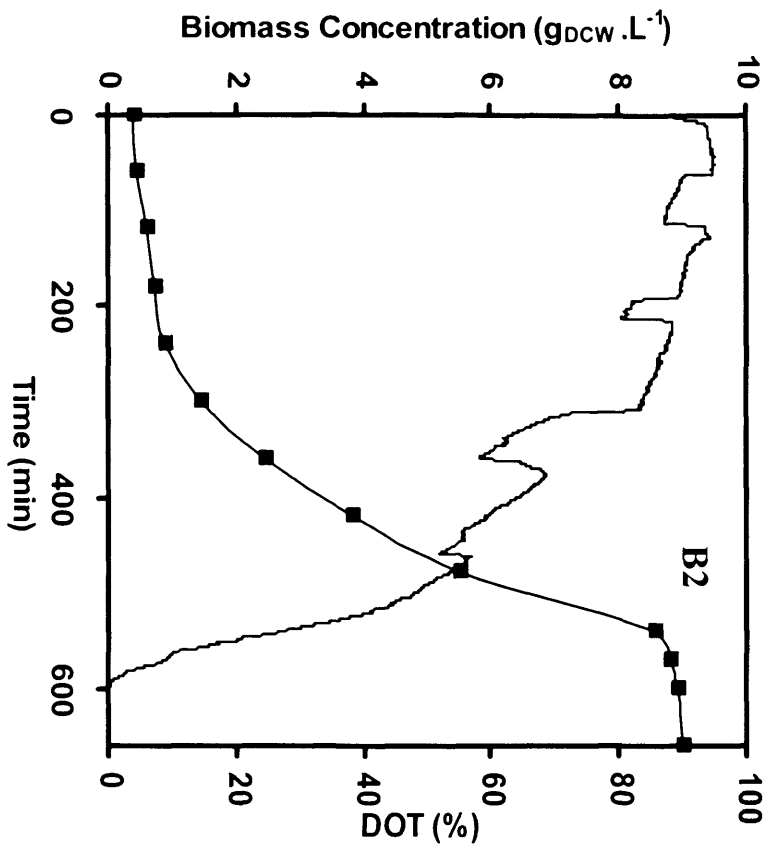
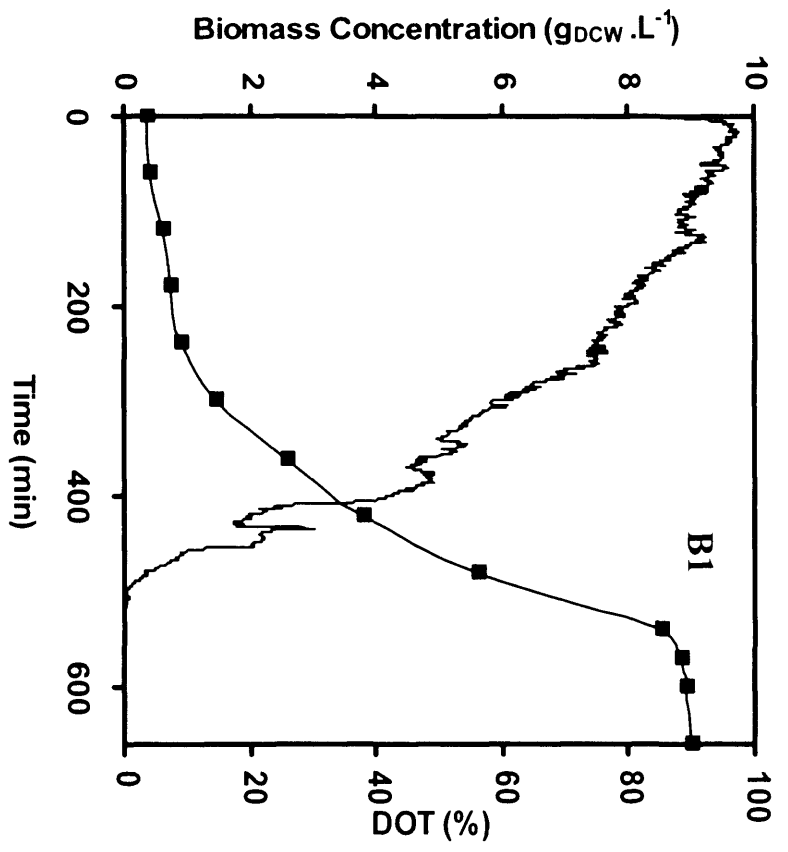
$$OTR_{\max} = k_L a C^* \quad \text{Eq. 3.4}$$

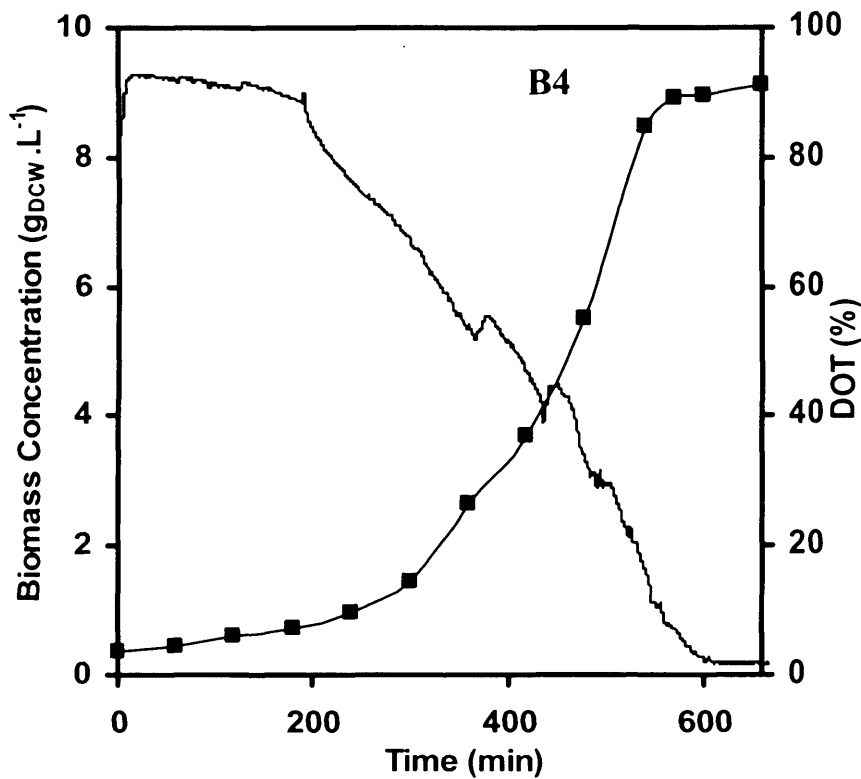
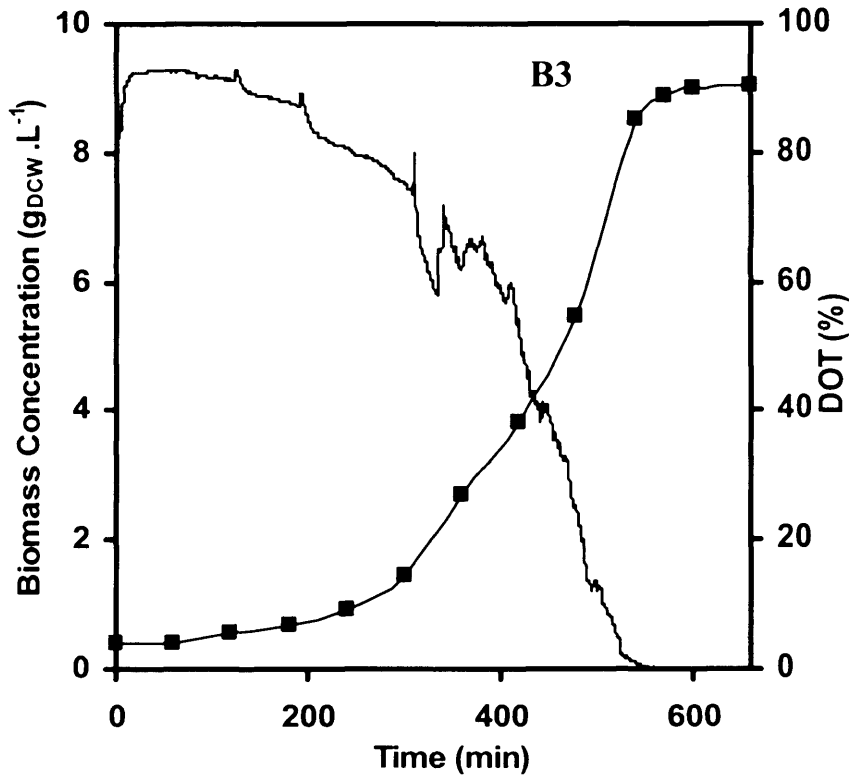
From Equation 3.2 the average  $OUR_{\max}$  for the fermentations shown in Figure 3.5 was calculated to be  $18.3 \pm 0.15 \text{ mmol.L}^{-1}.\text{h}^{-1}$ . In order to estimate the corresponding  $OTR_{\max}$  value from Equation 3.4, bioreactor  $k_L a$  values were measured by further gassing out experiments using spent biomedia containing the antifoam PPG used during fermentation experiments (Section 2.2.1). The presence of PPG is known to significantly reduce  $k_L a$  values (Morao *et al.*, 1999) and the measured value of  $0.03 \text{ s}^{-1}$  was not surprisingly 25% lower than the value measured in electrolyte solution. Using this lower  $k_L a$  value the calculated value of  $OTR_{\max}$  was thus estimated to be  $18.2 \text{ mmol.L}^{-1}.\text{h}^{-1}$  which is in excellent agreement with the calculated  $OUR_{\max}$  values.

### 3.4.2. Reproducibility of Parallel *B. subtilis* Fermentations

In addition to showing the reproducibility of parallel fermentations of *E. coli*, a facultative anaerobe, the flexibility of the miniature bioreactor system was shown using parallel fermentations of *B. subtilis*, a strict aerobe. Figure 3.6 shows typical biomass growth kinetics and DOT profiles for four parallel *B. subtilis* fermentations in the miniature bioreactors. These fermentations were carried out at a fixed impeller speed and aeration rate of 1500 rpm and 1 vvm (atmospheric air) respectively corresponding to a  $k_L a$  value of  $0.06 \text{ s}^{-1}$ , and the temperature and pH were controlled at  $32 \text{ }^\circ\text{C} \pm 0.2$  and  $6.8 \pm 0.1$  respectively. All biomass concentrations are reported as dry cell weight based on off-line  $OD_{600}$  measurements as described in Section 2.9.1.







**Figure 3.6.** Parallel batch fermentation kinetics of *B. subtilis* ATCC6633 grown under identical conditions: (■) biomass concentration; (-) DOT. Experiments performed at 1500 rpm and aerated with 1 vvm atmospheric air as described in Section 2.6.2.2. B1 – B4 refer to bioreactors one to four respectively.

Considering the first fermentation shown in Figure 3.6 (bioreactor B1) it can be seen that the entire fermentation lasted 660 minutes with the exponential phase of cell growth lasting until approximately 540 minutes. At this point the measured DOT again reached zero at which point the culture rapidly entered stationary phase and ceased to grow. As found with *E. coli*, very similar fermentation profiles for *B. subtilis* were obtained in all four miniature bioreactors in terms of cell growth and oxygen utilisation.

Table 3.2 shows the key kinetic parameters for *B. subtilis* derived from the individual fermentation profiles shown in Figure 3.6. The maximum specific growth rates were again very similar, giving an average value of  $0.45 \pm 0.01 \text{ h}^{-1}$  while the average final biomass concentration achieved was  $9.0 \pm 0.06 \text{ g.L}^{-1}$ . These results are comparable with those achieved in the bubble column block (Doig *et al.*, 2004), for the same  $k_L a$  value the maximum specific growth rate and final biomass concentration was  $0.47 \text{ h}^{-1}$  and  $10.4 \text{ g.L}^{-1}$  respectively. The average time taken for the DOT level to reduce to zero was  $565 \pm 33.7$  minutes. The level of variation seen for the *B. subtilis* fermentations is comparable to that determined for the earlier *E. coli* work and again indicates excellent reproducibility of the four-pot bioreactor system.

In addition to using the gassing out method to determine  $k_L a$  values (Section 3.3) in the case of a strict aerobe like *B. subtilis* an oxygen mass balance approach can also be used (Doig *et al.*, 2004):

$$\frac{dC_L}{dt} = k_L a (C^* - C_L) - OUR \quad \text{Eq. 3.5}$$

For this particular medium and strain of *B. subtilis*  $C_L$  and  $Y_{X,O_2}$  have been reported to be  $6.8 \text{ mg.L}^{-1}$  and  $1.6 \text{ g.g}^{-1}$  respectively (Doig *et al.*, 2004) with the contribution from cell maintenance to the overall oxygen requirement being negligible. Over a short time period  $dC_L/dt$  is constant and the  $k_L a$  was calculated as described in Appendix V. This method gave a  $k_L a$  value of  $0.062 \pm 0.001 \text{ s}^{-1}$  which is in excellent agreement with that measured using the gassing out technique under the same operating conditions.

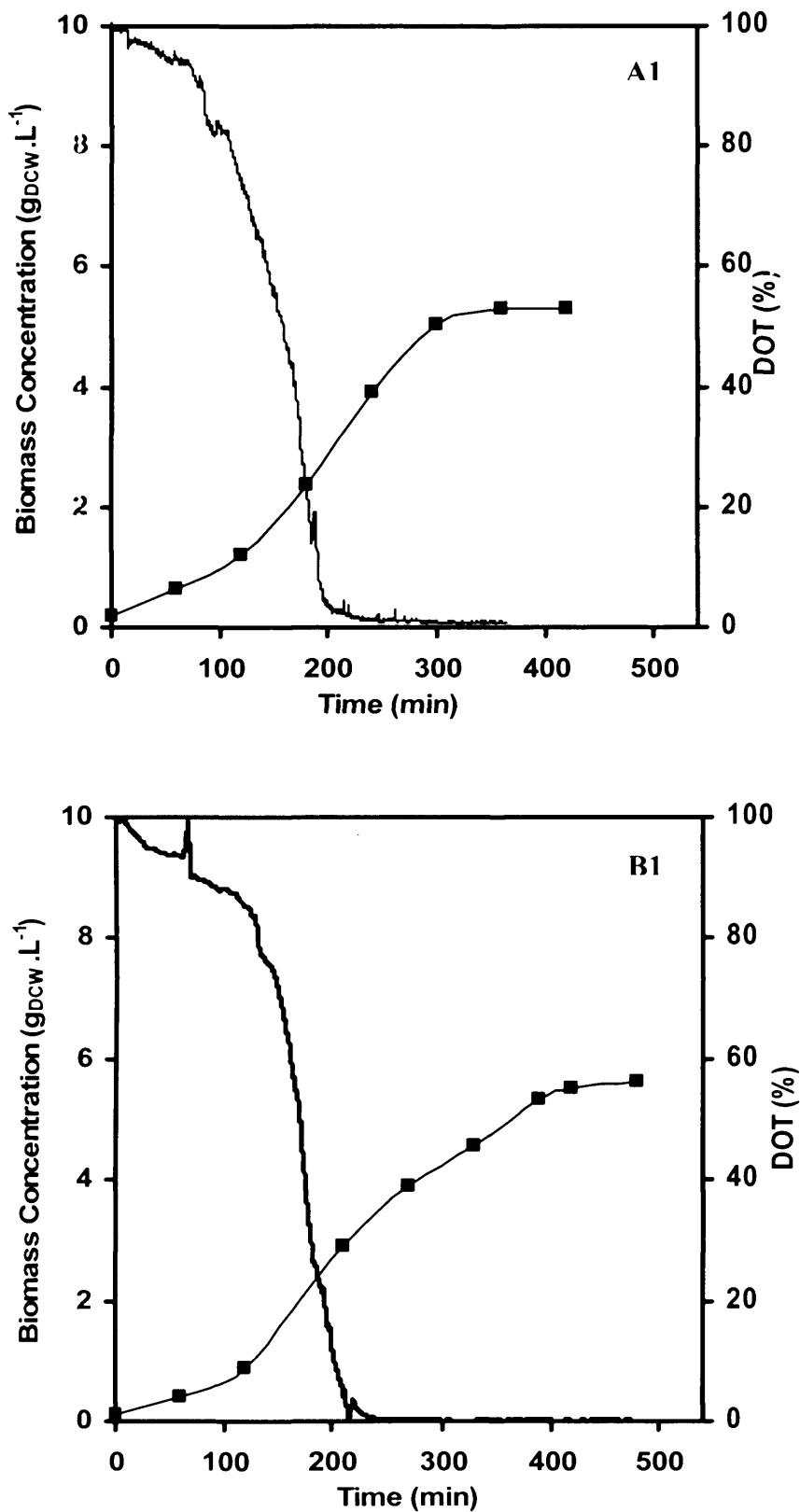
**Table 3.2** Reproducibility of batch *B. subtilis* ATCC6633 fermentation kinetics from four parallel fermentations. Kinetic parameters derived from the fermentation profiles shown in Figure 3.6. B1-B4 refer to bioreactors one to four respectively, while B<sub>AV</sub> indicates the mean values of the kinetic parameters (error indicated represents one standard deviation).

| Parameter                               | B1    | B2    | B3    | B4    | B <sub>AV</sub> |
|---|-------|-------|-------|-------|-----------------|
| $\mu_{\max}$ (h <sup>-1</sup> )         | 0.46  | 0.45  | 0.45  | 0.44  | 0.45 ± 0.01     |
| X <sub>final</sub> (g.L <sup>-1</sup> ) | 9.0   | 9.0   | 9.0   | 9.1   | 9.0 ± 0.06      |
| t <sub>DOT = 0</sub> (min)              | 529   | 572   | 550   | 608   | 565 ± 33.7      |
| k <sub>L</sub> a (s <sup>-1</sup> )     | 0.061 | 0.062 | 0.061 | 0.059 | 0.061 ± 0.001   |

### 3.5 Influence of Agitation and Aeration Conditions on *E.coli* Fermentations

The initial *E. coli* and *B. subtilis* fermentations reported in Section 3.4.1 and 3.4.2 were carried out at relatively low k<sub>L</sub>a values and so oxygen limitations were observed in both cases. To explore the oxygen uptake requirements of the *E. coli* strain further, a series of fermentations were carried at higher agitation rates of 1500 and 2000 rpm (aeration rate remained constant at 1 vvm) and higher aeration rates of 1.5 and 2 vvm (agitation rate remained constant at 1000 rpm). Aeration was with either atmospheric air or oxygen-enriched air utilising the gas-blending capability of the miniature bioreactor system, as described in Section 2.6.1.2 and 2.6.1.3.

Figure 3.7 shows representative examples of biomass concentration and DOT profiles under the different agitation and aeration conditions. The derived kinetic parameters from the entire series of experiments are summarised in Table 3.3. For aeration with atmospheric air there is a significant increase in both the maximum growth rate (0.75 to 0.94 h<sup>-1</sup>) and final biomass concentration (5.1 to 5.6 g.L<sup>-1</sup>) in all cases when compared to the values obtained with the lowest agitation and aeration conditions used previously in Section 3.4.1 (0.68 h<sup>-1</sup> and 3.8 g.L<sup>-1</sup>). These increases in cell growth rate are broadly in line with the measured increases in k<sub>L</sub>a values. The largest value of OUR<sub>max</sub> was calculated to be 46.8 mmol.L<sup>-1</sup>.h<sup>-1</sup>.



**Figure 3.7.** Influence of agitation and aeration rates on batch fermentation kinetics of *E. coli* TOP10 pQR239: (■) biomass concentration; (-) DOT. Experimental conditions: (A) 2000 rpm, 1 vvm; (B) 1000 rpm, 2 vvm. Fermentations performed as described in Section 2.6.1.2.

**Table 3.3.** Variation of bioreactor oxygen mass transfer coefficient and *E. coli* TOP10 pQR239 fermentation kinetics as a function of agitation and aeration conditions including the use of oxygen enrichment to control DOT levels. (A1) and (B1) correspond to the fermentation profiles shown in Figure 3.7; (A2) and (B2) correspond to the fermentation profiles shown in Figure 3.8. Oxygen mass transfer coefficient and values derived from Figure 3.4. ND = not determined.

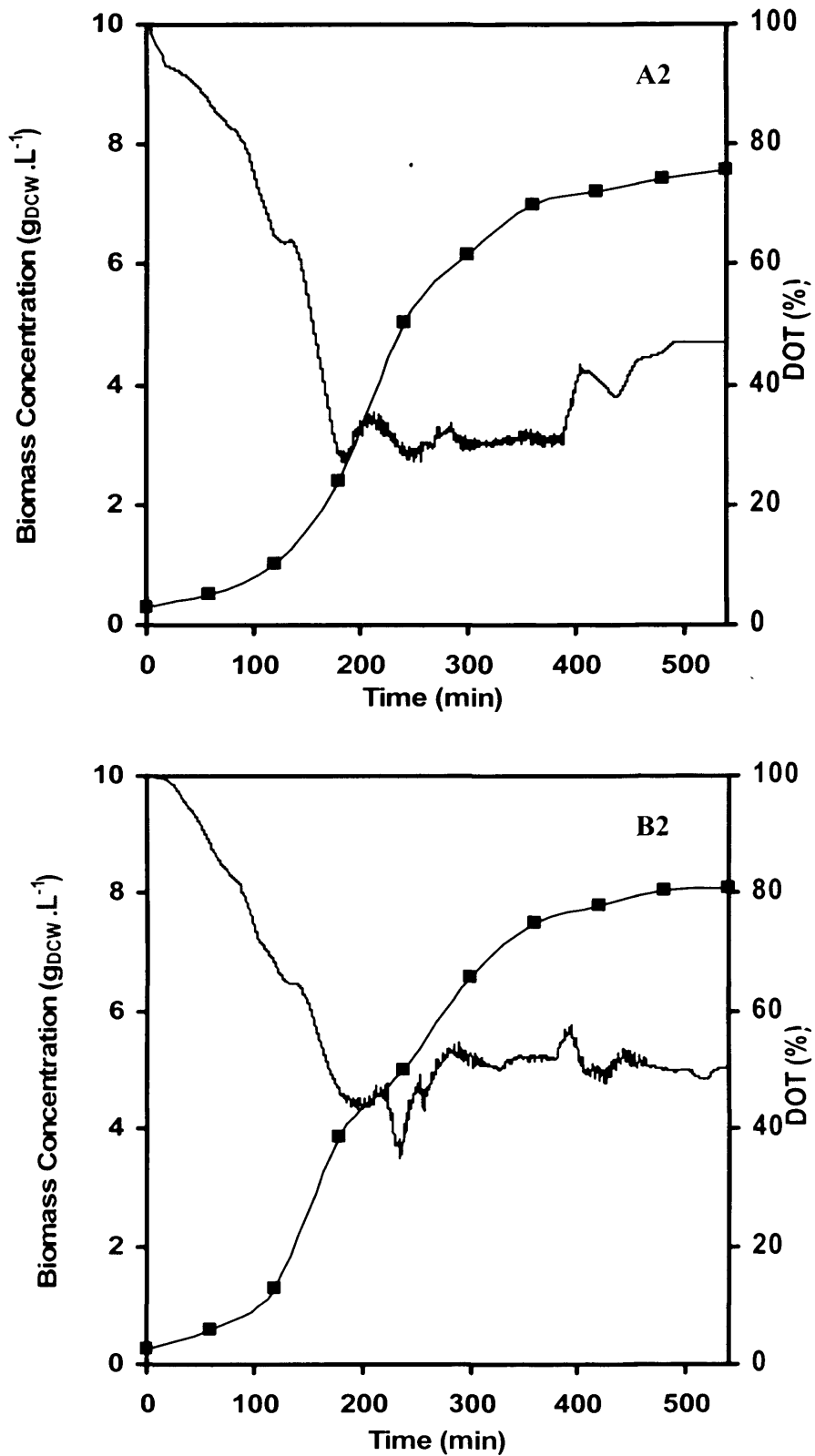
| Parameter  | Agitation and Aeration Conditions |                   |                        |                     |                       |                        |                        |
|--|-----------------------------------|-------------------|------------------------|---------------------|-----------------------|------------------------|------------------------|
|  | 1000 rpm<br>1 vvm                 | 1500 rpm<br>1 vvm | 2000 rpm<br>1 vvm (A1) | 1000 rpm<br>1.5 vvm | 1000rpm<br>2 vvm (B1) | 2000 rpm<br>1 vvm (A2) | 2000 rpm<br>1 vvm (B2) |
| Set Point DOT                                    | -                                 | -                 | -                      | -                   | -                     | 30%                    | 50%                    |
| $k_{L,a}$ ( $s^{-1}$ )                           | 0.04                              | 0.06              | 0.08                   | 0.06                | 0.06                  | ND                     | ND                     |
| $\mu_{max}$ ( $h^{-1}$ )                         | 0.68                              | 0.83              | 0.94                   | 0.75                | 0.79                  | 0.86                   | 0.93                   |
| $X_{final}$ ( $g \cdot L^{-1}$ )                 | 3.8                               | 5.1               | 5.3                    | 5.6                 | 5.6                   | 7.6                    | 8.1                    |
| $OUR_{max}$ ( $mmol \cdot L^{-1} \cdot h^{-1}$ ) | 18.4                              | 35.7              | 46.8                   | 26.3                | 27.5                  | ND                     | ND                     |

For all of the fermentations aerated with atmospheric air oxygen transfer limitations were observed to remain irrespective of the agitation and aeration rate used. The measured DOT reached zero at some point during the course of the individual fermentations. In order to overcome this problem the bioreactors could be aerated with oxygen-enriched air such that the DOT was maintained at a constant set point value. For agitation at 2000 rpm and aeration at 1 vvm in this case, graphs (A2) and (B2) in Figure 3.8 show that the DOT could be maintained and controlled at a minimum level of 30 or 50% respectively. In the absence of oxygen limitations the maximum growth rate of the culture increased further to  $0.93 \text{ h}^{-1}$  and the highest biomass concentration obtained was  $8.1 \text{ g.L}^{-1}$ . While gas blending can perhaps be avoided during the initial stages of fermentation process development it will be necessary to implement it during the later stages when high cell density cultures must be attained in the miniature bioreactors (García-Arrazola *et al.*, 2005).

### **3.6 Comparison with Other Miniature Bioreactors**

Several miniature bioreactor systems for rapid bioprocess development have been reported in recent years. A number of designs have been investigated but the recent trend has been toward mechanically stirred bioreactors as these are most widely used in industry for development and large scale operation. The majority of the bioreactors have been designed with parallel operation in mind and there is a consensus that 10's of experiments be performed in parallel for the systems to be of value. In this respect the "bioreactor block" (Puskeiler *et al.*, 2005a) currently gives the highest degree of parallelisation, 48, but must be operated on the deck of a dedicated laboratory automation platform. The smaller units (1 – 10 mL) tend to be single use disposable items while the larger ones (100 – 200 mL) like the bioreactor designed here can be repeatedly steam sterilised.

In terms of agitation and aeration systems those bioreactors featuring mechanical agitation tend to have the highest  $k_L a$  values. Stirrer speeds necessarily increase dramatically as the working volume of the bioreactors drop below about 10 mL. In many cases non-standard gas-sparging impellers (Puskeiler *et al.*, 2005a) and gas



**Figure 3.8.** Influence of oxygen enrichment on batch fermentation kinetics of *E. coli* TOP10 pQR239: (■) biomass concentration; (-) DOT. Experimental conditions: (A) 2000 rpm, 1 vvm and DOT controlled at 30%; (B) 2000 rpm, 1 vvm and DOT controlled at 50%. Fermentations performed as described in Section 2.6.1.3.



blending (Puskeiler *et al.*, 2005b; Betts *et al.*, 2006) have been implemented to maintain sufficient oxygen transfer rates. The highest  $k_La$  reported to date for any of the miniature bioreactors has been for the bioreactor block, achieving  $0.4 \text{ s}^{-1}$  (Puskeiler *et al.*, 2005a).  $k_La$  values of this order are necessary to support the microbial cell densities that could be achieved in approximately half of the designs that are capable of fed-batch or continuous operation. Betts and co-workers (2006) have reported  $k_La$  values in the order of  $0.1 \text{ s}^{-1}$  for a 10 mL stirred miniature bioreactor (Lamping *et al.*, 2003). The commercially available Cellstation (Fluorometrix, USA) (Kostov *et al.*, 2001; Harms *et al.*, 2006) allows up to 12 stirred bioreactors to be operated in a single run with working volumes of 35 mL. However the oxygen transfer rates are significantly lower compared to other systems described in this section ( $0.01 \text{ s}^{-1}$ ), due to the fact that agitation was achieved by a small magnetic stirrer bar and the sparger was positioned above the stirrer. Ideally the sparger should be positioned such that the air bubbles feed directly into the stirrer region to increase the time the air bubbles are in the solution.

In addition to stirred vessels, small scale bubble columns have also been designed in recent years, highlighting the importance and the need for a variety of bioreactor systems to address different process applications. Currently a 200 mL bubble column is available from Infors, Switzerland and is reported to achieve  $k_La$  values of up to  $0.16 \text{ s}^{-1}$  (Dilsen *et al.*, 2001; Weuster-Botz *et al.*, 2001b), with the capacity to operate up to 16 vessels in parallel. Doig *et al.* (2004) have characterised a system with up to 48 miniature bubble columns operating in parallel with working volumes of 2 mL, producing  $k_La$  values of around  $0.06 \text{ s}^{-1}$ . Although these systems lack the mixing capability of mechanical agitation, sufficient aeration and to a lesser extent efficient mixing are achieved by direct sparging. These researchers have also demonstrated a good correlation with a laboratory scale bubble column (100 mL) in terms of oxygen transfer and volumetric power consumption (Doig *et al.*, 2005).

Virtually all the miniature bioreactor designs feature the standard on-line probes expected for effective bioreactor monitoring and control though a number feature novel probes for on-line monitoring of culture optical density (Puskeiler *et al.*, 2005a; Kostov *et al.*, 2001; Harms *et al.*, 2006). The striking trend is the switch from standard probe technologies to fluorescent/optical probes once the bioreactor volume

drops below about 10 mL. All the designs for which parallel operation has been demonstrated feature dedicated PC-based software necessary for the supervision of multiple units.

### 3.7 Discussion

In this work a 4-pot parallel miniature bioreactor system has been designed and constructed. Each miniature bioreactor is of standard geometry (100 mL maximum working volume) and is fitted with a magnetically driven six-blade turbine impeller (Figure 2.1) operating in the range 100 - 2000 rpm. Aeration is achieved via a sintered sparger at flow rates in the range of 0 - 2 vvm. Continuous on-line monitoring of each bioreactor is possible using miniature pH, dissolved oxygen, temperature probes and a novel optical probe for optical density measurement. The control of key parameters such as temperature and pH has been achieved using a dedicated software system. Initial experiments (Figure 3.1) showed the bioreactor was capable aseptic operation and precise control of pH and temperature (Figure 3.2).

The reproducibility of both *E. coli* and *B. subtilis* has been demonstrated (Figure 3.5 and 3.6) with calculated kinetic parameters (Table 3.1 and 3.2) for the maximum specific growth rates and final biomass concentrations being  $0.68 \pm 0.01 \text{ h}^{-1}$  and  $3.8 \pm 0.05 \text{ g.L}^{-1}$  respectively for *E. coli* (1000 rpm, 1 vvm); and  $0.45 \pm 0.01 \text{ h}^{-1}$  and  $9.0 \pm 0.06 \text{ g.L}^{-1}$  for *B. subtilis* (1500 rpm, 1 vvm). In the case of *B. subtilis*, fermentations were carried out at matched  $k_L a$  values ( $0.06 \text{ s}^{-1}$ ) to those reported for the bubble column block (Doig *et al.*, 2004), producing comparable results of  $0.47 \text{ h}^{-1}$  and  $10.4 \text{ g.L}^{-1}$  for the maximum specific growth rate and final biomass concentration respectively. The final biomass concentrations achieved for *E.coli* is higher than those reported for batch *E.coli* fermentation ( $2.3 \text{ g.L}^{-1}$ ) in the Cellstation™ miniature bioreactor (Kostov *et al.*, 2001), since this system was operating at a much lower  $k_L a$  value.

The oxygen transfer characteristics of the bioreactor have also been examined using the dynamic gassing out technique (Figure 3.3), with the maximum  $k_L a$  determined as

0.11 s<sup>-1</sup> (Figure 3.4). This value is within the range that is typically achieved in conventional laboratory scale bioreactors (Doig *et al.*, 2006). For aeration with atmospheric air this led to oxygen limitation for both *E. coli* and *B. subtilis*. The highest OUR supported was 46.8 mmol.L<sup>-1</sup>.h<sup>-1</sup> for *E. coli* when operating at an agitation rate of 2000 rpm and aeration rate of 1 vvm (Table 3.3). Despite the continued oxygen limitation at higher agitation and aeration rates, biomass growth kinetics were seen to significantly improve with increases in agitation and aeration rates (Figure 3.7).

The integration of a gas blending system enabled oxygen enriched fermentations to be carried out by controlling the DOT at set point values of 30% and 50% (Figure 3.8). This improvement in the oxygen transfer capability of the system enabled  $\mu_{\max}$  and  $X_{\text{final}}$  as high as 0.93 h<sup>-1</sup> and 8.1 g.L<sup>-1</sup> (Table 3.3) respectively to be achieved. Gas blending is a common choice for maintaining sufficient oxygen transfer rates at this scale and has been readily implemented in the miniature stirred bioreactors of Puskeiler *et al.* (2005b) and Betts *et al.* (2006b).

In summary this chapter has described the oxygen transfer characteristics of the miniature bioreactors and their related to cell growth. Parallel operation generating reproducible results has been demonstrated for both *E. coli* and *B. subtilis* fermentations. In the following chapter the application of the miniature bioreactors to the optimisation of cell growth and heterologous protein expression will be described.

# 4. APPLICATION TO FERMENTATION PROCESS OPTIMISATION

---

---

## 4.1 Introduction and Aims

### 4.1.1 Statistical Design of Experiments (DoE)

In the previous chapter the basic performance of the miniature bioreactor system has been illustrated with regard to *E.coli* cell growth. In most commercial applications however, the product of interest is usually a heterologously expressed protein (Hilker *et al.*, 2006; Bird *et al.*, 2002). The optimisation of cell growth and/or protein expression during fermentation is thus a good example of a multi-objective, multi-variable problem usually requiring a larger number of experiments to be performed (Doig *et al.*, 2004; Puskeiler *et al.*, 2005a). Since development time is key to commercial success, approaches that increase the rate at which these experiments can be carried out are of great value and therefore high throughput methodologies are of increasing interest (Lye *et al.*, 2003).

In most cases of optimising the efficiency of recombinant protein expression, interactions between the most influential variables can be of importance. This increases the complexity of identifying which of these are key to improving protein expression. Some are target protein specific (protein construct length and expression vector) whilst others are related to fermentation conditions (media type and fermentation time) or protein induction conditions (inducer concentrations and induction time) (Islam *et al.*, 2007). Environmental factors such as oxygen transfer rate, temperature and pH will influence both cell growth and protein expression (Stanbury *et al.*, 2003; Uzura *et al.*, 2001; Rosso *et al.*, 2002; Qader *et al.*, 2006).

Most screening approaches are unstructured and result in a limited understanding of

the process under investigation. Determination of the true optimal expression conditions can therefore be a resource intensive process and may be impractical for large numbers of variables (Islam *et al.*, 2007). The classical experimental strategy of assessing one factor at a time (OFAT) does not provide a suitable structured approach that is less demanding in terms of time and cost given the large quantity of experiments required to evaluate the effects of each variable (Eriksson *et al.*, 2000). More importantly, such a strategy also fails to consider any possible interactions between variables which may not lead to finding the true optimum, since the optimal setting for one variable remains constant irrespective of the other variable settings (Montgomery, 2005).

Statistical Design of Experiments (DoE) provides a useful tool for overcoming the limitations of the OFAT method, as it is a more structured approach for determining the quantitative relationships between multiple variables affecting a process and the output of that process (Montgomery, 2005). DoE enables the investigation of the key combinations of the critical variables that directly affect the process, therefore fewer more relevant experiments are required providing more useful and precise information. Interactions between variables are resolved by applying the appropriate form of experimental design. The resulting model is then capable of predicting the overall optimal variable settings, or region, for maximum protein expression. Identification of the true optimum output, and its sensitivity to small changes in the underlying variables, is often not achieved based on the OFAT experiments. The identification of optimal and robust experimental conditions is of key importance here with regards to subsequent bioprocess development and scale-up.

In recent years the DoE approach has been used for a variety of applications including improving biomass yields (Vázquez and Martin, 1998; He *et al.*, 2004) and optimisation of protein expression based on a range variables investigating either media formulation (Nikerel *et al.*, 2005; Ren *et al.*, 2006; Zhang *et al.*, 2006) or protein induction conditions (Cao, 2006; Swalley *et al.*, 2006; Urban *et al.*, 2003; Wang *et al.*, 2005).

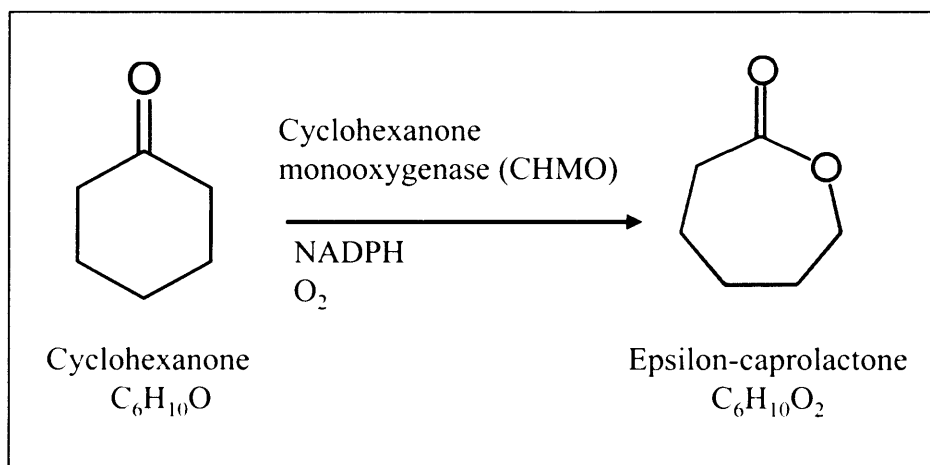
### ***4.1.2 Model System and Aims***

The aim of this chapter is to illustrate the utility of the miniature bioreactor system described in Chapter 3 for the rapid evaluation and optimisation of conditions for the expression of a recombinant protein. In particular it will examine the expression of cyclohexanone monooxygenase (CHMO) expressed in *E.coli* TOP10 pQR239 by evaluating three critical factors: temperature, pH and L-arabinose concentration, which are thought to have a significant effect on CHMO production.

CHMO is one of a class of potentially commercially important biocatalysts, the Baeyer-Villiger Monooxygenases (BVMOs) (Lander, 2003). The Baeyer-Villiger reaction is an extremely useful reaction in synthetic organic chemistry. These are enzymes capable of using molecular oxygen to mediate the nucleophilic oxygenation of linear or cyclic ketones yielding the corresponding esters and lactones (Doig *et al.*, 2001). CHMO is an attractive choice for synthetic purposes since reactions proceed with excellent selectivity with a wide variety of natural and synthetic substrates. Furthermore these biocatalytic oxidations are less hazardous, polluting and energy consuming than conventional chemical based methodologies (Zambianchi *et al.*, 2001). For the model protein expression system used for this study, the level of CHMO activity will be detected using the reaction in Figure 4.1, where CHMO carries out an oxygen insertion reaction on cyclohexanone to form the cyclic product epsilon-caprolactone (Sheng *et al.*, 2001).

The specific objectives of this chapter will be to:

- Illustrate operation of the miniature bioreactors over a range of operating conditions and set points.
- Demonstrate the potential for accelerated fermentation process development by the combined application of DoE with parallel experimentation.
- Establish appropriate conditions for both cell growth and CHMO expression to be used in subsequent scale-up studies.

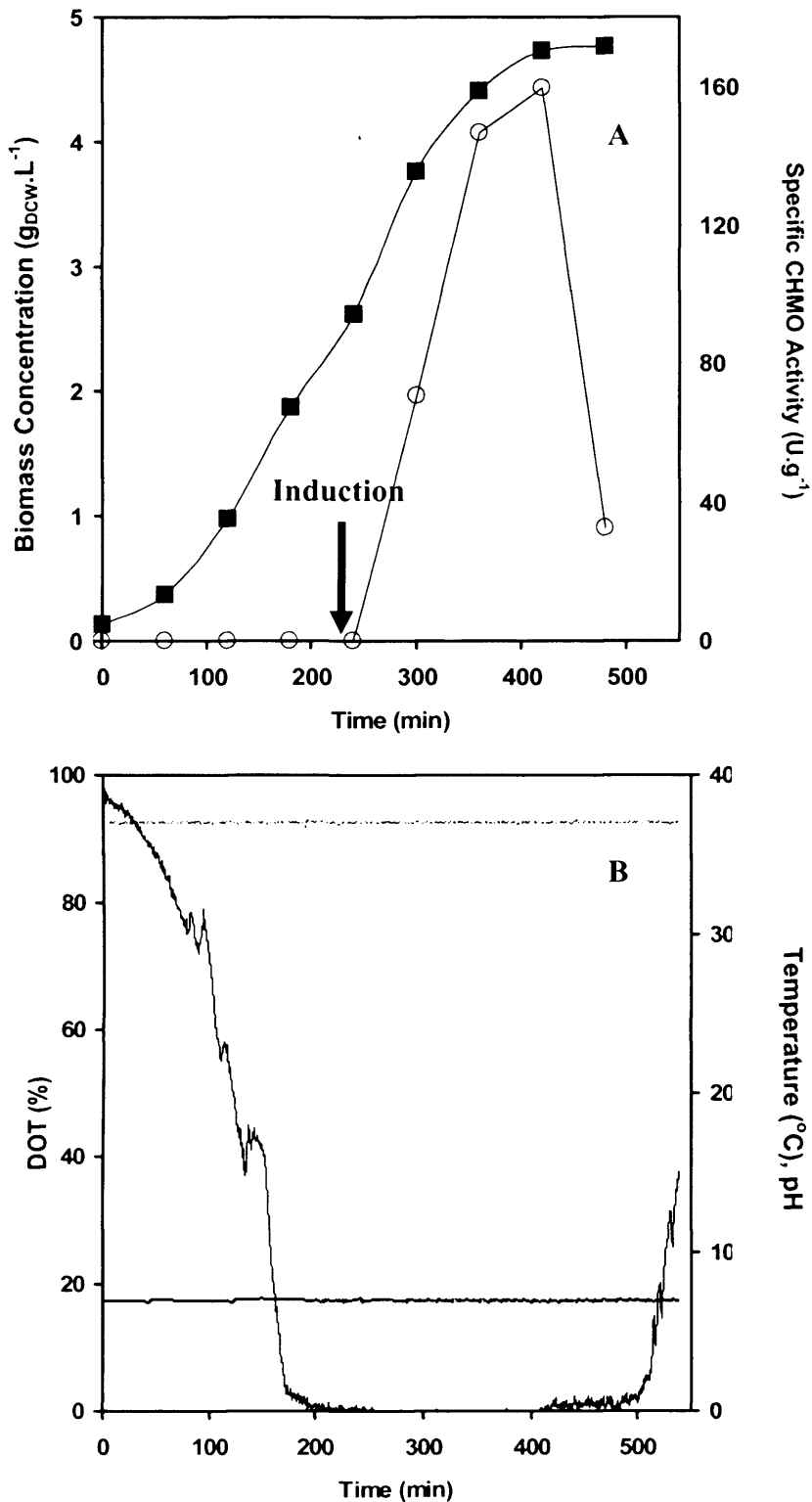


**Figure 4.1.** The reaction scheme for the CHMO catalysed bioconversion studied in this work.

## 4.2 Initial Evaluation of Cell Growth and Enzyme Expression

An *E.coli* TOP10 pQR239 fermentation was carried out at 37°C, pH 7 and induced with 0.1 % w/v L-arabinose, in order to initially examine the time course of CHMO expression over the course of the fermentation. These initial conditions were based on previous work using the same biocatalyst (Doig *et al.*, 2001; Lander, 2003). Figure 4.2 (A) shows a typical growth profile for the *E.coli* fermentation, determined from off-line OD<sub>600</sub> measurements and the specific intracellular CHMO titre, determined as described in Section 2.9.2, of the recombinant *E.coli* biocatalyst. Also shown in Figure 4.2 (B) are the continuous online measurements of pH, temperature and DOT. pH and temperature were automatically controlled at 7 and 37°C respectively.

It can be seen in Figure 4.2 (A) that the duration of the fermentation was a total of 480 minutes with the end of exponential cell growth occurring at approximately 200 minutes. This was followed by a period of linear growth which coincides with the point at which the measured DOT falls below <5%. A reduced DOT has been reported to be favourable for CHMO expression (Doig *et al.*, 2001) as the presence of oxygen can be inhibiting to CHMO activity. Overall the profiles for cell growth and DOT are similar to that achieved by Doig and co-workers (2001). However, in terms



**Figure 4.2.** Results from a typical 100 mL *E.coli* TOP10 pQR239 fermentation at pH 7, 37°C and induced with 0.1 % w/v L-arabinose. (A) Cell growth and volumetric CHMO activity versus time: (■) biomass concentration; (♦) specific CHMO activity. (B) Online measurement of pH, temperature and DOT: (- -) pH; (-) temperature; (-) DOT. Experiments performed at 1000 rpm and aeration with atmospheric air at 1 vmm as described in Section 2.7.2.



of quantitative values for maximum specific growth rate and final biomass concentrations achieved, for this particular fermentation the results of  $0.78 \text{ h}^{-1}$  and  $4.76 \text{ g.L}^{-1}$  respectively were lower than reported by Doig *et al.* (2001). This is most likely due to this experiment being performed at a lower  $k_{\text{LA}}$  of  $0.04 \text{ s}^{-1}$  compare to  $0.08 \text{ s}^{-1}$ . Induction of CHMO activity occurred after 240 minutes when the cell culture was in mid exponential phase, and the time course of CHMO expression was also qualitatively similar to that achieved by Doig *et al.* (2001) with a maximum specific CHMO activity of  $159.2 \text{ U.g}^{-1}$  obtained at approximately 420 minutes. The CHMO activity from lysed cells was calculated from the rate of NADPH utilisation upon the addition of cyclohexanone substrate, as described in Section 2.9.2.2.

### **4.3 Optimisation of Enzyme Expression: Selection of Variables and Ranges**

In order to obtain the highest level of expressed CHMO activity it is important to consider how fermentation process variables will affect both cell growth and the specific level of CHMO expression (Doig *et al.*, 2001). The key variables that will affect cell growth include pH, temperature, and the type and concentration of carbon source (Stanbury *et al.*, 2003; Uzura *et al.*, 2001; Rosso *et al.*, 2002; Qader *et al.*, 2006). These will also influence the expression of CHMO as will the concentration of the inducer used, L-arabinose. Temperature and pH are important variables to consider as they are key operating parameters during fermentations (Bailey and Ollis, 1986; Islam *et al.*, 2007). Alternations to either parameter would likely have a direct impact on both *E.coli* growth and CHMO expression. The *E.coli* TOP10 pQR239 strain contains L-arabinose inducible CHMO, therefore variations in the concentration of L-arabinose would be expected to affect the level of CHMO activity. Investigation of the influence of the critical factors: temperature, pH and L-arabinose, would potentially enable identification of the optimum conditions for both cell growth and enzyme expression that would yield the highest overall catalytic activity.

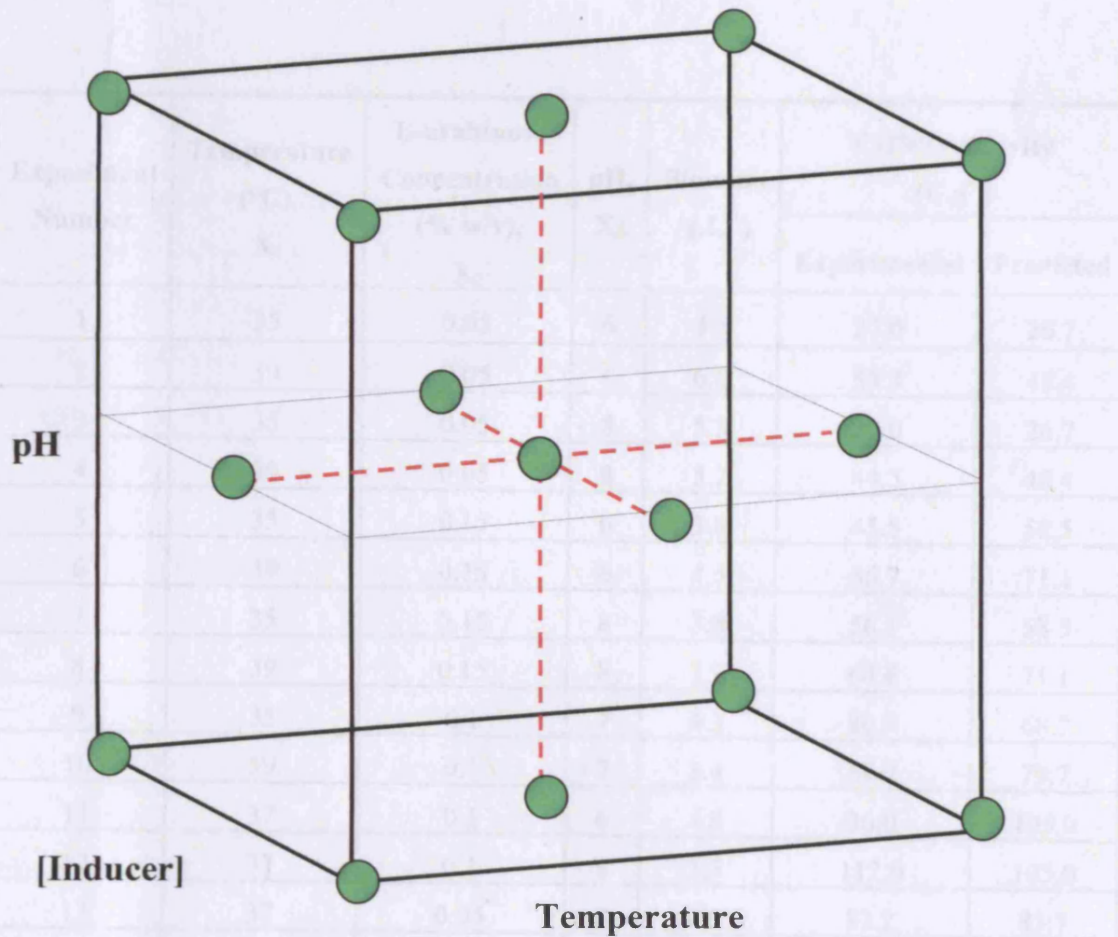
The level of catalytic activity will depend on both the number of cells and that amount of enzyme produced per cell, therefore, the most suitable response variables were

biomass concentration and CHMO activity. Biomass provides a direct indication of cell growth therefore, the effects of any changes in operating conditions would be immediately apparent. Similarly the CHMO activity was measured as it is produced intracellularly in *E.coli*, and although certain combinations of the operating variables may have a positive effect on the biomass concentration, this may not necessarily be the case for the CHMO activity and vice versa (Rosso *et al.*, 2002; Chandra *et al.*, 1980; Qader *et al.*, 2006). It is therefore important to assess both these response variables together.

A Central Composite Face (CCF) design was used to determine the optimal levels of the three key variables. This design requires each factor to be varied over three levels only (low, medium and high) and fewer experiments are needed compared to an equivalent Box-Behnken or three-level full factorial design (Montgomery, 2005). Figure 4.3 illustrates the CCF design region using three variables and can be modelled on a cube to represent the experimental region being explored. All factors were coded as described in Section 2.7.1. Table 4.1 shows the experimental plan for optimisation in which three factors are investigated in 20 experimental runs, including six replicated centre point experiments for estimations of pure error. The centre point values of 37 °C, pH 7 and 0.1 % w/v L-arabinose were chosen as they are the most widely reported for this particular strain of *E.coli* (Doig *et al.*, 2001; Lander, 2003; Doig *et al.*, 2002). The high and low levels of the three factors were as follows: temperature ranged from 35 – 39 °C, pH ranged from 6 – 8 and L-arabinose concentration ranged from 0.05 – 0.15 % w/v.

In the case of the temperature, a low value of 35 °C was chosen since it is known that heterologous protein expression can be higher at lower temperatures (Kamerbeek *et al.*, 2003). A higher value of 39 °C was deliberately chosen above the optimum temperature to identify potential interactions between factors. The optimal growth pH for *E.coli* is typically between 6.4 and 7.2 (Manderson *et al.*, 2006), therefore values just outside the optimal range were chosen (pH 6 – 8), so as not to severely affect cell growth and still be able to identify potential factor interactions. In the case of the inducer concentration the upper limit was set to 0.15% w/v since Doig *et al.* (2001) have previously showed that CHMO activity reaches a plateau at inducer concentrations above 0.1% w/v. Below this concentration Doig *et al.* (2001) observed

Table 4.1 shows the Central Composite Face (CCF) design matrix of uncoupled independent variables for the optimisation of ChMO conversion in multiple fermenter experiments. The table shows the corresponding factor and transformation ranges and experimental design factor ChMO activities. Experiments performed as described in Section 4.2.1. The material measurements were 420 minutes after induction. Product = ChMO activity values based on Equation 4.2.



**Figure 4.3.** CCF design region using three variables can be modelled on a cube to represent the experimental region being explored. Each corner of the cube represents a combination of the factors used in an experiment, with additional points at the centres of the faces to approximate a sphere. A centre point is included and in this case has been replicated six times to determine reproducibility and detect non-linear responses.

**Table 4.1.** Central Composite Face (CCF) design matrix of uncoded independent variables for the optimisation of CHMO expression in miniature bioreactor experiments. Table also shows the corresponding biomass concentration results and, experimental and predicted CHMO activities. Experiments performed as described in Section 2.7.2. Experimental measurements were 420 minutes after induction. Predicted CHMO activity values based on Equation 4.2.

| Experiment Number | Temperature (°C), $X_1$ | L-arabinose Concentration (% w/v), $X_2$ | pH, $X_3$ | Biomass (g.L <sup>-1</sup> ) | CHMO Activity (U.g <sup>-1</sup> ) |           |
|-------------------|-------------------------|--|-----------|------------------------------|------------------------------------|-----------|
|                   |                         |  |           |                              | Experimental                       | Predicted |
| 1                 | 35                      | 0.05                                     | 6         | 4.5                          | 27.0                               | 26.7      |
| 2                 | 39                      | 0.05                                     | 6         | 6.0                          | 53.3                               | 48.4      |
| 3                 | 35                      | 0.05                                     | 8         | 5.3                          | 29.0                               | 26.7      |
| 4                 | 39                      | 0.05                                     | 8         | 5.2                          | 44.5                               | 48.4      |
| 5                 | 35                      | 0.15                                     | 6         | 3.8                          | 45.5                               | 58.5      |
| 6                 | 39                      | 0.15                                     | 6         | 4.5                          | 86.7                               | 71.1      |
| 7                 | 35                      | 0.15                                     | 8         | 3.8                          | 56.1                               | 58.5      |
| 8                 | 39                      | 0.15                                     | 8         | 3.9                          | 64.6                               | 71.1      |
| 9                 | 35                      | 0.1                                      | 7         | 4.3                          | 80.6                               | 68.7      |
| 10                | 39                      | 0.1                                      | 7         | 3.4                          | 69.7                               | 79.7      |
| 11                | 37                      | 0.1                                      | 6         | 4.8                          | 36.0                               | 105.0     |
| 12                | 37                      | 0.1                                      | 8         | 3.5                          | 112.0                              | 105.0     |
| 13                | 37                      | 0.05                                     | 7         | 4.5                          | 83.2                               | 83.7      |
| 14                | 37                      | 0.15                                     | 7         | 5.2                          | 99.9                               | 98.6      |
| 15                | 37                      | 0.1                                      | 7         | 5.1                          | 101.5                              | 105.0     |
| 16                | 37                      | 0.1                                      | 7         | 5.1                          | 102.0                              | 105.0     |
| 17                | 37                      | 0.1                                      | 7         | 4.9                          | 105.9                              | 105.0     |
| 18                | 37                      | 0.1                                      | 7         | 5.2                          | 106.4                              | 105.0     |
| 19                | 37                      | 0.1                                      | 7         | 4.9                          | 102.8                              | 105.0     |
| 20                | 37                      | 0.1                                      | 7         | 5.1                          | 102.8                              | 105.0     |

an approximately linear relationship between the final CHMO titre and inducer concentration at a fixed temperature and pH of 37 °C and 7 respectively.

## 4.4 DoE Results, Model Formulation and Optimisation

### 4.4.1. DoE Results and Modelling

Experimentally determined values for both biomass and CHMO activity based on the CCF experimental plan are listed in Table 4.1. These were determined from samples taken at 420 minutes, the time at which the CHMO activity peaked in the initial expression studies (Section 4.2). The behaviour of the system was modelled using the following quadratic equation:

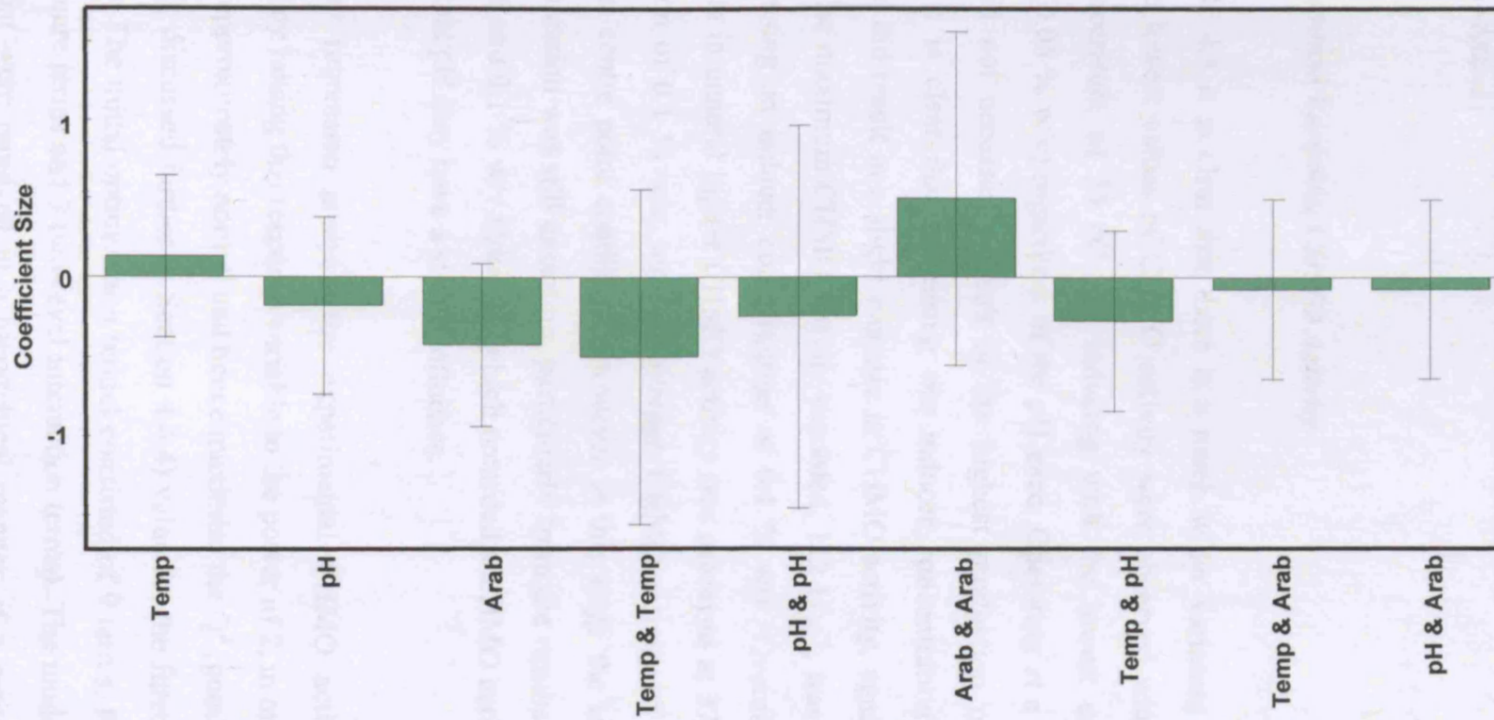
$$Y_i = \beta_0 + \beta_1x_1 + \beta_2x_2 + \beta_3x_3 + \beta_{11}x_1^2 + \beta_{22}x_2^2 + \beta_{33}x_3^2 + \beta_{12}x_1x_2 + \beta_{13}x_1x_3 + \beta_{23}x_2x_3$$

Eq. 4.1

where  $i$  is the predicted response,  $x_1$ ,  $x_2$  and  $x_3$  are independent variables,  $\beta_0$  is the constant term,  $\beta_1$ ,  $\beta_2$  and  $\beta_3$  are linear effects,  $\beta_{11}$ ,  $\beta_{22}$  and  $\beta_{33}$  are squared effects, and  $\beta_{12}$ ,  $\beta_{13}$  and  $\beta_{23}$  are interaction terms. Model terms with confidence intervals that included zero were removed from the regression models in a stepwise manner, starting with the least significant terms.

### 4.4.2. Response Variable: Biomass Concentration

From the measured biomass concentrations (Table 4.1), it can be seen that there is not a wide variation in biomass yield over the ranges of temperature, pH and inducer concentration studied. This is most probably due to the fact that the chosen ranges used for each factor were rather narrow given that *E.coli* is a relatively adaptable microorganism (Stelling *et al.*, 2002) and able to withstand such moderate changes to its environment. The coefficient plot in Figure 4.4 also confirms that none of the



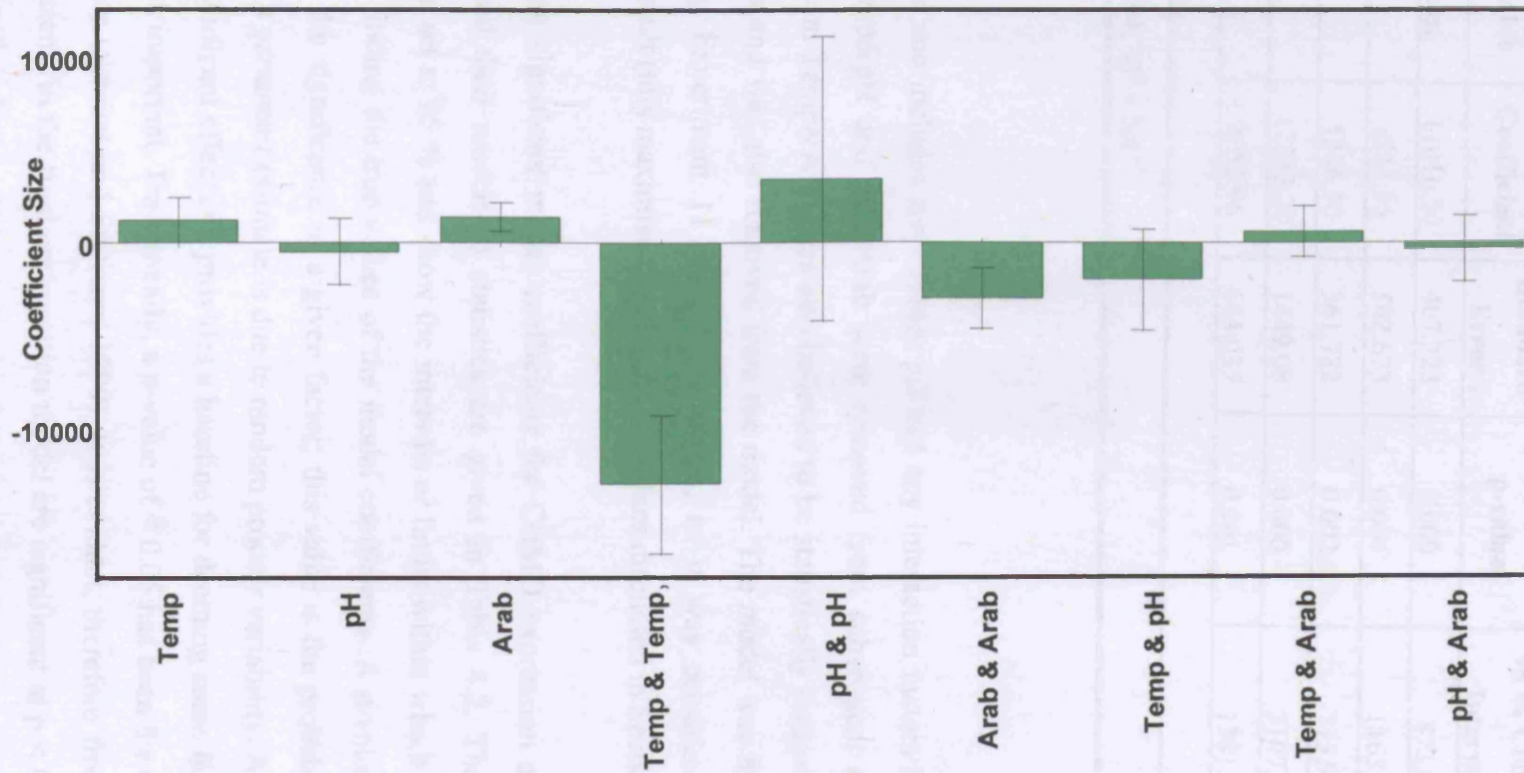
**Figure 4.4.** Coefficient plot with confidence intervals (set at 95%) for biomass concentration. The size of each bar (or coefficient) represents the relative importance upon *E. coli* cell growth.

factors over the ranges studied appeared to have any significant affect on cell growth, since all of the confidence intervals include zero. As a result it was not possible to produce a regression model for predicting biomass concentration, over the range of conditions studied.

#### **4.4.3. Response Variable: CHMO Activity**

From Table 4.1 it is clear that there is a much wider variation in CHMO activity levels. The lowest values of CHMO activity were observed when operating at the lowest temperature of 35 °C and inducing with the lowest concentration of L-arabinose (0.05 % w/v) regardless of the pH used. Operating at a higher temperature (39 °C) did not necessarily result in the highest production of CHMO activity. However, it is clear that increasing the inducer concentration at this particular temperature did result in a slight increase in CHMO activity, again regardless of the pH used. The maximum CHMO activity recorded, 112 U.g<sup>-1</sup>, was achieved at 37°C, pH 8 and using an inducer concentration of 0.1 % w/v. Overall the CHMO data suggests that in general higher CHMO activity was achieved at 37°C and an inducer concentration of 0.1 % w/v, with an average CHMO activity of 103.6 ± 2.1 U.g<sup>-1</sup> recorded for centre point conditions. However at this stage the influence of pH on CHMO expression was still uncertain, particularly from the results of Experiment 11 (37°C, pH 6 and 0.1 % w/v inducer), which recorded a CHMO activity of 36.0 U.g<sup>-1</sup>, suggesting that pH may have a strong influence.

Prior to any regression analysis the experimental CHMO activity results were transformed by raising this response variable to the power of 2, in order to render their distribution approximately normal and hence maximise the Q<sup>2</sup> (goodness of prediction of the model, discussed further in Section 4.4.4) value for the fitted model (Eriksson *et al.*, 2000). The initial optimisation model consisted of 9 terms, Figure 4.5 (3 main effects, 3 square terms and 3 two-level interaction terms). The model terms that were not significant were removed in a hierarchical manner; if a main effect term was removed then all higher order terms containing that factor, such as squared terms and interaction terms were also removed. From Figure 4.5 pH was seen to be statistically insignificant as the indicated confidence interval is much larger compared to the



**Figure 4.5.** Coefficient plot with confidence intervals (set at 95%) for CHMO activity. The size of each bar (or coefficient) represents the relative importance upon CHMO expression.

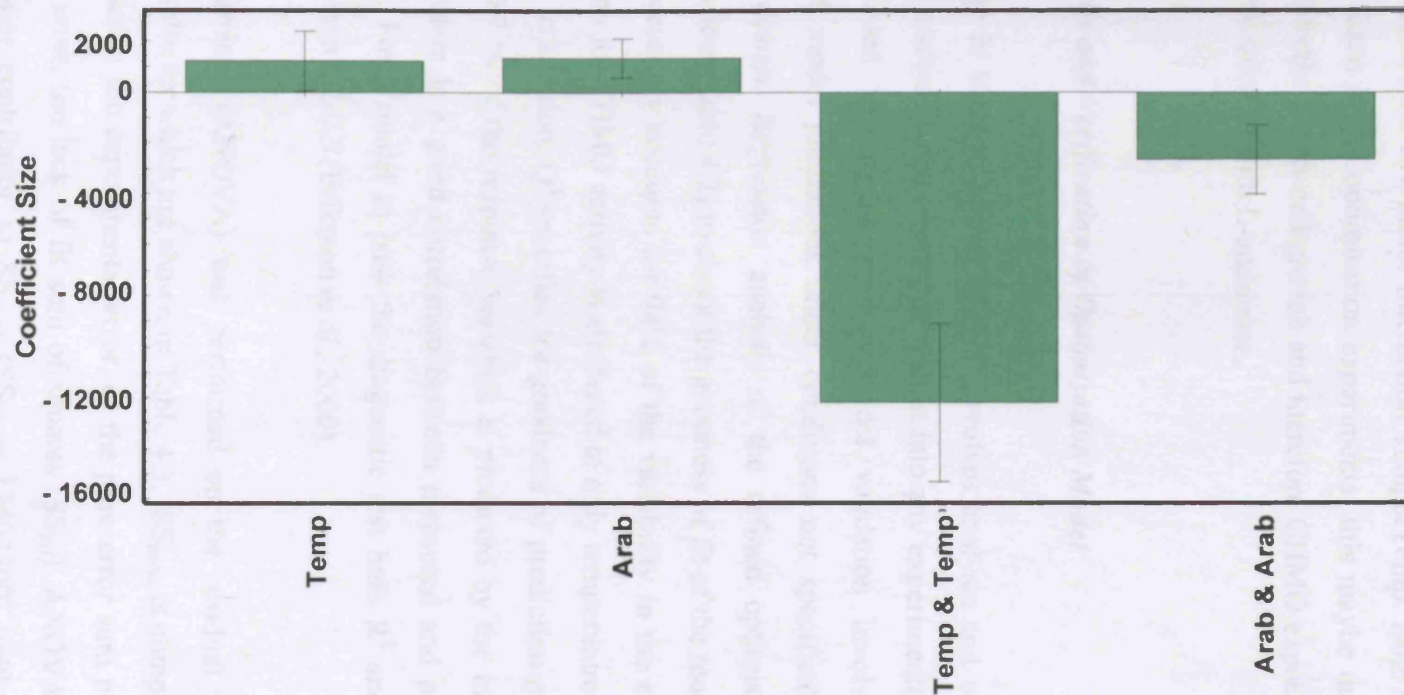


**Table 4.2.** Estimated regression coefficients of the reduced optimisation model (Equation 4.1) for CHMO expression. The corresponding p-values and confidence intervals are also shown.  $X_1$  = temperature and  $X_2$  = L-arabinose concentration.

| Variable                 | Coefficient | Standard Error | p-value | 95 % Confidence Interval ( $\pm$ ) |
|--------------------------|-------------|----------------|---------|------------------------------------|
| Constant                 | 11016.50    | 407.323        | 0.000   | 873.63                             |
| $X_1$                    | 1215.55     | 542.673        | 0.004   | 1163.93                            |
| $X_2$                    | 1356.30     | 361.782        | 0.002   | 775.953                            |
| $X_1^2$                  | 12213.20    | 1449.08        | 0.000   | 3107.99                            |
| $X_2^2$                  | 2652.96     | 644.035        | 0.001   | 1381.33                            |
| $R^2 = 0.94, Q^2 = 0.87$ |             |                |         |                                    |

response area and includes zero. Hence pH and any interaction factors involving pH, pH&pH, Temp&pH and pH&Arab were removed from subsequent analysis. The interaction term Temp&Arab was also believed to be statistically insignificant for the same reasons and was also removed from the model. The model was further refined by excluding Experiment 11 from the analysis, as it was considered to be an anomalous result (this maximised the  $R^2$  and  $Q^2$  values discussed in Section 4.4.4).

The remaining significant model coefficients for CHMO expression are shown in Figure 4.6 and their associated statistics are given in Table 4.2. The confidence intervals were set at 95 % and show the intervals or limits within which there is a 95 % chance of finding the true values of the model coefficients. A p-value is a means for assessing the significance of a given factor; this value is the probability that the magnitude of a parameter estimate is due to random process variability. A low p-value indicates a significant effect and provides a baseline for deeming some factors critical and others less important. Traditionally, a p-value of  $< 0.05$  has been the cut-off point for significance (Strobel and Sullivan, 1999). It is evident, therefore from Table 4.2 that all coefficients in the final optimisation model are significant at  $p < 0.05$ . Only 2 (temperature and inducer concentration) of the original 3 factors were found to significantly influence the expression of CHMO. The squared terms for both



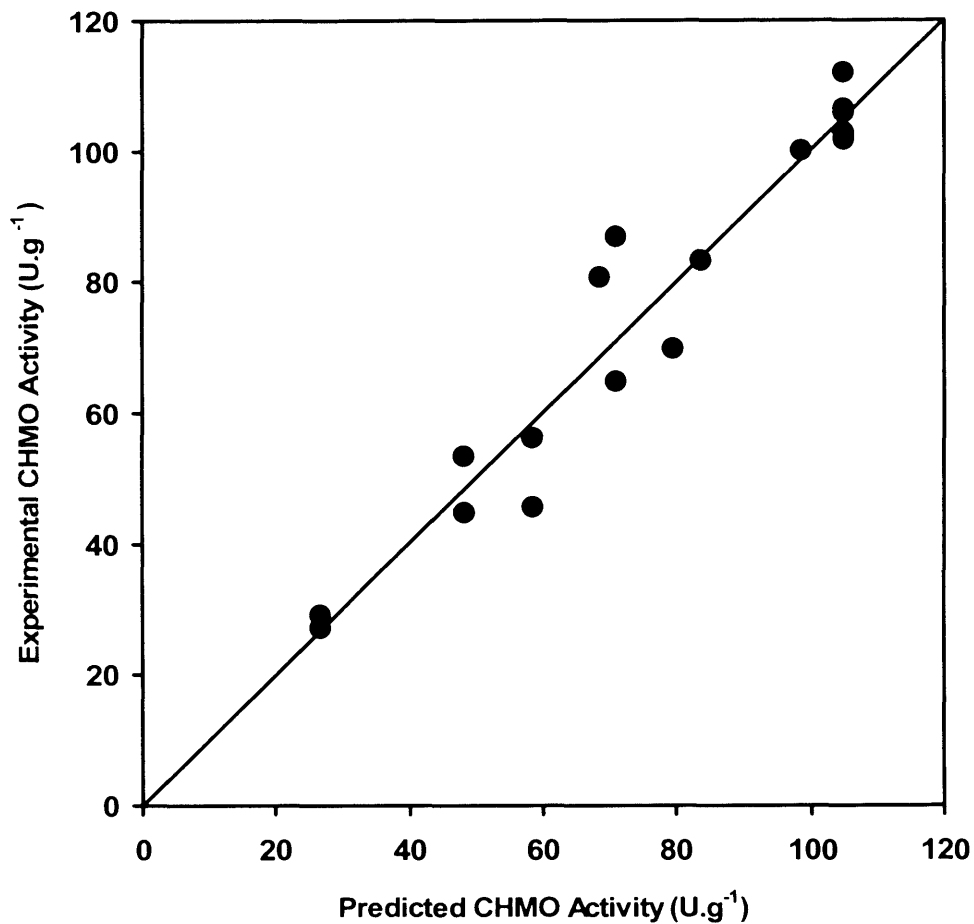
**Figure 4.6.** Coefficient plot for final optimisation model for CHMO activity, complete with confidence intervals (set at 95%) for CHMO activity ( $Y$  transformed as  $Y^2$ ). The original model consisted of 9 terms. However terms whose confidence intervals included the value zero were deemed insignificant and so were removed in a hierarchical manner.

temperature and inducer concentration are significant and indicate that the optimum levels for these factors lie within the ranges studied. Although the main effect of temperature may be considered a lower order term and less significant, this term is not deleted from the refined model because it contributes to the formation of a higher order term, namely, the two factor interaction Temp&Temp. Both these factors have become significant in the optimisation experiments; this maybe due to the fact that temperature directly effects cell growth and therefore CHMO expression which relies completely on induction with L-arabinose.

#### ***4.4.4. Analysis and Verification of Optimisation Model***

The final stage in the application of DoE involves analysis and verification of the model. Model analysis helps to provide insight into any experimental issues that may not be accounted for in the model. Model validation involves experimental verification of model predictions under conditions not specifically tested in the experimental design. Regression analysis of the refined optimisation model for CHMO expression (Table 4.2) to check the goodness of fit of the model,  $R^2$ , indicates the model successfully accounts for 94% of the variability in the response and that sample variation for CHMO activity is attributed to only temperature and L-arabinose concentration. In addition,  $Q^2$  specifies the goodness of prediction of the model, and confirms that 87 % of the response variation is predicted by the model. Figure 4.7 confirms that there is a good correlation between measured and predicted CHMO activity values. For a model to pass the diagnostic test both  $R^2$  and  $Q^2$  should not differ by more than 0.2-0.3 (Eriksson *et al.*, 2000).

Analysis of variance (ANOVA) was performed on the residual sum of squares ( $SS_{resid}$ ), the results for which are shown in Table 4.3.  $SS_{resid}$  is comprised of the sum of two components: the experimental error, or the pure error sum of squares ( $SS_{pe}$ ) and the model error, the lack of fit sum of squares ( $SS_{lof}$ ). ANOVA concludes that  $SS_{lof}$  is the major contributor to  $SS_{resid}$  ( $SS_{lof} \sim 17402300$ ), with the pure error associated with the replicate experiments being relatively low ( $SS_{pe} \sim 921760$ ).



**Figure 4.7.** Parity plot of experimental and predicted CHMO activities used to produce the regression model. Experimental values taken from experiments described in Table 4.1. Predicted values calculated from refined regression model, Equation 4.2. Solid line indicates parity.

The final regression model was comprised of the coefficients shown in Table 4.2 and assumed the form of a second-order polynomial equation that enables reliable predictions of CHMO activity (Y) based on the interaction of temperature ( $X_1$ ) and L-arabinose concentration ( $X_2$ ):

$$Y^2 = 11016.5 + 1215.55X_1 + 1356.3X_2 - 12213.2X_1^2 - 2652.96X_2^2 \quad \text{Eq. 4.2}$$

**Table 4.3.** ANOVA results for analysis of the reduced optimisation model (Equation 4.2) for CHMO expression. Model terms as described in Table 4.2.

| Source                 | Degrees of Freedom (DF) | Sum of Squares (SS) | Mean Squares (MS) | F statistic | p-value |
|------------------------|-------------------------|---------------------|-------------------|-------------|---------|
| <b>Total</b>           | 19                      | 1164110000          | 61269000          |             |         |
| <b>Constant</b>        | 1                       | 869096000           | 869096000         |             |         |
|                        |                         |                     |                   |             |         |
| <b>Total Corrected</b> | 18                      | 295015000           | 16389700          |             |         |
| <b>Regression</b>      | 4                       | 276691000           | 69172800          | 52.849      | 0.000   |
| <b>Residual</b>        | 14                      | 18324100            | 1308860           |             |         |
|                        |                         |                     |                   |             |         |
| <b>Lack of Fit</b>     | 9                       | 17402300            | 1933590           | 10.489      | 0.009   |
| <b>Pure Error</b>      | 5                       | 921760              | 184352            |             |         |

## 4.5 Response Surface Plot: Optimisation of Enzyme Expression

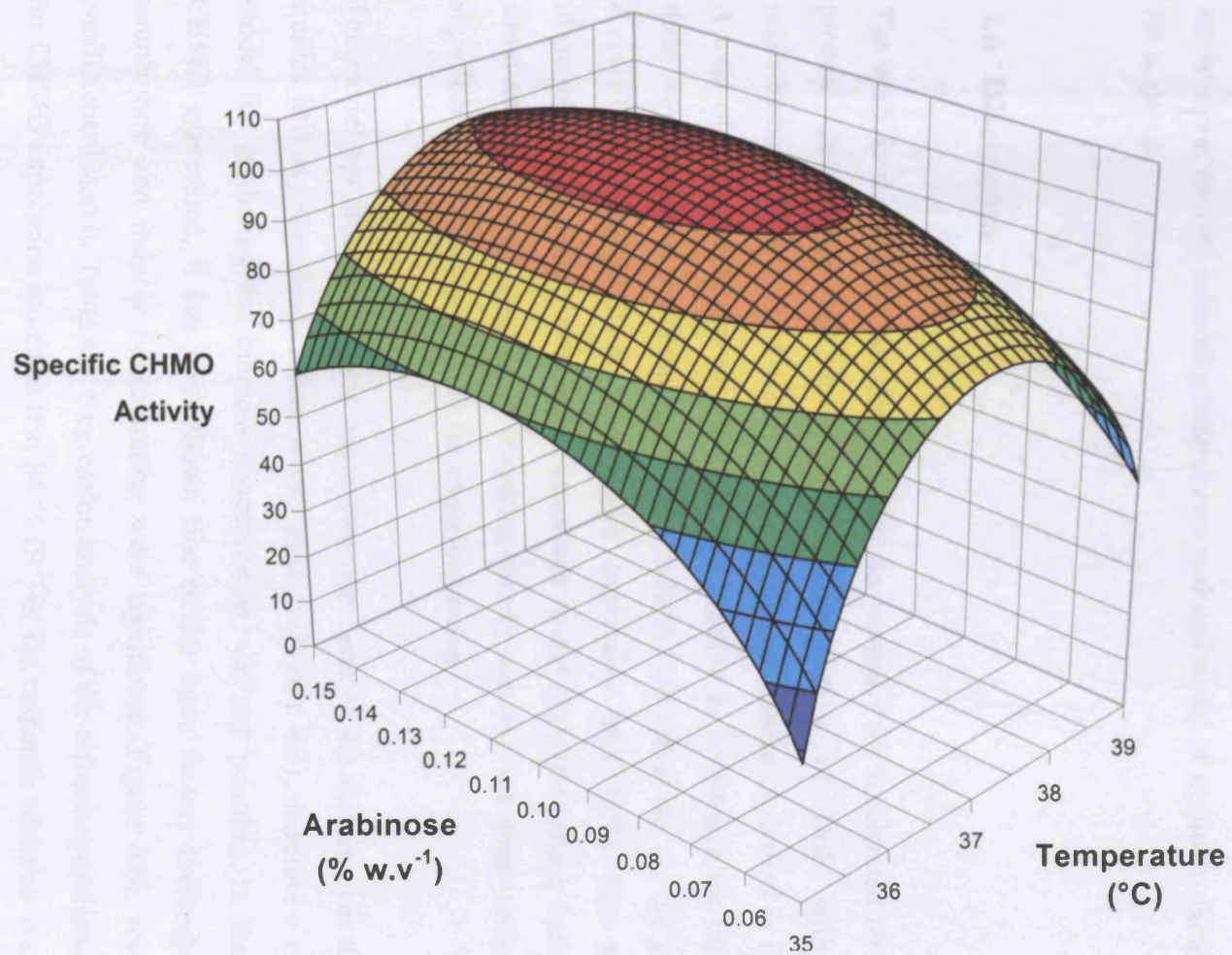
### 4.5.1. Response Variable: Biomass Concentration

Further analysis of the data described in Table 4.1 was carried out using a response surface approach (Adinarayana and Ellaiah, 2002). The response surface plot displays the combined influence of two key variables, in this case: temperature and L-arabinose concentration, on the desired response: CHMO activity. The response surface plots are derived based on using the DoE model that has been developed to predict the response value for any factor setting in the experimental region and identifying factor settings that correspond to an optimum response for the chosen variable. (Adinarayana and Ellaiah, 2002; Eriksson *et al.*, 2000). The maximum predicted yield is indicated by the surface confined in the response surface diagram.

In the case of biomass concentration, it has already been shown in Section 4.4.2 that there was no influence of the selected variables on the measured biomass concentration. The measured biomass concentration was found to be relatively constant over all experimental conditions investigated. Consequently no statistically significant model could be obtained for predicting biomass concentrations; hence no response surface could be drawn.

### 4.5.2. Response Variable: CHMO Activity

In the case of the CHMO activity, two of the factors, temperature and inducer concentration were shown to have a significant effect on CHMO expression, hence a suitable regression model was derived (Equation 4.2). The three-dimensional graph obtained from the calculated response surface is shown in Figure 4.8. The response surface plot illustrates the strong interaction effects between inducer concentration and temperature; and the squared terms for both these factors also signify that optimum values of these factors are within the ranges studied. A maximum specific CHMO activity of  $105.9 \text{ U.g}^{-1}$  was predicted from the response surface plot, achieved at a temperature of  $37.1 \text{ }^\circ\text{C}$  and inducer concentration of  $0.11 \text{ \% w/v}$ . This is



**Figure 4.8.** Response surface plot showing variation of expressed CHMO activity and the strong interaction effects between temperature and L-arabinose concentration. Response surface generated based on the data in Table 4.1 and using Equation 4.2.

comparable with the experimentally measured CHMO activity results at the centre points, and Experiment 12 which were carried out under similar condition, 37 °C and 0.1% w/v L-arabinose. The optimum operating conditions for temperature and inducer concentration predicted from the model are similar to the conditions previously established by Doig *et al.* (2001). Therefore although no direct enhancement in CHMO production was achieved, the response surface plot provides a good basis for establishing process operating boundaries and definition of optimum factor settings for scale-up.

## 4.6 Discussion

The work in this chapter has demonstrated the potential for accelerated fermentation process development by the combined application of DoE with parallel experimentation using the 4-pot miniature bioreactor system described in Chapter 3. A total of 20 fermentations (Table 4.1) were required to investigate the influence of three key variables, temperature, pH and inducer concentration, on the growth of *E.coli* TOP10 pQR239 and heterologous expression of CHMO. This study has illustrated the miniature bioreactors capability to run high throughput fermentations simultaneously over a range of operating conditions and set point values, hence significantly reducing time scales for experimentation.

The model optimisation process has shown that none of the factors over the ranges studied had any significant affect on cell growth (Figure 4.4), therefore a regression model for predicting the biomass concentration was not possible. In the case of CHMO expression, it has been shown that of the three factors investigated only temperature and inducer concentration were significant (Figure 4.6), with model coefficients listed in Table 4.2. Regression analysis of the refined optimisation model for CHMO expression indicates that 94 % ( $R^2$ ) of the response variation is explained by the model and 87 % ( $Q^2$ ) of the response variation is predicted by the model, hence confirming a good correlation between measured and predicted CHMO activity (Figure 4.7).



The final regression model (Equation 4.2) produced the response surface plot shown in Figure 4.8, and clearly shows strong interaction effects between inducer concentration and temperature; and the squared terms for both these factors also signify that optimum values of these factors are within the ranges studied. The DoE model predicted the optimum conditions for temperature and inducer concentration of 37.1 °C and 0.11 % w/v respectively. These conditions are similar to those previously established by Doig *et al.* (2001). At these conditions a maximum specific CHMO activity of 105.9 U.g<sup>-1</sup> was achieved. This is in reasonably good agreement with the experimentally determined average CHMO activity of 103.6 U.g<sup>-1</sup> for the centre point conditions (37 °C and 0.1 % w/v L-arabinose).

The strong dependence of CHMO expression on both temperature and L-arabinose concentration is most likely due to that fact that the enzyme is produced intracellularly. Therefore any temperature changes directly affect the cells metabolic pathways as well as its immediate environment, and *E.coli* adjusts its internal environment to adapt to changes (Babu and Aravind, 2006). In addition, enzyme production is induced only by L-arabinose; the concentration of L-arabinose is thus critical and will directly affect the level of CHMO activity. Baneyx (1999) has reported that the arabinose inducer system is somewhat weaker promoter and although it is commonly believed that *araBAD* can be used to achieve graded levels of protein expression by varying the arabinose concentration, there is extensive heterogeneity in cell populations treated with subsaturating concentrations of the inducer, with some bacteria fully induced and others not at all. It has also been recently found that that interferon- $\alpha$  and human granulocyte-colony stimulating factor (*hG-CSF*) were expressed relatively slower in the L-arabinose promoter system, compared to other *E. coli*-inducible promoters such as *tac* and *pL* promoter (Choi *et al.*, 2001). This maybe due to the nature of the *araBAD* regulon of *E. coli* shown to exhibit all-or-nothing induction (Siegele and Hu, 1997). In such cases those cells that contain sufficient transporters to accumulate inducer at the time the sugar is added induce the synthesis of additional transporters that catalyze uptake of more sugar leading to further induction (Morgan-Kiss *et al.*, 2002). This autocatalytic induction cycle continues until this subpopulation of cells becomes fully induced. In contrast, cells having transporter levels that fall below the threshold number of transporters required for inducer accumulation never capture sufficient sugar to become induced (Morgan-Kiss

*et al.*, 2002).

In the case of pH however, as a variable does not directly affect CHMO activity as changes in pH generally only affect the pH of the external environment and thus have minimal influence on the intracellular pH and biosynthesis including production of CHMO. Generally the internal environment of the cell is closer to neutral (~ pH 7) and is usually fairly insensitive to the external environment. Microorganisms are able to regulate their internal pH homeostasis for normal growth (Zulkifli *et al.*, 2006).

Thus the basic utility of the miniature bioreactor system has been demonstrated together with its application to the rapid establishment of optimum fermentation conditions at small scale. In the next chapter the engineering basis for the scale-up of the optimum miniature bioreactor results will be considered.

# 5. SCALE-UP OF MINIATURE BIOREACTOR PERFORMANCE<sup>†</sup>

---

---

## 5.1 Introduction and Aims

In the previous chapters the potential of the miniature bioreactor system to accelerate fermentation process development has been established. For the results obtained to be of use by industry, however, it is important that those obtained in the miniature bioreactor can be reproduced at the conventional laboratory scales currently used to mimic larger industrial scales. There is no standard method for fermentation scale-up, since the basis for scale-up is very much related to the characteristics of the microorganism and individual processes. The process characteristics which have been most commonly suggested to be maintained constant during scale-up include  $k_L a$ , power per unit volume, oxygen transfer rate, impeller tip speed and mixing time (Stanbury *et al.*, 2002; Ju and Chase, 1992; Oosterhuis and Kossen, 1985; Hosobuchi and Yoshikawa, 1999), these parameters have been discussed in detail in Section 1.2.3.

The aim of this chapter is to further characterise the mixing and oxygen transfer characteristics of the miniature bioreactor and to establish a quantitative basis for process scale-up. The specific objectives include:

- Measurement of the ungasged and gasged power input of the miniature impeller as a function of agitation and aeration rates.
- Establishment of predictive correlations for the miniature bioreactor relating  $P_g/V$  and  $k_L a$  to bioreactor operating conditions.

---

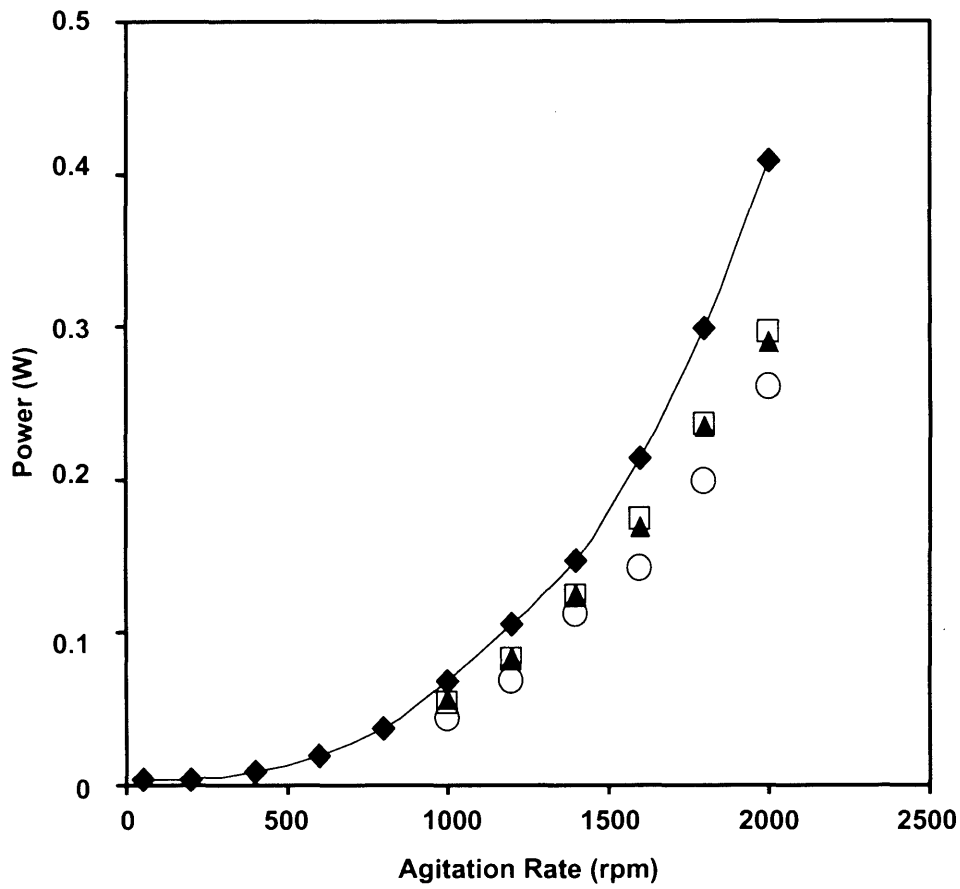
<sup>†</sup> The majority of the results presented in this chapter have been submitted for publication as: N. K. Gill, M. Appleton, G. J. Lye, Quantification of Power Consumption and Oxygen Transfer Characteristics of a Stirred Miniature Bioreactor for Predictive Scale-up, *Biotechnol. Bioeng.* (2007) submitted.

- Performance of a series of miniature and conventional scale *E.coli* fermentations at matched  $P_g/V$  and  $k_L a$  values in order to define a suitable engineering basis for scale-up.
- Verification of both the chosen basis for scale-up and the DoE results from chapter 4 based on the accurate reproduction of the optimum miniature bioreactor results at the laboratory scale.

## 5.2 Power Characteristics of the Miniature Turbine Impeller

For any novel impeller design it is important to understand its mixing and energy dissipation characteristics. The impeller power consumption in the case of aerated systems is always lower than that in unaerated systems since the transfer of power from the impeller to the fluid is greatly influenced by aeration. This power reduction is due to the formation of cavities behind the impeller blades and the different density of the fluid under gassed and ungassed conditions (Sensel *et al.*, 1993). The affect of aeration has been extensively studied by Nienow *et al.* (1977) (as referenced by Yawalkar *et al.*, 2002) and Warmoeskerken and Smith (1981) (as referenced by Oosterhuis and Kossen, 1981) for a single impeller system as studied here. It has been shown that the gassed power input is approximately 30-40 % of the ungassed power input (Oosterhuis and Kossen, 1985).

The results in Figure 5.1 illustrate how the measured power consumption of the miniature turbine impeller, for both gassed and ungassed conditions increases exponentially with agitation rate. There is a clear trend showing that the power consumption under ungassed conditions is on average 25.7 % higher than that of the gassed power consumption. The maximum power consumption determined was 0.41 W at an agitation rate of 2000 rpm. The measured power consumption under gassed conditions was found to decrease with increasing aeration rate. The maximum values measures at an agitation rate of 2000 rpm were 0.30, 0.29 and 0.26 W for aeration rates of 1, 1.5 and 2 vmm respectively. The difference between ungassed and gassed power inputs is more significant at higher stirrer speeds. As the stirrer speed decreases to <1000 rpm the gassed power consumption approaches the ungassed power



**Figure 5.1.** Ungassed and gassed power requirements of the miniature turbine impeller over a range of agitation rates: (◆) ungasged power; gassed power with aerating at (□) 1 vvm, (▲) 1.5 vvm and (○) 2 vvm. Experiments performed with water as described in Section 2.5.

consumption with a maximum difference of 0.024 W. Visual observations suggested that this was a result of poor gas dispersion at lower stirrer speeds.

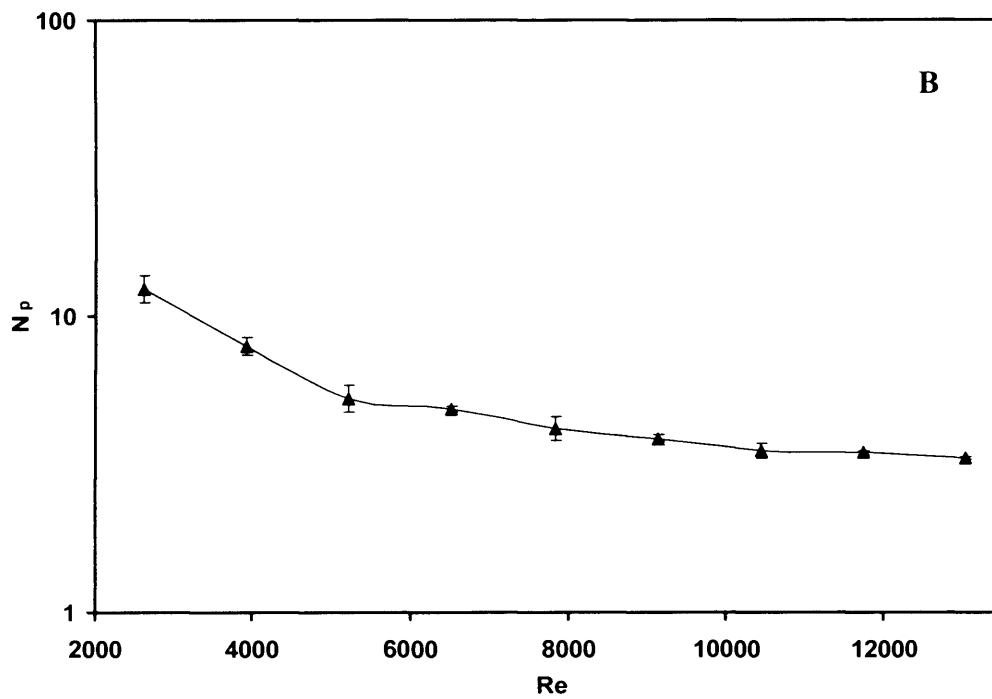
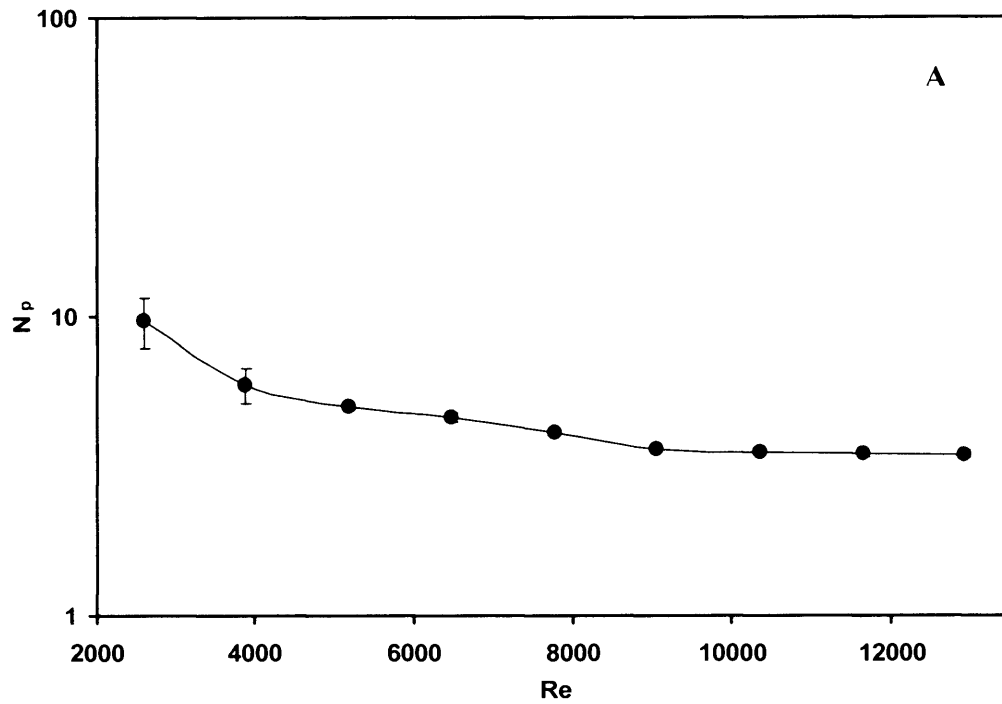
For the ungasged power input data Figure 5.2 shows the relationship between the calculated Power number,  $N_p$ , of the miniature turbine impeller and the impeller Reynolds number,  $Re$ . The  $N_p$  values have been calculated by substituting the measured ungasged power input data (Figure 5.1) into Equation 5.1:

$$P_{ug} = N_p \rho N^3 d_i^5 \quad \text{Eq. 5.1}$$

where  $P_{ug}$  is the ungasged power input of the impeller,  $N_p$  is the Power number,  $\rho$  is the density of the liquid,  $N$  is the agitation rate and  $d_i$  is the impeller diameter. Results are shown for agitation of both water and clarified fermentation broth. At low agitation rates, the Power numbers are higher than usually reported for a single Rushton turbine. This may be due to vibrations of the rigid arm attached to the top plate of the air bearing which led to the large error bars indicated. The variation of  $N_p$  with  $Re$  is very similar for both process fluids and as  $Re$  increases, a constant value of 3.5 for  $N_p$  is achieved. Visual observation of the vessel suggested that the turbulent motion of the liquid was achieved at  $Re > 8000$ .

This measured value of a  $N_p$  of 3.5 is lower than that typically reported in literature for a six blade Rushton turbine of 6 (Nienow *et al.*, 1994) in the turbulent region. However, Bujalski *et al.* (1987) have reported that geometric parameters such as the thickness of the disk and the impeller blades can have an appreciable effect on the Power number. Rutherford *et al.* (1996) also concluded that  $N_p$  reduced as the ratio of impeller blade thickness to impeller diameter was increased from 0.008 to 0.033. The  $N_p$  correlation derived by Rutherford *et al.* (1996) is shown below,

$$N_p = 6.57 - 54.771 \left( \frac{b_t}{d_i} \right) \quad \text{Eq. 5.2}$$



**Figure 5.2.** Variation of the measured Power number with increasing Reynolds number for the miniature turbine impeller: (A) in water; (B) in clarified fermentation broth. Power number calculated as described in Section 5.2. Error bars represent one standard deviation.

where  $N_p$  is the Power number,  $b_t$  is the impeller blade thickness and  $d_i$  is the impeller diameter. This computes a Power number of 3.8 for the miniature turbine impeller designed here having a blade thickness ratio of 0.05. This predicted value is in good agreement with the experimentally determined Power number. In relation to other miniature impeller designs this measured  $N_p$  is within the same range as those reported for the magnetically driven bioreactor block ( $d_T = 20$  mm,  $d_i = 14.5$  mm) described by Puskeiler *et al.* (2005), who estimated a value of 3.7 based on CFD analysis, and Betts *et al.* (2006b) who predicted a Power number of 3 for a triple impeller system ( $d_T = 0.023$  m,  $d_i = 8.5$  mm) based on directly measuring the electrical energy input of the agitator motor.

### 5.2.1. Variation of $P_g/P_{ug}$ Ratio with Flow Number

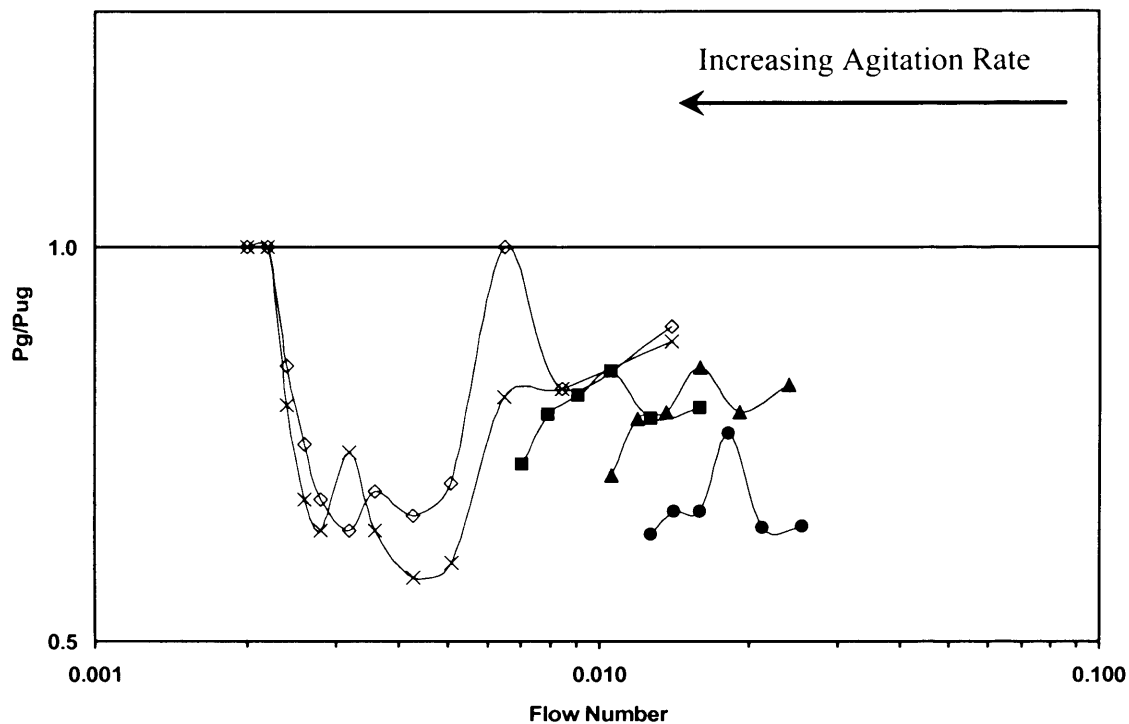
In aerated systems the ratio of  $P_g/P_{ug}$  will determine the actual power input during fermentation operation and can also give insight into the gas dispersion characteristics of the impeller. The extent of power decrease in a gassed compared to an ungassed system,  $P_g/P_{ug}$ , ranges from 0.3 – 1, depending on the type of impeller and aeration rate (Abia *et al.*, 1973).

The nature of the gas-liquid flow regime within the vessel maybe described by the Flow number which defined as:

$$Fl = \frac{Q_g}{Nd_i^3} \tag{Eq 5.3}$$

where  $Q_g$  is the volumetric gas flow rate,  $N$  is the agitation rate and  $d_i$  is the impeller diameter (Hall *et al.* 2005). Figure 5.3 shows the measured  $P_g/P_{ug}$  ratio (solid symbols) as a function of the Flow number. For comparison data from Hall *et al.* (2005) has also been included (open symbols). Their system consisted of a 0.045 m diameter glass vessel with a mechanically driven, eccentrically fitted 6-blade up pumping pitched blade turbine ( $d_i = 0.024$ m) and is the only compatible data available in the literature at this scale. In the case of Hall *et al.* (2005) gas was introduced at a





**Figure 5.3.** Comparison of the ratio of gassed/ungassed power,  $P_g/P_{ug}$ , against Flow number for the miniature bioreactor and the results reported by Hall *et al.* (2005) for a miniature reactor with a 0.045m vessel diameter. Miniature bioreactor aeration rates: (■) 1 vvm, (▲) 1.5 vvm and (●) 2 vvm. Hall *et al.* (2005) miniature reactor aeration rate of 0.5 vvm: (×) sparger positioned beneath the impeller axis; (◇) sparger positioned away from the impeller.

single flow rate of 0.5 vvm via a sintered glass sparger mounted at the base of the vessel. Two different configurations were used for the position of the sparger in the vessel: the first had the active area of the sparger located directly below the eccentrically positioned impeller, whilst the second had the active part of the sparger located opposite the impeller on the other side of the vessel. From Figure 5.3 it can be seen that the ratio of  $P_g/P_{ug}$  is of the same order of magnitude for both systems and in the range of 0.58-0.85, suggesting similar gas dispersion characteristics. However to obtain similar values of  $P_g/P_{ug}$  the miniature bioreactor studied here needs to operate at significantly higher flow numbers. This is probably due to the thicker blades of the miniature impeller design used here as described in Section 5.2.

To ensure economical gas-liquid dispersion in a stirred tank reactor and to better understand the various flow patterns that occur, some knowledge of the minimum agitation rate ( $N_{CD}$ ) for complete dispersion of the sparged gas is necessary. Nienow *et al.* (1977) proposed the following correlation:

$$N_{CD} = \frac{4Q_g^{0.5} d_T^{0.25}}{d_i^2} \quad \text{Eq. 5.4}$$

where  $N_{CD}$  is the minimum agitation rate for complete dispersion of the sparger gas ( $\text{rev}\cdot\text{s}^{-1}$ ),  $Q_g$  is the volumetric gas flow rate,  $d_T$  is the vessel diameter  $d_i$  is the impeller diameter. At agitation rates below  $N_{CD}$ , gas dispersion becomes inefficient resulting in little or no gas in the region below the impeller and potential oxygen starvation in the case of aerobic fermentations. In Figure 5.3  $N_{CD}$  is represented by the minimum  $P_g/P_{ug}$  values in each data set. The flow pattern at this operating condition is characterised by a fully dispersed bubbled regime throughout the fluid without any flooding of the impeller. At this point however the gas hold up is not sufficient to promote gross recirculation of bubbles throughout the dispersion. The point at which gross recirculation sets in is normally taken as the left hand maximum of the curves (Hall *et al.*, 2005).

In the case of the miniature bioreactor the data in Figure 5.3 suggests that complete

dispersion of gas occurred at flow numbers of 0.014, 0.019 and 0.028 for aeration rates of 1, 1.5 and 2 vvm respectively. These flow numbers are achieved at significantly higher agitation rates, compared to those calculated by Equation 5.4 which predicts flow numbers of 0.033, 0.040 and 0.047 for achieving complete dispersion. These differences are again most likely a result of the thicker impeller blades as described in Section 5.2.

### 5.3 Correlation of Miniature Bioreactor Energy Dissipation Rates

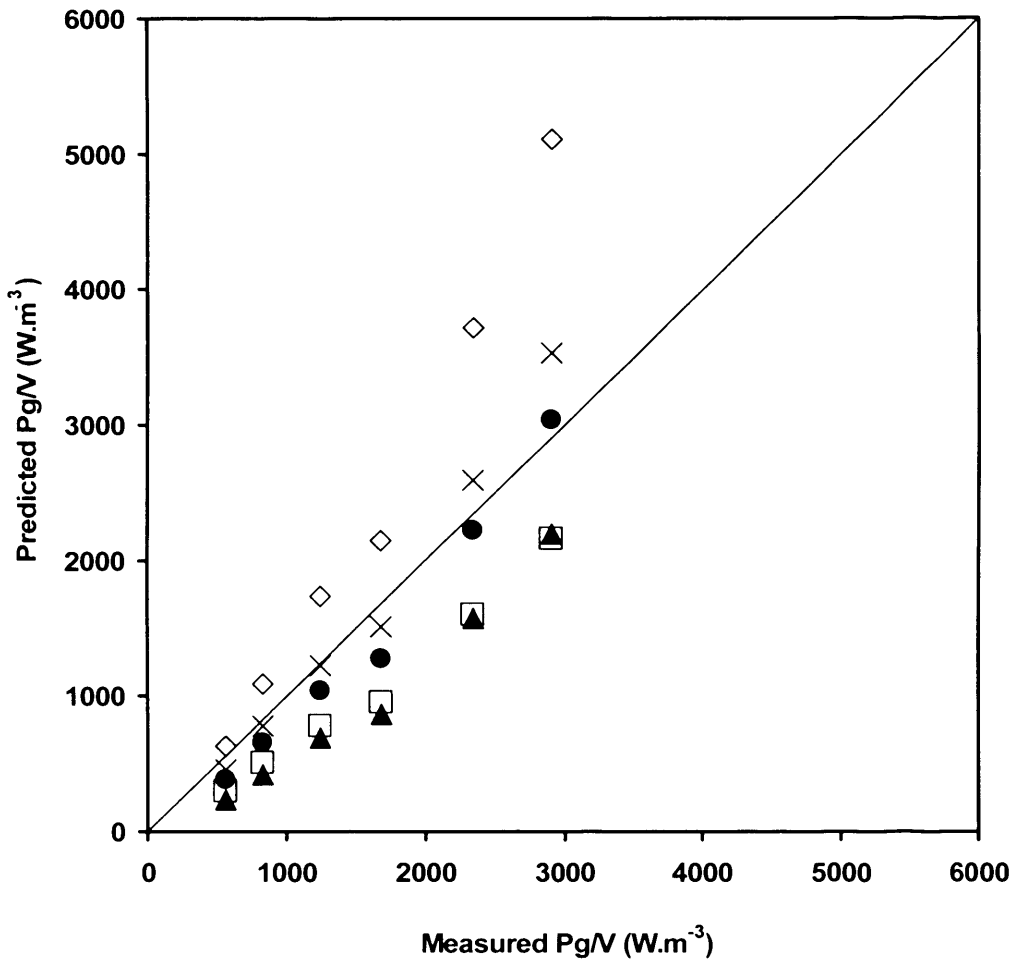
For the purpose of process design and scale-up it is useful to correlate the measured power input data shown in Figure 5.1 with the bioreactor geometry and operating conditions. The ungasged power requirement,  $P_{ug}$ , of an impeller in a stirred bioreactor can be easily calculated from the Power number (Equation 5.1). However since the transfer of power from the impeller to the fluid is influenced very much by aeration, as described in Section 5.2, the power uptake for the gassed situation is lower than that for the ungasged situation. Much research has been done to correlate  $P_g/P_{ug}$  values to bioreactor design and operation. Table 5.1 lists some of the most commonly used correlations derived by various authors with a particular emphasis on smaller vessels with single impellers ( $d_T = 0.165-1.83$  m).

Figure 5.4 shows a parity plot comparing the measured  $P_g/V$  values here with those predicted from the correlations listed in Table 5.1. The dual correlation proposed by Cui *et al.* (1996) provides the closest predictions to the experimental miniature bioreactor data. In their work the correlations were based on 526 data sets for single impeller systems with errors below 6 %. Cui *et al.* (1996) concluded that gassed power reductions can vary considerably at the same Flow number, which means that the Flow number alone is not sufficient to describe the value of  $P_g/P_{ug}$ . Consequently they derived two separate criteria for predicting the  $P_g/P_{ug}$  depending of the value of the Flow number.

In terms of the other correlations, Mockel *et al.* (1983) derived an empirical equation which gave good agreement with measured and literature data. This correlation is

**Table 5.1.** Comparison of the most commonly reported gassed to un-gassed power ( $P_g/P_{ug}$ ) correlations for smaller scale vessels.

| Reference                   | Vessel Diameter (m) | Impeller Characteristics |   |             | Proposed Correlation   |
|-----------------------------|---------------------|--------------------------|---|-------------|--|
|                             |                     | Type                     | Number                                    | D/T         |  |
| Cui <i>et al.</i> (1996)    | 0.23 - 1.83         | flat blade turbine       | 1-2                                       | 0.33 - 0.5  | $\frac{QN^{0.25}}{D^2} \leq 0.055: 1 - \frac{P_g}{P_{ug}} = 9.9 \left( \frac{QN^{0.25}}{D^2} \right)$ $\frac{QN^{0.25}}{D^2} > 0.055: 1 - \frac{P_g}{P_{ug}} = 0.52 + 0.62 \left( \frac{QN^{0.25}}{D^2} \right)$ |
| Mockel <i>et al.</i> (1983) | 0.4 - 7             | flat blade turbine       | 1 (Z = 750)<br>2 (Z = 490)<br>3 (Z = 375) | 0.25 - 0.4  | $\frac{P_g}{P_{ug}} = \frac{1}{\sqrt{1 + Z \frac{U_s}{\sqrt{gD}}}}$  |
| Hughmark (1980)             | 0.165 - 1           | flat blade turbine       | 1   | 0.33        | $\frac{P_g}{P_{ug}} = 0.1 \left[ \frac{Q}{NV} \right]^{-0.25} \left[ \frac{N^2 D_i^4}{gW_i V^3} \right]^{-0.2}$  |
| Michel and Miller (1962)    | 0.165 - 0.305       | flat blade turbine       | 1   | 0.25 - 0.46 | $P_g = 0.72 \left[ \frac{P_{ug}^2 ND^4}{Q^{0.56}} \right]^{-0.45}$   |
| Luong and Volesky (1979)    | 0.222               | 6 blade turbine          | 1   | 0.33        | $\frac{P_g}{P_{ug}} = 0.497 \left( \frac{Q}{ND^3} \right)^{-0.38} \left( \frac{N^2 D^3 \rho}{\sigma} \right)^{-0.18}$  |



**Figure 5.4.** Parity plot comparing the measured  $P_g/V$  at an aeration rate of 1.5 vvm, with those predicted from the most commonly reported literature correlations: ( $\square$ ) Hughmark (1980); ( $\blacktriangle$ ) Michel and Miller (1962); (x) Cui et al. (1996); ( $\diamond$ ) Luong and Volesky (1979); ( $\bullet$ ) Mockel et al. (1990). Experimental measurements as shown in Figure 5.1. Correlations as described in Table 5.1. Solid line represents line of parity.

unique in that it only takes into account the superficial gas velocity and impeller diameter together with a single constant,  $Z$ , which varies depending on the number of impellers. Although the correlation does not appear to be as widely used as some, it does show reasonably good agreement with the measured  $P_g/V$  data here, but with a tendency to over predict the experimental values. The correlation presented by Hughmark (1980) for a six-bladed disc turbine has been applied over a wide range of system configurations and operating parameters. The correlation was based on 391 data sets with a standard deviation of 0.1117 and is considered to be very reliable (Hughmark, 1980; van't Riet and Tramper, 1991; Yalwalkar *et al.*, 2002). Although Koloini *et al.* (1989) reported that Hughmark's correlation predicted higher values for power input compared to their experimental data, in the case of the miniature bioreactor this correlation also slightly under estimates the power input compared to the measured values, especially at higher stirrer speeds. The original  $P_g/P_{ug}$  correlation suggested by Michel and Miller (1962) follows the same general trend as that predicted by Hughmark, but it is known that this correlation was derived over a limited variable range (Van't Riet and Tramper, 1991; Nagata, 1975). Finally the Luong and Volesky (1979) correlation based on the use of dimensionless groups and Newtonian fluids, is seen to greatly over predict the measured values and is unsuitable.

#### 5.4 Correlation of Miniature Bioreactor $k_L a$ Values

Given the previously established importance of the  $k_L a$  value on cell growth kinetics in the miniature bioreactor (Table 3.3), correlations for the prediction of  $k_L a$  values were also examined. These correlations usually relate  $k_L a$ , power consumption and superficial gas velocity, and take the form:

$$k_L a = C \left( \frac{P_g}{V} \right)^\alpha u_s^\beta \quad \text{Eq. 5.5}$$

where  $k_L a$  is the volumetric mass transfer coefficient,  $P_g/V$  is the impeller gassed

power per unit volume,  $u_s$  superficial gas velocity,  $C$  is a constant and  $\alpha$  and  $\beta$  are exponents. Various authors have predicted values for the constant,  $C$ , and exponents ( $\alpha$  and  $\beta$ ) for a variety of different systems and these are listed in Table 5.2. Figure 5.5 shows the  $k_L a$  values for a range of different agitation rates that have been predicted according to the correlations listed in Table 5.2. The  $P_g/V$  values substituted into these correlations were the measured previously (Figure 5.1).

The correlations derived by Linek *et al.* (2004), Smith *et al.* (1977) and Zhu *et al.* (2001) all under estimate the  $k_L a$  values for the miniature bioreactor. It can be seen in Figure 5.5 however, that they have very similar gradients to the measured  $k_L a$  values. The van't Reit (1979) and Vilaca *et al.* (2000) correlation predicted  $k_L a$  values that are in the same order of magnitude as the measured  $k_L a$ , but grossly over and under estimated over a wide range of stirrer speeds.

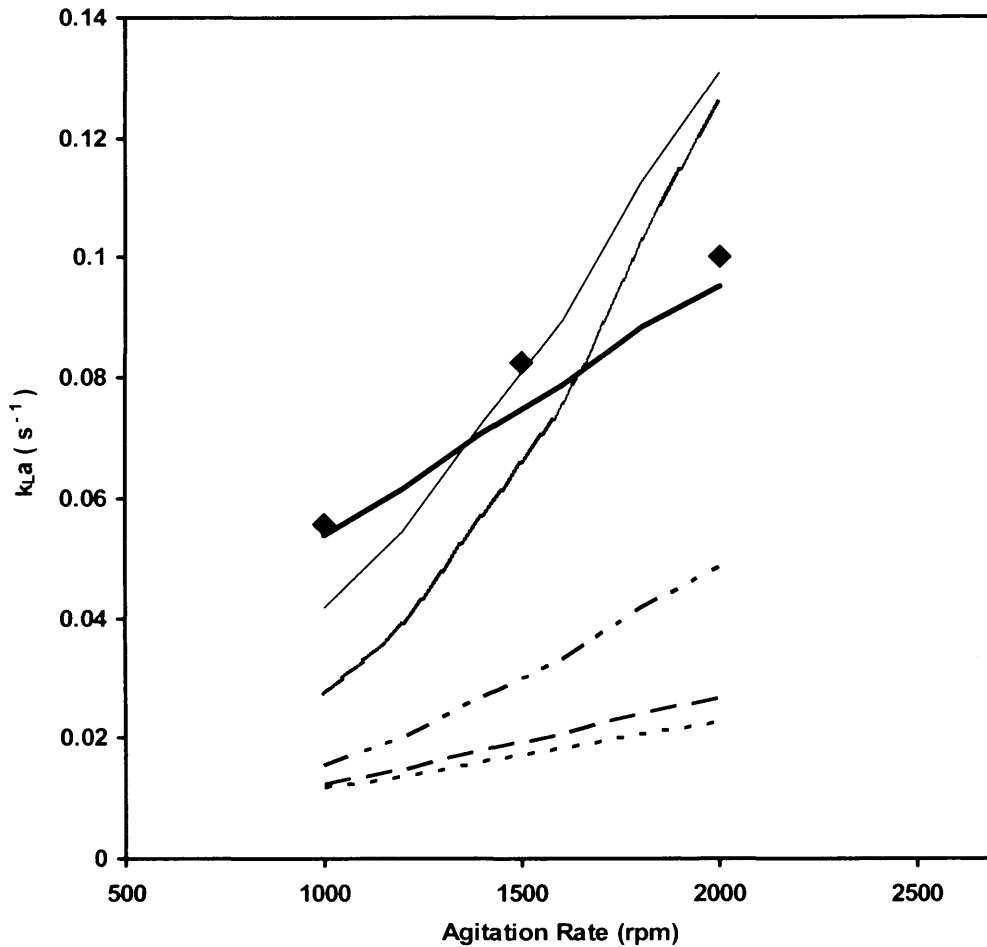
All of the existing  $k_L a$  correlations appear unsuitable for predicting accurate  $k_L a$  values for the miniature bioreactor and is most probably due to the fact that they have been developed for much larger scale vessels. As a result an empirical relationship was derived here specifically for the miniature bioreactor based on  $k_L a$  values that were previously measured at different operating conditions (Figure 3.4) and the corresponding gassed power measurements (Figure 5.1). The values determined for the constant  $C$ ,  $\alpha$  and  $\beta$  from Equation 5.5 were 0.224, 0.35 and 0.52 respectively, as described in Appendix VI.

The correlations proposed by Van't Reit (1979) and Vilaca *et al.* (2000) have much larger values for  $\alpha$  than  $\beta$ , implying that the stirrer speed has a more significant influence on  $k_L a$ . In the case of the miniature bioreactor correlation  $\beta > \alpha$ , suggesting that in fact there is much less dependence on  $P_g/V$ . This may be attributed to the lower Power number of the miniature turbine impeller and the efficiency of gas bubble breakage. Also, as the superficial gas velocity is a more significant parameter here than in larger scale bioreactors, this might imply that the miniature bioreactor has certain bubble column characteristics. It can be seen from Figure 5.5 that the correlations of Linek *et al.* (2004), Smith *et al.* (1977) and Zhu *et al.* (2001) show a similar gradient to the miniature bioreactor correlation. The difference between  $\alpha$  and  $\beta$  for these correlations is also less. The correlation from Zhu *et al.* (2001) has very

**Table 5.2.** Comparison of the most commonly reported correlations relating  $k_L a$  to gassed power per unit volume and superficial gas velocity. NR: Figures not reported as a variety of previously published data was analysed, vessel volumes ranged from 0.002 -2.6 m<sup>3</sup>.

| Reference                   | Vessel Diameter (m) | Impeller Characteristics |          | Proposed Correlation   |
|-----------------------------|---------------------|--------------------------|----------|--|
|                             |                     | Type                     | D/T      |  |
| This work                   | 0.06                | Rushton turbine          | 0.33     | Air-Water with ions:<br>$k_L a = 0.224 \left( \frac{P_g}{V} \right)^{0.35} u_s^{0.52}$                     |
| Van't Riet (1979)           | Various             | Various                  | Various  | Air-Water with ions:<br>$k_L a = 2 \times 10^{-3} \left( \frac{P_g}{V} \right)^{0.7} u_s^{0.2}$            |
| Vilaca <i>et al.</i> (2000) | 0.21                | Rushton turbine          | 0.4      | Air-Water-sulfite solution<br>$k_L a = 6.76 \times 10^{-3} \left( \frac{P_g}{V} \right)^{0.94} u_s^{0.65}$ |
| Linek <i>et al.</i> (2004)  | 0.29                | Rushton turbine          | 0.33     | Air-Water:<br>$k_L a = 0.01 \left( \frac{P_g}{V} \right)^{0.699} u_s^{0.581}$                              |
| Smith <i>et al.</i> (1977)  | 0.61-1.83           | Disc turbine             | 0.5-0.33 | Air-Water:<br>$k_L a = 0.01 \left( \frac{P_g}{V} \right)^{0.475} u_s^{0.4}$                                |
| Zhu <i>et al.</i> (2001)    | 0.39                | Disc turbine             | 0.33     | Air-Water:<br>$k_L a = 0.031 \left( \frac{P_g}{V} \right)^{0.4} u_s^{0.5}$                                 |





**Figure 5.5.** Comparison of the experimentally determined  $k_{La}$  values at an aeration rate of 1.5 vvm, with those predicted from the miniature bioreactor correlation and various literature correlations (Table 5.2): ( $\blacklozenge$ ) Measured values; ( $\text{—}$ ) miniature bioreactor correlation; ( $\text{—}$ ) van't Riet (1979); ( $\text{—}$ ) Vilaca *et al.* (2000); ( $\text{— - -}$ ) Linek *et al.* (2004); ( $\text{— — —}$ ) Smith *et al.* (1977); ( $\text{----}$ ) Zhu (2001). Experimental  $k_{La}$  values taken from Figure 3.4.

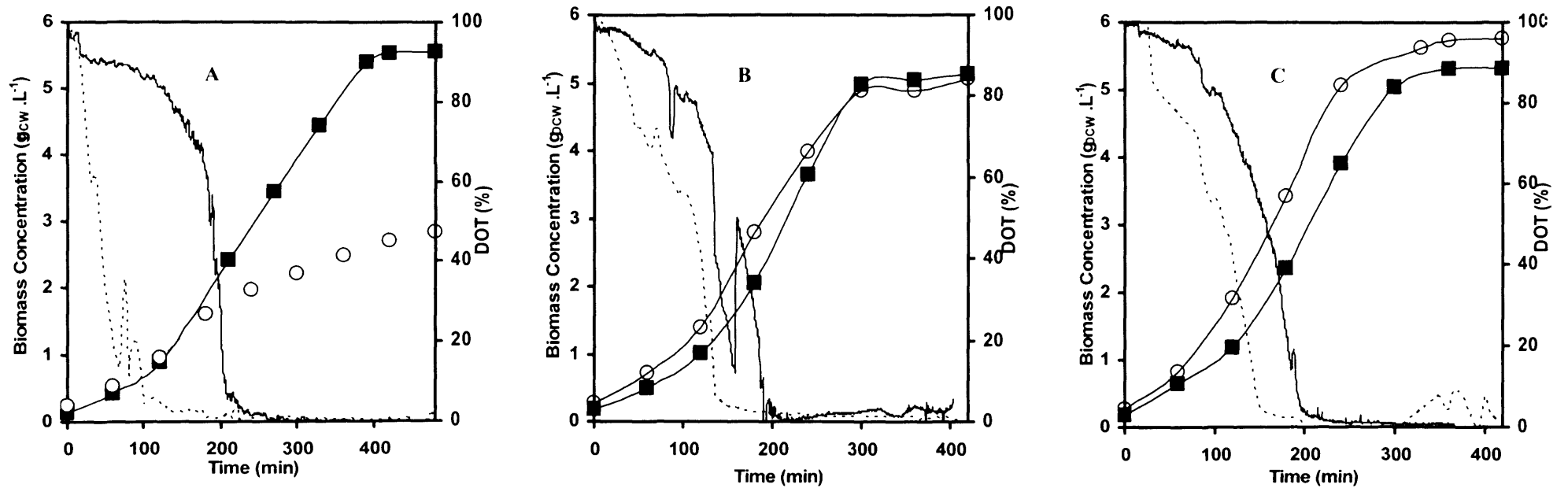
similar exponents as those determined for the miniature bioreactor.

## 5.5 Fermentation Scale Translation at Matched $P_g/V$ and $k_L a$ Values

### 5.5.1 Scale-up Based on Constant $P_g/V$

In order to explore the ability of the miniature bioreactor to provide data representative of conventional laboratory scale bioreactors a series of fermentations were performed at matched  $P_g/V$  and matched  $k_L a$  values. The 2 L bioreactor used in this work was fitted with two six blade Rushton turbine impellers. In the case of matched  $P_g/V$  values the operating conditions required in the 2 L bioreactor were determined using the Hughmark correlation (1980). Although this correlation was primarily derived for single impeller systems, the few multiple impeller correlations available are either very specific to the vessel geometry (Cui *et al.*, 1996) or based on larger impeller spacing. In the latter case the clearance between the two impellers must be sufficiently large to consider them as fully separate (Paglianti *et al.*, 2001) i.e when the impeller spacing is  $>2d_i$ ; (Gogate *et al.*, 2000) which is not the case for the 2 L vessel used here. Taking into account the importance of impeller spacing, a dual power number of 10.5 was used to compute the various operating condition required for the 2 L. This was estimated based on the ratio of impeller spacing to impeller diameter (Hudcova *et al.*, 1989). Table 5.3 summaries the key parameters and operating conditions required for each bioreactor over a range of matched  $P_g/V$  values.

Figure 5.6 compares the performance of the two bioreactor scales at each matched  $P_g/V$  value. The fermentation kinetic parameters are summarised in Table 5.3. At the lowest  $P_g/V$  value of  $657 \text{ W.m}^{-3}$ , the 2 L bioreactor significantly underperforms compared to the miniature bioreactor, achieving a final biomass concentration of almost  $3 \text{ g.L}^{-1}$  less. This is likely to be the result of operating at a reduced agitation rate, and the poor gas-liquid dispersion that was observed at the 2 L scale at these operating conditions. Given the poor oxygen transfer at the 2 L scale, the DOT reduced to zero much earlier, and cell growth is clearly seen to be oxygen limited. The



**Figure 5.6.** Comparison of growth and DOT profiles for batch *E. coli* TOP10 pQR239 fermentations carried out at matched  $P_g/V$  at miniature (100 mL) and conventional laboratory bioreactor (1.5 L) scales: (A)  $P_g/V = 657 \text{ W}\cdot\text{m}^{-3}$ ; (B)  $P_g/V = 1487 \text{ W}\cdot\text{m}^{-3}$ ; (C)  $P_g/V = 2960 \text{ W}\cdot\text{m}^{-3}$ . Miniature bioreactor: (■) cell density, (—) DOT; laboratory bioreactor: (○) cell density, (---) DOT. Matched  $P_g/V$  operating conditions as described in Table 5.3. Miniature bioreactor experiments performed as described in Section 2.8.1 and laboratory scale bioreactor experiments performed as described in Section 2.8.2.

**Table 5.3.** Summary of batch *E. coli* TOP10 pQR239 fermentations carried out in miniature and conventional laboratory bioreactors using constant  $P_g/V$  as a basis for scale translation. Kinetic parameters derived from data in Figure 5.6.

| $P_g/V$ ( $W \cdot m^{-3}$ )     | 657                        |               | 1487                       |               | 2960                       |               |
|----------------------------------|----------------------------|---------------|----------------------------|---------------|----------------------------|---------------|
| Bioreactor                       | 0.1 L Miniature Bioreactor | 2L Bioreactor | 0.1 L Miniature Bioreactor | 2L Bioreactor | 0.1 L Miniature Bioreactor | 2L Bioreactor |
| Agitation Rate (rpm)             | 1000                       | 650           | 1500                       | 900           | 2000                       | 1100          |
| Aeration Rate (vvm)              | 1.5                        | 0.67          | 1                          | 0.67          | 1                          | 0.67          |
| $\mu_{max}$ ( $h^{-1}$ )         | 0.75                       | 0.72          | 0.84                       | 0.82          | 0.94                       | 0.91          |
| $X_{final}$ ( $g \cdot L^{-1}$ ) | 5.6                        | 2.8           | 5.1                        | 5.1           | 5.3                        | 5.8           |

performance of the 2 L bioreactor is improved at higher  $P_g/V$  values ( $> 1000 \text{ W}\cdot\text{m}^{-3}$ ), with very similar  $\mu_{\max}$  and  $X_{\text{final}}$  values obtained at both scales. The trends for oxygen depletion during the linear growth phase as well as the time taken for both systems to become oxygen limited are similar and reproducible at these two higher  $P_g/V$  values. However, in both cases oxygen limitation occurs slightly earlier in the 2 L vessel.

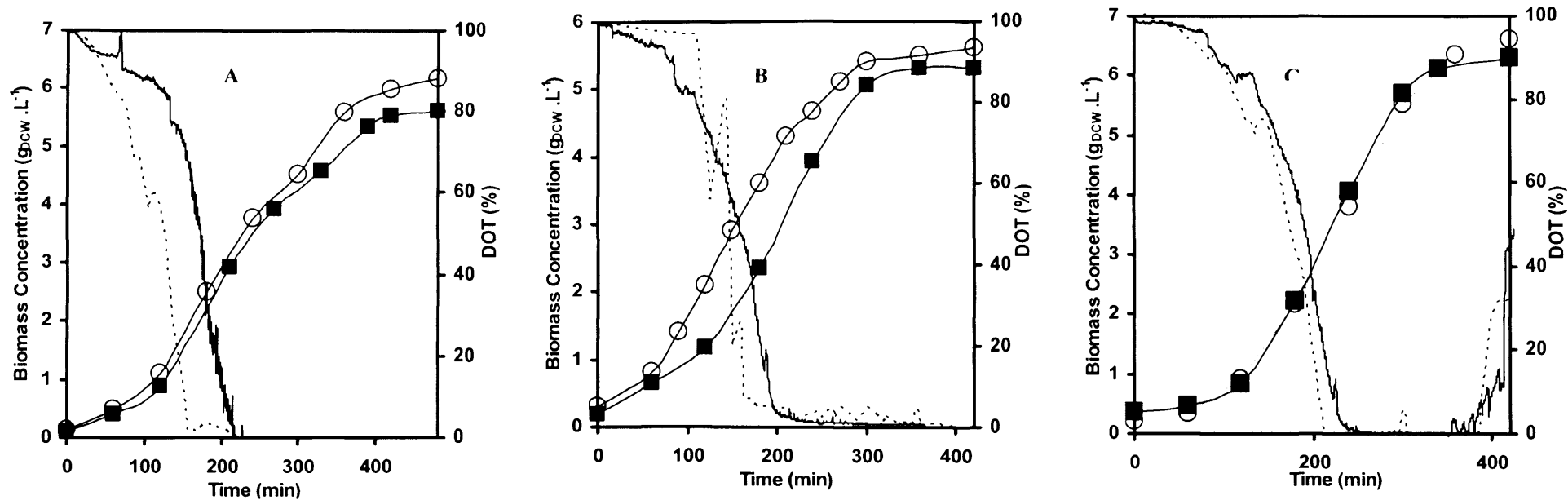
### **5.5.2 Scale-up Based on Constant $k_{La}$**

For experiments at matched  $k_{La}$  values of 0.06, 0.08 and  $0.11 \text{ s}^{-1}$  were used. At both scales these  $k_{La}$  values were experimentally determined using the dynamic gassing out technique as described by in Section 2.4. Figure 5.7 compares the performance of the two bioreactor scales at these matched  $k_{La}$  values. The operating conditions in each case, together with the derived growth kinetic parameters are given in Table 5.4. Compared to the earlier experiments at matched  $P_g/V$  values (Figure 5.6) there appears to be much better agreement in terms of cell growth and DOT profiles across the range of  $k_{La}$  values studied. There is particularly good agreement at the two higher  $k_{La}$  values. The trends for oxygen depletion during the linear growth phase as well as time taken for both systems to become oxygen limited are similar and reproducible in both cases.

Based on the results presented in Figures 5.6 and 5.7, in the case of aerobic fermentations, and cases where oxygen supply is critical, it would appear that  $k_{La}$  provides a better basis for scale translation over a range of operating conditions compared to matched  $P_g/V$ .

## **5.6 Scale-up of Optimised Conditions for Cell Growth and Enzyme Expression**

Having established  $k_{La}$  as the most suitable basis for scale-up based on cell growth (Figure 5.7), the optimum conditions for both cell growth and recombinant enzyme expression found in Section 4.5.2 were also scaled-up to the 2 L scale. These



**Figure 5.7.** Comparison of growth and DOT profiles for batch *E. coli* TOP10 pQR239 fermentations carried out at matched  $k_{La}$  at miniature (100 mL) and conventional laboratory bioreactor (1.5 L) scales: (A)  $k_{La} = 0.06 \text{ s}^{-1}$ ; (B)  $k_{La} = 0.08 \text{ s}^{-1}$ ; (C)  $k_{La} = 0.11 \text{ s}^{-1}$ . Miniature bioreactor: (■) cell density, (—) DOT; laboratory bioreactor: (○) cell density, (---) DOT. Matched  $k_{La}$  conditions as described in Table 5.4. Miniature bioreactor experiments performed as described in Section 2.8.1 and laboratory scale bioreactor experiments performed as described in Section 2.8.2.

**Table 5.4.** Summary of batch *E. coli* TOP10 pQR239 fermentations carried out in miniature and conventional laboratory bioreactors using constant  $k_L a$  as a basis for scale translation. Kinetic parameters derived from data in Figure 5.7.

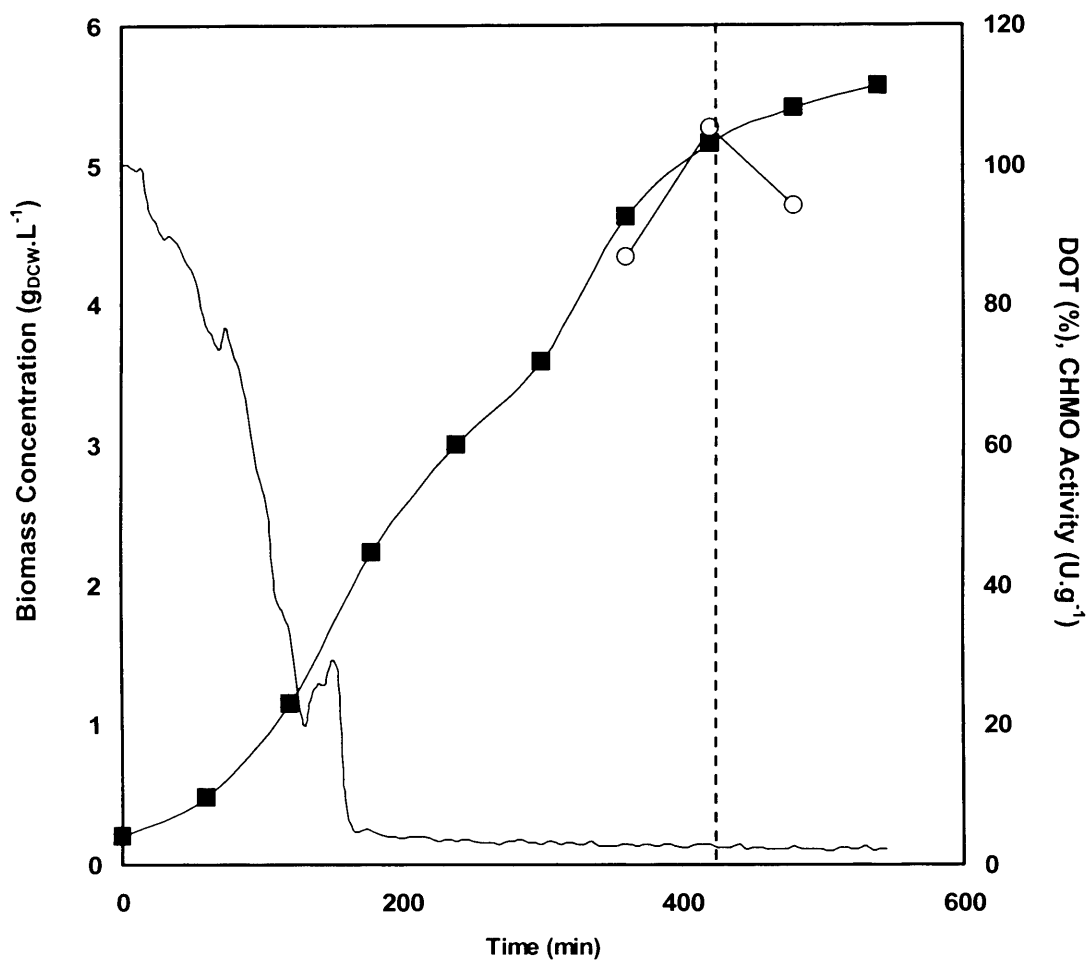
| $k_L a$ ( $s^{-1}$ )             | 0.06                       |               | 0.08                       |               | 0.11                       |               |
|----------------------------------|----------------------------|---------------|----------------------------|---------------|----------------------------|---------------|
| Bioreactor                       | 0.1 L Miniature Bioreactor | 2L Bioreactor | 0.1 L Miniature Bioreactor | 2L Bioreactor | 0.1 L Miniature Bioreactor | 2L Bioreactor |
| Agitation Rate (rpm)             | 1000                       | 900           | 2000                       | 1000          | 2000                       | 1100          |
| Aeration Rate (vvm)              | 2                          | 1.33          | 1                          | 0.67          | 2                          | 1.33          |
| $\mu_{max}$ ( $h^{-1}$ )         | 0.79                       | 0.78          | 0.94                       | 0.90          | 0.99                       | 0.98          |
| $X_{final}$ ( $g \cdot L^{-1}$ ) | 5.6                        | 6.2           | 5.3                        | 5.5           | 6.3                        | 6.6           |

experiments were performed at a matched  $k_{La}$  value of  $0.04\text{ s}^{-1}$ , as used in the DoE experiments (Section 4.3), which is slightly outside the range of the  $k_{La}$  values used in the previous scale-up study (Section 5.5.2). Table 5.5 summaries the operating conditions at the two scales necessary to achieve the desired  $k_{La}$  value, and the corresponding kinetic parameters derived from the fermentation data. Figure 5.8 shows the biomass growth kinetic and DOT profiles for *E. coli* in the 2 L vessel. The specific CHMO titre, determined as described in Section 2.9.2 was only measured at three time points with maximum CHMO activity achieved at the same time point (420 minutes) as the miniature bioreactor. The results shown in Table 5.5 again indicate almost identical cell growth at the two scales of operation verifying the results seen previously in Section 5.5.2. In addition they show excellent agreement in the induced CHMO activities, indicating comparable levels of enzyme expression after CHMO induction with L-arabinose.

**Table 5.5.** Comparison of the optimum fermentation conditions for enzyme expression in *E.coli* TOP10 pQR239 derived from the DOE investigation in Section 4.5.2 and corresponding conditions in the 2 L bioreactor for scale-up on the basis of constant  $k_{La}$ . Experiments performed as described in Sections 2.7.2 and 2.8.2. Biomass and CHMO values both determined at 420 minutes.

| <b>Parameter</b>   | <b>Miniature Bioreactor</b> | <b>2 L Bioreactor</b> |
|--|-----------------------------|-----------------------|
| <b>Temperature (°C)</b>  | 37.1                        | 37.1                  |
| <b>pH</b>  | 7                           | 7                     |
| <b>Arabinose Concentration (% w/v)</b>   | 0.11                        | 0.11                  |
| <b>Agitation Rate (rpm)</b>  | 1000                        | 900                   |
| <b>Aeration Rate (vvm)</b>   | 1                           | 1                     |
| <b><math>k_{La}</math> (<math>\text{s}^{-1}</math>)</b>                          | 0.04                        | 0.04                  |
| <b>X (<math>\text{g}\cdot\text{L}^{-1}</math>) (t = 420 minutes)</b>             | 4.9                         | $5.1 \pm 0.19$        |
| <b>CHMO Activity (<math>\text{U}\cdot\text{g}^{-1}</math>) (t = 420 minutes)</b> | 105.9                       | $105.2 \pm 1.52$      |





**Figure 5.8.** The optimum fermentation conditions for enzyme expression in *E.coli* TOP10 pQR239 derived from the DOE investigation in Section 4.5.2 were scaled-up to the 2 L bioreactor based on a constant  $k_{La}$  value of  $0.04 \text{ s}^{-1}$ : (■) cell density, (—) DOT, (○) specific CHMO activity. Dashed line represents time point used in original DoE experiments with miniature bioreactor (Chapter 4). Experiments performed as described in Sections 2.7.2 and 2.8.2. Biomass and CHMO values both determined 420 minutes.

## 5.7 Discussion

In this chapter the engineering characteristics of the miniature bioreactor have been further examined in terms of mixing and oxygen transfer in order to establish a reliable criterion for the predictive scale-up of fermentation results. Initially the power consumption of the miniature turbine impeller under both ungasged and gasged conditions were determined as a function of agitation and aeration rates (Figure 5.1). As expected the measured power consumption under gasged conditions becomes significantly lower with increasing aeration rate. The ungasged power measurement yielded a Power number of 3.5 for the miniature turbine impeller (Figure 5.2). This value was in good agreement with that predicted by the correlation derived by Rutherford *et al.* (1996) and is in the same range as the values predicted for the magnetic impeller for the bioreactor block which has a  $N_p$  of 3.7 (Puskeiler *et al.*, 2005a) and the mechanically driven miniature bioreactor described by Betts *et al.* (2006b) which has a  $N_p$  of 3.

Investigation of the gas dispersion of the miniature turbine impeller showed that complete dispersion of the sparged gas occurred at Flow numbers of 0.0135, 0.0194 and 0.028 for aeration rates of 1, 1.5 and 2 vvm respectively (Figure 5.3). However the correlation proposed by Nienow *et al.* (1977) predicts complete dispersion of gas to be achieved at lower agitation rates and hence higher Flow numbers. The main reason for these differences is most probably due to the thicker impeller blades of the miniature turbine impeller used in this work. Comparison of the miniature bioreactor with a miniature reactor described by Hall *et al.* (2005) showed that the bioreactor used in this work needs to operate at significantly higher flow numbers to achieve similar values for  $P_g/P_{ug}$ . This is once again likely to be the result of the thicker blades of the miniature turbine impeller.

Various literature correlations for predicting  $P_g/P_{ug}$  for the miniature bioreactor have been evaluated (Table 5.1). Correlations by Cui *et al.* (1996) and Mockel *et al.* (1983) provided the closest predictions to the experimental miniature bioreactor data (Figure 5.4). Similarly several literature correlations were evaluated for the estimation of the miniature bioreactor  $k_L a$  values (Table 5.2). However all of these correlations proved

to be unsuitable for the reliable predictions of the  $k_{L}a$  values for the miniature bioreactor over a range of agitation rates (Figure 5.5), since they were initially designed for much larger vessels. As a result an empirical correlations relating  $k_{L}a$ , gassed power per unit volume and superficial gas velocity was specifically derived for the miniature bioreactor as follows:

$$k_{L}a = 0.224 \left( \frac{P_g}{V} \right)^{0.35} u_s^{0.52} \quad \text{Eq. 5.6}$$

Finally a series of miniature and conventional scale *E.coli* TOP10 pQR239 fermentations were performed at matched  $P_g/V$  and  $k_{L}a$  values to define a suitable basis for scale-up of fermentation results. In the case of scale-up based on constant  $P_g/V$ , comparable results at both scales were only achieved at  $P_g/V$  values greater than  $1000 \text{ W.m}^{-3}$  (Figure 5.6), with very similar results for calculated maximum specific growth rate and final biomass concentrations (Table 5.3). Scale-up at matched  $k_{L}a$  values showed good agreement of fermentation results at both scales over the whole range of  $k_{L}a$  values studied (Figure 5.7). It would thus appear that  $k_{L}a$  is the most suitable criterion for scale-up of miniature bioreactor results. This was confirmed by reproduction of the optimum CHMO expression in *E.coli*. These results were scaled-up to the 2 L scale at a matched  $k_{L}a$  of  $0.04 \text{ s}^{-1}$  (Figure 5.8). Successful scale-up of the DoE results was achieved (Table 5.5), with good agreement between the biomass concentrations and specific enzyme expression at both scales.

Of the miniature bioreactors that have been reported to date, very few have carried out detailed scale-up studies as described in this work. Some very general scale comparison studies have been carried out comparing the growth and productivity of *Bacillus subtilis* RB50 and the productivity of riboflavin (Knorr *et al.*, 2006) in the bioreactor block (Puskeiler *et al.*, 2005a) and a 7 L bioreactor. Betts *et al.* (2006) have carried out more rigorous scale-up studies using a defined scale-up criterion based on constant power per unit volume given the geometric similarity between their vessel and a conventional bioreactor. Comparing the results of the miniature bioreactor and

the 7 L vessel concluded reasonable agreement in terms of maximum specific growth rates for *E.coli* DH5 $\alpha$  producing plasmid DNA.

In this chapter the engineering characteristics of the miniature bioreactor in terms of mixing and oxygen transfer have been further evaluated and the most suitable criterion for scale translation to conventional laboratory scales defined. In the following chapter alternative methods for continuous on-line monitoring of the miniature bioreactor cultures using a novel optical density probe and the natural heat generation of growing cells are described.

# 6. *IN-SITU* MONITORING OF CELL GROWTH DURING PARALLEL BIOREACTOR OPERATION

---

---

## 6.1 Introduction and Aims

The current state of bioprocess monitoring has evolved from chemical engineering and as a result sensors useful for *in-situ* monitoring of biotechnological processes are comparatively few; they measure physical and chemical variables rather than biological ones (Sonnleitner, 1999). The reasons are generally due to the fact that biologically relevant variables are much more difficult and complex to measure than physical ones. The most widely used on-line sensors for bioprocess monitoring have been discussed in Section 1.3.1, of which the most common conventional probes are for temperature, pH and dissolved oxygen. Techniques for on-line monitoring become increasingly important as bioprocesses are scaled down handling significantly reduced process volumes. In such cases taking large numbers of samples becomes unrealistic and alternative methods for continuous online monitoring to obtain the same type of information are necessary. Some researchers have integrated commercially available optical density probes for continuous monitoring of biomass growth to replace repeated offline sampling (Sarrafzadeh *et al.*, 2005; Wu *et al.*, 1995).

Alternative non-invasive methods for on-line monitoring include calorimetric techniques. Given that heat generation is a natural occurrence for the majority of bioprocesses (von Stockar and Marison, 1989), a wealth of information can be inferred from simple measurements of heat production by microbes which can be valuable for assessing the state of the culture and deciding on corrective actions ensuring proper control of the process. Such an indicator not only constitutes a potentially valuable diagnostic tool for laboratory work, but also holds promising

potential for control of such processes on an industrial scale (von Stockar and Briou, 1989).

In previous chapters the potential of the miniature bioreactors for parallel process development has been demonstrated. While accurate data for process design and scale-up can be obtained in parallel it is still necessary for the operator to aseptically remove and then analyse samples for biomass growth and protein expression. The aim of this final chapter is to briefly explore the potential of two *in-situ* approaches for the determination of biomass growth kinetics, namely optical density and thermal profiling methods. The specific objectives of this chapter are to:

- Explore the use of a novel optical density probe for monitoring changes in culture absorbance.
- Explore the use of thermal profiling techniques for monitoring changes in culture heat generation.
- Correlate the above measurements to known dry cell weight concentrations.
- Demonstrate the *in-situ* collection and quantification of biomass growth kinetic data.

## **6.2 *In-situ* Optical Density Measurements**

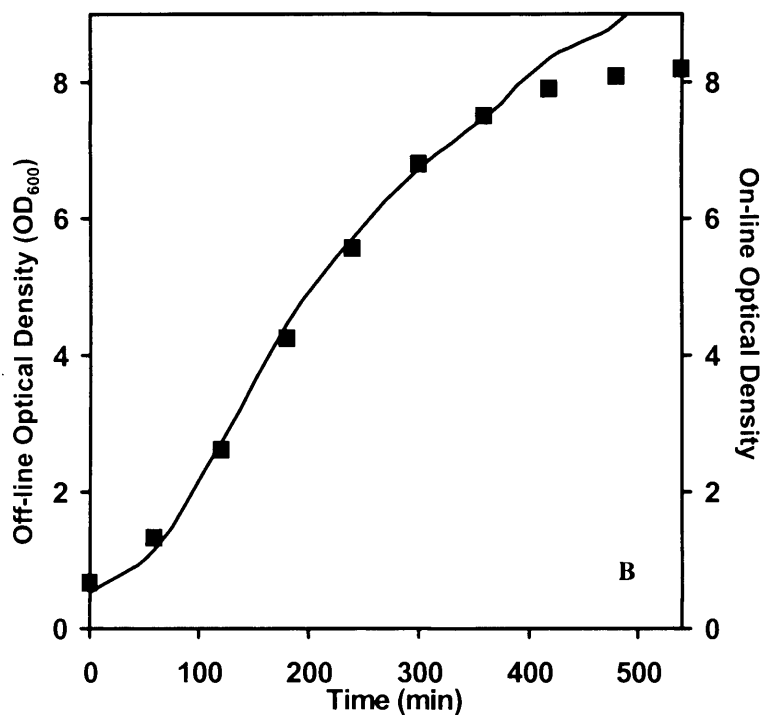
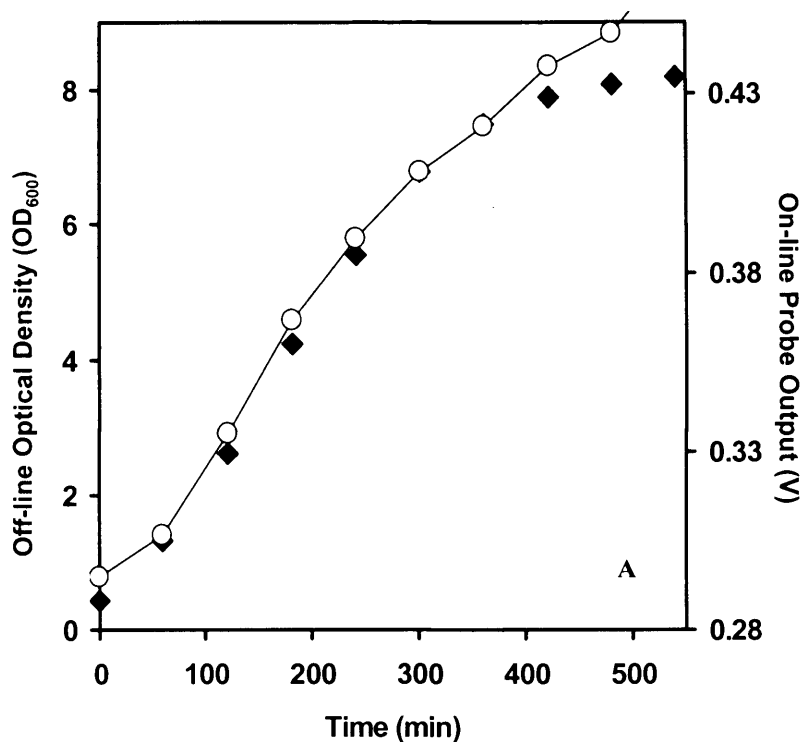
Off-line measurements of optical density of microbial cultures at 600 nm are the standard way of monitoring cell growth kinetics. Combined with a suitable calibration curve (Figure A.III.1) their OD<sub>600</sub> measurements can be used to estimate biomass dry cell weight concentrations as a function of a time. As described in Section 2.3.2, each miniature bioreactor was equipped with a novel on-line OD probe that screwed into a specifically designed port in the head plate. The probe was designed to facilitate continuous on-line monitoring of biomass growth kinetics which was considered important given the small volume of each bioreactor (which limits the number and volume of samples that can be withdrawn) and the potential supervision of up to sixteen bioreactor units in parallel by a single operator. A detailed description of the

design of the probe can be found in Section 2.3.2.2 and a schematic illustration of its operation is shown in Figure 2.3.

In order to assess the reliability and reproducibility of the OD measurements from the probe, nine identical *E.coli* TOP10 fermentations were carried out as described in Section 2.6.1 at a constant agitation rate and aeration rate of 1000 rpm and 1 vvm respectively. Figure 6.1 (A) shows an example for one representative fermentation of how well the on-line raw signal from the OD probe compared with off-line OD measurements. It is clear from Figure 6.1 (A) that the *E.coli* growth curve derived from on-line measurements is virtually identical to the off-line measurements, apart from during the final stages of the culture when the log phase ended after 420 minutes.

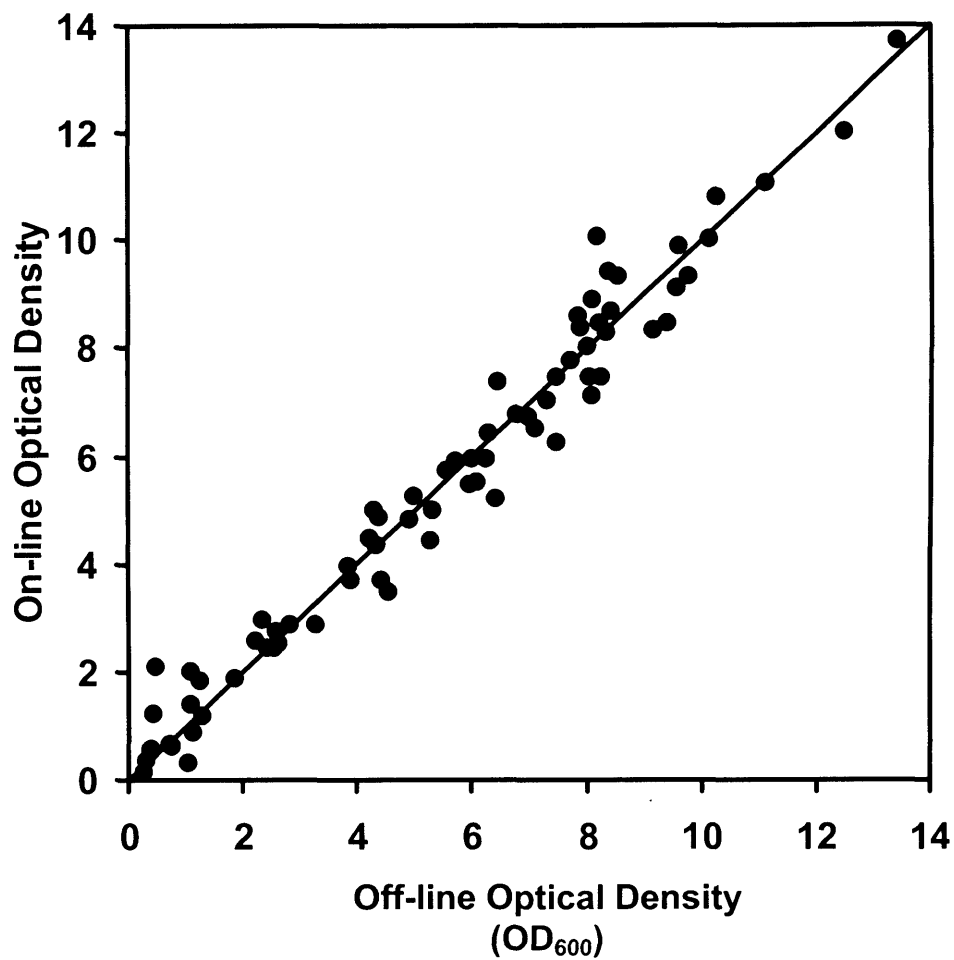
Having confirmed that the OD probe provides useful information on biomass growth over the course of the fermentation, for subsequent fermentations the voltage output of the probe was initially calibrated against the OD<sub>600</sub> of the sterilised culture medium. Figure 6.1 (B) shows the comparison between on-line and off-line OD results based on this calibration. Again, for this typical fermentation there is good agreement between the two profiles apart from the point when the stationary phase is reached. The calculated values of the culture maximum specific growth rate were 0.67 h<sup>-1</sup> and 0.68 h<sup>-1</sup> respectively, indicating that the on-line data can also be used for quantitative analysis of cell growth kinetics.

Figure 6.2 shows a parity plot of on-line and off-line OD data collected during all nine *E. coli* fermentations. There is seen to be excellent correlation between the two types of OD data indicating the robustness of the probe after repeated cycles of sterilisation and fermentation.



**Figure 6.1.** On-line measurement of optical density in *E. coli* TOP10 pQR239 fermentations. (A) Comparison of the off-line OD and un-calibrated voltage output of the OD probe: (♦) off-line optical density; (○) on-line voltage output. (B) Comparison of off-line and calibrated on-line biomass growth kinetics from an individual fermentation: (■) off-line optical density; (—) on-line optical density. Experiments performed at 1000 rpm and 1 vvm as described in Section 2.6.1.





**Figure 6.2.** Parity plot of on-line and off-line optical density data from nine identical fermentations. Linear Regression gives an  $R^2$  value of 0.96. Experiments performed at 1000 rpm and 1 vvm as described in Section 2.6.1. Solid line indicates parity.

## 6.3 *In-situ* Culture Heat Generation Measurements

### 6.3.1. *Thermal Profiling of Cell Growth*

There have been several publications on the application of calorimetric techniques for monitoring and controlling various bioprocesses. A number of examples have previously been discussed in Section 1.3.2. The majority of researchers have reported on work carried out in modified calorimeters such as RC1 (Marison *et al.*, 1998) developed by Mettler-Toledo and the BSC-81 (Meier-Schneiders *et al.*, 1995) developed by Ciba-Geigy that were initially designed for calorimetric investigation of chemical processes. In some cases a conventional bioreactor has been altered in order for it to perform as a calorimeter (van Kleeff *et al.*, 1993; Meier-Schneiders and Schafer, 1996). Data collection in both cases is based on conventional calorimetric techniques i.e. a complete heat balance, and the resulting data can yield the precise quantity of heat generated at different points during a bioprocess.

Although data collected in this way may be interesting and useful for deriving enthalpic parameters (Marison and von Stockar, 1986; Meir-Schneiders and Schafer, 1996), it is necessary to accurately determine all heat flows that result from stirring, aeration, loss to the environment, from acid and base feeds and carbon dioxide vaporisation (Voisard *et al.*, 2002). In most cases however, particularly those applications for which the miniature bioreactor has been designed, a more general knowledge of the rate at which heat is released provides sufficiently useful information on the level of microbial activity. In the case of the parallel miniature bioreactors being used for high throughput process development this latter approach represents a useful tool for on-line monitoring. As described in Appendix A.VII this information on culture heat generation can readily be extracted from the existing temperature control system of each miniature bioreactor. Given the absence of a detailed heat balance this approach is referred to here as ‘thermal profiling’ rather than calorimetry.

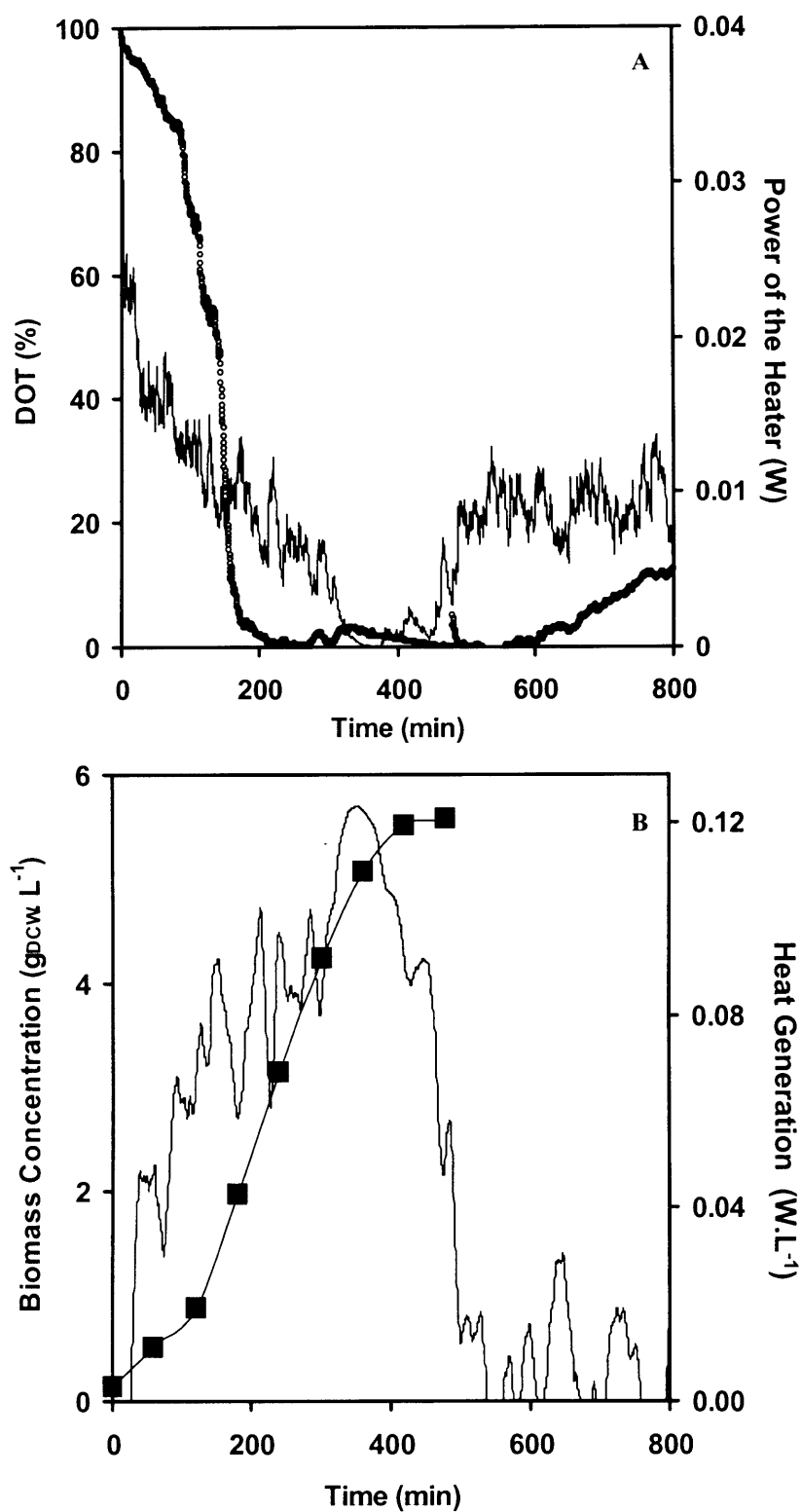
The temperature control system of each miniature bioreactor system employs an external electrical disc heater (50 W) positioned directly beneath the vessel driven by PWM (pulse-width modulation). The PWM drive regime was derived from a

continuously variable parameter termed the 'request power' (expressed as a percentage) that was determined by a PID control loop. This involved the heater being turned on and off at a fixed level to maintain the set-point temperature.

Previous experiments carried out by HEL Ltd. (UK) on an analogous system have demonstrated that the requested power of the heater is linearly related to the heater power. It was shown that on the introduction of a known power source into the vessel, the change in the requested power was proportional to the magnitude of the introduced power. Careful lagging the entire vessel ensured all the heat losses were constant throughout a given fermentation experiment. Thus as the fermentation progressed and generated heat, the requested power backed off accordingly to compensate for the additional heat from the fermentation in order to maintain the set point temperature. The calibration relating requested power and heat input into the vessel is described in Appendix A.VII.

### ***6.3.2. Analysis of the Thermal Profiling Results during E.coli TOP10 pQR239 Fermentations***

In order to test the thermal profiling approach a total of ten identical *E.coli* TOP10 pQR239 fermentations were carried out as described in Section 2.3.2.3. Considering a single typical fermentation, Figure 6.3 (A) shows the power delivered from the electrical heater to maintain the bioreactor at a constant temperature of 37 °C throughout the fermentation. It can be seen that the power required from the electrical heater gradually decreased from 0.023 W to 0.0003 W suggesting that less heat is required to maintain the fermentation temperature. This is most probably due to the increasing heat evolved from the microbial culture. At approximately 355 minutes the heater power reduces to a minimum value of  $1.85 \times 10^{-5}$  W which coincided with the time at which the fermentation was in the late log phase, as shown by the biomass growth profile in Figure 6.3 (B). Once the microbial culture entered stationary phase, there was a corresponding shift in the power supplied by the electrical heater, as it began to increase and stabilised at approximately 0.01 W in order to compensate for the reduction in the heat evolved by the microbial culture as growth and cellular



**Figure 6.3.** On-line heat measurements during a typical *E.coli* TOP10 pQR239 fermentation. (A) On-line dissolved oxygen profile and the power supplied by the heater to maintain the fermentation temperature at 37 °C: (o) DOT; (-) heater power. (B) Comparison of biomass growth kinetics from off-line OD<sub>600</sub> measurements and the heat generation: (■) biomass concentration; (-) heat generation. Experiments performed as described in Section 2.3.2.3.

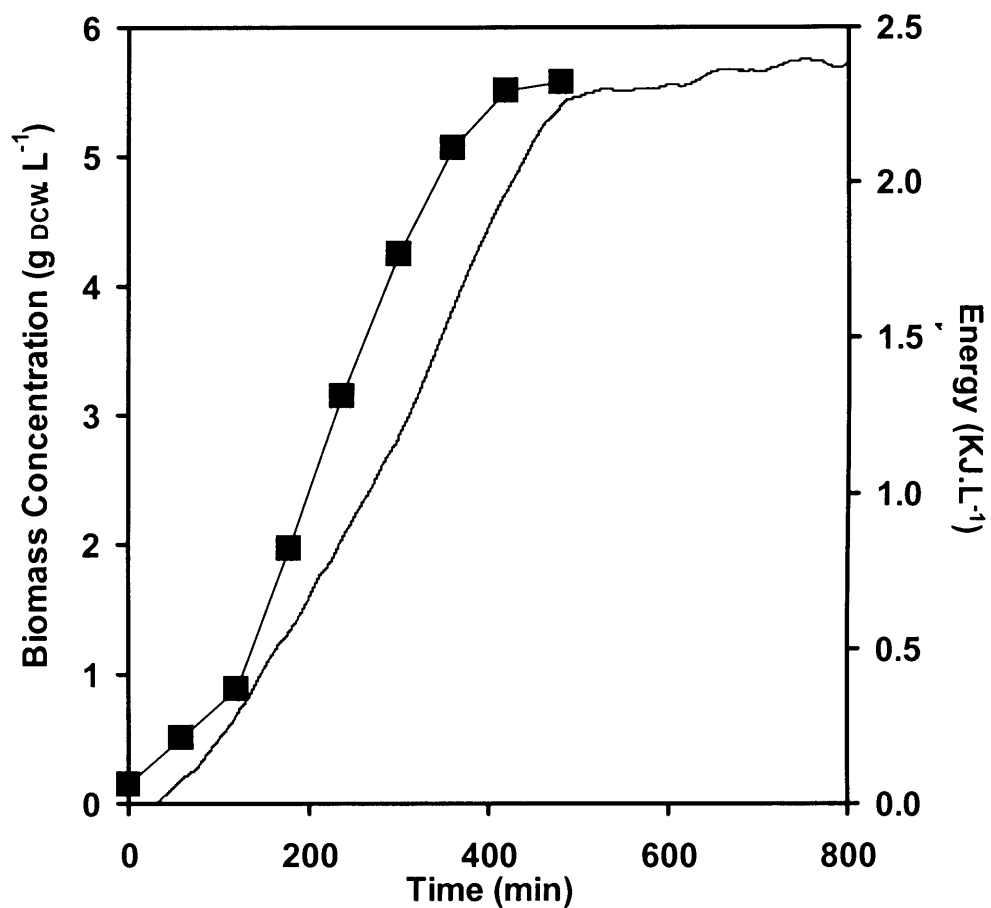
process slowed down. From Figure 6.3 (B) it can be seen that the actual rate of heat evolution increased with biomass concentration, achieving a maximum value of  $0.12 \text{ W.L}^{-1}$ , until the culture entered stationary phase. At this time (370 minutes into the fermentation) the heat signal fell dramatically to a lower value, implying the end of rapid cell growth.

After 370 minutes a series of small peaks in the heat signal were recorded, although no measurable increase in biomass was detected. This pattern is typical of fermentations on complex media, since various substrates that are still present and can be slowly oxidised (Voisard *et al.*, 2002). This could also be the result of the oxidation of a small level of products formed during the initial growth phase (Marison and von Stockar 1986). During the exponential phase, there was an instantaneous reduction in the heat signal at approximately 183 and 228 minutes after inoculation as a result of the onset of oxygen limitation causing a potential shift in metabolism as the cells re-adjust to their environment, however further work would be necessary to confirm this.

The integrated heat curve based on the data in Figure 6.3 (B) is shown in Figure 6.4. This is seen to follow the same basic pattern as the off-line biomass concentration curve, achieving a maximum heat evolution of  $2.4 \text{ KJ.L}^{-1}$ . During exponential growth of the culture heat evolution also increased exponentially. The calculated rate constant for heat generation was similar to that of biomass production,  $0.68 \text{ h}^{-1}$  and  $0.65 \text{ h}^{-1}$  respectively. The data collected from the ten identical *E. coli* fermentations provide an overall good agreement between the maximum specific growth rates predicted from the off-line biomass measurements and heat curve,  $0.66 \pm 0.04 \text{ h}^{-1}$  and  $0.69 \pm 0.05 \text{ h}^{-1}$  respectively.

## 6.4 Discussion

In this Chapter two novel approaches to the on-line monitoring of parallel miniature bioreactors have been demonstrated. In the case of the miniature optical density probe



**Figure 6.4.** Comparison of biomass growth kinetics from a typical *E.coli* TOP10 pQR239 fermentation, off-line OD<sub>600</sub> measurements and the integrated heat generation curve: (■) biomass concentration; (-) integrated heat curve. Experiments were carried out as described in Section 2.3.2.3 and heat generation was calculated directly by the IQ software.

it has been shown that the initial voltage signal of the probe can be calibrated with off-line OD<sub>600</sub> measurements to provide a good quantification of culture OD over the time course of a fermentation (Figure 6.1 and 6.2). Evaluation of culture maximum specific growth rates from both off-line and on-line measurements were 0.67 and 0.68 h<sup>-1</sup> respectively, confirming that the on-line data can also be used for quantitative analysis of cell growth kinetics.

Comparing the off-line and on-line OD data of nine identical fermentations (Figure 6.2) confirms that the OD probe is robust over long periods operation, repeated sterilisation and reliable for accurately monitoring cell growth during fermentation. Thus it is a valuable sensor for the parallel monitoring of multiple fermentations with just end point samples being removed for off-line OD measurements and product analysis. Such a probe could also be combined with OD versus DCW calibration to give direct DCW measurements on-line.

The preliminary thermal profiling results have also demonstrated that a wealth of information can be gained simply from monitoring the natural heat generated by a microbial culture during fermentation. It has been shown that quantitative information regarding biomass growth kinetics can be easily obtained from the standard temperature control system of the miniature bioreactors, without any additional modifications that are necessary with conventional calorimetry methods (Maskow and Babel 1998; Voisard *et al.* 1998; Bou-Diab *et al.* 2001; Voisard *et al.* 2002; Jassen *et al.* 2005). This technique of thermal profiling is thus a novel and simplistic operation that could be valuable for parallel monitoring of several miniature bioreactors simultaneously.

Initial thermal profiling data has clearly shown that an increasing amount of heat is produced during a typical *E.coli* fermentation, since the amount of heating required from the electrical heater to maintain the set-point temperature of 37 °C gradually decreased as the fermentation progressed (Figure 6.3 (A)). The rise in the cultures heat production was particularly significant when the cell culture entered the log phase, increasing in cell number and generating a maximum of 0.12 W.L<sup>-1</sup> prior to entering the stationary phase (Figure 6.3 (B)). As the culture ceased to grow further, no further heat was produced since the response of the temperature controller caused

the power requested from the heater to rapidly increased in order to maintain the set point temperature of the fermentation broth.

The integrated heat curve (Figure 6.4) follows the same pattern as the off-line biomass concentration curve, achieving a maximum heat evolution of  $2.4 \text{ KJ.L}^{-1}$ . As a result it was possible to estimate the maximum specific growth rate from the heat curve; data from 10 identical fermentations estimated a value of  $0.69 \pm 0.05 \text{ h}^{-1}$  which is good agreement with estimates from off-line biomass measurements,  $0.66 \pm 0.04 \text{ h}^{-1}$ .

The OD measurements shown in Figure 6.1 provide valuable information about cell growth but, relies solely on turbidity changes of the fermentation broth to estimate this. Although some of the changes in the appearance of the fermentation broth (getting darker/ cloudy) can be attributed to growth and increase in cell number, this measurement is not able to differentiate between active cells, dead cells, cell fragments or any other particulates that may have accumulated during the fermentation (Kaiser *et al.*, 2007). However, simply looking at the changes in the natural heat evolved from (Figure 6.3) active cells potentially provides a valuable quantitative indicator of the metabolic state of a microbial culture and has some parallel with more accurate biocalorimetry methods.

In the case of the miniature bioreactor system simply monitoring a characteristic that is already naturally occurring (the generation of heat) during cell cultivation, provides an excellent and extremely valuable real-time monitoring tool, producing qualitative results of biomass growth during a microbial fermentation. The added benefits of this technique is that no additional insertions into the bioreactor are required, reducing the risk of contamination and potentially excessive sampling. There is thus a trade off to be made between qualitative heat measurement methods or the added expense of an OD probe that would allow quantitative measurements.



# 7. CONCLUSIONS AND FUTURE WORK

---

---

## 7.1 Conclusions

In this study a parallel miniature bioreactor system (100 mL working volume) designed to be geometrically similar to conventional laboratory scale stirred bioreactors has been constructed (Section 2.3) and evaluated. The oxygen transfer characteristics of the miniature bioreactor were first evaluated in terms of the oxygen mass transfer coefficient,  $k_{La}$ , as a function of agitation and aeration rates (Figure 3.4). Values of  $k_{La}$  as high as  $0.11 \text{ s}^{-1}$  could be achieved and are comparable to those typically found in laboratory scale bioreactors. Measurements of power consumption under ungasged conditions predicted a Power number of 3.5 for the miniature turbine impeller (Figure 5.2). Further engineering characterisation in terms of mixing and oxygen transfer led to the derivation of a correlation specifically for the miniature bioreactor, relating  $k_{La}$ , gassed power per unit volume and superficial gas velocity (Equation 5.6), since none of the existing literature correlations (Table 5.2) were suitable for predicting these parameters at this scale.

Parallel high throughput fermentation has been demonstrated with excellent reproducibility between parallel *E. coli* (Figure 3.5) and *B. subtilis* (Figure 3.6) fermentations in terms of the calculated maximum specific growth rates ( $0.68 \pm 0.01 \text{ h}^{-1}$  and  $0.45 \pm 0.01 \text{ h}^{-1}$  for *E. coli* and *B. subtilis* respectively). Biomass growth rates and yields for *E. coli* could be improved, and oxygen transfer limitations overcome, by increases in agitation and aeration rates and by the implementation of a gas blending system (Table 3.3).

The miniature bioreactor has proved to be a valuable tool for screening and optimisation investigations, involving DoE techniques which demand multiple experiments to be carried out for the evaluation of a range of operational conditions

for a given bioprocess (Chapter 4). In this study a total of 20 experiments were necessary to derive a suitable regression model for the optimisation of a heterologously expressed protein, CHMO, in *E.coli* TOP 10 pQR239. The application of the miniature bioreactor system for this study enabled a series of 4 parallel fermentations to run simultaneously, significantly reducing the experimental time frames by up to 75 %. This investigation concluded that both temperature and inducer concentration significantly affected CHMO expression, with optimum CHMO activity predicted at 37.1 °C and 0.11 % w/v respectively (Figure 4.7).

Rigorous scale-up studies were carried out in order to establish a reliable and reproducible criterion for scale translation from the miniature bioreactor to conventional laboratory scale. This was assessed for three different  $k_{La}$  (Figure 5.7) and  $P_g/V$  (Figure 5.6) conditions. Scale-up based on constant  $k_{La}$  was found to be the most reliable basis for scale-up with good agreement between biomass and DOT profiles, and maximum specific growth rates (Table 5.4) at both scales over the whole range of  $k_{La}$  conditions investigated. Furthermore, accurate scalability of the optimum conditions for CHMO expression derived from the DoE studies (Figure 5.8 and Table 5.5) has also been demonstrated. The ability to obtain quantitative and scaleable data from potentially up to sixteen miniature bioreactors in parallel, therefore makes the system described here a valuable tool for the rapid optimisation of microbial fermentation processes.

To achieve further advances in bioprocess optimisation, information on key process variables describing the potentials and limits of the biological system need to be available on-line (Section 1.3). In the final part of this work two methods for parallel on-line monitoring, a novel optical density probe (Section 6.2) and thermal profiling (Section 6.3), have been implemented and evaluated. Both these methods of continuous on-line monitoring have successfully correlated well with off-line cell growth results and potentially provide a means for further automation with reduced frequency of sampling. In particular, the thermal profiling technique is a valuable measure and very competitive when compared to other on-line quantitative techniques especially since heat is a global measurement of metabolic activity. Therefore can be used for the same kind of purposes as other microbiological techniques, compared to which it presents some clear advantages, such as simplicity of technology and

procedures, potentially improved accuracy of results, applicability to almost any microbial growth process and growth media and the easy modifications of growth conditions.

Parallel automated operation and reduced process volumes are the key requirements for high throughput cell cultivation to rationally speed up bioprocess design (Section 1.1). Although a variety of different miniature bioreactor systems currently exist, as described in Table 1.1 and A.1.1, the nature, complexity and variety of different bioprocess present ever increasing challenges which makes it difficult to find a single system able to satisfy all the requirements. Therefore different systems maybe used at various stages of bioprocess development depending on the nature of the process and the level of monitoring, control and sampling required. The miniature bioreactor described in this work has shown to be particularly suitable for parallel high throughput fermentation applications with potential for scale-up based on the reliable scale-up criterion.

## 7.2 Future Work

The work in this thesis has demonstrated and validated the 4-pot miniature bioreactor systems capability for high throughput fermentation applications generating reproducible and accurately scaleable results. Further work is required for the complete characterisation of the system and evaluation of its generic application.

- Further studies similar to those described in Chapter 3 should be performed to explore the use of the miniature bioreactor with other microorganisms and more challenging culture conditions such as the culture of a *Streptomyces* species on industrial fermentation media (Davies *et al.*, 2000). This will test longer term aseptic operation of the bioreactors and also the ability to agitate and aerate more viscous media. Indeed some initial studies were started with this microorganism during the course of this investigation, however the time constraints of the project did not permit a comprehensive set of results to be obtained.

- For a more complete understanding of the miniature bioreactor performance liquid phase mixing times and also gas-liquid distribution within each bioreactor should be explored in more detail. For example, these might be studied by high speed video photography (Hall *et al.*, 2005). This will provide a fundamental insight into the performance of the miniature turbine impeller and possibly provide further explanation the  $P_g/P_{ug}$  versus Flow number results in Figure 5.3 and may ultimately lead to a better impeller design.
- Based on the initial DoE results in Chapter 4, further DoE studies over a wider range of conditions to those investigated should be explored. This study should also include other critical variables such as media type and induction times so that their impact on cell growth can be modelled and a proper trade-off between cell growth and enzyme expression can be made.
- Explore the robustness of the most suitable scale-up criterion based on constant  $k_{La}$  conditions established in this work with a wider range of microbial fermentations, for example *Streptomyces* fermentations described above.
- Based on the initial thermal profiling results in Chapter 6, perform a more detailed study of the relationship between heat generation and biomass growth kinetics, to potentially gain more quantitative data on-line. Perhaps further investigation looking at shifts in the heat curves at points of induction and enzyme expression could provide further insight to the process.
- Finally in order to further enhance the miniature bioreactor design and to improve its industrial utility work is needed to:
  - (i) Study fed-batch operation based on the gas blending capability of the miniature bioreactor (which was only implemented in the later stages of the project).
  - (ii) Re-design or re-fabrication of the impeller to give better oxygen transfer characteristics. There is the possibility to fabricate it from a different

material to reduce the blade thickness and therefore increase both the Power number and  $k_L a$ .

- (iii) Improve the general mechanical design of the system for commercial applications, for instance recently the foot print of the unit has been reduced, accommodating 6 miniature bioreactors instead of 4. The fitting of the headplate to the glass vessel has been improved providing a more even seal and making preparation and cleaning easier.

## 8. REFERENCES

---

---

S. Abia, A. E. Humphrey, N. Millis, Biochemical engineering, 2<sup>nd</sup> ed, New York Academic press (1973)

K. Adinarayana, P. Ellaiah, Response surface optimisation of the critical medium components for the production of alkaline protease by a newly isolated *Bacillus* sp., J. Pharm. Pharmaceut. Sci. 5 (2002) 272-278

Akgün, B. Maier, D. Peris, B. Roth, R. Klingelhöfer, J. Büchs, A novel parallel shaken bioreactor system for continuous operation, Biotechnol. Prog. 20 (2004) 1718-1724

Antoce, L. D. Dinu, K. Takahashi, Microcalorimetry, a convenient technique for microbial growth monitoring, Roum. Biotechnol. Lett. 6 (2001) 243-251

Atkinson, F. Mavituna, Biochemical Engineering and Biotechnology Handbook, 2<sup>nd</sup> ed, Stockton press (1999)

Bailey and Ollis, Biochemical Engineering Fundamentals, McGraw-Hill International, (1986)

F. Baneyx, Recombinant protein expression in *Escherichia coli*, Curr. Opin. Biotechnol. 10 (1999) 411-421

A.F. Barnes, M. J. Hardy, T. J. Lever, Review of the applications of thermal methods within the pharmaceutical industry, J. Thermal Analysis. 40 (1993) 499-509

E. H. Battley, The development of direct and indirect methods for the study of the thermodynamics of microbial growth, *Thermochim. Acta* 309 (1998) 17-37

J. I. Betts, F. Baganz, Miniature bioreactors: current practices and future opportunities, *Microbial Cell Factories* 5 (2006) 1-14

J. I. Betts, S. D. Doig, F. Baganz, Characterisation and application of a miniature 10 mL stirred tank bioreactor, showing scale-down equivalence with a conventional 7 L reactor, *Biotechnol. Prog.* 22 (2006) 681-688

P. A. Bird, J.M. Woodley, D. C.A. Sharp, Using biocatalysts at useful reactant and product concentrations monitoring and controlling biocatalytic processes, *BioPharm International* (2002) 14-24

Birou, I. W. Marison, U. von Stocker, Calorimetric investigation of aerobic fermentations. *Biotech. Bioeng.* 30 (1987) 650-660

Blomberg, C. Larsson, L. Gustafsson, Microcalorimetric monitoring of growth of *Saccharomyces cerevisiae*: osmotolerance in relation to physiological state, *J Bacteriol.* 170 (1988) 4562-4568

P. Bonvillani, M. P. Ferrari, E. M. Ducrós, J. A. Orejas, Theoretical and experimental study of the effects of scale-up on mixing time for a stirred tank, *Brazilian J. Chem. Eng.* 23 (2006) 1-7

Bou-Diab, B. Schenker, I. Marison, S. Ampuero, U. von Stockar, Improvements of continuous calibration based on temperature oscillation and application to biochemical reaction calorimetry. *Chem. Eng.* 81 (2001) 113-127

R. Brettel, I. Lamprecht, B. Schaarschmidt, Microcalorimetric investigations of the metabolism of yeasts. VII. Flow-calorimetry of aerobic batch cultures, *Radiat Environ Biophys.* 18 (1980) 301-9

E. Brown, Industrial scale operation of microbial processes, J. Chem. Technol. Biotechnol. 32 (1982) 34-46

J. Buchs, Introduction to advantages and problems in shaken cultures, Biochem. Eng. J. 7 (2001) 91-98

W. Bujalski, A. W. Nienow, S. Chatwin, M. Cook, The dependency on scale of power numbers of Rushton turbines, Chem. Eng. Sci. 42 (1987) 317-326

Y. Cao, Optimization of expression of *dhaT* gene encoding 1, 3-propanediol oxidoreductase from *Klebsiella pneumoniae* in *Escherichia coli* using the methods of uniform design and regression analysis, J. Chem. Technol. Biotechnol. 81 (2006) 109-112.

A.K.Chandra, S. Medda, A.K. Bhadra, Production of extracellular thermostable  $\alpha$ -amylase by *Bacillus licheniformis*, J. Ferment. Technol. 58 (1980) 1-10

M. Charles, J. Wilson, Encyclopaedia of bioprocess technology: fermentation, biocatalysis, and bioseparation, New York, Wiley (1999)

S. Choi, D. Park, K. Jung, Development and optimization of two-stage cyclic fed-batch culture for hG-CSF production using L-arabinose promoter of *Escherichia coli*, Bioproc. Biosys. Engin. 24 (2001) 1615-7605

Clementsich, K. Bayer, Improvement of bioprocess monitoring: development of novel concepts, Microbial Cell Factories 5 (2006) 1-11

M. A. Cooper, Label-free screening of bio-molecular interactions, Analytical Bioanalytical Chem. 377 (2003) 834-842

Y. Q. Cui, R. G. J. M. van der Lans, K. Ch. A. M. Luyben, Local power uptake in gas-liquid systems with single and multiple Rushton turbines, Chem. Eng. Sci. 51 (1996) 2631-2636



J. L. Davies , F. Baganz , A. P. Ison , G. J. Lye, Studies on the interaction of fermentation and microfiltration operations: erythromycin recovery from *Saccharopolyspora erythraea* fermentation broths, *Biotechnol Bioeng.* 69 (2000) 429-39

S. de Buruaga, A. Echevarria, P. D. Armitage, J. C. de la, On-line control of a semibatch emulsion polymerization reactor based on calorimetry, *AIChE J.* 43 (1997) 1069 - 1081

S. Dilsen, W. Paul, D. Herforth, A. Sandgathe, J. Altenbach-Rehm, R. Freudl, C. Wandrey, D. Weuster-Botz, Evaluation of parallel operated small-scale bubble columns for microbial process development using *Staphylococcus carnosus*, *J. Biotechnol.* 88 (2001) 77-84

Diaz, F. Acevedo, Scale-up strategy for bioreactors with Newtonian and non-Newtonian broths, *Bioprocess Eng.* 21 (1999) 21-23

S.D. Doig, A. Diep, F. Baganz, Characterisation of a novel miniature bubble column bioreactor for high throughput cell cultivation, *Biochem. Eng. J.* 23 (2004) 97-105

S.D. Doig, F. Baganz, G.J. Lye, High throughput screening and process optimisation, In Ratledge C, Kristiansen B (Eds.), *Basic Biotechnology*, 3<sup>rd</sup> ed, Cambridge University Press, UK (2006)

S. D. Doig, K. Ortiz-Ochoa, J. M. Ward, F. Baganz, Characterization of oxygen transfer in miniature and lab-scale bubble column bioreactors and comparison of microbial growth performance based on constant  $k_{La}$ , *Biotechnol. Prog.* 21 (2005) 1175-1182

S.D. Doig, L.M. O'Sullivan, S. Patel, J.M. Ward, J.M. Woodley, Large scale production of cyclohexanone monooxygenase from *Escherichia coli* TOP10 pQR239, *Enz. Microb. Technol.* 28 (2001) 265-274

P. M. Doran, *Bioprocess Engineering Principles*, 5th edition, Academic Press Limited (2000)

P. Duboc, U. von Stockar, Energetic investigation of *Saccharomyces cerevisiae* during transitions 1. Mass balances, *Thermochim. Acta* 251 (1995) 119-130

P. Duboc, I Marison, U. von Stockar, *Quantitative calorimetry and biochemical engineering*, Elsevier. (1999)

W. A. Duetz, L. Ruedi, R Hermann, K. O. Connor, J. Buchs, B. Witholt, Methods of intense aeration, growth, storage and replication of bacterial strains in microtitre plates, *Appl. Environ. Microbiol.* 66 (2000) 2641-2646

W. A Dutez, B. Witholt, Effectiveness for orbital shaking for the aeration of syuspended bacterial cultures in square deepwell microtitre plates 7 (2001)113-115

I.J. Dunn, A.J. Einsele, Oxygen transfer coefficients by the dynamic method, *J. Appl. Chem. Biotechnol.* 25 (1975) 707-720

A. Dybko, Errors in chemical sensor measurements, *Sensors.* 1 (2001) 29-37

Elmahdi, F. Baganz, K. Dixon, T. Harrop, D. Sugden, G.J. Lye, pH control in microwell fermentations of *S. erythraea* CA340: Influence on biomass growth kinetics and erythromycin biosynthesis, *Biochem. Eng. J.* 16 (2003) 299-310

Eriksson, L.; Johansson, E.; Kettaneh-Wold, N.; Wikström, C.; Wold, S. *Design of Experiments: Principles and Applications*; Umeå / Learnways AB: Stockholm, 2000.

P. Fernandes, J. M. S. Cabral, Review: microlitre/millilitre shaken bioreactors in fermentative and biotransformation process 24 (2006) 237-252

Ferreira-Torres, M. Micheletti, G.J. Lye, Microscale process evaluation of recombinant biocatalyst libraries: Application to Baeyer-Villiger mono-oxygenase catalysed lactone synthesis, *Bioproc. Biosystems Eng.* 28 (2005) 83-93

R. Flores, F. Perez, M. De La Torre, Scale-up of *Bacillus thuringiensis* fermentation based on oxygen transfer, J. of Ferment. Bioeng. 83 (1997) 561-564

S. A. Freyer, M. Konig, A. Kunkel, Validating shaking flasks as representative screening systems, Biochem. Eng. J. 17 (2004) 196-173

García-Arrazola, P. Dawson, I. Buchanan, B. Doyle, T. Fearn, N. Titchener-Hooker, F. Baganz, Evaluation of the effects and interactions of mixing and oxygen transfer on the production of Fab' antibody fragments in *Escherichia coli* fermentation with gas blending , Bioproc. Biosys. Eng. 27 (2005) 365-374

Giron, Applications of thermal analysis and coupled techniques in pharmaceutical industry, J. Thermal Analysis and Calorimetry 68 (2002) 335–357

P. R. Gogate, A. A. C. M. Beenackers, A. B. Pandit, Multiple-impeller systems with a special emphasis on bioreactors: a critical review, Biochem. Eng. J. 6 (2000) 109-144

Gupta, G. Rao, A study of oxygen transfer in shake flasks using a non-invasive oxygen sensor, Biotechnol. Bioeng. 84 (2003) 351 - 358

L. Guzman, D. Belin, M. J. Carson, J. Bechwith, Tight Regulation, Modulation, and High-Level Expression by Vectors Containing the Arabinose PBAD Promoter, J. Bacteriology 177 (1995) 4121–4130

J. F. Hall, M. Barigou, M. J. H Simmons, E. H. Stitt, A PIV study of hydrodynamics in gas-liquid high throughput experimentation (HTE), reactors with eccentric impeller configurations, Chem. Eng. Sci. 60 (2005) 6403-6413

L. D. Hansen, D. J. Eatough, Comparison of the detection limits of microcalorimeters, Thermochim. Acta (1983) 70: 257-268

P. Harms, Y. Kostov, G. Rao, Bioprocess monitoring, Curr. Opinion in Biotech. 13 (2002) 124-127

P. Harms, Y. Kostov, J. A. French, M. Soliman, M. Anjanappa, A. Ram, G. Rao, Design and performance of a 24-station high throughput microbioreactor, *Biotech. Bioeng* 93 (2006) 6-13

G.Q. He, Q. Kong, L.X. Ding Response surface methodology for optimizing the fermentation medium of *Clostridium butyricum*, *Lett. App. Microbiol.* 39 (2004) 363-368

E.G. Hibbert, F. Baganz, H.C. Hailes, J.M. Ward, G.J. Lye, J. M. Woodley, P.A. Dalby, Directed evolution of biocatalytic processes, *Biomolecular Eng.* 22 (2005) 11-19

J. Higuera-Guisset, J. Rodriguez-Viejo, M. Chacon, F. J. Munoz, N. Vignes, J. Mas, Calorimetry of microbial growth using a thermopile based microreactor, *Thermochim. Acta* 427 (2005) 187-191

Hilker, C. Baldwin, V. ronique Alphan, R. Furstoss, J. Woodley, R. Wohlgemuth, On the Influence of Oxygen and Cell Concentration in an SFPR Whole Cell Biocatalytic Baeyer–Villiger Oxidation Process, *Biotechnol. Bioengin.* 93(2006) 1138-1144

M. Hosobuchi, H. Yoshikawa, *Manual of industrial microbiology and biotechnology*, 2<sup>nd</sup> ed. Washington, D.C. ASM Press (1999)

V. Hudcova, V. Machon, A. W. Nienow, Gas-liquid dispersion with dual Rushton turbine impellers, *Biotech. Bioeng.* 34 (1989) 617-628

A. Hughmark, Power requirements and interfacial area in gas-liquid turbine agitated systems, *Ind. Eng. Chem. Proc. Des. Dev.* 19 (1980) 638-641

Y. Ishikawa, Y. Nonoyama, M. Shoda, Microcalorimetric study of aerobic growth of *Escherichia coli* in batch culture, *Biotech. Bioeng.* (1981) 2825-2836

R. S. Islam, D. Tisi, M. S. Levy, G. J. Lye, A framework for the rapid optimisation of soluble protein expression in *E.coli* combining microscale experiments and statistical experimental design, *Biotechnol. Prog.* (2007) submitted.

N.B. Jackson, J.M. Liddell, G.J. Lye, An automated microscale technique for the quantitative and parallel analysis of microfiltration operations. *J. Membrane Sci.* (2006) in press

M. Jassen, R. Patino, U. von Stockar, Application of bench-scale biocalorimetry to photoautotrophic cultures, *Thermochim. Acta* 435 (2005) 18-27

T. John, I. Kilmant, C. Wittmann, E. Heinzle, Integrated optical sensing of dissolved oxygen in microtitre plates: a novel tool for microbial cultivation, *Biotechnol. Bioeng.* 81 (2003) 829-836

R. E. Johnston, M. W. Thring, *Pilot plant, models and scale-up methods*, McGraw Hill, New York (1957)

L. K. Ju, G. G. Chase, Improved scale-up strategies of bioreactors, *Bioproc. Eng.* 8 (1992) 49-53

H. Junker, Scale-Up Methodologies for *Escherichia coli* and Yeast Fermentation Processes, *J. Biosci. Bioeng.* 97 (2004) 347-364

Kaiser, J. P. Carvell, R. Luttmann, A Sensitive, Compact, In Situ Biomass Measurement System: Controlling and Monitoring Microbial Fermentations Using Radio-Frequency Impedance, *Bioprocess Int.* 5 (2007) 52-56

N. M. Kamerbeek, A. J. J. Olsthoorn, M. W. Fraaije, D. B. Janssen, Substrate Specificity and Enantioselectivity of 4-Hydroxyacetophenone Monooxygenase. *Appl Environ Microbiol.* 69 (2003) 419-426

Kane, Feedback control system, United States Patent 20060237664 (2006)

H. Kato, Tanaka, Development of a novel box-shaped shake flask with efficient gas exchange capacity, *J. Ferm. Bioeng.* 85 (1998) 404-409

R. B. Kemp, A historical review of developments in cellular microcalorimetry, *Pure Appl. Chem.* 65 (1993) 1875-1880

R. B. Kemp, Y. H. Guan, Microcalorimetric studies of isolated animal cells, *Quantitative calorimetry and biochemical engineering*, Elsevier. (1999)

Knorr, H. Schlieker, H. P. Hohmann, D. Weuster-Botz, Scale-down and parallel operation of the riboflavin production process with *Bacillus subtilis*, *Biochem. Eng. J.* (2006) in press

T. Koloini, I. Plazl, M. Zumer, Power consumption, gas hold-up and interfacial area in aerated non-Newtonian suspensions in stirred tank of square cross section, *Chem. Eng. Res. Des.* 67 (1989) 526-536

Konstantinov, S. Chuppa, E. Sajan, Y. Tsai, S. Yoon, F. Golini, *Trends Biotechnol.* 12 (1994) 324-333

Y. Kostov, P. Harms, L. Randers-Eichhorn, G. Rao, Low-cost microbioreactor for high-throughput bioprocessing, *Biotechnol. Bioeng.* 72 (2001) 346-352

Y. Kostov, P. Harms, L. Randers-Eichhorn, G. Rao, Low-cost microbioreactor for high-throughput bioprocessing, *Biotechnol. Bioeng.* 72 (2001) 346-352

S. Kumar, C. Wittman, E. Heinzle, Minibioreactors, *Biotechnol. Lett.* 26 (2004) 1-10

S.R. Lamping, H. Zhang, B. Allen, P. Ayazi-Shamlou, Design of a prototype miniature bioreactor for high throughput automated bioprocessing, *Chem. Eng. Sci.* 58 (2003) 747-758

Lamprecht, Calorimetry and thermodynamics of living systems. *Thermochim. Acta* 405 (2003) 1-13

S. Lander, *In-situ* product recovery from a Baeyer-villiger monooxygenase catalysed bioconversion, PhD thesis (2003)

R. N. Landau, Expanding the role of reaction calorimetry, *Thermochim. Acta* 289 (1996) 101-126

G. Larsson, M. Tornkvist, E. Stahl Wernersson, C. Traigardh, H. Noorman, S. O. Enfors, Substrate gradients in bioreactors: origin and consequences, *Bioproc. Eng.* 14 (1996) 281-289

D. Lilly, Problems in process scale-up. Bioactive microbial products 2. Development and production, Academic Press (1983)

V. Linek, M. Kordac, M. Fugasova, T. Moucha, Gas-liquid mass transfer coefficient in stirred tanks interpreted through models of idealised eddy structure of turbulence in the bubble vicinity, *Chem. Eng. Proc.* 43 (2004) 1511-1517

C. Loureiro-Dias, J. D. Arrabaca, Flow microcalorimetry of a respiration-deficient mutant of *Saccharomyces cerevisiae*, *Z Allg Mikrobiol.* 22 (1982) 19-22

H. T. Luong, B. Volesky, Mechanical power requirements of gas-liquid agitated systems, *AIChE J.* 25 (1979) 893-895

G.J. Lye, P. Ayazi-Shamlou, F. Baganz, P.A. Dalby, J.M. Woodley, Accelerated design of bioconversion processes using automated microscale processing techniques, *Trends Biotech.* 21 (2003) 29-37

U. Maier, J. Buchs, Characterisation of the gas-liquid mass transfer in shaking bioreactors, *Biochem. Eng. J.* 7 (2001) 99-106

Manderson, R. Dempster, Y. Chisti, A recombinant vaccine against hydatidosis: production of the antigen in *Escherichia coli*, *J. Ind. Microbio. Biotechnol.* 33 (2006) 173-182

L. Maranga, A. Cunha, J. Clemente, P. Cruz, M. J. T. Carrondo, Scale-up of virus-like particles production: effects of sparging, agitation and bioreactor scale on cell growth, infection kinetics and productivity J. Biotechnol. 107 (2004) 55-64

Marison, J. S. Liu, S. Ampuero, U. von Stockar, B. Schenker, Biological reaction calorimetry: development of high sensitivity bio-calorimeters, Thermochem. Acta 309 (1998) 157-173

W. Marison, U. von Stockar, The application of a novel heat flux calorimeter for studying growth of *Escherichia coli* W in aerobic batch cultures, Biotech. Bioeng. 28 (1986) 1780-1793

Marison, U. von Stockar, A novel bench scale calorimeter for biological process development work, Thermochem. Acta 85 (1985) 493-496

S. Marose, C. Lindemann, R. Ulber, T. Scheper, Optical sensor systems for bioprocess monitoring Trends Biotechnol. 17 (1999) 30-34

T. Maskow, W. Babel, Calorimetric investigations of bacterial growth on phenol- efficiency and velocity of growth as a function of the assimilation pathways, Thermochem. Acta, 309 (1998) 97-103.

F. Mavituna, Strategies for Bioreactor scale-up, Computer and information science application in bioprocess engineering, Kluwer Academic (1996)

Mehrvar, C. Bis, J. M. Scharer, M. Moo-Young, J. H. Luong, Fibre-optic biosensors – trends and advances, Analy. Sci. 16 (2000) 677-692

M. Meier-Schneiders, F. Schafer, Quantification of small enthalpic differences in anaerobic microbial metabolism – a calorimetry supported approach, Thermochem. Acta 275 (1996) 1-16



M. Meier-Schneiders, U. Gosshans, C. Busch, G. Eigenberger, Biocalorimetry-supported analysis of fermentation processes, *Appl. Microbiol. Biotechnol.* 43 (1995) 431-439

M. Micheletti, T. Barrett, S.D. Doig, F. Baganz, M.S. Levy, J.M. Woodley, G.J. Lye, Fluid mixing in shaken bioreactors: Implications for scale-up predictions from microlitre scale microbial and mammalian cell cultures, *Chem. Eng. Sci.* 61 (2006) 2939-2949

J. Michel, S. A. Miller, Power requirements of gas-liquid agitated systems, *AIChE J.* 8 (1962) 262-266

H. O. Mockel, H. Weissgärber, K. Börner, Der leistungseintrag in belüfteten rührsystemen mit niedrigviskosen median, *Chem. Techn.* 35 (1983) 344-347

Morao, C.I. Maia, M.M.R. Fonseca, J.M.T. Vasconcelos, S.S. Alves, Effect of antifoam addition on gas-liquid mass transfer in stirred fermenters, *Bioprocess. Eng.* 20 (1999) 165-172

R. M. Morgan-Kiss, C. Wadler, J. E. Cronan Jr., Long-term and homogeneous regulation of the *Escherichia coli araBAD* promoter by use of a lactose transporter of relaxed specificity, *Biochemi.* 99 (2002) 7373-7377

C. Montgomery, Design and analysis of experiments, 6<sup>th</sup> edition, John Wiley & sons (2005)

R. Narayanaswamy, Tutorial review-optical chemical sensors: transduction and signal processing, *Analyst*, 118 (1993) 317-322

S. Nagata, Mixing principle and applications, Kodansha LTD, A Haisted press, Tokyo (1975)

W. Nienow, G. Hunt, B. C. Buckland, A fluid dynamic study of the retrofitting of large agitated bioreactors: Turbulent flow, *Biotechnol. Bioeng.* 44 (1994) 1177 - 1185

W. Nienow, D. Miles, A dynamometer for the accurate measurement of mixing torque, J. Sci. Instrum. 2 (1969) 994-995

W. Nienow, D. J. Wisdom, J.C. Middleton, Effect of scale and geometry on flooding, recirculation and power in stirred vessels, Proc. Eur. Conf. Mix. 2 (1977) F1

E. Nikerel, E.Toksoy, B. Kirdar, R.Yildirim, Optimizing medium composition for *TaqI* endonuclease production by recombinant *Escherichia coli* cells using response surface methodology. Proc. Biochem. 40 (2005) 1633-1639.

J. Y. Oldshue, Fermentation mixing scale-up techniques, Biotechnol. Bioeng. 8 (1966) 3-24

J. Y. Oldshue, Chemical engineering: concepts and reviews, volume 1: Mixing of liquids by mechanical agitation, Gordon and Breach Science publishers (1985)

M. G. Oosterhuis, N. W. F. Kossen, Modelling and scale-up of bioreactors, Biotechnology vol. 2, Verlagsgesellschaft , Berlin (1985)

N. M. G. Oosterhuis, N. W. F. Kossen, Power input measurements in a production scale bioreactor, Biotechnol. Lett. 3 (1981) 645-650

G. Orellana, Luminescent optical sensors, Analyt. Bioanalyt.Chem. 379 (2004) 344-346

Paglianti, K. Takenaka, W. Bujalski, Simple model for power consumption in aerated vessels stirred by Rushton disc turbines, AIChE J. 47 (2001) 2673-2683

R. E. Pérez, A. M. Lasa, R. S. Rodríguez, E. C. Menéndez, J. G. Suárez, H. D. Balaguer, Scale-up of recombinant Opc protein production in *Escherichia coli* for a meningococcal vaccine, J. Biotechnol. 127(2006) 109-114

R. Puskeiler, K. Kaufmann, D. Weuster-Botz, Development, parallelisation, and automation of a gas inducing millilitre-scale bioreactor for high-throughput bioprocess design (HTBD), *Biotechnol. Bioeng.* 89 (2005a) 512-523

R. Puskeiler, A. Kusterer, G.T. John, D. Weuster-Botz, Miniature bioreactors for automated high-throughput bioprocess design (HTBD): Reproducibility of parallel fed-batch cultivations with *Escherichia coli*, *Biotechnol. Appl. Biochem.* 42 (2005b) 227-235

S. A. U. Qader, S. Bano, A. Aman, N. Syed, A. Azhar, Enhanced production and extracellular activity of commercially important amylolytic enzyme by a newly isolated strain of *Bacillus* sp. AS-1, *Turk. J. Biochem.* 31(2006) 135–140

Randolph T, Marison I, Martens D, Von Stockar U. (1990). Calorimetric control of fed batch fermentations. *biotech. Bioeng.* 36. 678-684

K. Rege, M. Pepsin, B. Falcon, L. Steele, M, Heng, High-throughput process development for recombinant protein purification, *Biotech. Bioeng.* 93 (2006) 618-630

H. B. Reisman, Problems in scale-up of biotechnology production processes. *Crit. Rev. Biotechnol.* 13 (1993) 195-223

X. Ren, D. Yu, S. Han, Y. Feng, Optimization of recombinant hyperthermophilic esterase production from agricultural waste using response surface. *Bioresource Technol.* 97 (2006) 2345-2349.

M. Rosso, S. A. Ferrarotti, N. Krymkiewicz, B. Clara. Nudel, Optimisation of batch culture conditions for cyclodextrin glucanotransferase production from *Bacillus circulans* DF 9R, *Microb Cell Fact.* 1 (2002)

K. Rutherford, S. M. S. Mahmoudi, K. C. Lee, M. Yianneskis, The influence of Rushton impeller blade thickness on the mixing characteristics of stirred vessels, *Trans. IChemE* 74 Part A (1996) 369-378

M. H. Sarrafzadeh, L. Belloy, G. Estaban, J. M. Navarro, C. Ghommidh, Dielectric monitoring of growth and sporulation of *Bacillus thuringiensis*, *Biotechnol. Lett.* 27 (2005) 511-517

T.H. Scheper, J.M. Hilmer, F. Lammers, C. Miiller, M. Reinecke, Review: Biosensors in bioprocess monitoring, *J. Chromatography A*, 725 (1996) 3-1 2

F. R. Schmidt, Optimization and scale up of industrial fermentation processes, *Appl. Microbiol. Biotechnol.* 68 (2005) 425–435

M. E. Sensel, K.J. Myers, J. B. Fasano, Gas dispersion at high aeration rates in low to moderately viscous Newtonian liquids, *AIChE Symp. Series* 293, 89 (1993) 76

L. K. Shay, H. R. Hunt, G. H. Wegner, High-productivity fermentation process for cultivating industrial microorganisms, *J. Ind. Microbio. Biotechnol.* 2 (1987) 79-85

Sheng , D. P. Ballou , V. Massey, Mechanistic studies of cyclohexanone monooxygenase: chemical properties of intermediates involved in catalysis, *Biochem.* 18 (2001) 11156-11167

S. Shin, M. S. Hong, J. Lee, Oxygen transfer correlation in high cell density culture of recombinant *E.coli*, *Biotechnol. Techn.* 10 (1996) 679-682

V. B. Shukla, U. Parasu Veera, P. R. Kulkarni, A. B. Pandit, Scale-up of biotransformation process in stirred tank reactor using dual impeller bioreactor, *Biochem. Eng. J.* 8 (2001) 19-29

A. Siegele, J. C. Hu, Gene expression from plasmids containing the *araBAD* promoter at subsaturating inducer concentrations represents mixed populations, *Proc. Natl. Acad. Sci. USA* 94 (1997) 8168-8172

J. Singh, reaction calorimetry for process development: recent advances, process safety progress (1997) 16: 43-49

J. M. Smith, K. van't Riet, J. C. Middleton, Scale up of agitated gas-liquid reactors for mass transfer, in Proceedings of 2<sup>nd</sup> European conference on mixing, Cambridge, UK F4 (1977) 51-66

Sonnleitner, Instrumentation of Biotechnological Processes, Adv. Biochem. Eng. Biotechnol. 66 (1999) 1-64

F. Stanbury, A. Whitaker, S. J. Hall, Principles of fermentation technology, 2<sup>nd</sup> ed, Butterworth-Heinemann (2003)

Stärk, B. Hitzmann, K. Schügerl, T. Scheper, C. Fuchs, D. Köster, H. Märkl, Advances in biochemical engineering in-situ-fluorescence-probes: a useful tool for non-invasive bioprocess monitoring, Biotechnol. 74 (2002) 21-38

J. Stelling, S. Klamt, K. Bettenbrock, S. Schuster, E. Dieter Gilles, Metabolic network structure determines key aspects of functionality and regulation, *Nature* 420 (2002) 190-193

J. Strobel, G. R. Sullivan, Manual of industrial microbiology and biotechnology, 2<sup>nd</sup> ed. Washington, D.C. ASM Press (1999)

E. Swalley, J. R. Fulghum, S. P. Chambers, Screening factors effecting a response in soluble protein expression: Formalized approach using design of experiments. *Analy. Biochem.* 351 (2006) 122-127.

J. Suurkuusk, I. Wadso, A multichannel microcalorimetry system, *Chem. Scr.* 20 (1982) 155-163

Trudgill PW. Cyclopentanone 1,2 monooxygenase from *Pseudomonas* NCIMB 9872. *Meth Enzymol* 1990; 188: 77 – 81.

M. Türker, Development of biocalorimetry as a technique for process monitoring and control in technical scale fermentations, *Thermo. Acta* (2004) 419: 73-81

V. W. Uhl, J. A. von Essen, Scale-up of fluid mixing equipment, *Biotechnology processes: scale-up and mixing* AIChE (1987)

Urban, I. Ansmant, Y. Motorin, Optimisation of expression and purification of the recombinant Yol066 (Rib2) protein from *Saccharomyces cerevisiae*., *J. Chromatography B* 786 (2003) 187-195.

Uzura, T. Katsuragi, Y. Tani, Optimal conditions for production of (*R*)-1-Phenylpropanol by *Fusarium moniliforme* strain MS31, *J. Biosci. Bioeng.* 92 (2001) 288-293

M.E. Van Loo, P.E. Lengowski, Automated workstations for parallel synthesis, *Organic Process Research Dev.* 6 (2002) 833-840

H. A. van Kleeff, J. G. Kuenen, G. Honderd, J. J. Heijnen, Using heat-flow measurements for the feed control of a fed batch fermentation of *Saccharomyces cerevisiae*, *Thermo. Acta* (1998) 309: 175-180

H. A. van Kleeff, J. G. Kuenen, J. J. Heijnen, Heat-flux measurements for the fast monitoring of dynamic responses to glucose additions by yeast that were subjected to different feeding regimes in continuous culture, *Biotechnol. Prog.* 12 (1996) 510-518

H. A. van Kleeff, J. G. Kuenen J. J. Heijnen, Continuous measurement of microbial heat production in laboratory fermenter, *Biotech. Bioeng.* 41 (1993) 541-549

K. van't Riet, Review of measuring methods and results in non-viscous gas liquid mass transfer in stirred vessels, *Ind. Eng. Chem. Process Design Dev.* 18 (1979) 357-364

K. van't Riet, J. Tramper, *Basic bioreactor design*, Marcel Dekker, Inc, New York, NY (1991)

M.I Vázquez, A. M. Martín, Optimization of *Phaffia rhodozyma* continuous culture through response surface methodology, *Biotechnol. Bioeng.* 57 (1998) 314 - 320

P. Vellanki, G. Jayaraman, I. W. Marison, J. S. Liu, K. Jayaramnan, Calorimetric optimisation of growth and sporulation of *Bacillus thuringiensis* var *galleriae*, *Thermochim. Acta* 309 (1998) 105-110

P. R. Vilaca, A. C. Badino Jr., M. C. R. Facciotti, W. Schmidell, Determination of power consumption and volumetric oxygen transfer coefficient in bioreactors, *Bioproc. Eng.* 22 (2000) 261-265

Voisard , P. Pugeaud, A. R. Kumar, K. Jenny, K. Jayaraman, I. W. Marison, U. von Stockar, Quantitative calorimetric investigation of fed-batch cultures of *Bacillus sphaericus* 1593M, *Thermochim. Acta* 394 (2002) 99-111

Voisard, C. Claivaz, L. Menoud, I. W. Marison, U. von Stocker, Use of reaction calorimetry to monitor and control microbial cultures producing industrially relevant secondary metabolites, *Thermochim. Acta* 309 (1998) 87-96

U. von Stockar, B. Birou, The heat generation by yeast cultures with mixed metabolism in the transition between respiration and fermentation, *Biotech. Bioeng.* 34 (1989) 86-10

U. von Stockar, I. W. Marison, The use of calorimetry in biotechnology, *Adv. Biochem. Eng. Biotechnol.* 40 (1989) 93-136

U. von Stockar, L. C. Auberson, Chemostat cultures of yeasts, continuous culture fundamentals and simple unstructured mathematical models, *J. Biotechnol.* 22 (1992) 69-87

U. von Stocker, I. W. Marison, Large scale calorimetry and biotechnology, *Thermochim. Acta* 193 (1991) 215-242

U. von Stockar, P. Duboc, L. Laurent, , On-line calorimetry as a technique for process monitoring and control in biotechnology, *Thermochim. Acta* 300 (1997) 225-236

I. C. Wang, C. L Cooney, A. I. Demian, P. Dunhill, A. E. Humphrey, M. D. Lilly, *Fermentation and enzyme technology*, New York, J. Wiley & Sons (1979)

Y. H. Wang, C. F. Jing, B. Yang, G. Mainda, M. Dong, Xu, A Production of a new sea anemone neurotoxin by recombinant *Escherichia coli*: Optimization of culture conditions using response surface methodology, *Proc. Biochem.* 40 (2005) 2721-272

M. M. C. G. Warmoeskerken, J. M. Smith, Surface contamination effects in stirred tank reactors, *Proceedings of 8<sup>th</sup> conference of mixing* (1981) 9

Weiss, G. T. John, I. Kilmant, E. Heinzle, Modeling of mixing in 96-well microplates observed with fluorescence indicators, *Biotechnol. Prog.* 18 (2002) 821-230

Wittmann, H. M. Kim, G. John, E. Heinzle, Characterisation and application of an optical sensor for quantification of dissolved oxygen in shake flasks, *Biotech. Lett.* 25 (2003) 377-380

Weuster-Botz, J. Altenbach-Rehm, M. Arnold, Parallel substrate feeding and pH control in shaking flasks, *Biochem. Eng. J.* 7 (2001b) 163-170

Weuster-Botz, J. Altenbach-Rehm, A. Hawrylenko, Process-engineering characterisation of small-scale bubble columns for microbial process development, *Bioproc. Biosystems Eng.* 24 (2001a) 3-11

Weuster-Botz, Parallel reactor systems for bioprocess development, *Adv. Biochem. Eng Biotechnol.* 92 (2005) 125-143



Wong, A. Hernández, M. A. García, R. Segura, I. Rodríguez, Fermentation scale up for recombinant K99 antigen production cloned in *Escherichia coli* MC1061, *Proc. Biochem.* 37 (2002) 1195-1199

P. Wu, S. S. Ozturk, J. D. Blackie, J. C. Thrift, C. Figueroa, D. Naveh, Evaluation and applications of optical cell density probes in mammalian cell bioreactors, *Biotechnol. Bioeng.* 45 (1995) 495-502

Wadso, On the accuracy of results from microcalorimetric measurements on cellular systems, *Thermochim. Acta* 219 (1993) 1-15

Wadso, Trends in isothermal micro calorimetry, *Chem. Soc. Rev.* 26 (1997) 79-86

A. Yawalkar, A. B. M. Heesink, G. F. Versteeg, V. G. Pangarkar, Gas-liquid mass transfer coefficient in stirred tank reactors, *Canadian J. Chem. Eng.* 80 (2002) 840-848

Zambianchi, P. Pasta, G. Carrea, S. Colonna, N. Gaggero, J. M. Woodley, Use of isolated cyclohexanone monooxygenase from recombinant *Escherichia coli* as a biocatalyst for Baeyer-Villiger and sulfide oxidations, *Biotechnol. Bioeng.* 78 (2002) 489-496.

Zentgraf, Biocalorimetry and laser flow cytometry for characterization of the physiological state of microorganism, *Thermo. Acta* (1996) 277: 7-16

Zentgraf, Bench scale calorimetry in biotechnology, *Thermochim. Acta* 193 (1991) 243-251

X. Zhang, Optimization of 1, 3-propanediol production by novel recombinant *Escherichia coli* using response surface methodology, *J. Chem. Technol. Biotechnol.* 81 (2006) 1075-1078.

Y. Zhu, P. C. Bandopadhyay, J. Wu, Measurement of gas-liquid mass transfer in an agitated vessel – a comparison between different impellers, *J. Chem. Eng. Japan* 34 (2001) 579-584

F. Zimmermann, Trauthwein, U. Dingerdissen, K. Huthmacher, Rapid evaluation of oxygen and water permeation through microplate sealing tapes, *Biotechnol. Prog.* 9 (2003) 1061-1063

Zogg, F. Stoessel, U. Fischer, K. Hungerbühler, Isothermal reaction calorimetry as a tool for kinetic analysis, *Thermochim. Acta* 419 (2004) 1-17

L. Zulkifli, N. Uozumi, Mutation of His-157 in the Second Pore Loop Drastically Reduces the Activity of the *Synechocystis* Ktr-Type Transporter, *J. Bacteriol.* 188 (2006) 7985–7987

# APPENDIX I

## COMMERCIAL EVALUATION, DESIGN AND VALIDATION OF A PARALLEL MINIATURE BIOREACTOR SYSTEM FOR USE IN THE BIOTECHNOLOGY-BASED INDUSTRIES

---

---

### A.I.1 Initial Market Survey

Miniature bioreactor systems have become increasingly popular for speeding up many areas of bioprocessing owing to their inherent high throughput capability, since several cell cultivations can be performed in parallel. There are a wide variety of applications of miniature bioreactors including media development, strain improvement, process optimisation and scale-up. And as a result a range of different miniature bioreactors have become commercially available for this purpose. Prior to designing a prototype of the parallel miniature bioreactor system, some background market research was carried out to review all of these commercially available miniature bioreactor systems and identify their key features. These are listed in Table A.I.1. The three main designs include stirred tank reactors, shake flask systems and microtitre plates. All of the systems that are commercially available are autoclavable, except the GRETA system which is constructed from stainless steel and is steam sterilised in place. The stirred tank reactors are all magnetically driven, in some cases offering a range of different impellers, while the shake flask and microtitre plate systems require orbital shakers. In terms of on-line monitoring and control, all of the systems offer either conventional or optical sensors for monitoring typical parameters including, temperature, pH, DOT, OD and in some cases also monitor antifoam.

In order to understand the key requirements and interests of potential users of the parallel miniature bioreactor system in the current market, a brief market survey was carried out in the form of a short questionnaire, Figure A.I.1. This questionnaire was distributed to several pharmaceutical companies that had an interest or were involved in fermentation process development. The results of the replies received have been summarised in Table A.I.2.

# **SPECIAL NOTE**

**ITEM SCANNED AS SUPPLIED  
PAGINATION IS AS SEEN**

**Table A.I.1.** Comparison of miniature bioreactor systems that are commercially available for parallel operation. Table shows key design features and operating characteristics. Quoted working volumes, number of parallel units and range of agitation rates reported. Nomenclature: T = temperature, DOT = dissolved oxygen, OD = optical density, Agt = agitation rate, Ant = antifoam, OUR = oxygen uptake rate, CER = carbon dioxide excretion rate, RQ = respiratory quotient. All information last updated 01.08.06.

| Manufacturer and Product  | Working Vol. mL | Parallel Operation | Sterilisation | Agitation  | Aeration                | Sensors & Control       |
|---|-----------------|--------------------|---------------|--|-------------------------|-------------------------|
| <i>Stirred Bioreactors</i>  |                 |                    |               |  |                         |                         |
| Xplorer, Bioxplore<br><a href="http://www.bioxplore.net">www.bioxplore.net</a>                          | 100             | 4-16               | Autoclave     | Miniature turbine, Magnetic drive, 10-2000 rpm           | Sparger                 | pH, DOT, T, Agt, OD, TP |
| Biofst Q12, Sartorius BBI Systems GmbH<br><a href="http://www.sartorius.de">http://www.sartorius.de</a> | 500 - 1000      | 12                 | Autoclave     | Stirrer bar, Magnetic drive                              | Sparger                 | pH, DOT, T, Agt         |
| Stirrer- Pro flask, DASGIP<br><a href="http://www.dasgip.com">http://www.dasgip.com</a>                 | 150 - 300       | 4-8                | Autoclave     | Orbital Shaker, 10-1000 rpm                              | Gas blending            | pH, DOT, T, Agt, Ant    |
| Sixfors, Ecogen Infors HT<br><a href="http://www.ecogen.com">http://www.ecogen.com</a>                  | 300 - 1000      | 1-6                | Autoclave     | Range of stirrers, Magnetic drive, 50-2000 rpm           | Sparger<br>Gas blending | pH, DOT, T, Agt         |
| Multifors, Ecogen Infors HT<br><a href="http://www.ecogen.com">http://www.ecogen.com</a>                | 500             | 2-6                | Autoclave     | Range of stirrers, Magnetic drive, 30-1200 rpm           | Sparger<br>Gas blending | pH, DOT, T, Agt         |
| Cellstation, Fluorometrix<br><a href="http://www.fluorometix.com">http://www.fluorometix.com</a>        | 35              | 12                 | Autoclave     | Stirrer bar, Magnetic drive, 10-1000 rpm                 | Sparger                 | pH, DOT, T, OD          |
| Minifor, Lambda<br><a href="http://www.lambda-instruments.com">http://www.lambda-instruments.com</a>    | 35 - 200        | 1-6                | Autoclave     | Perforated stirring discs<br>Magnetic Vibromixer         | Sparger<br>Gas blending | pH, DOT, T, Agt         |
| Mini- Reactor Vario 500, Meredos GmbH<br><a href="http://www.meredos.com">http://www.meredos.com</a>    | 50-500          | 1-8                | Autoclave     | Marine propeller or paddle<br>Magnetic drive, 0-2000 rpm | Frit<br>Gas blending    | pH, DOT, T, Agt         |

|  |          |      |                |                               |                       |                         |
|--|----------|------|----------------|-------------------------------|-----------------------|-------------------------|
| GRETA, Belach Bioteknik<br><a href="http://www.belach.com">www.belach.com</a>                      | 200-1000 | 6    | <i>In-situ</i> | Magnetic drive                | Sparger               | pH, DOT, T, Agt,<br>OD  |
| <b><i>Shake Flask</i></b>  |          |      |                |                               |                       |                         |
| Shake-Pro Flask, DASGIP<br><a href="http://www.dasgip.com">http://www.dasgip.com</a>               | 50-500   | 4-16 | Autoclave      | Orbital shaker, 20-400 rpm    | Head space<br>gassing | pH, DOT, T              |
| RAMOS, HiTec-Zang GmbH<br><a href="http://www.hitec-zang.com">www.hitec-zang.com</a>               | 290      | 8    | Autoclave      | Orbital shaker                | Head space<br>gassing | Measure OUR, CTR,<br>RQ |
| <b><i>Microtitre Plates</i></b>  |          |      |                |                               |                       |                         |
| Micro 24, FT Applikon Ltd<br><a href="http://www.ftapplikon.co.uk">http://www.ftapplikon.co.uk</a> | 3-5      | 24   | Disposable     | Orbital shaker, Up to 800 rpm | Sparging              | pH, DOT, T              |

I am an Engineering Doctorate (EngD) student at University College London and my project involves developing a miniature bioreactor that will be fully automated. My supervisor, Dr Gary Lye, has suggested that I write to you as part of my market research since your input would be very useful. Any reply will only take 2 minutes of your time.

An important feature of the miniature bioreactor (50-100 mL total volume) is that it will have the potential for parallel operation. At the moment we plan to have up to 16 vessels running independently at any one time. If you feel it appropriate please could you respond to the three brief questions below?

1. As a person with fermentation development experience would you have a preference for metal bioreactors, that can be setup and sterilised *in-situ* automatically, or would you prefer glass vessels that would require being autoclaved separately?

Steel vessels sterilised *in-situ*

Glass vessel sterilised in an autoclave

2. What fermentation parameters would you like to be able to monitor?

Temperature       pH       Dissolved oxygen

CER       OUR       RQ

Optical density       Other, please specify

3. Would you be interested in on-line thermal profiling data that would allow parallel determination of growth kinetics or bioconversion rates?

Yes       No

Thank you for taking the time to respond to this email. Any further comments you would like to make would be very welcome.

Yours sincerely

Naveraj Kaur Gill

**Figure A.I.1.** Market survey questionnaire distributed to individuals in several pharmaceutical companies involved in fermentation processes.

**Table A.I.2.** Results from the initial market survey questionnaire from Figure A.I.1. Nomenclature: T = temperature, DOT = dissolved oxygen, OD = optical density, Agt = agitation rate, Ant = antifoam, OUR = oxygen uptake rate, CER = carbon dioxide evolution rate, RQ = respiratory quotient, G = residual glucose, Lp = residual lipid/ phosphates, F = feed, Agt = agitation rate.

| Company                     | Sterilisation | Parameters                             | Thermal Profiling | Additional Comments  |
|-----------------------------|---------------|--|-------------------|--|
| Eli Lilly and Co. Ltd.      | SIP           | T, pH, DOT, CER, OUR, RQ, OD, G, Lp, F | ✓                 | <ul style="list-style-type: none"> <li>• Advantage of SIP is that it mimics the plant operations in stirred tanks.</li> <li>• Sampling required</li> <li>• Fed batch operation required</li> </ul> |
| Eli Lilly and Co. Ltd.      |               | T, pH, DOT, G                          |                   |  |
| Safoni-Aventis              | SIP           | T, pH, DOT, OUR, OD                    | ✓                 |  |
| ML Laboratories Plc.        | Autoclave     | T, pH, DOT                             |                   | <ul style="list-style-type: none"> <li>• Sampling required</li> </ul>  |
| DSM Ltd.                    | Autoclave     | T, pH, DOT, CER, OUR                   | ✓                 |  |
| Abbott Laboratories Ltd     | Autoclave     | T, pH, DOT, Agt, Are, RQ, OD, G, Lp, F |                   | <ul style="list-style-type: none"> <li>• Glass autoclaved vessel would be cheaper and more practical</li> <li>• Flexibility with interchangeable stirrers</li> </ul>                               |
| Abbott Laboratories Ltd     | Autoclave     | T, pH, DOT, OD, Agt, RQ                |                   |  |
| Biotica Ltd.                | SIP           | T, pH, DOT                             | ✓                 |  |
| Pfizer Ltd.                 | Autoclave     | T, pH, DOT, CER, OUR, RQ               | ✓                 | <ul style="list-style-type: none"> <li>• Easier to maintain glass autoclaved vessel - cheap, no need to supply steam to the unit</li> <li>• additional ports for custom sensors</li> </ul>         |
| Cobra Biomanufacturing Plc. | Autoclave     | T, pH, DOT, OD                         | ✓                 | <ul style="list-style-type: none"> <li>• Some development labs may not have steam supplies and so autoclavable options may be more versatile</li> </ul>  |
| Serologicals Ltd.           | Autoclave     | T, pH, DOT, CER, OUR, RQ, OD           | ✓                 | <ul style="list-style-type: none"> <li>• Would like to have the option to be able to monitor any data wherever possible</li> </ul>   |



The overall market survey identified some key commercial opportunities and the main conclusions were:

- Autoclaving is the most suitable mode of sterilisation at this scale since it is a much cheaper and more practical, also some development labs may not have a steam supply, so autoclavable options may be more versatile.
- Although some mode of aseptic sampling is required, it is preferred to have as much information available on-line as possible.
- Flexibility of the system is necessary in terms of interchangeable stirrers, and additional ports on the headplate for custom ports.
- Options for fed batch operation are required in most cases.
- A strong interest was expressed for the use of thermal profiling as an additional technique for continuous on-line monitoring of fermentation processes and is not currently offered by any of the systems listed in Table A.I.1.

### **A.I.2 Required Features for Bioreactor Design and Operation**

In order to design a robust and reliable miniature bioreactor system for commercial applications, key considerations that the miniature bioreactor system described in this work must fulfil include:

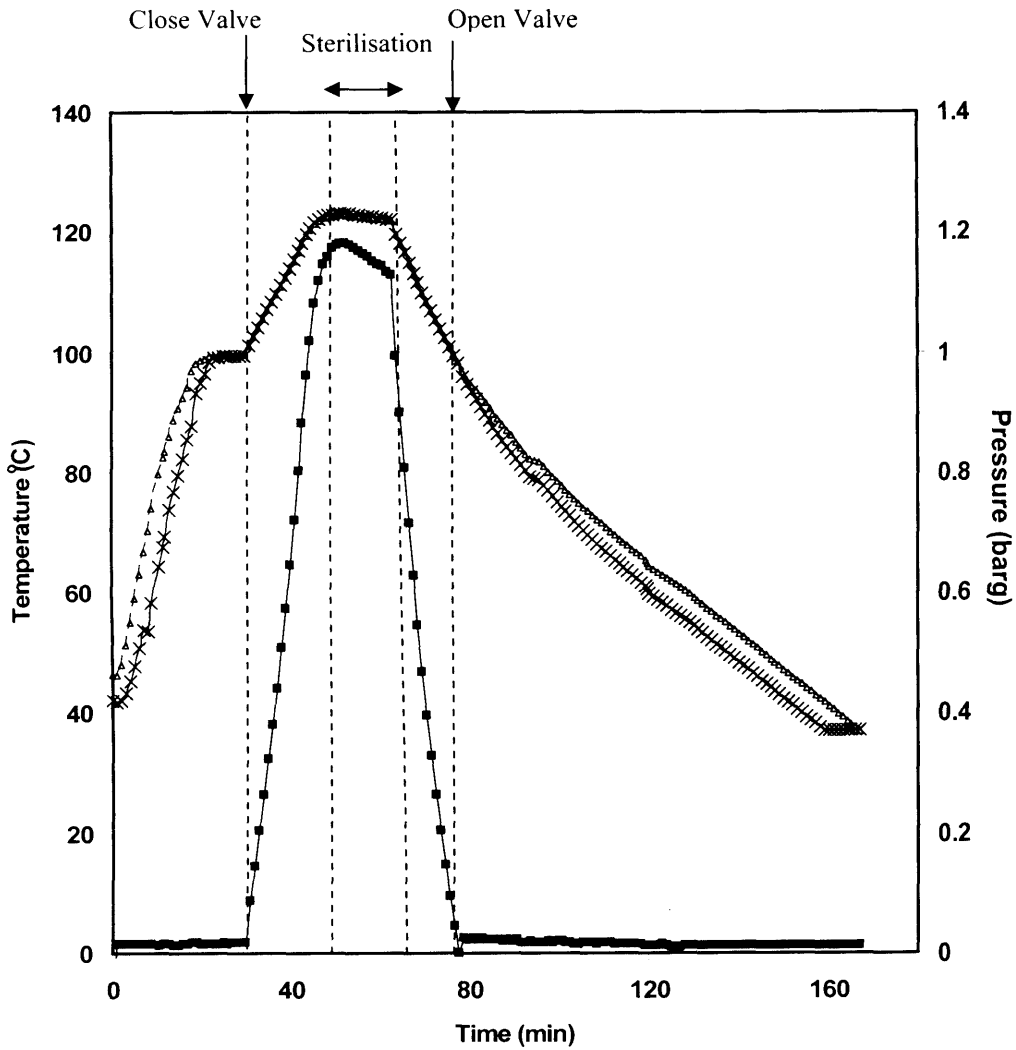
- Maintenance of sterility over prolonged periods.
- Robust sensors and control system, providing as much information about the process on-line as possible.
- Parallel operations to facilitate high throughput fermentations, 4 – 16 units are considered feasible to operate.
- Flexibility for each miniature bioreactor to be operated simultaneously and independently of each other at different operating conditions.
- Flexibility with modes of operation, batch and fed batch.
- User-friendly software that allows flexibility to carry out a variety of automated bioprocesses with complete on-line monitoring of key process parameters.

At the early development stages of the miniature bioreactor system some work was carried out to assess the feasibility of *in-situ* sterilisation without using an external steam supply in order to further automate the miniature bioreactor system. Initial work to test this method of *in-situ* sterilisation involved temperature mapping studies of reactor contents and head space temperatures and pressure studies, Figure A.I.2. The gas outlet port on the reactor head plate was fitted with a pressure relief valve which vented all the air out of the system as the vessel was heated up to 100 °C (using the systems own heater and temperature control), at which point the valve is closed and the vessel was allowed to heat up further to 121 °C for the sterilisation period of 15 minutes. Following this as the reactor was cooled back to 100 °C the valve is re-opened and once the vessel and its contents cooled to the desired temperature, it was ready for the next stage of the fermentation process.

Although this method of sterilisation has been shown to work, the whole process of achieving sterilisation and cooling the vessel to the fermentation temperature (37 °C) took over 2 hours. This is much longer compared to conventional sterilisation in the autoclave (1.5 hours). In addition sufficient reproducibility between sterilisation runs proved difficult to achieve and including a pressure relief valve on the headplate of the bioreactor would have compromised the design, but more importantly there were a number of safety issues and precautions that would have to be taken during the sterilisation procedure. This method of sterilisation would become increasingly challenging when dealing with several miniature bioreactors simultaneously with no added benefits in terms of speeding up the process and additional safety concerns. As a result of these trials this method of sterilisation was not pursued.

### **A.I.3 Validation of Prototype Bioreactor Design**

Ultimately the miniature bioreactor system has been designed and constructed for an intended purpose and a series of validation tests were carried out to demonstrate that the system is capable of fulfilling these under realistic conditions. The initial validation involved demonstrating the miniature bioreactors capability to maintain sterility over prolonged periods, this was successfully achieved over a period of 4



**Figure A.I.2.** Temperature mapping and pressure tests for *in-situ* sterilisation of the miniature bioreactor without an external steam supply: (■) pressure, (Δ) temperature of the reactor contents, (x) headspace temperature. Experiments performed as described in Section A.I.2.

days (Figure 3.1). For fermentation applications the need to tightly control process parameters such as temperature and pH is critical, this was also been demonstrated over prolonged periods of operation (Figure 3.2).

For any given aerobic fermentation process the oxygen transfer capability of the bioreactor is critical. With a maximum  $k_{La}$  value of  $0.11 \text{ s}^{-1}$  (Figure 3.4), the miniature bioreactors performance is comparable to conventional laboratory scale bioreactors (Doig *et al.*, 2006). In terms of parallel operation and reproducibility of results, this has been demonstrated with *E.coli* (Figure 3.5 and Table 3.1) and *B.subtilis* (Figure 3.6 and Table 3.2) fermentations carried out under identical conditions. This not only confirms reproducibility of results but also shows that system is sensitive to difference between microorganisms and operating conditions. However to asses the miniature bioreactors full potential further testing is probably necessary with a more challenging microorganism such as *Streptomyces* sp.

Potential industrial bioprocesses identified from the initial evaluation and screening at this scale, ultimately need to be scaled up. In this work it has been shown that the most reliable criterion for scale translation from the miniature bioreactor to a convention 2 L laboratory bioreactor can be achieved based on constant  $k_{La}$ . This scale-up criterion has been validated over a range of three different  $k_{La}$  values showing comparable results at both scales in all cases (Figure 5.7).

Finally preliminary validation testing was also carried out for assessing the novel optical density probe and the use of thermal profiling for monitoring microbial growth kinetics. In both cases there was good agreement between maximum specific growth rates calculated from off-line OD data and the on-line OD and thermal profiling data (Figure 6.1 and 6.4 respectively).

In terms of commercial validation it is necessary to fulfil the ISO9000 requirements for the quality standards of production equipment. This typically involves up to date documented procedures and regular auditing. CE marking is also is a mandatory safety mark for production equipment, to certify that the product complies with strict standards including the electrical safety standards, generic immunity standards and emissions standards.

## APPENDIX II

### MECHANICAL DRAWINGS OF THE MINIATURE BIOREACTOR SYSTEM

---

---

The figures in this appendix illustrate the detailed design features and dimensions of the main components of the miniature bioreactor. They were prepared by HEL Ltd., U.K. Note: All measurements are given in millimetres. Materials of construction: borosilicate glass, stainless steel (316L StSt) and polyether-ether-ketone (PEEK).

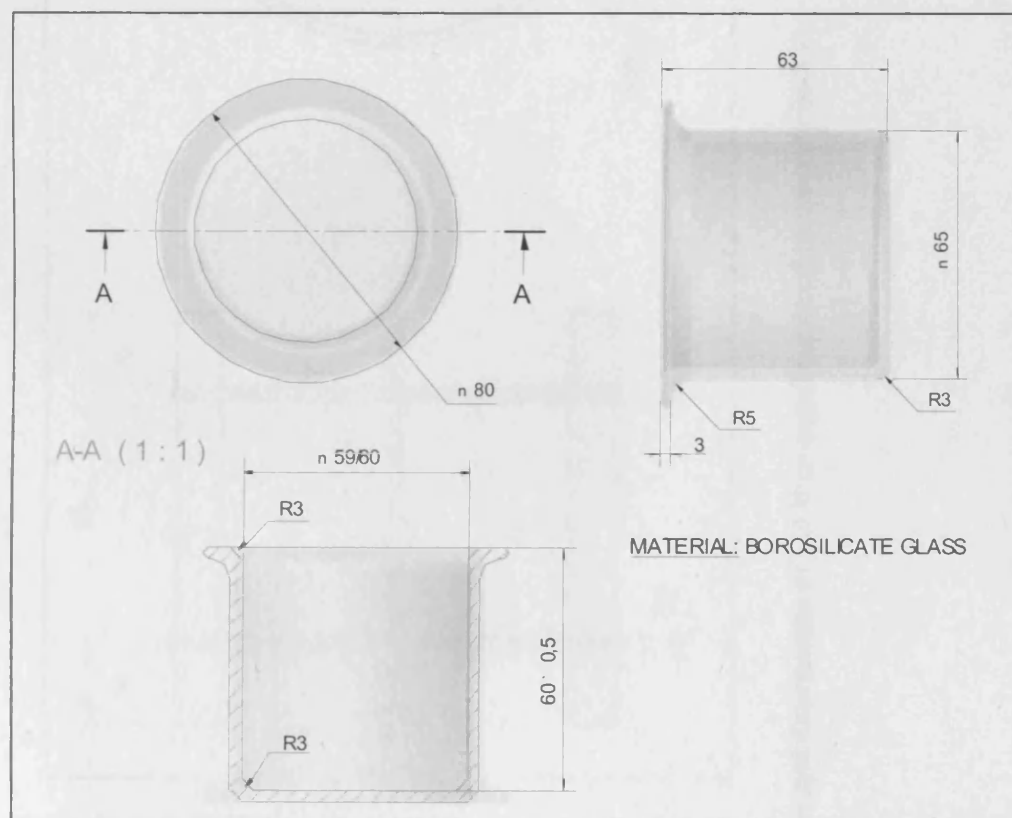
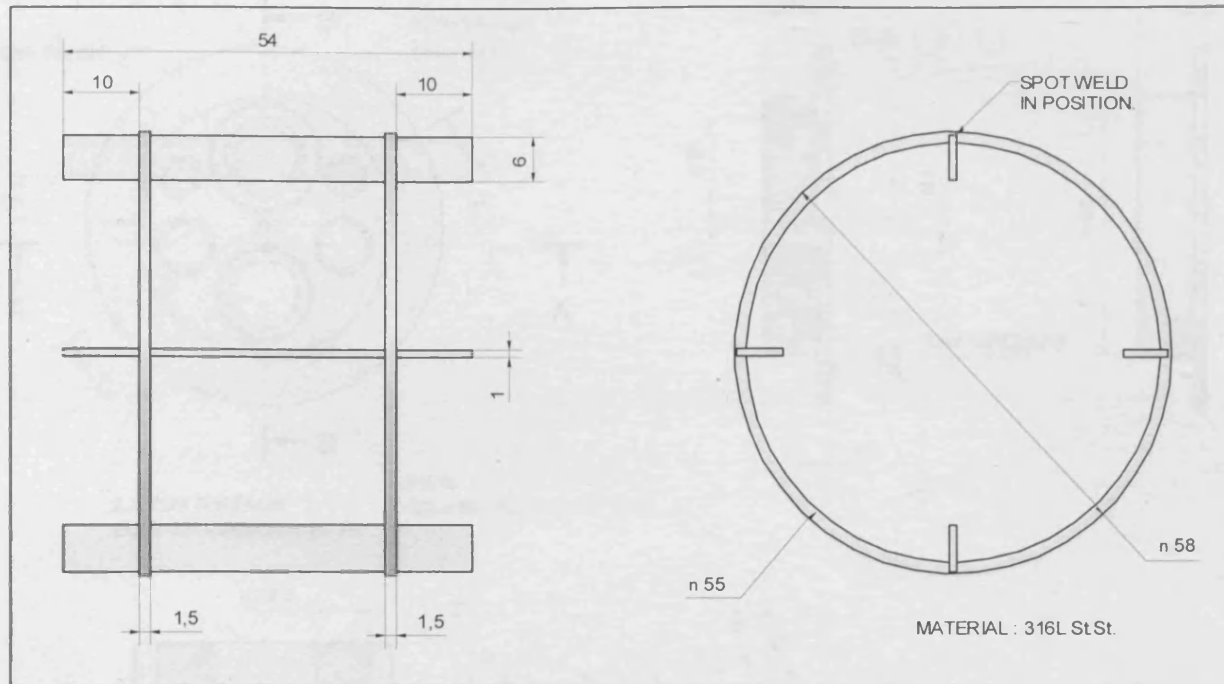
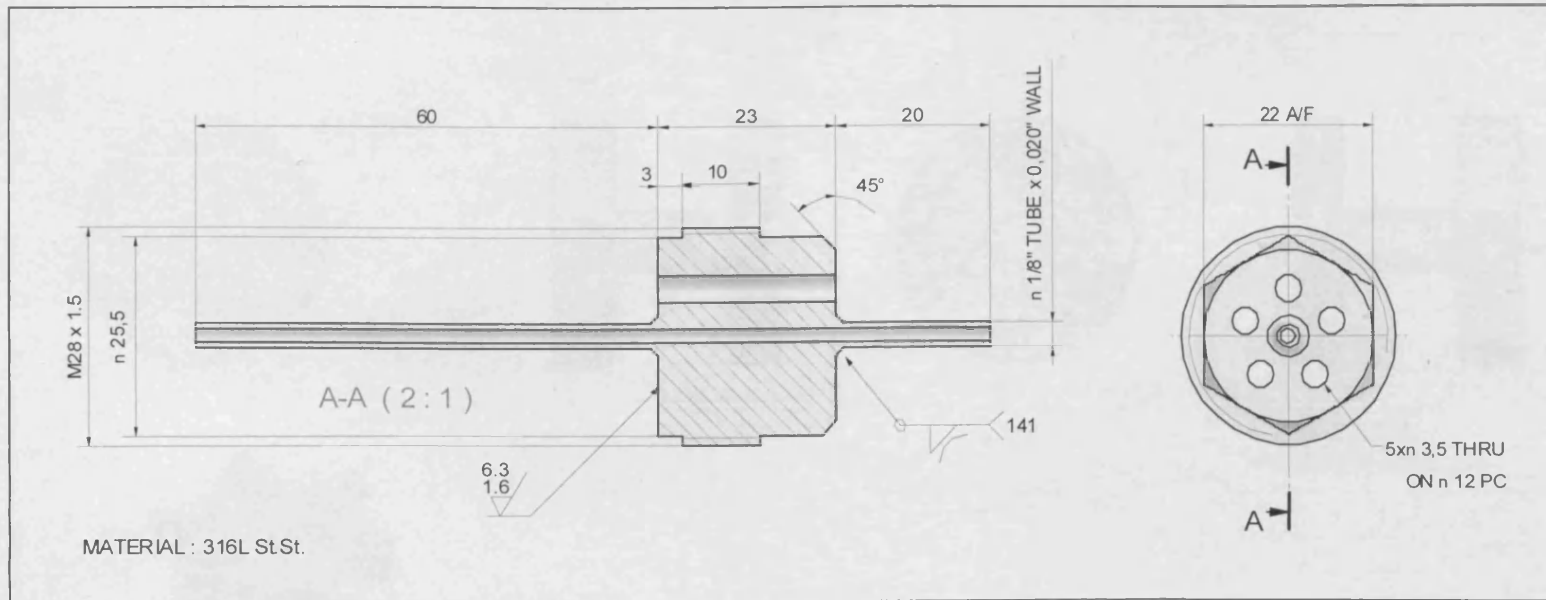


Figure A.II.1. Design and dimensions of miniature bioreactor glass vessel.



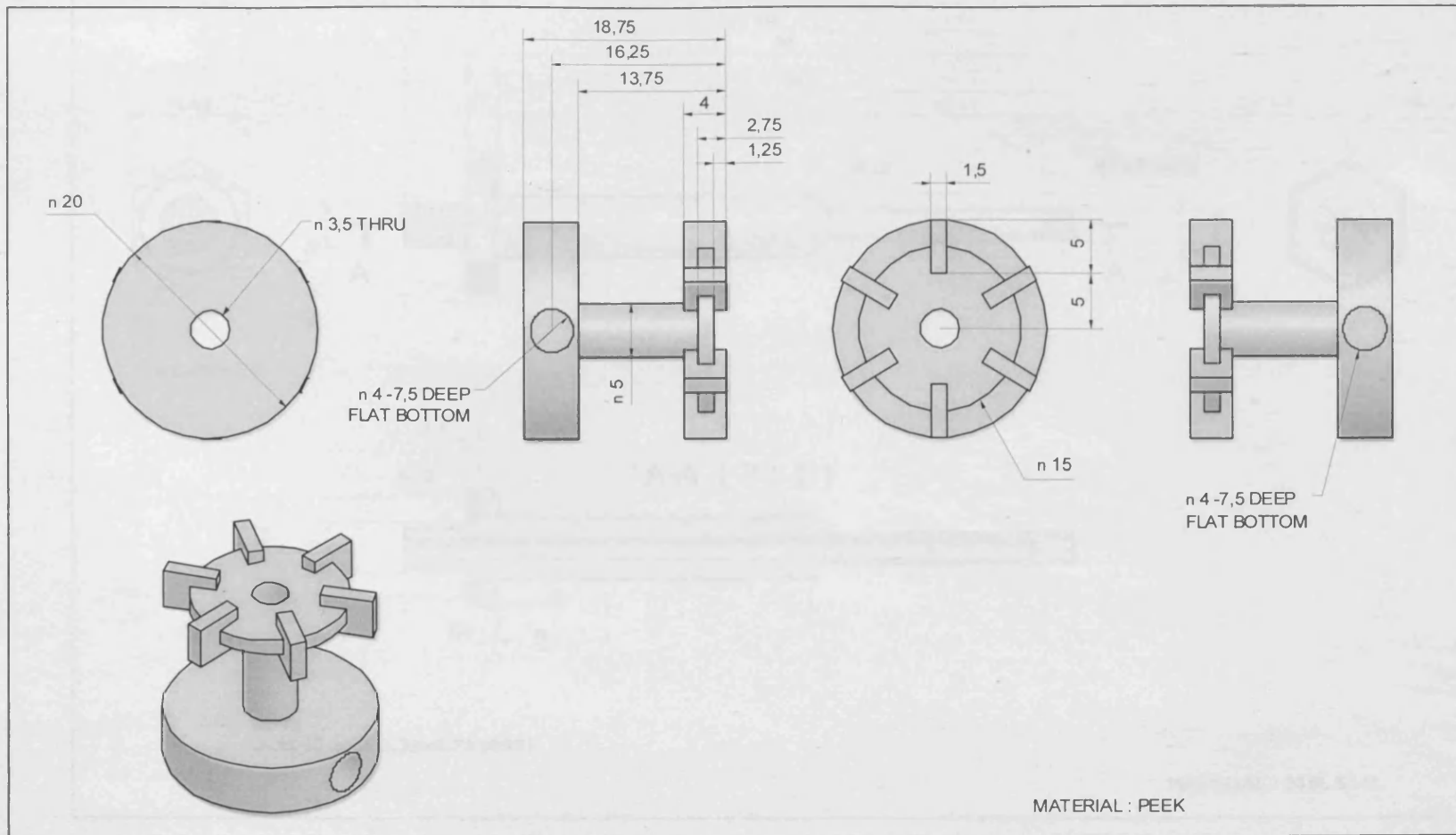
**Figure A.II.2.** Design and dimensions of the four equally spaced removable baffles.



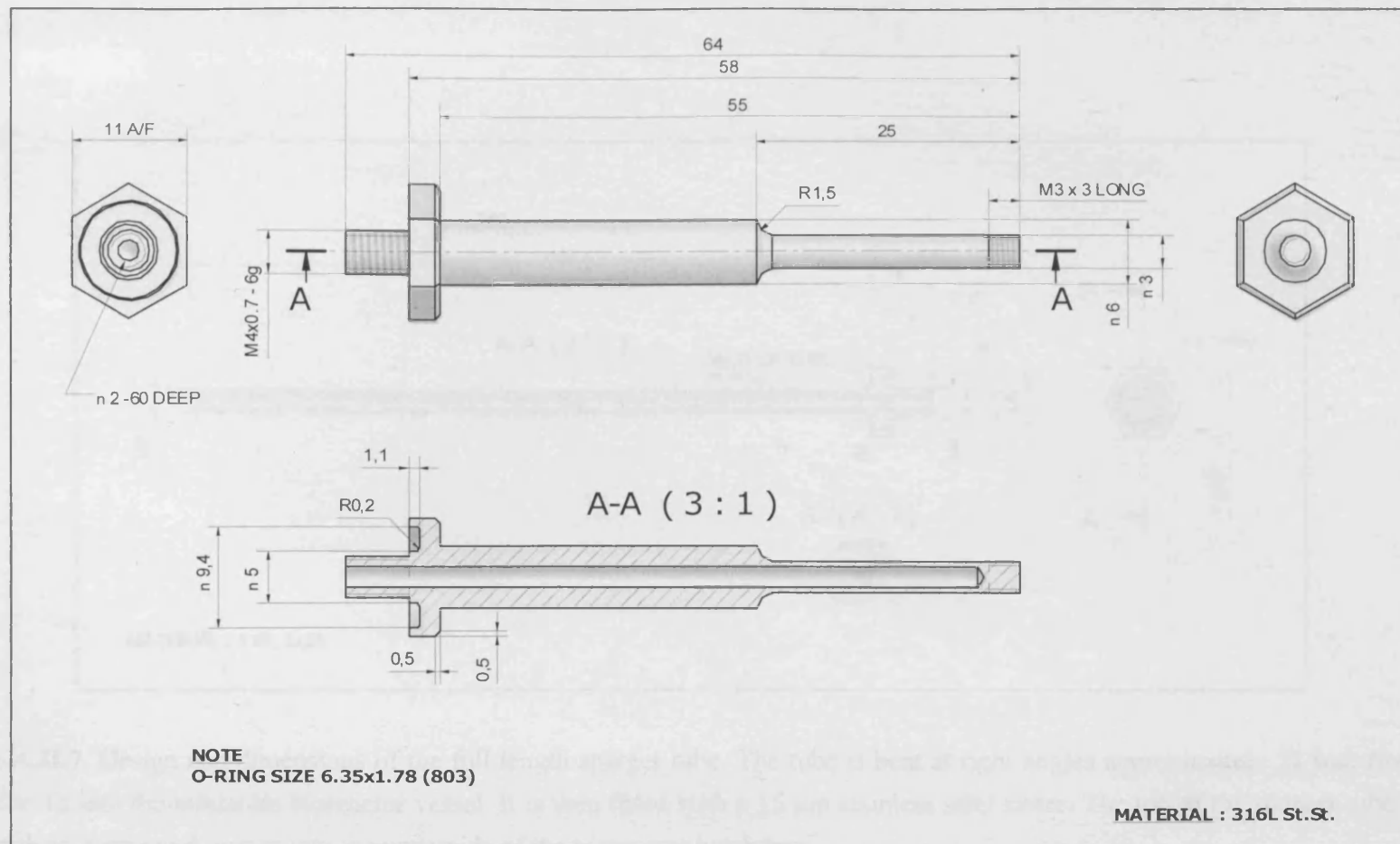


**Figure A.II.4.** Design and dimensions of the multiport fitting that screws into the bioreactor headplate. Up to five additions can be made using sterile hypodermic needles via a self-sealing septum. The centre of the multiport consists of a long hollow tube which functions as a sampling tube.

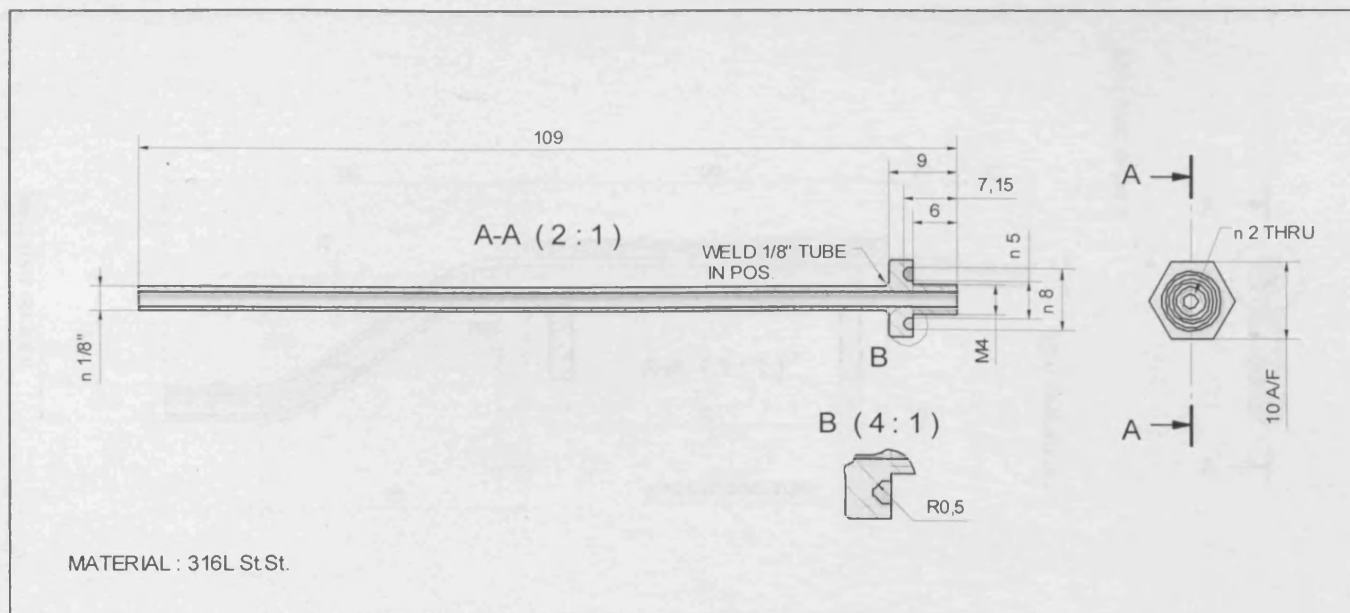




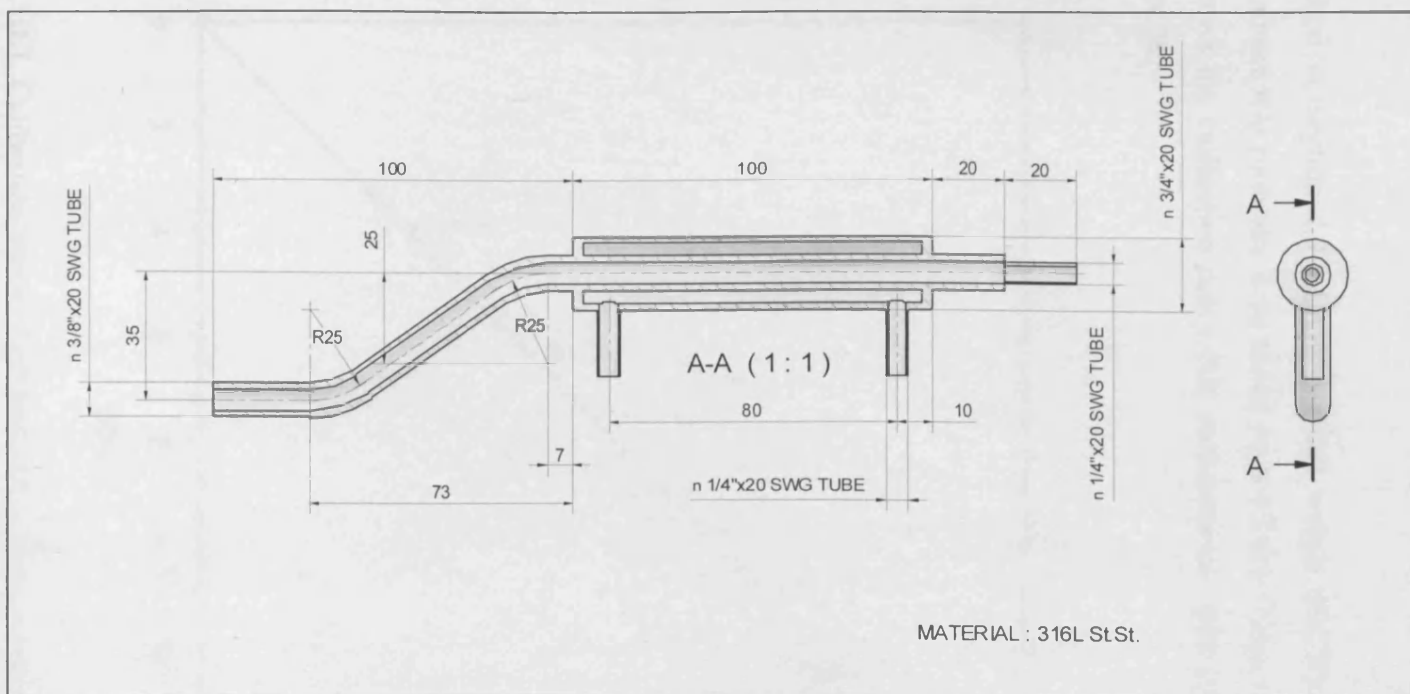
**Figure A.II.5.** Design and dimensions of the magnetically driven, miniature six-blade turbine impeller. The impeller has been designed to incorporate a flat disk at the end of the impeller drive shaft, this disc housed a total of eight cylindrical magnets.



**Figure A.II.6.** Design and dimensions of the hollow stirrer shaft, which also functions as a thermowell to hold the thermocouple. The miniature turbine impeller is mounted on the bottom half of the shaft and held in place with a nut. The top of the stirrer shaft is fitted with an o-ring and screws into the underside of the bioreactor headplate.



**Figure A.II.7.** Design and dimensions of the full length sparger tube. The tube is bent at right angles approximately 22 mm from the end to fit into the miniature bioreactor vessel. It is then fitted with a 15  $\mu$ m stainless steel sinter. The top of the sparger tube is fitted with an o-ring and screws into the underside of the bioreactor headplate.



**Figure A.II.8.** Design and dimensions of the off-gas condenser fitted onto the gas outlet port of the bioreactor headplate. Cooling was achieved using a chilled water supply.

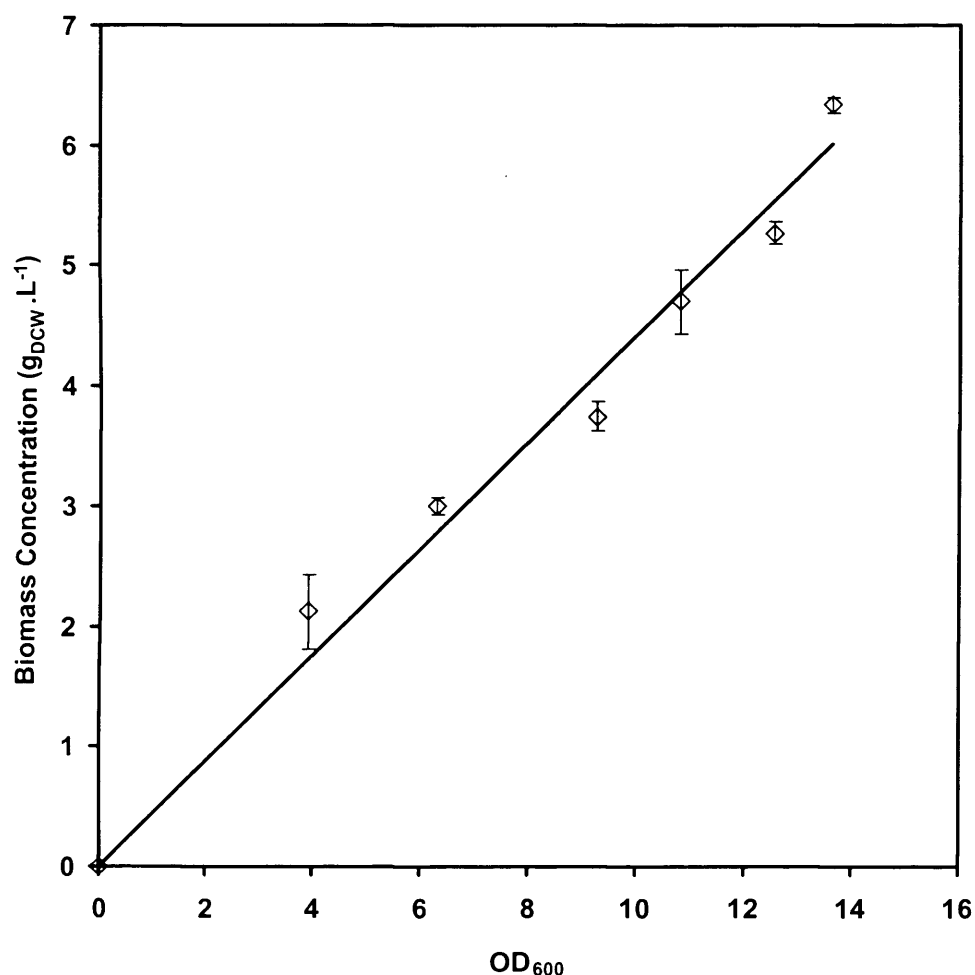
## APPENDIX III

### CALIBRATION OF OFF-LINE OD<sub>600</sub> MEASUREMENTS WITH BIOMASS DRY CELL WEIGHT

---

---

As described in Section 2.9.1.1 the dry cell weight (DCW) of an *E.coli* TOP10 pQR239 culture was routinely determined from off-line OD<sub>600</sub> measurements. Figure A.III.1 shows the calibration curve that correlates the measured OD<sub>600</sub> values with biomass DCW.



**Figure A.III.1.** Calibration curve of off-line OD<sub>600</sub> measurements from *E.coli* TOP10 pQR239 fermentation with DCW measurements. OD<sub>600</sub> and DCW were determined as described in Sections 2.9.1.2 and 2.9.1.1 respectively. Linear least squares fitting gave an R<sup>2</sup> value of 0.981. Error bars show one standard deviation of triplicate determinations.

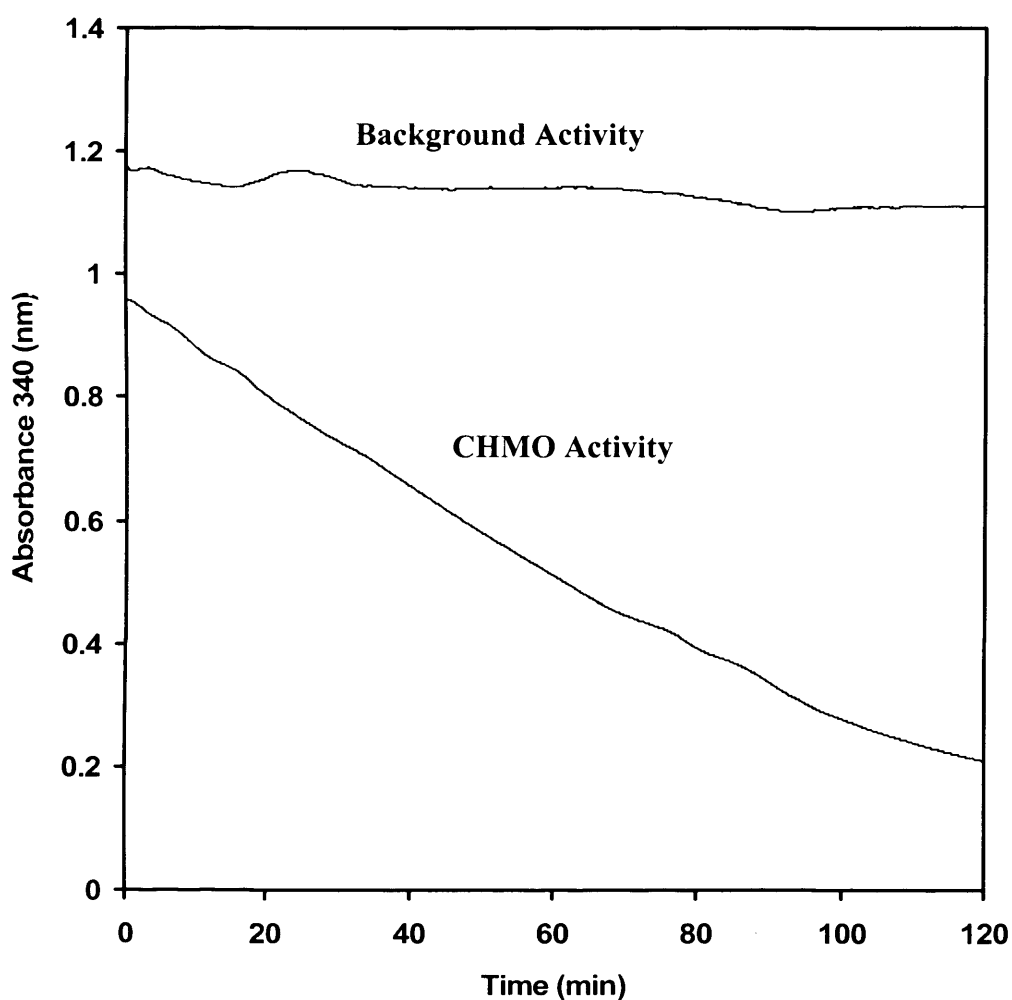
## APPENDIX IV

### QUANTIFICATION OF INTRACELLULAR CHMO ACTIVITY BASED ON THE SPECTROPHOTOMETRIC ASSAY

---

---

A sample curve for the determination of the activity of CHMO in cell lysate using the spectrophotometric assay described in Section 2.9.2 is shown in Figure A.IV.1. Background activity was determined prior to cyclohexanone addition.



**Figure A.IV.1.** Example of the background absorbance change with time and the absorbance change with time after addition of the cyclohexanone substrate for a typical spectrophotometric assay of CHMO in a clarified *E.coli* TOP10 pQR239 lysate. The details of the assay are described in Section 2.9.2.

The activity of the enzyme extract was expressed in Units (U) with one unit being defined as the amount of CHMO which catalyses the cyclohexanone induced oxidation of 1  $\mu\text{mol}$  of NADPH per minute. Calculation of the concentration of NADPH in the cuvette was based on Beer's Law, Equation (A.IV.1):

$$A_{340} = \epsilon c l \quad (\text{A.IV.1})$$

Where  $A_{340}$  is the absorbance at 340 nm,  $\epsilon$  is the extinction coefficient,  $c$  is the NADPH concentration in cuvette and  $l$  is the light path length.

The extinction coefficient of NADPH is  $6.22 \text{ mL} \cdot \mu\text{mol}^{-1} \cdot \text{cm}^{-1}$  (Doig *et al.* 2001). Therefore, the background activity and the activity of the sample can be calculated using the following equation:

$$\text{Number of units in the cuvette} = \frac{\Delta A_{340}}{l \epsilon \Delta t} \quad (\text{A.IV.2})$$

For the example shown in Figure A.IV.1 the initial linear rate of absorbance change (over two minutes) after addition of substrate is,  $0.008 \text{ A}_{340} \cdot \text{min}^{-1}$ . Subtraction of the background rate (over the same time period) of  $0.0027 \text{ A}_{340} \cdot \text{min}^{-1}$  gives  $0.0053 \text{ A}_{340} \cdot \text{min}^{-1}$ . From Equation A.IV.2 the number of units in the cuvette can be calculated to be  $0.0511 \text{ U} \cdot \text{mL}^{-1}$ . Knowing that the light path length is 1 cm, volume of the cuvette is 1 mL and the dilution factor is 10, the volumetric activity of the cell extract was calculated to be  $511 \text{ U} \cdot \text{L}^{-1}$ . The biomass concentration in the fermentation medium from which the lysate was originally prepared was  $3.53 \text{ g} \cdot \text{L}^{-1}$  so the specific intracellular CHMO activity titre is  $145 \text{ U} \cdot \text{g}^{-1}$ .

## APPENDIX V

### K<sub>L</sub>A DETERMINATION BASED ON THE FERMENTATION KINETICS OF A TYPICAL *B. SUBTILIS* ATCC6633 FERMENTATION

---

---

During a typical aerobic microbial fermentation, under steady state conditions oxygen absorption and consumption rates must balance (OTR = OUR) thus,

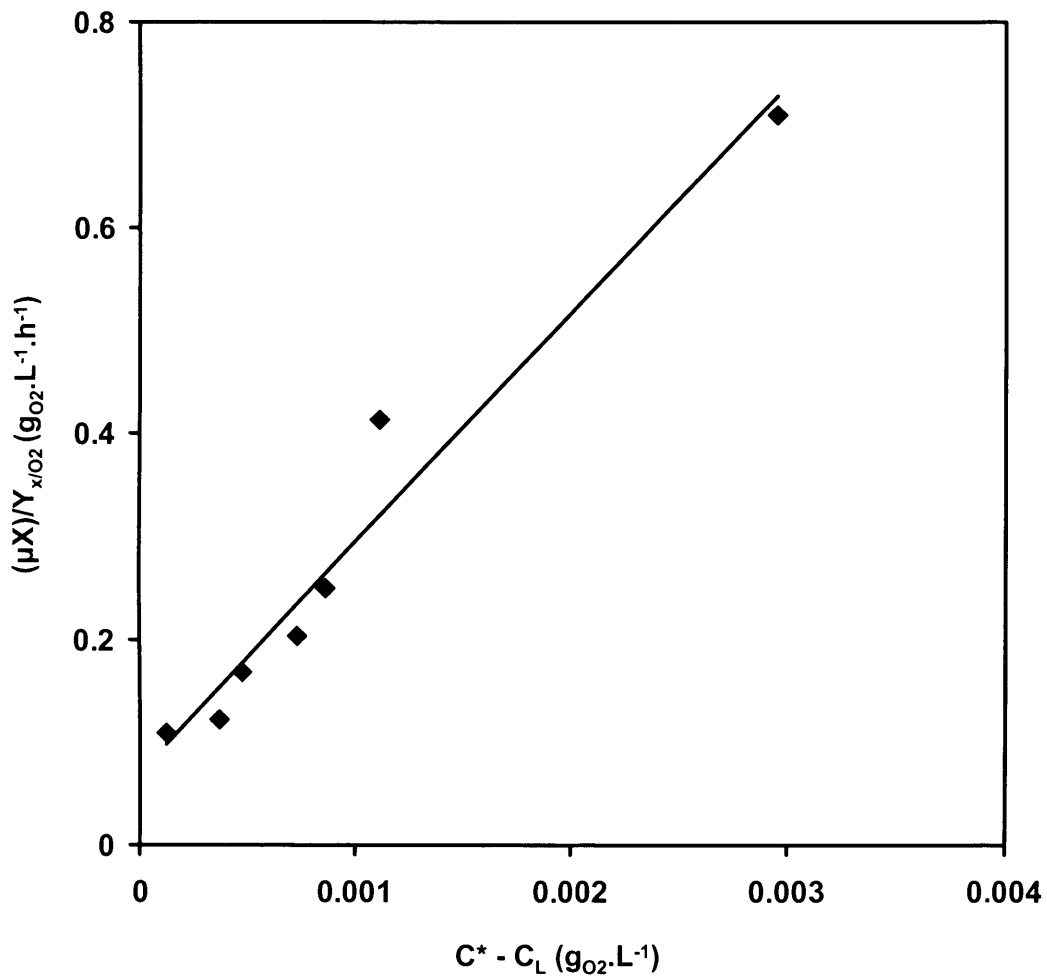
$$\frac{\mu}{Y_{X/O_2}} \cdot X = k_L a \cdot (C^* - C_L) \quad \text{Eq. A.V.1}$$

where  $\mu$  is the specific growth rate,  $X$  is biomass concentration,  $Y_{X/O_2}$  is the yield of biomass on oxygen,  $C^*$  is the saturation dissolved oxygen concentration in the medium,  $C_L$  is the actual concentration of dissolved oxygen.  $C_L$  and  $Y_{X/O_2}$  have been reported to be  $6.8 \text{ mg.L}^{-1}$  and  $1.6 \text{ g.g}^{-1}$  respectively (Doig *et al.*, 2004).

The linear relationship given by Equation A.V.1 can therefore be used to determine a value for  $k_L a$  from the kinetic data derived from an aerobic microbial fermentation. The  $k_L a$  value is given by the gradient of the line of  $(C^* - C_L)$  versus  $(\mu X)/Y_{X/O_2}$ . This has been illustrated in Figure A.V.1 using the fermentation data of a typical *B.subtilis* fermentation as shown in Figure 3.5 (B2).

A  $k_L a$  value of  $223.36 \text{ h}^{-1}$  ( $0.062 \text{ s}^{-1}$ ) is obtained and is in good agreement with that determined from the dynamic gassing out method (Section 2.4) under the same operating conditions.





**Figure A.V.1.** Determination of  $k_L a$  value based on fermentation data from a typical *B.subtilis* fermentation as shown in Figure 3.5 (B2). Linear least square fitting gave an  $R^2$  value of 0.958.

## APPENDIX VI

### DERIVATION OF THE PARAMETERS FOR THE MINIATURE BIOREACTOR $k_L a$ CORRELATION

---

---

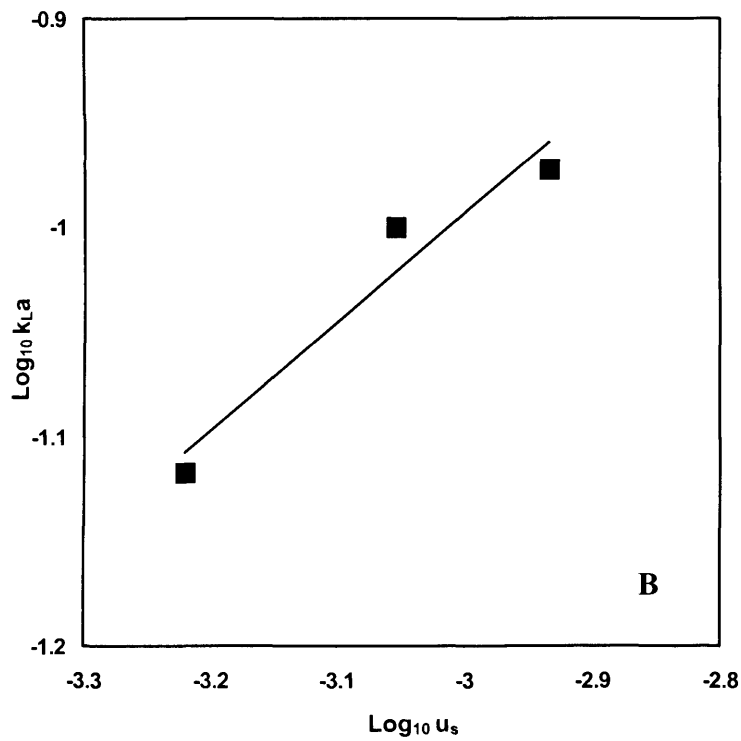
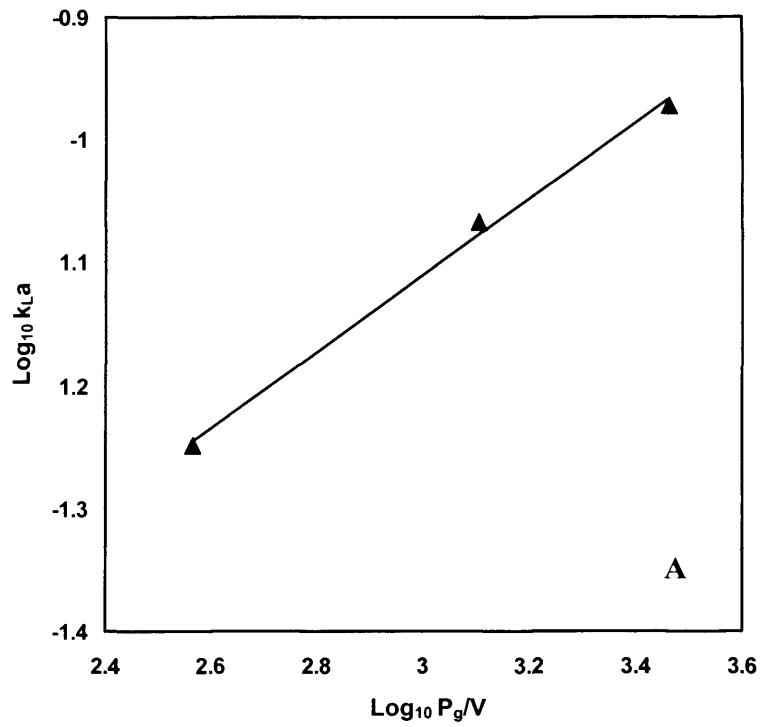
The values for the constant  $C$  and the exponents  $\alpha$  and  $\beta$  in Equation A.VI.1 were determined from the experimental  $k_L a$  data (Figure 3.4) and the gassed power input data (Figure 5.1):

$$k_L a = C \left( \frac{P_g}{V} \right)^\alpha u_s^\beta \quad \text{Eq. A.VI.1}$$

where  $k_L a$  is the volumetric mass transfer coefficient,  $P_g/V$  is the impeller gassed power per unit volume,  $u_s$  superficial gas velocity,  $C$  is a constant and  $\alpha$  and  $\beta$  are exponents. These parameters are determined as follows:

- A plot of  $\log_{10} k_L a$  versus  $\log_{10} P_g/V$  at constant superficial gas velocity for the three aeration rates 1, 1.5 and 2 vvm is needed; the average of the gradients of these lines will give the value for the exponent  $\alpha$ .
- A plot of  $\log_{10} k_L a$  versus  $\log_{10} u_s$  at constant  $P_g/V$  for three agitation rates, 1000, 1500 and 2000 rpm is needed; the average of the gradients of these lines will give the value for the exponent  $\beta$ .
- $C$  is determined from the substitution of  $\alpha$  and  $\beta$  for a given set of  $k_L a$  and  $P_g/V$  data.

A sample plot for the calculation of  $\alpha$  for at a constant aeration rate of 2 vvm is shown in Figure A.VI.1 (A). Similarly a sample plot for the calculation of  $\beta$  at a constant agitation rate of 2000 rpm is shown in Figure A.VI.1 (B).



**Figure A.VI.1.** Determination of exponents  $\alpha$  and  $\beta$ : (A) constant aeration rate of 2 vvm, gradient gives  $\alpha$ ; (B) constant agitation rate of 2000 rpm, gradient gives  $\beta$ .

From Figure A.VI.1 the exponents  $\alpha$  and  $\beta$  are determined to be 0.32 and 0.52 respectively. Therefore for agitation and aeration conditions of 2 vvm and 2000 rpm, when the  $k_L a$  and  $P_g/V$  and  $u_s$  equal  $0.11 \text{ s}^{-1}$ ,  $2900.96 \text{ W.m}^{-3}$  and  $0.00117 \text{ m.s}^{-1}$  respectively, the constant  $C$  is calculated to be 0.22 from Equation A.VI.1. This procedure was carried out at three different agitation (1000, 1500 and 2000 rpm) and aeration (1, 1.5 and 2 vvm) rates and the final values for  $C$ ,  $\alpha$  and  $\beta$  were taken from the average of the determinations.

## APPENDIX VII

### QUANTIFICATION OF REQUESTED HEATER POWER USING A PT100 CALIBRATION HEATER

---

---

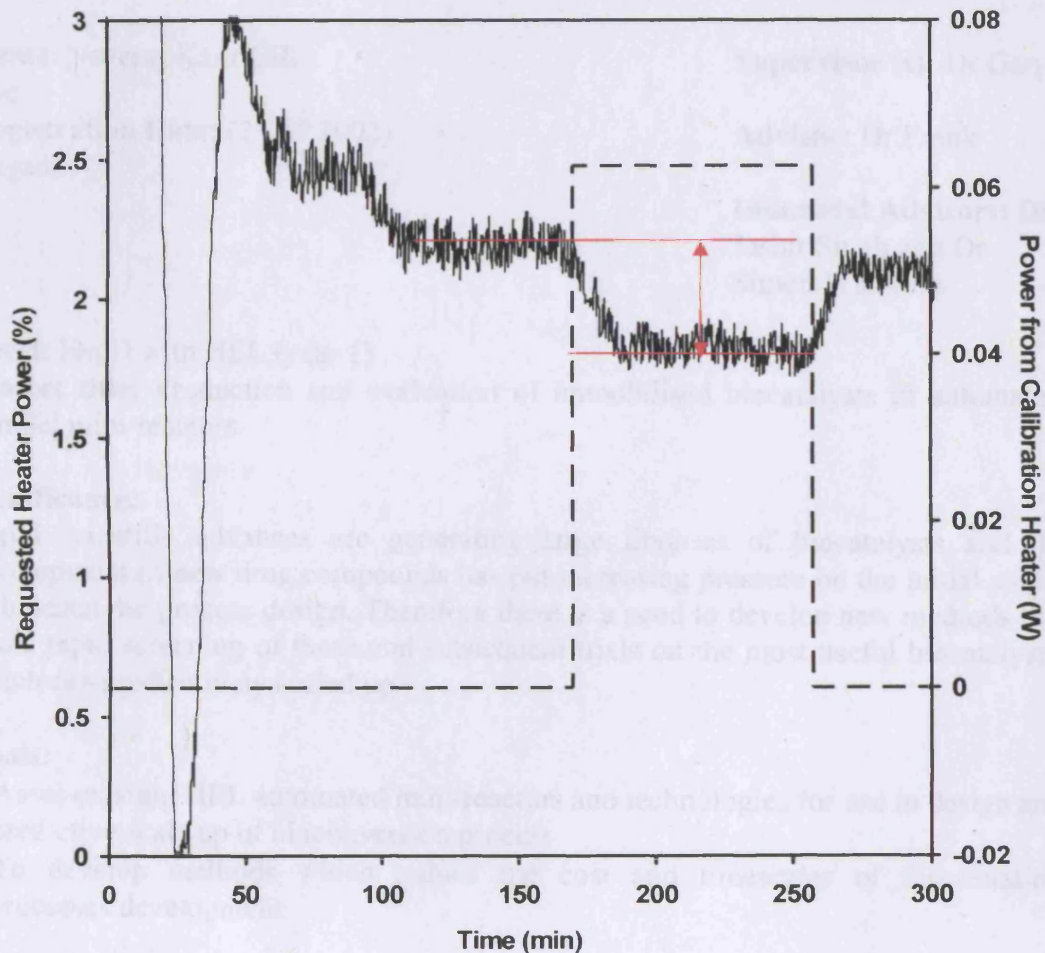
Temperature control of the miniature bioreactor was achieved via an electrical disc heater (50 W) positioned directly beneath the vessel driven by PWM (pulse-width modulation), i.e. a train of pulses with the heater being turned on and off at a fixed level to achieve the set-point temperature. This prohibits direct power measurement. However, PWM heaters have a “requested power” output which controls the portion of a fixed control period for which the heater is activated. This field is controlled by a standard PID controller. Previous experiments carried out by HEL Ltd. (UK) on an analogous system have demonstrated that the requested power of the heater is linearly related to the heater power. Therefore to determine the actual power output during a microbial fermentation a calibration procedure was undertaken, involving carefully lagging the entire vessel containing media to keep heat losses constant and to maintain the vessel temperature at 37 °C. A “calibration heater” then was placed into the reactor and once the requested power had stabilised, the calibration heater was activated at a known power and the magnitude of the control system response was recorded. The calibration heater used was a stainless steel-cased 100Ω resistor which was driven at 2.5 V (using a bench power supply), giving an output of 0.0625 W as calculated from equation A.VII.1:

$$P_{ch} = \frac{V_{ch}^2}{R_{ch}} \quad \text{A.VII.1}$$

where  $P_{ch}$  is the power output of the heater (W),  $V_{ch}$  is the voltage supplied to the calibration heater (V) and  $R_{ch}$  is the resistance of the calibration heater (Ω).

It can be seen from Figure A.VII.1 that when the calibration heater was activated the miniature bioreactor temperature control system backed off by 0.4% giving a calibration ratio of approximately 0.16 W per %. This calibration approach can be

justified in that the conditions in the fermentation and calibration experiments were kept as similar as possible.



**Figure A.VII.1.** Calibration of the requested power of the electrical heater (-) used for controlling the temperature of the miniature bioreactor. A known quantity of power was introduced to the vessel using a calibration heater (---). The average decrease in requested power when the calibration heater was activated, as indicated by the arrow, was 0.4 %. Calibration was performed using a well lagged vessel containing fermentation medium.

## APPENDIX VIII

### ENGD PROFORMAS

---

---

#### **Proforma 1:**

|  |  |
|--|--|
| <b>Name:</b> Naveraj Kaur Gill<br>Lye            | <b>Date:</b> 05.12.2002  |
| <b>Registration Date:</b> (23.09.2002)<br>Baganz | <b>Supervisor (s):</b> Dr Gary   |
|  | <b>Advisor:</b> Dr Frank   |
|  | <b>Industrial Advisors:</b> Dr<br>Jasbir Singh and Dr<br>Simon Waldram |

**Level:** EngD with HEL (year 1)

**Project title:** Production and evaluation of immobilised biocatalysts in automated, parallel mini-reactors.

#### **Significance:**

Rapid scientific advances are generating large libraries of biocatalysts and the development of new drug compounds has put increasing pressure on the initial stages of biocatalytic process design. Therefore there is a need to develop new methods that allow rapid screening of these and subsequent trials on the most useful biocatalysts, which can predicatively scaled up.

#### **Goals:**

- Asses existing HEL automated mini-reactors and technologies for use in design and predictive scale up of bioconversion process
- To develop methods which reduce the cost and timescales of fermentation processes development

#### **Conceptual Challenges:**

To establish if the Automate is suitable for running both chemical and biochemical processes, the advantages of using automated, parallel systems. Also to identify the basis for scale up.

#### **Results:**

In the past scale down studies have been a useful way of obtaining specific design information for large-scale reactors and process optimisation that can be scale up. However there is a growing demand for new approaches to bioprocess design in order to asses the process performance of new novel biocatalysts more rapidly that provides data that can be readily scaled-up, enabling expensive pilot trials to focus on the most favourable biocatalyst process combination. HEL's miniature reactors have the

potential to fulfil these requirements, however it is necessary to identify the key features of conventional biochemical reactors and construct a suitable automated reactor. The study will examine the key issues in automated production and evaluation of immobilised enzyme biocatalysts using asymmetric carbon-carbon bond formation by the enzyme transketolase as a model reaction.

Initial work has involved carrying out a series of shake flask fermentations using *E.coli* JM107/PQR711 grown on LB media, in order to obtain a growth curve and practice laboratory procedures. 1ml of the seed culture was used to inoculate 150ml of LB broth in a 500ml shake flask, which was incubated in an orbital shaker at 37°C and 250rpm. 1ml samples were taken every hour and the optical density was measured. While preparing the media the pH was adjusted to pH 7.0 using 1M NaOH prior to autoclaving.

The second fermentation was conducted in a 2L fermenter, using LB media. The 150ml inoculum was grown in a 500ml shake flask in the same way as before for approximately 12hours. 3M H<sub>3</sub>PO<sub>4</sub> and 3M NaOH were used to regulate the pH during the fermentation. Again samples were taken hourly and the optical density measured to develop a growth curve. At the end of the fermentation a large sample was taken and a series of dilutions were made and the dry cell weight (samples were dried over night in a drying oven) and corresponding optical density was measured for each sample to make a calibration curve.

**Intellectual Property:**

At this stage the main intellectual property would be to compare the similarities and difference between chemical and biochemical reactors. Also to assess and make modifications to the design of the HEL reactors in order to operate the system aseptically, so that samples can be taken and additions made without compromising the sterility of the system.

**Publications:**

None to date.

**Previous milestones:**

None, this is proforma 1.

**Research targets:**

**6 months:**

- Become competent with the relevant laboratory procedures i.e. aseptic techniques, seed stock preparation, media preparation, sampling and set-up and operation of a 2L fermenter.
- Perform reproducible *E.coli* fermentations in shake flask and at 2L scale
- Prepare a detailed explanation of microbial fermentation for HEL
- Spend time at HEL to learn about their software and control system and become familiar with their Automate.
- On going market research into miniature chemical reactors and bioreactors that are currently available and analysis of their designs and special features.

**Milestone(s):** to give at least 4 milestones



- Successfully complete shake flask and 2L fermentations using LB and glycerol based media
- Present 'an introduction to microbial fermentation' to HEL
- Tabulate all the information found about miniature reactors already being manufactured
- Carry out sterilisation tests and perform a fermentation at HEL using their miniature reactor
- Produce an initial draft of literature review for the first year report

**Research targets:**

**6 months to 1 year:**

- Define changes to the design of HEL's miniature reactors to enable a microbial fermentation to be run efficiently
- Complete market survey about miniature reactors
- Investigate the oxygen transfer rates in the Automate
- Comparative studies of bioreactors and the Automate, e.g. assess the agitator design, investigate its potential to use as a scale up parameter

**Milestone (s):**

- Implement the suggested changes to the existing Automate and have a bioreactor made for subsequent tests
- Definition of suitable bioreactors and the potential market
- Carry out oxygen transfer rate experiments
- Assess the fermentation efficiency in the Automate using a range of different agitator types and compare with 2L bioreactor.

**Time spent with collaborate company in the last six months:**

None, set date for 6<sup>th</sup> January 2003

**Training profile**

**Educational Background:** MEng, Chemical Engineering with Biochemical Engineering, University of Birmingham.

**Training profile:** MBI modules and relevant graduate school courses.

**Year 1**

**Core Training:**

| Course or Management activity  | Dates *   | Progress & Assessment                  |
|--|---|--|
| <b>Graduate school board skills e.g. Personal and Professional Management Skills</b> | Personal Skills Development (PPMS, IMR)<br>Sept 02 – Feb 03 | Course due to be completed by Feb 2003 |

|  |   |                                      |
|--|---|--------------------------------------|
| <b>Graduate school technical courses</b><br>e.g. Statistics    | Booked a Statistics course for Jan 03             | To be completed                      |
| <b>Department training modules</b><br>e.g. Fermentation module | MBI Fermentation<br><br>MBI Process Validation    | To be taken<br><br>To be taken 02/03 |
| <b>Management activities</b><br>e.g. Demonstratorship          | Demonstrating Homogenisation<br>Nov 02- March 03  |                                      |
| <b>Workshops Attended</b><br>e.g. Gene meetings                | Biotech Exhibition<br>Weekly Biocatalyst meetings |                                      |
| <b>Total number of courses taken</b>                           |   |                                      |

\* these may be checked

## Proforma 2

**Date:** 15.05.2003

**Name:** Naveraj Kaur Gill  
Lye

**Registration Date:** (23.09.2002)  
Baganz

**Supervisor (s):** Dr Gary

**Advisor:** Dr Frank

**Industrial Advisors:** Dr  
Jasbir Singh and Dr  
Simon Waldram

**Level:** EngD with HEL (year 1)

**Project title:** Production and evaluation of immobilised biocatalysts in automated, parallel mini-reactors.

### **Significance:**

Rapid scientific advances are generating large libraries of biocatalysts and the development of new drug compounds has put increasing pressure on the initial stages of biocatalytic process design. Therefore there is a need to develop new methods that allow rapid screening of these and subsequent trials on the most useful biocatalysts, which can predicatively scaled up.

### Goals:

- Assess existing HEL automated mini-reactors and technologies for use in design and predictive scale up of bioconversion process
- To develop methods which reduce the cost and timescales of fermentation processes development

### Conceptual Challenges:

To establish if the Automate is suitable for running both chemical and biochemical processes, the advantages of using automated, parallel systems. Also to identify the basis for scale up.

### Results:

- **Sterilisation Test 1:** initially we wanted to be able to sterilise the entire reactor and its contents (media) *in-situ*, this would involve raising the temperature of the system to 121°C and holding this temperature for 20- 30 minutes. Such a high temperature in the Automate can only be reached if the vessel is completely sealed to allow the pressure to build and raise the temperature, and it is very important that all parts of the reactor including the headspace and dead-leg (area furthest from the liquid, i.e. in the ports) areas reach this temperature. Therefore this experiment was designed to assess the time taken to reach 121°C in three major parts of the reactor: the liquid, the headspace and the dead-leg. This was done by inserting a thermocouple into each of these areas. Water was used for these experiments, and the results show that the system had to be raised to 125°C for all parts of the reactor to reach a satisfactory sterilising temperature.
- **Sterilisation Test 2:** This experiment involved setting the Automate up as a bioreactor containing LB media. The reactor had an air inlet and outlet and a pH probe (not steam sterilisable). The objective of this experiment was to sterilise the vessel and its contents *in-situ* and run a fermentation without inoculating with any microorganisms for a few days to see if any microbes (contaminants) entered the system and if the media had been adequately sterilised.
- **Problems:** The air filters could not be sterilised *in-situ* with the reactor and had to be sterilised separately in an oven and attached to the reactor after sterilisation. Since we did not have a dissolved oxygen probe we had to rely on the pH values as an indicator of any microbial growth in the reactor. Unfortunately there were a few problems associated with the stirrer half way through the experiment and the heating system broke down temporarily and reduced the temperature of the system which in turn caused the pH to reduce.
- **Results:** At the end of the experiment samples of the media were taken and grown on 8 LB agar plates, however no microbial growth was detected indicating that the media was successfully sterilised and no contaminants entered the system. In addition to this 2 agar plates were left open to the atmosphere all day, 1 near the reactor and the other outside the working area in order to get some idea of the potential contaminants that could enter the system.

- **Sterilisation Test 3:** Repeat Sterilisation test 2, using LB media, only difference is method of sterilisation, reactor and its contents together with all fittings was sterilised in an oven (no autoclave available). Run experiment for 136.95 hours.
- **Problems:** the pH probe was giving a lower reading for the media which was set at pH 7. This may be due to the fact that the probe was initially calibrated at approx 19°C, and the experiment was run at 37°C. Since the media was actually at pH 7 at the start of the fermentation, all the measured pH values were adjusted by adding 0.75 (this is the difference between the measured pH at the start and the actual pH, 7).
- **Results:** At the end of the experiment samples of the media were taken and grown on 10 LB agar plates, incubate at 37°C. 7 plates have shown microbial growth (white circular colonies, and on some plates the growth was at the edges of the plate and the centre was clear). Therefore the system was contaminated – likely sources: stopper port and the insertion of the pH probe after sterilisation (washed with ethanol).

#### **Intellectual Property:**

At this stage the main intellectual property would be to compare the similarities and difference between chemical and biochemical reactors. Also to asses and make modifications to the design of the HEL reactors in order to operate the system aseptically, so that samples can be taken and additions made without compromising the sterility of the system.

#### **Previous milestones:**

- Successfully complete shake flask and 2L fermentations using LB and glycerol based media
- Present 'An introduction to microbial fermentation' to HEL
- Tabulate all the information found about miniature reactors already being manufactured
- Carry out sterilisation tests and perform a fermentation at HEL using their miniature reactor
- Produce an initial draft of literature review for the first year report

#### **Research targets:**

##### **6 months:**

- Make changes to the Automate that have been suggested so far, decide on if the bioreactor system will be autoclaved or sterilised *in-situ*
- Research gas analysers and inform HEL of the information found
- Test the selected bakers yeast fermentation and bioconversion system (conversion of a ketone to an alcohol). First carry out shake flask fermentations, once confirmed the system is a suitable demonstration of fermentation and bioconversion, carry out in the Automate.
- Find a chemical test that confirms that the ketone has been converted to an alcohol, preferably show a colour change.
- Continue making recommendation for the re-design of the Automate and test the new designs till a suitable bioreactor is obtained.

- Prepare a brief presentation for first year seminar

**Milestone(s):**

- Fabricate a new Automate according to the suggested changes and repeat sterilisation tests and confirm sterilisation mechanism.
- Successfully complete shake flask experiments using bakers yeast also complete in the Automate.
- Present an introduction to my project at the first years seminar

**Research targets:**

**6 months to 1 year:**

- Finalise the design of the Automate for it to perform efficiently as a bioreactor
- Review the existing software and adapt it for the control and monitoring microbial fermentations
- Look into the mechanism of sparging and agitation
- Decide on a novel bioprocess/ bioconversion to investigate, that can be used to assess the efficiency of the automate

**Milestone (s):**

- Fabricate the Automate bioreactor
- Make changes to the software, e.g. incorporate the sterilisation of the entire system as a single step in the recipe that is pre-program and carried out automatically.
- Decide on a suitable sparger and impeller design
- Carry out the novel bioprocess that has been chosen to base the remainder of the project on.

**Time spent with collaborate company in the last six months:**

- Time spent at HEL 06.01.03 – 10.02.03
- Introduction to laboratory infrastructure at HEL.
- Training on the Automate reactor system and software for planning, running and viewing experiments, (WinIso). Software for off-line viewing of data.
- Prepared two PowerPoint presentations for HEL: 'Introduction to microbial fermentation' and 'Progress with the Automate reactor so far'.
- Carried out a series of sterilisation tests on the Automate: capability of achieving sterilisation conditions, possibility of *in-situ* sterilisation and sterilisation by autoclaving.
- Obtain suitable miniature, steam sterilisable pH and dissolved oxygen probes for use in subsequent sterilisation and fermentation experiments

**Training profile**

**Educational Background:** MEng, Chemical Engineering with Biochemical Engineering, University of Birmingham.

**Training profile:** MBI modules and relevant graduate school courses.

**Year 1**

**Core Training:**

| <b>Course or Management activity</b>   | <b>Dates *</b>  | <b>Progress &amp; Assessment</b> |
|--|---|----------------------------------|
| <b>Graduate school board skills<br/>e.g. Personal and Professional<br/>Management Skills</b> | Personal Skills<br>Development<br>(PPMS, IMR)<br>Sept 02 – Feb 03           | Completed Feb 2003               |
| <b>Graduate school technical<br/>courses<br/>e.g. Statistics</b>                             |   |                                  |
| <b>Department training modules<br/>e.g. Fermentation module</b>                              | MBI Validation  | Completed April 03 2003          |
| <b>Management activities<br/>e.g. Demonstratorship</b>                                       |   |                                  |
| <b>Workshops Attended<br/>e.g. Gene meetings</b>   | -Weekly Biocatalyst<br>meetings<br>-Microwell research<br>planning meetings |                                  |
| <b>Total number of courses taken</b>   |   |                                  |

\* these may be checked

**Proforma 3:**

**Date:** 10.11.2003

**Name:** Naveraj Kaur Gill  
Lye  
**Registration Date:** (23.09.2002)  
Baganz

**Supervisor (s):** Dr Gary

**Advisor:** Dr Frank

**Industrial Advisors:** Dr  
Jasbir Singh and Dr  
Simon Waldram

**Level:** EngD with HEL (year 2)

**Project title:** Production and evaluation of immobilised biocatalysts in automated, parallel mini-reactors.

**Significance:**

Rapid scientific advances are generating large libraries of biocatalysts and the development of new drug compounds has put increasing pressure on the initial stages of biocatalytic process design. Therefore there is a need to develop new methods that allow rapid screening of these and subsequent trials on the most useful biocatalysts, which can predicatively scaled up.

**Goals:**

- Asses existing HEL automated mini-reactors and technologies for use in design and predictive scale up of bioconversion process
- To develop methods which reduce the cost and timescales of fermentation processes development
- Using calorimetry to monitor bioprocesses

**Conceptual Challenges:**

To establish if the Automate is suitable for running both chemical and biochemical processes, the advantages of using automated, parallel systems. Also to identify the basis for scale up. Assessing the sensitivity of HEL's calorimetry methods for monitoring bioprocesses.

**Results:**

- *In-situ* sterilisation of the miniature Automate reactor and 4 successful bakers yeast fermentation were carried out at HEL. Only the pH and dissolved oxygen were monitored during the fermentations and provided the expected results for a typical aerobic yeast fermentation.
- Two 1L fermentations were carried out at UCL, the purpose of these fermentations was to try and achieve similar results to what was found with the fermentations carried out in the Automate. At UCL further analysis of cell density and glucose concentration could be done. Similar pH and dissolved oxygen profiles were obtained.
- The first miniature bioreactor prototype has been made and a number of tests have been carried out, such as pressure test, temperature mapping tests and sterilisation tests. Unfortunately the design of the head plate and arrangement of ports were not very suitable, also the Rushton turbine was much too large for a bioreactor.
- The initial pressure test showed that pressures as high as 3bar were achieved within the reactor during *in-situ* sterilisation. A hydrostatic pressure test was also done with the glass reactors and concluded that the reactors can handle up to 8bar.
- A second prototype has been carefully designed, particularly concentrating on the Rushton turbine, arrangement of the sparger and ensuring the vessel can be sealed sufficiently to enable *in-situ* sterilisation without compromising the sterility at any time.
- Some crude calorimetry tests have been done, monitoring the requested power of the external heater used to control the temperature of the system during the fermentation. The results showed that there is a reduction in the requested power for the heater during a fermentation, as the yeast generate heat.

**Intellectual Property:**

At this stage the main intellectual property would be to compare the similarities and difference between chemical and biochemical reactors. Also to asses and make modifications to the design of the HEL reactors in order to operate the system aseptically, so that samples can be taken and additions made without compromising the sterility of the system.

**Publications:****Previous milestones:**

- Fabricate a new Automate according to the suggested changes and repeat sterilisation tests and confirm sterilisation mechanism.
- Successfully complete shake flask experiments using bakers yeast also complete in the Automate.
- Present an introduction to my project at the first years seminar

**Research targets:****6 months:**

- Produce detailed mechanical drawings of the head plate, sparger and stirrer.
- Have the second prototype made, and carry out pressure, temperature mapping and sterilisation tests. Having done these tests carry out a yeast fermentation.
- Review the parameters that must be controlled and monitored for a bioprocess and how it will be achieved.
- Design of the base on which the reactors will sit.
- Decide on how feeds, acid, base and air are going to be supplied to the system, e.g. peristaltic pumps, rotary valve, rotameters.
- Do some scale-up experiments in the miniature bioreactor and a lab scale fermenter at UCL. These experiments should be done at constant  $P_g/V$ , constant tip speed and constant  $kLa$  so that the best scaling criteria can be define

**Milestone(s):**

- Have the second prototype made according to the mechanical drawings.
- Carry out the various tests on the new reactor.
- A second hydrostatic test with the new head plate.
- Have a base designed and made up with the pumps and rotameters etc accessibly positioned.

**Research targets:****6 months to 1 year:**

- Carry out some useful biocalorimetry experiments.
- Decide on a novel bioprocess/ bioconversion to investigated, that can be used to asses the efficiency of the automate

**Milestone (s):**

- Make changes to the software, e.g. incorporate the sterilisation of the entire system as a single step in the recipe that is pre-program and carried out automatically



- Carry out the novel bioprocess that has been chosen to base the remainder of the project on.

**Time spent with collaborate company in the last six months:**

I have spent most of my time since May 2003 at my company as all the facilities and expertise required at this stage of my project are at HEL. I have only returned to UCL to carry out further analysis for fermentations that can not be done at HEL and for demonstrating the homogenisation labs.

**Training profile**

**Educational Background:** MEng, Chemical Engineering with Biochemical Engineering, University of Birmingham.

**Training profile:** MBI modules and relevant graduate school courses.

**Year 1**

**Core Training:**

| <b>Course or Management activity</b>   | <b>Dates *</b>  | <b>Progress &amp; Assessment</b> |
|--|---|----------------------------------|
| <b>Graduate school board skills<br/>e.g. Personal and Professional<br/>Management Skills</b> | Personal Skills<br>Development<br>(PPMS, IMR)<br>Sept 02 – Feb 03           | Completed Feb 2003               |
| <b>Graduate school technical<br/>courses<br/>e.g. Statistics</b>                             |   |                                  |
| <b>Department training modules<br/>e.g. Fermentation module</b>                              | MBI Validation  | Completed April 03 2003          |
| <b>Management activities<br/>e.g. Demonstratorship</b>                                       | Homogenisation lab<br>demonstration (head<br>demonstrator)                  | Oct 2003 – March 2004            |
| <b>Workshops Attended<br/>e.g. Gene meetings</b>   | -Weekly Biocatalyst<br>meetings<br>-Microwell research<br>planning meetings |                                  |
| <b>Total number of courses taken</b>   |   |                                  |

\* these may be checked

## **Proforma 4:**

**Date:** 14.05.2004

**Name:** Naveraj Kaur Gill

**Supervisor (s):** Dr Gary Lye

**Registration Date:** (23.09.2002)

**Advisor:** Dr Frank Baganz

**Industrial Advisors:**

Dr Jasbir Singh and Dr Simon  
Waldram

**Level:** EngD with HEL (year 2)

**Project title:** Design and scale-up of parallel, automated miniature bioreactors.

### **Significance:**

Rapid scientific advances are generating large libraries of biocatalysts and the development of new drug compounds has put increasing pressure on the initial stages of biocatalytic process design. Therefore there is a need to develop new methods that allow rapid screening of these and subsequent trials on the most useful biocatalysts, which can predicatively scaled up.

### **Goals:**

- Asses existing HEL automated mini-reactors and technologies for use in design and predictive scale up of bioconversion process
- To develop methods which reduce the cost and timescales of fermentation processes development
- Scale-up from the 100ml scale to bench scale bioreactor
- Using calorimetry to monitor bioprocesses

### **Conceptual Challenges:**

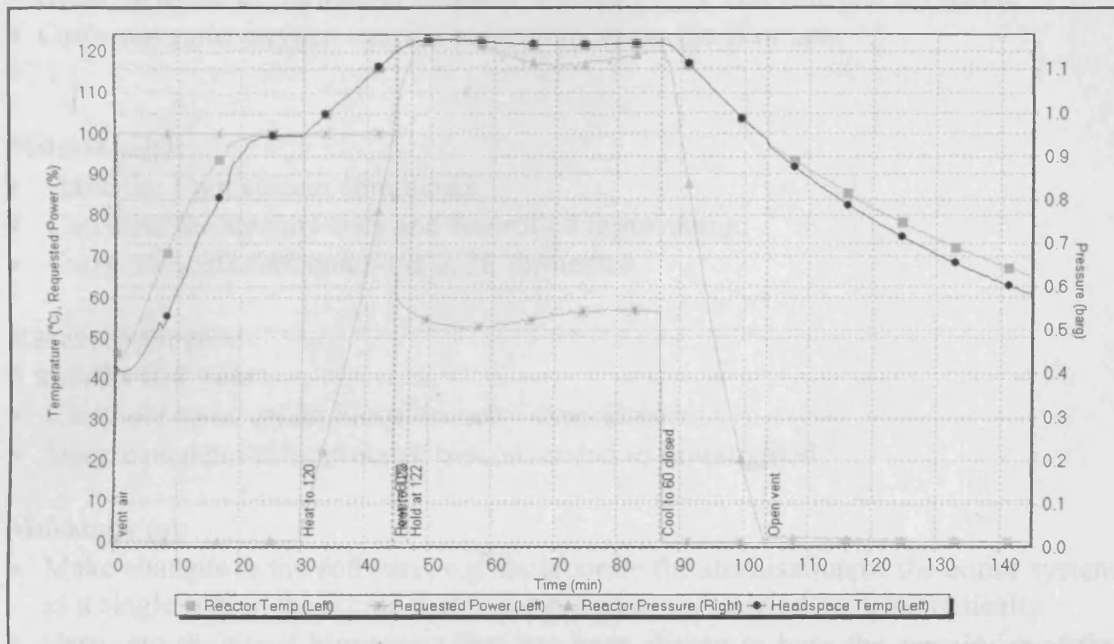
To establish if the Automate is suitable for running both chemical and biochemical processes, the advantages of using automated, parallel systems. Also to identify the basis for scale up. Assessing the sensitivity of HEL's calorimetry methods for monitoring bioprocesses. Using a suitable criteria for scale up, e.g. constant power per unit volume.

### **Results:**

- The design of the miniature bioreactor (Biomate) has been finalised and the reactor has been fabricated. The Biomate has a working volume of 100 ml, and is fitted with four equally spaced baffles and a six blade Rushton turbine which is magnetically driven.
- The head plate has been deigned with 7 ports for pH, dissolved oxygen, temperature and optical density probes. There are also ports allocated for air inlet

and exhaust gas outlet. A larger multiport has been designed for all the additions (acid, base, inoculum) and sampling.

- Air is sparged into the vessel via a stainless steel tube located directly beneath the Rushton turbine.
- Temperature mapping and pressure tests have been conducted to establish the conditions for *in-situ* sterilisation. The results are shown below.



- The results show that the bulk reactor system must be heated to 122°C to ensure the vessel internal and media are sterilised at 121°C. The maximum pressure generated during the sterilisation procedure was 2.1 bar, and these figures agree completely with data from steam tables.
- Two-way pH control has also been implemented. Peristaltic pumps are used for acid and base delivery
- Some work has been done using an optical density probe made in house.

### Intellectual Property:

At this stage the main intellectual property would be to assess the efficiency of the *in-situ* sterilisation and check that sterility is maintained. The Biomate has been designed to be geometrically similar to standard stirred tank bioreactors, therefore the potential for scale needs to be investigated.

**Publications:** None

### Previous milestones:

- Have the second prototype made according to the mechanical drawings.
- Carry out the various tests on the new reactor.
- A second hydrostatic test with the new head plate.
- Have a base designed and made up with the pumps and rotameters etc accessibly positioned.

**Research targets:****6 months:**

- Complete the sterilisation tests for the Biomate
- Complete the 1 pot biomate system equipped with probes, pumps and rotameter for use at UCL
- Carry out *e.coli* fermentation in the Biomate under controlled conditions.
- Scale up to the 2L fermenter based on constant  $P_g/V$  and constant tip speed.
- Carry out some oxygen transfer measurements in the Biomate.

**Milestone(s):**

- Have the 1 pot system completed.
- Carry out the sterility tests and controlled fermentation
- Carry out scale fermentations in 2L fermenter

**Research targets:****6 months to 1 year:**

- Carry out some useful biocalorimetry experiments.
- Decide on a novel bioprocess/ bioconversion to investigated

**Milestone (s):**

- Make changes to the software, e.g. incorporate the sterilisation of the entire system as a single step in the recipe that is pre-program and carried out automatically
- Carry out the novel bioprocess that has been chosen to base the remainder of the project on.

**Time spent with collaborate company in the last six months:**

I have been at HEL from May 2003 to March 2004, as all the facilities and expertise required at this stage of my project are at HEL. I have only returned to UCL to carry out further analysis for fermentations that can not be done at HEL and for demonstrating the homogenisation labs.

**Training profile**

**Educational Background:** MEng, Chemical Engineering with Biochemical Engineering, University of Birmingham.

**Training profile:** MBI modules and relevant graduate school courses.

**Year 1****Core Training:**

| Course or Management activity | Dates *         | Progress & Assessment |
|-------------------------------|-----------------|-----------------------|
| Graduate school board         | Personal Skills | Completed Feb 2003    |

|  |   |                         |
|--|---|-------------------------|
| <b>skills</b><br>e.g. <b>Personal and Professional Management Skills</b> | Development (PPMS, IMR)<br>Sept 02 – Feb 03   |                         |
| <b>Graduate school technical courses</b><br>e.g. <b>Statistics</b>       |   |                         |
| <b>Department training modules</b><br>e.g. <b>Fermentation module</b>    | MBI Validation  | Completed April 03 2003 |
| <b>Management activities</b><br>e.g. <b>Demonstratorship</b>             | Homogenisation lab demonstration (head demonstrator)  | Oct 2003 – March 2004   |
| <b>Workshops Attended</b><br>e.g. <b>Gene meetings</b>                   | -Weekly Biocatalyst meetings<br>-Microwell research planning meetings<br>- Weekly Departmental seminars<br>- IChemE seminar | April 2004              |
| <b>Total number of courses taken</b>                                     |   |                         |

\* these may be checked

### **Proforma 5:**

**Date:** 14.11.2005

**Name:** Naveraj Kaur Gill

**Supervisor (s):** Dr Gary Lye

**Registration Date:** (23.09.2002)

**Advisor:** Dr Frank Baganz

**Industrial Advisors:**  
Dr Mark Appleton

**Level:** EngD with HEL (year 3)

**Project title:** Design and scale-up of parallel, automated miniature bioreactors.

**Significance:**

Rapid scientific advances are generating large libraries of biocatalysts and the development of new drug compounds has put increasing pressure on the initial stages

of biocatalytic process design. Therefore there is a need to develop new methods that allow rapid screening of these and subsequent trials on the most useful biocatalysts, which can predicatively scaled up.

**Goals:**

- Asses existing HEL automated mini-reactors and technologies for use in design and predictive scale up of bioconversion process
- To develop methods which reduce the cost and timescales of fermentation processes development
- Scale-up from the 100ml scale to bench scale bioreactor
- Using calorimetry to monitor bioprocesses

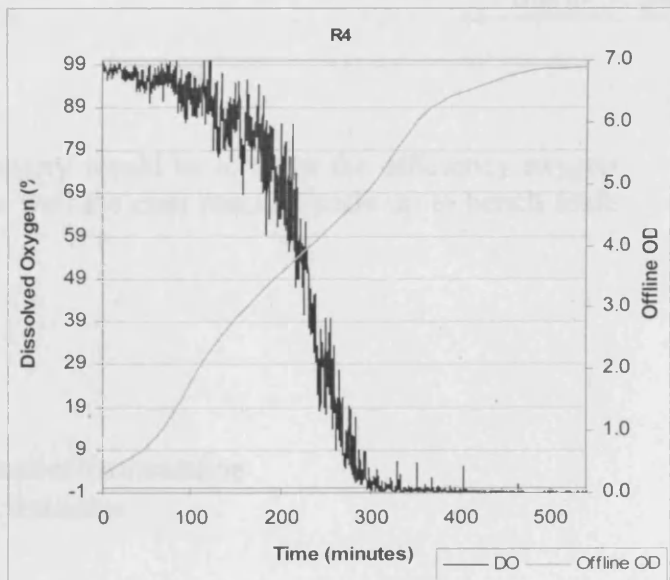
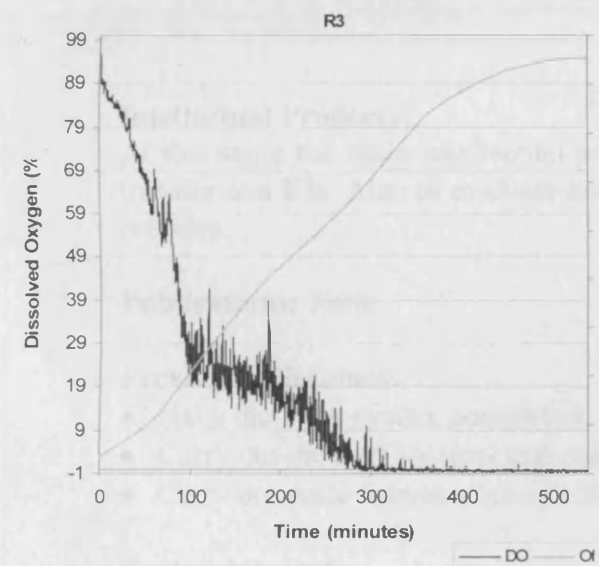
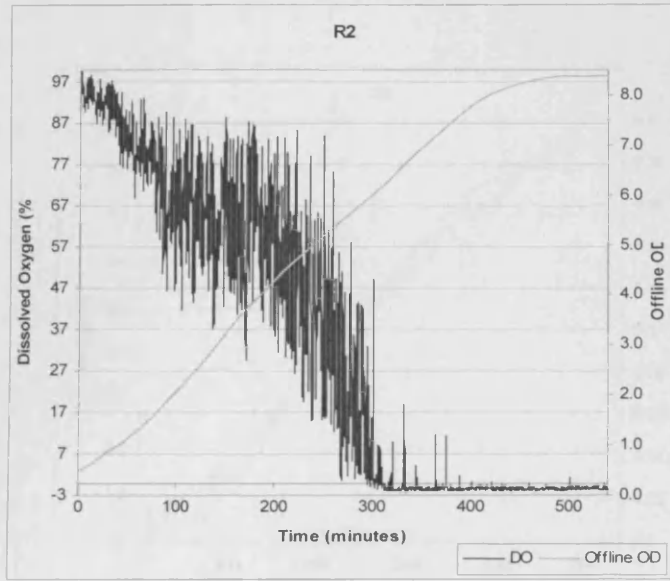
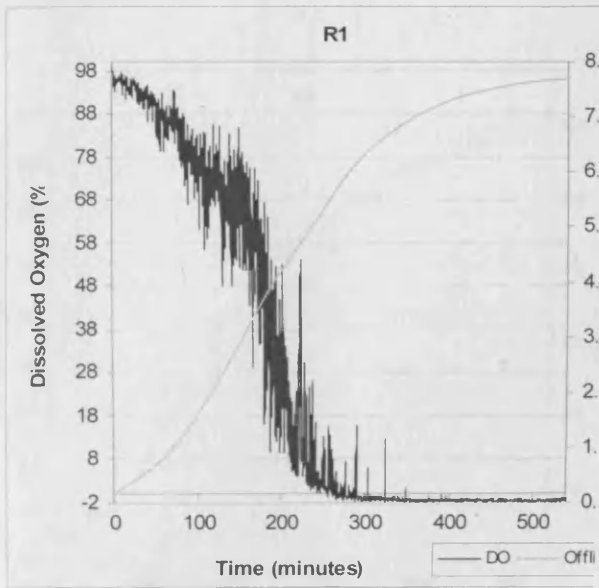
**Conceptual Challenges:**

To establish if the Automate is suitable for running both chemical and biochemical processes, the advantages of using automated, parallel systems. Also to identify the basis for scale up. Assessing the sensitivity of HEL's calorimetry methods for monitoring bioprocesses. Using a suitable criteria for scale up, e.g. constant power per unit volume.

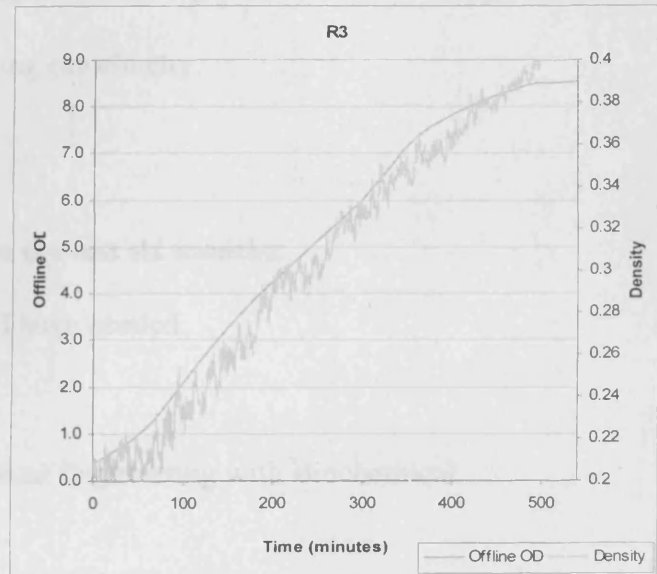
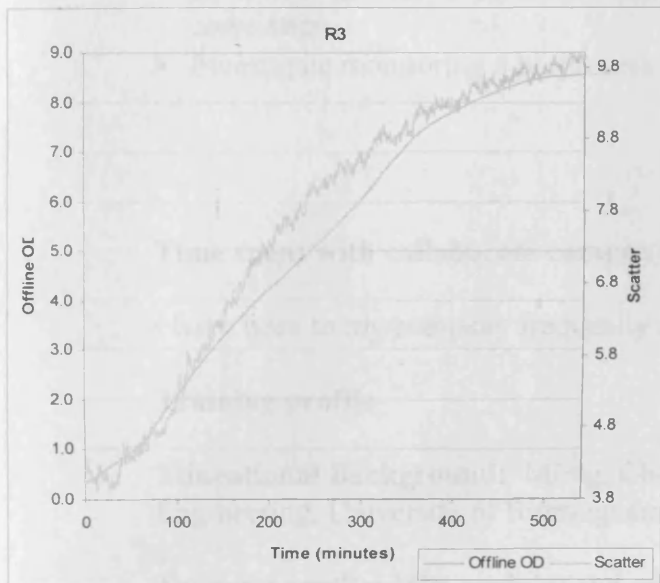
**Results:**

- Sterility tests for the miniature bioreactor is complete, and sterility was maintained after leaving the reactor running under fermentation condition for 4 days.
- A four pot miniature bioreactor system is complete.
- A series of four parallel fermentations have been carried out under identical conditions. Each of the reactors contained 100 ml of media and was inoculated with 2ml of broth grown overnight (2% inocula). The agitation rate in all reactors was maintained at 1000 rpm and the air flow rate for all the systems was constant at 1 vvm (100ml/min). 1ml samples were taken hourly from each reactor and the biomass concentration of *E.coli* was determined turbidimetrically at 600nm in a spectrophotometer. See figure 1.

Figure 1: Dissolved oxygen and off-line optical density profiles for all four reactors.



- HEL have created an on-line optical probe. The probe provides on-line optical density (transmitted light) data as well as scatter data (this is the light detected at 90° to the transmitted light). The graphs below show how the on-line optical data compares with the off-line data for reactor 3.



### Intellectual Property:

At this stage the main intellectual property would be to assess the efficiency oxygen transfer and  $K_{La}$ . Also to evaluate how well the mini reactors scale up to bench scale reactors.

**Publications:** None

### Previous milestones:

- Have the 1 pot system completed.
- Carry out the sterility tests and controlled fermentation
- Carry out scale fermentations in 2L fermenter

### Research targets:

#### 6 months:

- Carry out some oxygen transfer measurements in the Bioexplorer.
- Collect parallel fermentation and oxygen transfer data for first paper.
- Determine the power number of the mini impeller
- Scale up to 2L scale based on P/V

#### Milestone(s):

- Determine the max  $K_{La}$  for mini reactor
- Complete draft paper before Christmas
- Determine the power number of the impeller.

### Research targets:

#### 6 months to 1 year:

- Complete scale up experiments in 2L scale (and maybe larger) based on P/V



- Further investigation of biocalorimetry

**Milestone (s):**

- Establish the most suitable scale up criteria, e.g based on the Hughmark correlation.
- Investigate monitoring a bioprocess using calorimetry.

**Time spent with collaborate company in the last six months:**

I have been to my company frequently as I have needed.

**Training profile**

**Educational Background:** MEng, Chemical Engineering with Biochemical Engineering, University of Birmingham.

**Training profile:** MBI modules and relevant graduate school courses.

**Year 1**

**Core Training:**

| <b>Course or Management activity</b>   | <b>Dates *</b>  | <b>Progress &amp; Assessment</b> |
|--|---|----------------------------------|
| <b>Graduate school board skills</b><br>e.g. <b>Personal and Professional Management Skills</b> | Personal Skills Development (PPMS, IMR)<br>Sept 02 – Feb 03 | Completed Feb 2003               |
| <b>Graduate school technical courses</b><br>e.g. <b>Statistics</b>                             |   |                                  |
| <b>Department training modules</b><br>e.g. <b>Fermentation module</b>                          | MBI Validation  | Completed April 03 2003          |
| <b>Management activities</b><br>e.g. <b>Demonstratorship</b>                                   | Homogenisation lab demonstration (head demonstrator)        | Oct 2003 – March 2004            |
| <b>Workshops Attended</b><br>e.g. <b>Gene meetings</b>   | -Weekly Biocatalyst meetings<br>-Microwell research         |                                  |

|                                      |   |            |
|--------------------------------------|---|------------|
|                                      | planning meetings<br>- Weekly Departmental seminars<br>- IChemE seminar | April 2004 |
| <b>Total number of courses taken</b> |   |            |

\* these may be checked

### **Proforma 6:**

**Date:** 14.11.2005

**Name:** Naveraj Kaur Gill

**Supervisor (s):** Dr Gary Lye

**Registration Date:** (23.09.2002)

**Advisor:** Dr Frank Baganz

**Industrial Advisors:**  
Dr Mark Appleton

**Level:** EngD (year 4)

**Project title:** Design and Characterisation of Parallel Miniature Bioreactors for Rapid Process Optimisation and Scale-up

#### **Significance:**

Rapid scientific advances are generating large libraries of biocatalysts and the development of new drug compounds has put increasing pressure on the initial stages of biocatalytic process design. Therefore there is a need to develop new methods that allow rapid screening of these and subsequent trials on the most useful biocatalysts, which can predicatively scaled up.

#### **Goals:**

- Asses existing HEL automated mini-reactors and technologies for use in design and predictive scale up of bioconversion process
- To develop methods which reduce the cost and timescales of fermentation processes development
- Scale-up from the 100ml scale to bench scale bioreactor
- Using calorimetry to monitor bioprocesses

#### **Conceptual Challenges:**

To establish if the Automate is suitable for running both chemical and biochemical processes, the advantages of using automated, parallel systems. Also to identify the basis for scale up. Assessing the sensitivity of HEL's calorimetry methods for monitoring bioprocesses. Using a suitable criteria for scale up, e.g. constant power per unit volume.

**Results:**

- A series of  $k_{La}$  measurements have been carried out, giving a maximum  $k_{La}$  value of  $0.11 \text{ s}^{-1}$ .
- Fermentations were carried out to assess the influence of aeration rates and stirrer speeds.
- Experimentally determined a power curve for the miniature Rushton turbine, giving a power number of 3.5 in the turbulent flow regime.
- Successfully scaled up to 2L bench scale bioreactor based on constant  $k_{La}$ . Three different  $k_{La}$  values were investigated and there is very good agreement between biomass and DOT profiles at both scale.
- Scale up was also performed based on constant  $Pg/V$ , this was only successful at higher stirrer speeds.

**Intellectual Property:** design and fabrication of the 4-pot Xplorer system, unique software and novel optical density probe.

**Publications:**

**PAPER:** Design and Instrumentation of a Novel Miniature Bioreactor System for High Throughput Fermentation Optimisation  
N. K. Gill, M. Appleton, F. Baganz, M. Peacock, G. J. Lye

**POSTER:** Design and Instrumentation of a Novel Miniature Bioreactor System for High Throughput Fermentation Optimisation  
N. K. Gill, M. Appleton, F. Baganz, M. Peacock, G. J. Lye

**Previous milestones:**

- Establish the most suitable scale up criteria, e.g. based on the Hughmark correlation.
- Investigate monitoring a bioprocess using calorimetry.

**Research targets:****6 months:**

- Train MEng student to use the 4-pot Xplorer system.
- Use experimental design tools to assess the effects of varying temperature, pH and arabinose concentration on the biomass concentration and CHMO activity during a *e.coli* TOP10 fermentation.
- Collect all data for second paper, based on scale up

**Milestone(s):**

- Complete some trial fermentations with MEng student.
- Compile a series of experiments that need to be completed to investigate the parameter of interest
- Start writing draft of second paper

**Research targets:****6 months to 1 year:**

- Further investigation of biocalorimetry

**Milestone (s):**

- Investigate monitoring a bioprocess using calorimetry

**Time spent with collaborate company in the last six months:**

I have been to my company frequently as I have needed.

**Training profile**

**Educational Background:** MEng, Chemical Engineering with Biochemical Engineering, University of Birmingham.

**Training profile:** MBI modules and relevant graduate school courses.

**Year 1****Core Training:**

| <b>Course or Management activity</b>  | <b>Dates *</b>  | <b>Progress &amp; Assessment</b>                |
|---|---|---|
| <b>Graduate school board skills</b><br>e.g. Personal and Professional Management Skills | Personal Skills Development (PPMS, IMR)<br>Sept 02 – Feb 03   | Completed Feb 2003                              |
| <b>Graduate school technical courses</b><br>e.g. Statistics                             |   |   |
| <b>Department training modules</b><br>e.g. Fermentation module                          | MBI Validation  | Completed April 03 2003                         |
| <b>Management activities</b><br>e.g. Demonstratorship                                   | Homogenisation lab demonstration (head demonstrator)<br><br>Planning and organising careers seminar every month | Oct 2003 – March 2004<br><br>Oct 2005 – to date |
| <b>Workshops Attended</b><br>e.g. Gene meetings   | -Weekly Biocatalyst meetings<br>-Microwell research planning meetings   |   |

|                                      |   |                                |
|--------------------------------------|---|--------------------------------|
|                                      | <ul style="list-style-type: none"> <li>- Weekly Departmental seminars</li> <li>- IChemE seminar</li> <li>- RAFT conference</li> </ul> | <p>April 2004<br/>Nov 2005</p> |
| <b>Total number of courses taken</b> |   |                                |